The Pharmacology of Novel Illicit Synthetic Cannabinoids

Jordyn M. Stuart

Faculty of Human Sciences

Australian School of Advanced Medicine

Macquarie University

2015

A thesis submitted in fulfilment of the requirements for the degree of

Doctor of Philosophy in Advanced Medicine

TABLE OF CONTENTS

Table of Tables and Figures

Abbreviations

2-AG	2-arachydonoyl Glycerol
4-HNE	4-hydroynonenol
5-HT$_3$	5-hydroxytryptamine Serotonin Receptor
AC	Adenylate cyclase
AEA	Anandamide
AKI	Acute Kidney Injury
Aphla	α
Beta	β
BK	Bradykinin
BSA	Bovine Serum Albumin
Ca^{2+}	Calcium
cAMP	Cyclic adenosine monophosphate
CAP	Capsaicin
CAPZ	capsazepine
CB$_1$	cannabinoid receptor 1
CB$_2$	Cannabinoid Receptor 2
CBD	Cannabidiol
CDD	Cannabinoid Designer Drugs
CGRP	calcitonin gene-related peptide
CIN	Cinnamaldehyde
D$_2$	Dopamine 2 receptor
D$_4$AEA	Deuterium labelled anandamide
DA	Dopamine
DMEM	Dulbecco's Modified Eagles Medium
DMSO	Dimethyl sulfoxide
DRG	Dorsal Root Ganglia
ESI	Electrospray ionization
EtOH	Ethanol
EMCDDA	European Monitoring Center for Drug and Drug Abuse
EWS	Early Warning System
FAAH	Fatty Acid Amide Hydrolase
FBS	Fetal bovine serum
FS 3	FlexStation 3
Gamma	γ
GDP	Guanosine diphosphate
GIRK	G-protein gated inwardly rectifying potassium
GPCR	G-Protein Coupled Receptors
GTP	Guanosine triphosphate
HBSS	Hanks Balanced Salt Solution
HEK	Human Embryonic Kidney
HPLC	High performance liquid chromatography
IACM	International Association of Cannabinoid Medicine
ICE	International Collaborative Exercises
ICRS	International Cannabinoid Research Society
IDHC	India Hemp Drugs Commission
IP$_3$	Inositol triphosphate receptor
K+	Potassium

LEA	linolenoyl ethanolamide
MAP Kinase	Mitogen-Activated Protein Kinase
MeOH	Methanol
mGlu5	metabotropic glutamate receptor 5
MRM	Multiple reaction monitoring
Na$^+$	Sodium
NAc	Nucleus Accumbens
NAEs	N-acyl ethanolamides
NAGly	N-arachidonoyl Glycine
NPS	new psychoactive substances
OEA	Oleoyl ethanolamide
P/S	Penicillin/streptomycin
PBS	Phosphate-buffered saline
PCP	Phencyclidine
PEA	Palmitoyl ethanolamide
PLC	Phospholipase C
PSI	Product Ion Scan
PTX	Pertussis Toxin
RLB	Radioligand Binding
ROS	Reactive Oxidation Species
RT	Retention Time
SAR	Structure activity relationship
SC	Synthetic cannabinoid
SEA	stearoyl ethanolamide
SEM	Standard Error of the Mean
SRIF	Somatostatin
TG	Trigeminal Ganglia
THC	Tetrahydrocannabinol
TRPA	transient receptor potential ankyrin
TRPC	transient receptor potential canonical
TRPM	transient receptor potential melastatin
TRPML	transient receptor potential mucolipin
TRPP	transient receptor potential polycystin
TRPV	transient receptor potential vanilloid
UNODC	United Nations Office on Drugs and Crime
UNOSC	United Nations Office on Drugs and Crime
VTA	Ventral Tegmental Area
WADA	World Anti-Doping Agency
WHO	World Health Organization
WIN	WIN 55,212-2

DECLARATION

I certify that this work contains no material which has been submitted or accepted for the award of any other degree or diploma in any university or other tertiary institution in my name. The work presented was completed personally or where contributing researchers have been mentioned. This contains no material, to my knowledge, that has been previously published or written by another person, except where a reference has been given for such work. In addition, I certify that no part of this work will be used in a submission in my name, for any other degree or diploma in any university or other tertiary institution without the prior approval of the Macquarie University.

Contributions in this work from joint research or publications:

- All synthetic cannabinoids that were not purchased from listed vendors were synthesized at the University of Sydney in Sydney, Australia by either Samuel D. Banister or Shane M. Wilkinson in the lab of Dr. Michael Kassiou.
- Transfections of the rat cannabinoid receptors into AtT20 cells were completed and gifted to us by Ken Mackie from the Indiana University in Bloomington, IN USA.
- Transfections of the human cannabinoid receptors into AtT20 cells were completed and gifted to us by Michelle Glass from the University of Auckland in Auckland, New Zealand.
- Transfections of the human TRPV1 receptor into HEK293 cells were completed and gifted by Peter McIntyre from RMIT University in Melbourne, Australia.
- A small number of replicates of the fluorescent-based plate reader membrane potential and intracellular calcium assays were completed by Amelia Edington and Mark Connor and Macquarie University in Sydney Australia to supplement data generated by Jordyn Stuart.

ACKNOWLEDGEMENTS

ABSTRACT

Herbal smoking mixtures containing illicit synthetic cannabinoids (SCs), originally sold as legal substitutes to cannabis, have become the most rapidly growing class of recreational designer drugs since 2008. Legal restrictions on the first generation SCs created a chemist-driven structural evolution making identification and the study of their pharmacology and toxicology difficult. The consumption of these novel compounds is of major concern as the toxicity seems to be increasing with each new generation of structures. As very little is known about their pharmacological activity, it was pertinent to establish their actions at cannabinoid receptors CB_1 and CB_2. This was done using a high-throughput fluorescent-based plate reader membrane potential assay on AtT20 pituitary tumor cells stably transfected with either rat or human cDNA for CB_1 and human cDNA for CB_2. Relevant off target pathways, specifically the TRP channels, were also tested for activity by measuring the changes in intracellular calcium in a fluorescent-based plate reader assay on HEK293 cells transfected with human TRPA1 or human TRPV1. Approximately 60 SCs were tested and all showed activity at both CB_1 and CB_2 receptors with the majority having high efficacy and potency. Some compounds were up to 1,000 times more potent at CB_1 in comparison to Δ^9-THC, the main psychoactive ingredient in cannabis. Many also differed from Δ^9-THC by showing a selectivity for CB_2. The physiological implications of this outcome have yet to be determined but could play a role in toxicity. At the off target pathways only one SC showed partial agonist activity at TRPV1 but 28 showed agonist activity at TRPA1 ranging from partial to full agonists. As these ion channels have been implicated in the cardiovascular system, gastrointestinal system and CNS, their activation could be another mode of toxicity. Finally, a method was developed using reverse phase column chromatography and HPLC/MS/MS to measure endocannabinoid levels in cells lines after a drug stimulation. Preliminary data showed that SCs can affect the endocannabinoid system further proving their lack of specificity.

CHAPTER 1: INTRODUCTION

1 INTRODUCTION

1.1 HISTORY OF CANNABIS: PART ONE

Synthetic cannabinoid (SC) use and abuse has become an epidemic worldwide, especially in the past five years. Due to the rapidity of their structural evolution and the sheer number of different compounds in the market, little research has been able to be conducted regarding their pharmacology and toxicity. Much of what is known about the consumption of these compounds in humans has been taken from blogs, firsthand accounts from users and emergency room records. Therefore, to better understand how these drugs have come to infiltrate our society, an outline will be presented on the history of Δ^9-THC, the main psychoactive ingredient in the plant *Cannabis sativa*.

1.1.1 Cannabis sativa

Cannabis sativa, most commonly referred to today as marijuana or hashish, has had many uses throughout history; hemp was used for textile purposes, the plant itself was burned for religious incense, and extracts and tinctures of both the seeds and leaves were used in the treatment of a number of ailments (R. Pertwee, 2014; Russo, 2007). Its origins lie in Central Asia but spread to India, Western Asia, Egypt, and eventually Europe. It did not make its way into North America until the presence of the slave trade in the sixteen hundreds (Lee, 2012; Russo, 2007). Since written documentation appeared many years after what is assumed to be the beginning of its cultivation, it hard to pinpoint the exact location and time of its initial use by humans (Ben Amar, 2006). Some experts speculate cannabis extract was used for its medicinal purposes as far back as 5000 years ago (R. Pertwee, 2014) whereas the physical evidence of hemp dates back around 12,000 years ago (Russo, 2007).

Cannabis has been referred to by many different names depnding on the period and the culture; Egyptian: shemshemet, Chinese: ma, Sanskrit: bhang, Persian: Shadanaj, Hebrew: kaneh bosem and Greek: cannabis (Russo, 2007). Only some historical instances have actual physical DNA evidence to support that the plant described in ancient texts was in fact cannabis. Other instances deduced the plant in question was cannabis by its application and side effects (Russo, 2007). The following information will be presented assuming all experts were correct in their translation and identification of the plant.

1.1.2 **Medicinal uses of Cannabis: Past**

The medicinal purposes of cannabis are highly varied. Throughout ancient history and modern medicine cannabis has had antibacterial, antibiotic, anti-inflammatory, anti-parasitic, antitumor, insecticidal, anti-helminthic, antitussive and expectorant, vermicidal, antispasmodic and analgesic properties attributed to it; as well as being suggested as a digestive aid, appetite stimulant, diuretic, and an aphrodisiac (Russo, 2007; Zuardi, 2006).

The oldest complete medical papyri with mention of medicinal cannabis was written in Egypt in 1500 BC (Russo, 2007). Within this text, cannabis was cited as being inserted into the vagina to cool the uterus and also caused vaginal contraction (R. Pertwee, 2014). Emulsions made from cannabis seed oil and water were also useful in relieving pain associated with prolapsed uterus, inflammation of mucous membranes and symptoms of gonorrhoea (Dawson, 1934; Russo, 2007). This obstetric use of cannabis was also seen in ancient Israel. An archaeological dig uncovered the skeletal remains of a young woman with a partially born fetus within her pelvis. Upon further analysis, traces of Δ^8-THC was found in her abdomen assuming this meant cannabis was used to aid in the failed childbirth (Zlas et al., 1993). The Assyrians also documented its use for "female ailment" (assumed menstrual pain); many centuries later the same prescription was given to Queen Victoria for

her dysmenorrhea (Ben Amar, 2006). In the 19th century, cannabis continued to be used as a vaginal suppository to treat gynecological disorders, migraine and to prevent miscarriage (Russo, 2007).

The route of administration in most of these remedies was emulsions or inhalation, but cannabis was also used by both the Egyptians and Assyrians as a topical remedy for external conditions. It was ground up into honey and used in a poultice for infected toenails. Hemp fabric was also used to treat anal fissures (Russo, 2007). Its application to treat skin ailments ranged from bruising and inflammation to the treatment of parasitic worms (both internal and external) (Zuardi, 2006). It was even applied to stimulate hair growth (Zuardi, 2006). Cannabis tea, boiling the plant leaves in water, was also a direct route of administration for ailments, most often headache. Teas and inhalation were the two most popular forms of administration for ailments of the mind: anxiety, depression, mania and hysteria. The second century "Shen Nung Pen Tshao Ching," a transcribed version of Emperor Shen-Nung's rulings, stated that it would "even a man's moods" and said that "cannabis will keep you strong, fat and never senile"(Russo, 2007). This hints at potential neuroprotective properties and its utilization in the treatment of memory loss and dementia. In 2nd century China, cannabis, when mixed with wine, created a strong enough analgesia to be used as a surgical anesthetic (Russo, 2007).

Though the ancient texts mainly discuss cannabis in terms of its medicinal applications, the psychoactive properties and recreational use were described in China as early as 2737 BC (Li, 1973). In 1563, a man linked with Portugese royalty was quoted saying, "those of my servants who took it unknown to me said that it made them so as to not feel work, to be very happy, and to have a craving for food" (Russo, 2007). The consumption of the plant for one's pleasure would eventually lead to the claims that it

caused insanity, moral and intellectual deterioration and violence, resulting in a need for regulation (Ben Amar, 2006).

1.1.3 **ine or Drug: Early Legislation of Cannabis**

During the evolution of westernized medicine, three main psychoactive plants had the spotlight for their contribution in the health field: opium poppy (*Papaverus somniferum),* coca bush *(Erythroxylum coca),* and cannabis. As chemistry advanced, morphine, codeine, noscapine, papaverine and thebaine were separated from the opium poppy; cocaine was isolated from the coca plant and their derivatives were able to be identified and studied which solidified their place within the medical community (Musto, 1987). Cannabis constituents are unstable and many are nearly identical structurally making analytical separation and identification difficult. The tools needed for this level of analytical analysis had yet to be developed leaving the active ingredients of cannabis highly elusive (Di Marzo, 2004; R. Pertwee, 2014). Therefore, cannabis was suspended in a grey area between a recreational drug and a medicine. This ultimately dictated its legality with repercussions still felt to the present day.

Although cannabis use for medicinal purposes has been documented throughout history, it was not until 1839 that William O'Shaughnessy introduced cannabis back into western medicine, using it to treat rheumatism, cholera, tetanus and convulsions. Being the first to publish cannabis's value in a medical journal, he legitimized it uses in the medical profession (Backes & Weil, 2014). It became the equivalent of an over the counter medication, sold in pharmacies across the western countries (Ben Amar, 2006). A seven member team commissioned by the House of Commons of the United Kingdom to study the effects of cannabis use in Bengal, India, known as the Indian Hemp Drugs Commission (IDHC) of 1893-1894, established the first legislation of cannabis. They concluded

"moderate use of cannabis drugs has no appreciable physical effects on the body, no harmful effect on the brain (except possibly for those individuals predisposed to act abnormally) and no adverse influence on morality" (Mills, 2003; R. Pertwee, 2014). Their suggestion for government regulation was to implement a "system of taxation, control and restriction", fearing the prohibition of its sale and use would exacerbate the problem enticing smuggling or the use of more harmful substances (Mills, 2003; R. Pertwee, 2014).

At the Second Opium Conference, the "12 Powers" (Germany, United States, China, France, Great Britian, Italy, Japan, the Netherlands, Persia, Portugal, Russia and Siam) first discussed the control of cannabis stating that it had the same level of danger as opium. The outcome was limiting cannbis use for medicinal and scientific purposes only, placing it for the first time under international control (Law, 1913). In 1937, due to the combination of this ruling and an increase in the recreational use of cannabis, the United States followed closely behind by instituting the *Marihuana Tax Act.* This act was passed on the basis that the Second Opium Conference deemed cannabis a drug and not a medicine. The tax detrimentally affected the medical profession as the tax was imposed on the prescribing, stocking, sale and manufacturing of cannabis (Mikuriya, 1969). This, in conjunction with the increased use of opiates in medicine, resulted in a decline in medicinal cannabis use. In 1954, the World Health Organization (WHO) reported that cannabis had become medically obsolete and it was completely removed from all United States pharmacies (Ben Amar, 2006; R. Pertwee, 2014).

The United Nations Single Convention on Narcotic Drugs was the first to establish "scheduling" restrictions in 1961. The focus of the convention was to develop legislation that would limit drug possession and trafficking, which was done by limiting use of Scheduled substances to only medicinal and/or scientific purposes. They designed a scheduling system that organized psychoactive substances into different classes (Schedule I-

IV) depending upon their therapeutic value, their potential for abuse, and danger to health (Bewley-Taylor & Jelsma, 2011; R. Pertwee, 2014). All substances that may cause dependence or risk of abuse were limited to only medical and scientific purposes under Schedule I. Schedule II was similar to but less restrictive than Schedule I allowing for leniency in trading. Schedule III was least restrictive meant for preparations of substances that lacked ill effects and therefore could be readily traded. Schedule IV was for drugs that were perceived as being most dangerous to health and with the least recognized medicinal value. All drugs that were placed in Schedule IV were also placed in Schedule I to ensure the highest level of control possible. Cannabis resin was placed Schedules I and IV and therefore under the most regulation. Cannabis tinctures and extracts, on the other hand, were only placed in Schedule I, meaning they were only legal to use for scientific or medicinal purposes (Bewley-Taylor & Jelsma, 2011). Since the WHO declared cannabis medically obsolete in 1954, this meant all forms of cannabis were essentially prohibited (R. Pertwee, 2014). The signing of this treaty meant from that point forward the use of cannabis was deemed illegal worldwide (R. Pertwee, 2014).

1.2 THE MOLECULAR IDENTITY OF CANNABINOIDS AND THEIR RECEPTORS

Cannabinoids were originally defined as a "group of oxygen containing C_{21} aromatic hydrocarbon compounds typical of and present in *cannabis sativa*" (R. Mechoulam & Gaoni, 1967). This definition was then broadened to include their carboxylic acids, analogues and transformation products and now further includes their "synthetic analogues, endogenous cannabinoids and their congeners" (Di Marzo, 2004).

1.2.1 Discovery of Δ^9-THC

The first two cannabinoids isolated, cannabinol and cannabidiol (CBD), were both mistaken as the active component in cannabis until the isolation of tetrahydrocannabinol (THC) in 1942 (Di Marzo, 2004). The synthetic version of the THC congener $\Delta^{6a,10a}$-THC was produced but was not potent enough to be the main psychoactive component which indicated that the true psychoactive component must be chemically related. It was not until 1963-1964 that the correct structures for CBD and Δ^9- tetrahydrocannabinol (Δ^9- THC) were identified (Di Marzo, 2004; Gaoni & Mechoulam, 1964).
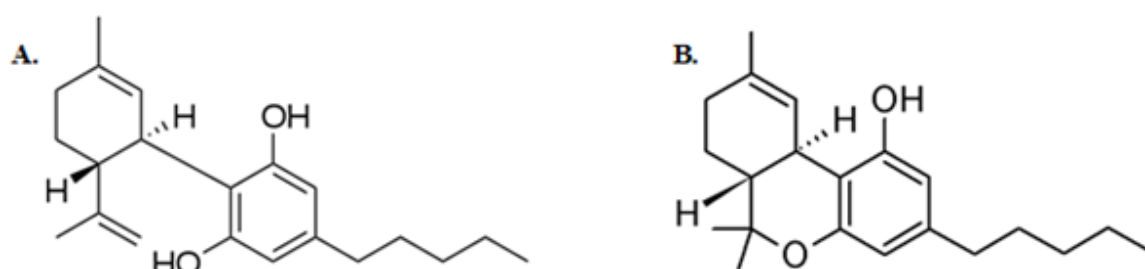
Figure 1: The chemical structures of two phytocannabinoids found in *Cannabis Sativa*. This figure shows the verified chemical structures for phytocannabinoids A) CBD and B) Δ^9-THC that have been isolated from *Cannabis sativa*. Structures were made using ChemDraw Professional 15.

This discovery, in conjunction with the increased prevalence of recreational cannabis use in Western countries, peaked interest in cannabinoid research leading to an increase in studies on its psychoactive properties (Roger G. Pertwee, 2006). Shortly after the confirmation of the true structures, synthetic versions of these compounds and novel structural analogues were synthesized. After the identification of Δ^9-THC as the main psychoactive constituent of cannabis using animal models, a study was done that administered synthetic Δ^9-THC and CBD intravenously to humans who used cannabis

chronically. The study found Δ^9-THC produced similar effects to that of cannabis with high potency whereas CBD had no psychoactive effects Raphael Mechoulam, Hanus, Pertwee, and Howlett (2014); (Perez-Reyes, Timmons, Davis, & Wall, 1973).

In 1974, the pharmaceutical company Pfizer launched a medicinal chemistry campaign to try and utilize cannabinoids to create nondependence producing analgesics. Instead of investigating the standard cannabinoid structural analogues, they developed a pharmacophore model. This means they derived structures from common molecular features of the drugs but not necessarily the whole chemical scaffold. The outcome was that Pfizer synthesised a new class of cannabinoids called "nonclassical" cannabinoids, most famously CP 55,940, CP 47,497, and CP 55,240 (R. Pertwee, 2014; R. S. Wilson, May, Martin, & Dewey, 1976). A radioligand binding assay using [H^3]CP 55,940 would eventually be used in the discovery of the first cannabinoid receptor.

1.2.2 **G-Protein Coupled Receptors**

The development of the radioligand binding assay advanced the exploration of molecule characterization, which made the study of interactions with G-protein coupled receptors (GPCRs) possible (Hill, 2006). GPCRs are a diverse family of cell surface receptors (around 800 human GPCR genes have been found) that are characterized by their common structure of seven transmembrane helices (Hill, 2006). They are commonly associated with G protein complexes - heterotrimers made up of alpha (α), beta (β), and gamma (γ) subunits, the latter two forming the beta-gamma complex (Hurowitz et al., 2000). In the presence of a ligand or through a spontaneous rearrangement (constitutive activity), the receptor will undergo a conformational change, to an active state. The active conformation catalyzes the release of a guanosine diphosphate (GDP) bound to the Gα

subunit. Guanosine triphosphate (GTP) then binds to the Gα subunit, resulting in a dissociation of the G protein from both the receptor and the Gα from the Gβγ subunit (Kukkonen, 2004). The dissociated subunits are released intracellularly to further signal transduction by interactions with downstream effectors depending on which type of Gα subunit (Table 1) was activated (Digby, Lober, Sethi, & Lambert, 2006). Gα subunits regulate adenylate cyclase (AC) activity, either increasing or decreasing depending upon the specific subunit, which in turn regulates the formation of cyclic adenosine monophosphate (cAMP) (Mackie, Lai, Westenbroek, & Mitchell, 1995). The βγ complex of the $Gα_{i/o}$ or $Gα_z$ proteins can activate G-protein gated inwardly rectifying potassium (GIRK) channels; close L-, N-, and P/Q type calcium channels; and activate mitogen-activated protein kinase (MAP kinase) (Mackie et al., 1995). Broad scope outcomes of GPCR signal transduction can range from rapid neuronal signalling to the regulation of synaptic plasticity, hormone release, chemotaxis and cell motility (Kukkonen, 2004).

Table 1: The four G-protein families and their interaction with the main cannabinoid receptors. This table shows the four G-protein families separated into their specific G-proteins and corresponding Gα subunits. Major signal transduction pathways (not comprehensive) are represented and their interactions with cannabinoid receptors are described as determined by a literature search (Kostenis, Waelbroeck, & Milligan, 2005).

G-Protein Family	G-Protein	Major Signal Transduction Pathways	Gα Subunit	Cannabinoid Receptor 1	Cannabinoid Receptor 2
G_i	G_i	Inhibition of AC, closes Ca^{2+} channels, opens GIRK channels (via β/γ subunits)	$\alpha_{i(1-3)}$	Yes[3]	Yes[3]
	G_o		α_o	Yes[3]	Yes[3]
	G_t	Activation of phosphodiesterase 6	α_t	N.D.	N.D.
	G_{gust}	Activation of phosphodiesterase 6	α_{gust}	N.D.	N.D.
	G_z	Inhibition of AC	α_z	Yes[4]	N.D.
G_s	G_s	Stimulation of AC, closes Ca^{2+} channels	α_s	Yes[3]	Yes[3]
	G_{olf}		α_{olf}	Potentially[7]	N.D.
$G_{q/11}$	$G_{q/11}$	Stimulation of phospholipase Cβ	α_q	Yes[8,9]	Yes[8]
			α_{11}	Yes[8,9]	Yes[8]
			α_{14}	Yes[2]	DNC[2]
			α_{15}	Yes[2]	DNC[2]
			α_{16}	Yes[2]	DNC[1]
$G_{12/13}$	$G_{12/13}$	Stimulation of the low-molecular-weight G-protein Rho and its downstream targets	α_{12}	Yes[5]	Yes[6]
			α_{13}	Yes[5]	Yes[6]

DNC = does not couple   N.D. = Not Determined from literature review
[1](New & Wong, 2003)   [2](B. Y. Ho, Uezono, Takada, Takase, & Izumi, 1999)
[3](A. C. Howlett, 2005)

[4](Garzón, de la Torre-Madrid, Rodríguez-Muñoz, Vicente-Sánchez, & Sánchez-Blázquez, 2009)
[5](Dalton, Peterson, & Howlett, 2013)   [6](Irving, 2011)
[7](Corbille et al., 2007)   [8](L. De Petrocellis et al., 2007)
[9](Lauckner, Hille, & Mackie, 2005)

It was discovered that cannabinoids inhibit Gs-stimulated adenylyl cyclase, a response sensitive to the pretreatment of pertussis toxin (PTX) a $G_{i/o}$ inhibitor, solidifying that the mechanism of action was G protein-coupled (A. C. Howlett, 1984, 1985; A. C. Howlett & Fleming, 1984). Using radiolabelled [H^3]CP 55,940 it was shown that the ligand was competitively displaced by cannabinoid agonists with a similar rank order of potency to agonist inhibition of AC and antinociception. These findings met the criteria for the presence of a stereoselective, high-affinity cannabinoid specific receptor, later identified to be cannabinoid receptor 1 (CB_1) (Raphael Mechoulam et al., 2014).

1.2.3 **Cannabinoid Receptor 1 (CB_1)**

The CB_1 receptor was first cloned from the rat cDNA library (Matsuda, Lolait, Brownstein, Young, & Bonner, 1990). As a GPCR, CB_1 signal transduction acts primarily through the $G_{i/o}$ pathway upon stimulation. This results in the activation of GIRK channels causing in an outflux of potassium into the intermembrane space. Not limited to the $G_{i/o}$ pathway, CB_1 has also been known for its promiscuity. It couples to G_s (activation of AC) and G_q (activation of phospholipase C to increase intracellular calcium) as best depicted in Figure 2 (Basavarajappa, Yalamanchili, Cooper, & Hungund, 2008; Glass, Faull, & Dragunow, 1997; Turu & Hunyady, 2010).
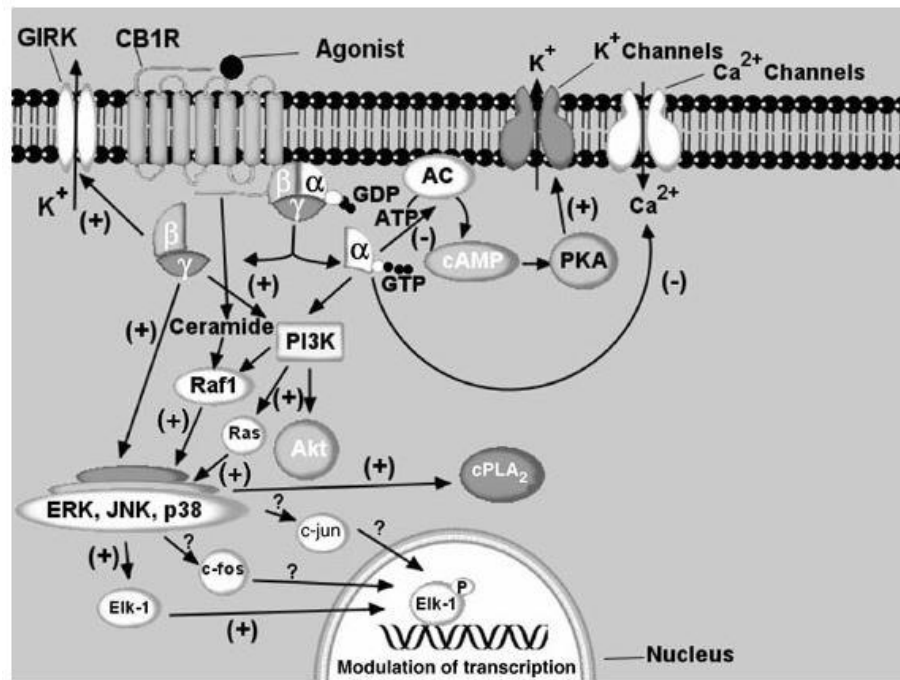
Figure 2: CB₁ signalling transduction pathways. As published by Basavarajappa et al. (Basavarajappa et al., 2008), this figure depicts recognized signalling transduction pathways of CB₁ receptor activation through G proteins and their subsequent effectors.

Primarily found throughout the central nervous system, CB₁ receptors are one of the most abundant GPCRs in the brain and their distributuion is highly heterogeneous. They show the highest density in the allocortex, substantia nigra, globus pallidus and cerebellum, and in regions of the association cortex (Glass et al., 1997; Allyn C. Howlett et al., 2004). More generally, CB₁ has high densities in areas associated with movement, high cognitive function and motor and sensory functions of the autonomic nervous system (Glass et al., 1997). Although the highest density of CB₁ receptors are in the brain, CB₁ has been indentified in the peripheral nervous system located with high densities found in the gut nervous system well as sensory, postganglionic and parasympathetic neurons (Calignano et al., 2000; Sibaev et al., 2009; Ständer, Schmelz, Metze, Luger, & Rukwied, 2005). On a cellular level, CB₁ receptors are found predominantly at central and peripheral presynaptic

axon terminals where they mediate inhibition of glutamatergic, GABA-ergic, cholinergic and noradrenergic neurotransmission (Freund, Katona, & Piomelli, 2003). CB$_1$ receptor activation decreases GABA-ergic inhibition and inhibits glutamate release which both increase the neuronal firing of the ventral tegmental area-nucleus accumbens (VTA-NAc) on dopamine (DA) neurons resulting in the release of dopamine from the NAc (Oleson & Cheer, 2012). This pathway is known as the mesolimbic reward pathway which plays a role in drug addiction, depression and schizophrenia (Gerdeman, Partridge, Lupica, & Lovinger, 2003). CB$_1$ receptor expression has also been associated with areas of the brain responsible for mood, autonomic function, sensation, central and peripheral regulation of food intake, fat accumulation, lipid and glucose metabolism and reward circuitry (Svizenska, Dubovy, & Sulcova, 2008).

1.2.4 Cannabinoid Receptor 2 (CB$_2$)

Through sequence homologuey, the second cannabinoid receptor (CB$_2$) was discovered in a human promyelocytic cDNA library and cloned in 1993 (Munro, Thomas, & Abu-Shaar, 1993). CB$_2$ receptors are located primarily in immune cells with high expression in leukocytes, monocyte/macrophages, NK cells, neutrophils, and B and T lymphocytes mainly of the spleen, tonsils and thymus (Roger G. Pertwee, 2006; Sipe, Arbour, Gerber, & Beutler, 2005). Although they are most known for their location in the periphery, it has been suggested in recent literature that they may also be located in the CNS within microglial cells and cerebellar neurons (Svizenska et al., 2008). Similar to CB$_1$, CB$_2$ receptors primarily signal through the G$_{i/o}$ pathway. This can result in the stimulation of GIRK channel activation and MAP kinase cascades while negatively coupling to AC and cAMP pathways as depicted in Figure 3 (Dhopeshwarkar & Mackie, 2014; Fernandez-Ruiz et al.,

2007; Svizenska et al., 2008). The inhibition of AC that occurs upon activation of the CB_2 receptor in B and T-cells within the immune system results in immune suppression by preventing antibody formation (Condie, Herring, Koh, Lee, & Kaminski, 1996).

Other than immune suppression, the main functions of CB_2 receptor activation are modulatory functions such T and B cell regulation, induction of apoptosis and induction of cell migration (Basu, Ray, & Dittel, 2011). The modulation of such immune functions has implicated the CB_2 receptor as a therapeutic target for many disease states. The activation of CB_2 receptors revealed that changes in cAMP levels resulted in the inhibition of T cell receptor signalling. This has implications in the treatment of neuropathic pain and inflammation (Cheng & Hitchcock, 2007). CB_2 activation in glioma and astrocytoma cells has been shown to cause apoptosis in tumor cells through the synthesis of ceramide, a sphingolipid secondary messenger. Manipulation of this system been implicated in increasing the effectiveness of some cancer treatments(Fernandez-Ruiz et al., 2007; Kolesnick, 2002). An upregulation of the receptor in reactive microglial cells has been thought to control the production of neurotoxic factors such as nitric oxide, cytokines, and reactive oxygen species could which could have therapeutic potential in the prevention of neurodegenerative diseases (Fernandez-Ruiz et al., 2007). It is thought that when Δ^9-THC is introduced into the system, there is a CB_2 mediated increase in the expression of Th2-type cytokines and a decrease in Th1-type immune stimulatory cytokines, resulting in an inhibited antitumor immunity which has therapuetic potential in the treatment of cancer and AIDS (A. C. Howlett, 2002).
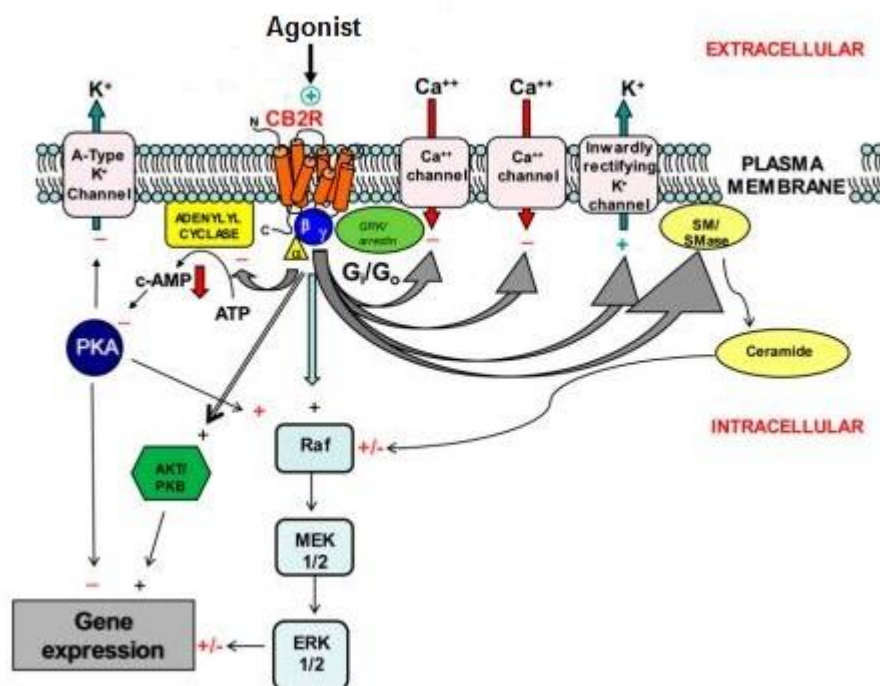
Figure 3: CB₂ signalling transduction pathways. Adapted from the publication by Dhopeshwarkar and Mackie, this figure depicts recognized signalling transduction pathways of CB_2 receptor activation through the $G\alpha_{i/o}$ mediated pathway and subsequent effectors.(Dhopeshwarkar & Mackie, 2014)

1.2.5 **Putative Cannabinoid Receptors**

Although only CB_1 and CB_2 receptors will be investigated in this thesis, it should be noted and will be briefly described that three orphan GPCRs have been implicated as potential non-CB_1/CB_2 cannabinoid receptors: GPR55, GPR119 and GPR18. The presence of cannabinoid like activity in cannabinoid receptor knockout mice stimulated the search for additional receptor targets (A. J. Brown, 2007). Their putative cannabinoid receptor status was determined by all three having agonist activity with exogenous and endogenous cannabinoids: GPR55 shown to be activated by Δ^9-THC, CP 55,940, AEA and virodhamine (Ryberg et al., 2007); GPR119, activated by endogenous ligands such oleoyl ethanolamide (OEA), an analogue of anandamide (Overton et al., 2006) ; and GPR18, N-

arachidonoyl Glycine (NAGly), an AEA metabolite (McHugh et al., 2010). GPR55 signaling has been thought to be involved in gastrointestional and bone function (Moreno et al., 2014; Staton et al., 2008)as well as playing a role in inflammation and neuropathic pain (Whyte et al., 2009). For further review on GPR55 see (Sharir & Abood, 2010) or (A. J. Brown, 2007). GPR119 has been localized in the pancreas and gastrointestinal tract. Although its physiological role has yet to be fully elucidated, it has been implicated in the regulation of blood glucose levels. For futher review see (Shah, 2009) or (A. J. Brown, 2007). Finally, GPR18 has been found to regulate the initiation of the migration of microglial cells following CNS injury or inflammation. For further review see (McHugh et al., 2010).

1.2.6 Endocannabinoids

Endogenous agonists had been found for other G protein coupled receptors, which inspired the search for an endogenous cannabinoid ligand (Raphael Mechoulam et al., 2014). In 1992, Devane et al. discovered N-arachidonoyl ethanolamide, most famously known as anandamide (AEA), as the first endogenous ligand of CB_1 in the porcine brain (Devane et al., 1992). Anandamide, which is a derivative of arachidonic acid, competitively inhibited $[^3H]$HU-243 binding to CB_1 on the synaptosomal membrane to an equivalent degree as what was seen with Δ^9-THC in the same experiment (Devane et al., 1992; Smith et al., 1994). AEA also displayed cannabimimetic activity by inhibiting the electrically stimulated twitch response in mouse vas deferens in a dose-dependent manner (Devane et al., 1992). After the discovery of CB_2, there was search for a peripheral endogenous agonist, resulting in the discovery of 2-arachidonoyl glycerol (2-AG) found in the canine gut. Although the motivation for its discovery was for it to be the CB_2 receptor agonist, 2-AG

actually binds to both CB_1 and CB_2 with potencies similar to Δ^9-THC and at higher potencies and efficacies than that of AEA at both receptors (Raphael Mechoulam et al., 2014).

Both AEA and 2-AG are lipophilic neurotransmitters that are synthesized on demand usually in the response to an increase in intracellular calcium related to a post-synaptic event (Raphael Mechoulam et al., 2014). Endocannabinoids act as retrograde messengers that activate presynaptic CB_1 receptors upon their release from GABAergic or glutamatergic synapses. Therefore, their role is to regulate the release of both excitatory and inhibitory neurotransmitters in the CNS. An example, AEA is released upon the activation of the dopamine 2 (D_2) receptor which acts as a retrograde messenger at presynaptic CB_1 which in necessary to induce long-term depression, an effect which produces withdrawal like symptoms seen in drug addiction (Wenger, Moldrich, & Furst, 2003). The effects associated with their release and subsequent receptor activation come on quickly but have a short duration. This is thought to be due to their rapid uptake into neurons from the intracellular space by ways of diffusion or potentially membrane-associated carriers followed by enzymatic degradation: fatty acid amide hydrolase (FAAH) for AEA and MAG lipase for 2-AG (Svizenska et al., 2008). The speed with which AEA is metabolised is tissue dependent having faster metabolism in the brain (<10 mins) and slower breakdown in the plasma ($\leq$30 mins) and the adrenal glands (>30 minutes) (Willoughby, Moore, Martin, & Ellis, 1997).

Production of AEA was often accompanied by a higher concentrations of other N-acyl ethanolamides (NAEs): palmitoyl ethanolamide (PEA), stearoyl ethanolamide (SEA), oleoyl ethanolamide (OEA), and linolenoyl ethanolamide (LEA) (W. S. Ho, Barrett, & Randall, 2008; Rahman, Tsuboi, Uyama, & Ueda, 2014). Although the NAEs are structurally similar to AEA, NAEs are not agonists at the main cannabinoid receptors

(various can activate GPR55 and OEA is thought to be the GPR119 receptor agonist). They potentially play a role in the endocannabinoid system by enhancing the effect of AEA through increasing affinity for receptors and/or by inhibiting the expression of FAAH (W. S. Ho et al., 2008; Schmid, Wold, Krebsbach, Berdyshev, & Schmid, 2002). Alternatively, OEA is thought to reduce AEA degradation by substrate competition for FAAH (W. S. Ho et al., 2008). The presence of PEA, although it acts through different pathways, has similar anti-inflammatory, antinociceptive, neuroprotective and anti convulsant properties as demonstrated by activation of the cannabinoid system (Re, Barbero, Miolo, & Di Marzo, 2007). LEA has also been shown to produce anti-inflammatory effects (Ishida et al., 2013).

1.2.7 **TRP Channels: TRPV1 and TRPA1**

The transient receptor potential (TRP) family consists of 28 mammalian ion channels separated into 6 subfamilies: canonical (TRPC1-7), vanilloid (TRPV1- 6), melastatin (TRPM1-8), ankyrin (TRPA1), polycystin (TRPP1-3) and mucolipin (TRPML1-3) (K. W. Ho, Ward, & Calkins, 2012). They have a common structure of 6 transmembrane domains with a pore located between the fifth and sixth domain. From this position within the plasma membrane they can mediate the flux of cations (Ca^{2+} and Na^+) down their electrochemical gradients. The rise of intracellular calcium and sodium results in a depolarization of the cell (K. W. Ho et al., 2012; Ramsey, Delling, & Clapham, 2006). The modes of activation are highly varied and are completely dependent on specific cellular conditions but can be generalized into three categories: receptor activation, activation of phospholipase C (PLC) by G-proteins or tyrosine kinases; ligand activation, activation of the channel itself by small organic molecules, endogenous lipids, purine nucleotides and inorganic ions and reactive compounds; direct activation, response to mechanical stimuli,

temperature change, channel phosphorylation, or coupling to IP_3 receptors (Ramsey et al., 2006). As somatosensory nociceptors, TRP channels are involved in a number of different processes including pain, temperature sensation, taste, pressure and vision.

By investigating the mechanism of action of vasodilation induced by endogenous AEA, Zygmunt et al. found this was mediated through the activation of transient receptor potential vanilloid type 1 (TRPV1). AEA was originally reported functioning as a full agonist but with a relatively low binding affinity at TRPV1 (Zygmunt et al., 1999). Alternatively, in electrophysiology experiments ,which look directly at the interaction of a drug and its target, AEA has only been shown to be a partial agonist at both the mouse and human TRPV1 receptors with efficacies less than the high efficacy reference compound capsaicin (Jerman et al., 2000; Roberts, Christie, & Connor, 2002). AEA activity has also been shown to depend on receptor reserve, being a partial agonist at low reserves and a full agonist at high reserves (Ross, 2003). As a low efficacy agonist, it can produce a maximal response in a high receptor system making it appear as a full agonist. It should be noted that in assays done on cells not containing native receptor, the receptor of interest is overexpressed to test for activity. Overexpression can vary in the amount of receptor significantly between different cell types. If receptor expression is not tested for, efficacy and potency can vary sometimes up to 1000x which should be taken into account when comparing potencies and efficacies in the literature. CBD and Δ^9-THC were both found to activate transient receptor potential ankyrin 1 (TRPA1) with EC_{50} values in the low μM range, transient receptor potential vanilloid 2 (TRPV2) with EC_{50} values also in the low μM range. CBD was also found to activate TRPV1 with an EC_{50} of approximately 1 μM solidifying the link between the cannabinoid system that the TRP channels (L. De Petrocellis et al., 2011; L. De Petrocellis et al., 2008).

1.2.7.1 TRPV1

TRPV1, the most widely studied TRP channel, is most famously known for its activation by capsaicin, the active ingredient in chilli peppers. Most commonly found on the end of sensory neurons, TRPV1 and the vanilloid family are known for thermosensitivity, converting relative changes in temperature into significant changes in action potential frequency to mediate neuronal excitability and homeostatic events such as regulation of body temperature or blood osmolatlity (Sudbury & Bourque, 2013). TRPV1 knockout animals have shown deficits in inflammation and both thermo and osmoregulation (Sudbury & Bourque, 2013) proving TRPV1 is necessary for thermal hyperalgesia (Caterina, 2007).

Heat is only one of five modes of activation/regulation of TRPV1 including voltage, vanilloids and lipids, protons and cations and secondary messengers (Pingle, Matta, & Ahern, 2007). Except for vanilloids and lipids, which interact with intercellular regions of TRPV1 and vanilloid binding sites respectively, the other four modes can activate the receptor with and without the presence of such ligands. In the presence of ligands, changes within these modes act to sensitize the receptor and to enhance the response produced by the ligand (Pingle et al., 2007).

During pain caused by inflammation, inflammatory mediators, such as prostaglandins, bradykinin (BK), serotonin, lipoxygenase, and adenosine, act through secondary messengers to sensitize the TRPV1 receptor resulting in hyperalgesia, allodynia and tissue acidification. This acidification then potentiates further activation due to the extra extracellular protons (Pingle et al., 2007). These mediators and acidification contribute to the TRPV1 mediation of airway hypersensitivity commonly associated with asthma. A similar mediation of the contractibility of tissues is seen within the vascular system, depending on TRPV1 mediated neuropeptide release, a tissue-specific

vasodilatation or vasoconstriction will occur. TRPV1 mediated processes have also been implicated within the gastrointestinal tract, urinary tract, ear, food intake pathways, taste, skin and brain (Pingle et al., 2007).

1.2.7.2 TRPA1

Although TRPA1 is frequently coexpressed with TRPV1, the modes of activation for TRPA1 signalling significantly differ from TRPV1 and some modes have yet to be fully elucidated. Cold stimulus, mechanical displacement, exogenous pungent compounds/ irritants and BK have all been thought to either directly or indirectly activate TRPA1 (Garcia-Anoveros & Nagata, 2007). It has been reported that TRPA1 has an activation temperature near the noxious cold threshold (<17°C) but some have reported no activation with lower temperatures. This discrepancy has been thought to be due to nonspecific changes in intracellular calcium that could affect the ion channel gating (Hill, 2006). Mechanical force, by itself, has not been proven as an activation mode, but there are implications of its influence in regards to TRPA1 nonessential participation in hair cell mechanotransduction complexes. Hypersensitivity associated with mechanical stimuli in relation to TNBS-induced colitis also requires the coexpression of TRPV1 and TRPA1 providing further evidence that mechanical stimuli may play a role in TRPA1 activation (D. M. Bautista, Pellegrino, & Tsunozaki, 2013).

There are a wide variety of agonists, both plant-derived and synthetic compounds that activate TRPA1. Many of the agonists are considered pungent or irritants that cause neurogenic inflammation and pain. Icilin, the first compound found to activate TRPA1, has been found to produce a cold and prickling sensation that is not present upon activation by the other TRPA1 agonists: isothiocyanates (wasabi mustard oil, horseradish), cinnamaldehyde (cinnamon), allicin (garlic), acrolein (byproducts of tear gas), methyl salicylate (mouthwashes), gingerol (ginger), and eugenol (clove) (Garcia-

Anoveros & Nagata, 2007). Only a few agonists have similar structures (some share α,β unsaturated double bonds), therefore, it is thought that reactivity, such as electrophilic character, contributes more to agonist activity (Hinman, Chuang, Bautista, & Julius, 2006). It is thought that agonists form adducts that covalently modify specific cysteine residues located in the ankyrin repeat domains of the N-terminus as the N-terminal cysteine residues are required for activation (D. M. Bautista et al., 2013; Hinman et al., 2006). Non-covalent binding of fatty acids at TRPA1 has also been documented suggesting TRPA1 activity may act through more than one binding site (Redmond, Gu, Camo, McIntyre, & Connor, 2014). A common hydrophilicity and slow reaction time amongst agonists suggests that activation may rely directly or indirectly on the compound's ability to enter the lipid membrane. TRPA1 has also been known to be activated by secondary signalling pathways such BK activation of PLC through the Gq-coupled BK receptor. This suggests that other proalgesic and proinflammatory mediators that stimulate the PLC pathway may also effect TRPA1 (Garcia-Anoveros & Nagata, 2007). Other endogenous inflammatory agents, when released after tissue damage, can create metabolites that can directly interact with TRPA1, for example reactive oxygen species (ROS) can undergo lipid peroxidation to create 4-hydroynonenol (4-HNE), a TRPA1 agonist (D. M. Bautista et al., 2013)

TRPA1 is expressed in a subset of C-fiber afferents that have cell bodies in the vagus nerve, dorsal root ganglia (DRG) and trigeminal ganglia (TG) that innervate peripheral targets such as the skin, airways, bladder, GI tract and cardiovascluar system (D. M. Bautista et al., 2013; Redmond et al., 2014). The expression of TRPA1, and coexpression with TRPV1, in these areas and their involvement in inflammation and pain regulation have therefore made them major targets for therapeutics, and have helped to elucidate potential mechanisms of action for medicinal cannabis.

1.2.8 **Effect of cannabinoid activation by THC in humans**

With such a broad distribution of cannabinoid receptors throughout the body, the endocannabinoid system has been implicated in a myriad of physio and psychological processes such as cognition, memory, anxiety, control of appetite, emesis, motor behaviour, sensory, autonomic and neuroendocrine responses, male and female reproduction, hypotension and bradycardia, inhibition of cell growth, affect energy metabolism and modulate immune responses (Marzo, Bifulco, & Petrocellis, 2004; R. Pertwee, 2014). Therefore, the introduction of an exogenous cannabinoid agonist, such as Δ^9-THC, to the endocannabinoid system of the human body has physiological repercussions in a number of biological processes. Cannabinoid consumption has been linked with side effects such as: short-term memory deficits, cognitive impairments, changes in perception of time, mood alterations, enhanced body awareness, a reduced ability to focus attention, loss of coordination and sleepiness (Svizenska et al., 2008).

Within the central nervous system, exogenous cannabinoids, specifically Δ^9-THC, inhibit glutamatergic synaptic transmission. This mediates their rewarding effects for cannabinoid enhanced brain reward and reward-related behaviors within both the VTA and NAc. This occurs by enhancing VTA-NAc DA neuronal firing which is accompanied by DA neuronal burst firing that increases the release of axonal DA. This combination of neuronal firing and bursting is thought to then lead to the increase of NAc DA. Neuronal firing was also decreased upon the administration of a CB_1 antagonist, furthering evidence of endocannabinoid mediation. The increases in NAc DA brought on by Δ^9-THC are similar to that of other drugs of abuse as well as its increase in electrical reward stimulation and the decrease after withdrawal (R. Pertwee, 2014).

Δ^9-THC also displays effects on neuronal placisity (R. Pertwee, 2014). It has been shown that chronic use of Δ^9-THC alters both the structure and function of the

hippocampus (Scallet, 1991). Due to the high density of CB_1 in the hippocampus and prefrontal cortex, Δ^9-THC has a detrimental effect on memory, both episodic and working, by reducing neuronal activity and reducing blood flow to this area of the brain which may be a consquence of the former (Block et al., 2002; Hermann et al., 2007). Depending on the age of the user, this can lead to irreversible learning and neuropsychological deficits (Meier et al.).

Peripherally, Δ^9-THC consumption causes and increase in diastolic blood pressure in a dose dependent manner resulting in tachychardia. Chronic users who develop a tolerance to these effects can actually reverse this effect resulting in bradycardia. Dilation of blood vessels can occur at high doses causing orthostatic hypotension which can lead to dizziness, fainting or even heart attack (Mittleman, Lewis, Maclure, Sherwood, & Muller, 2001). Daily Δ^9-THC intake has also been shown to increase the risk of liver cirrhosis in patients with hepatitis C (Hézode et al., 2008).

1.3 HISTORY OF CANNABIS: PART TWO

1.3.1 Medical uses of Cannabis/Synthetic Δ^9-THC and Analogues

Research into the endocannabinoid system revived the interest in cannabis and related synthetic analogues, for their medicinal properties. Nabilone (Cesamet®), a synthetic analogue of Δ^9-THC, and dronabinol (Marinol®), synthetic THC, were the first synthetic cannabinoids to be clinically trialled (Raphael Mechoulam et al., 2014; R. Pertwee, 2014). Nabilone and dronabinol have been administered for their antiemetic properties in the treatment of nausea in chemotherapy patients. They were found to provide more relief than that of the other antiemetic drugs: prochlorperazine, metoclopramide, chlorpromazine,

domperidone, thiethylperazine and haloperidol (Ben Amar, 2006). In a clinical trial comparing orally delivered THC to smoked cannabis, only 25% of patients (n=20) found relief and the majority preferred the orally delivered method over inhalation. Due to negative psychoactive effects, cannabinoid treatment for antiemetic relief could not compete with the more recent efficacious 5-HT$_3$ receptor antagonists (Ben Amar, 2006).

Cannabinoids have also been used in clinical trials as an appetite stimulant, mainly for anorexics, HIV sufferers and terminal cancer patients. Earlier clinical trials only using dronabinol (Marinol®) at very low doses in advanced cancer patients found an increase in body weight of patients when the administration was combined with synthetically derived progesterone (oral megestrol). In a study treating HIV patients comparing higher doses of Marinol® and smoked cannabis, both showed statistically greater weight gain than placebo while not disrupting the protease inhibitors used in the HIV treatment (Ben Amar, 2006). Marinol® preparations have also provided benefits to patients in clinical trials pertaining to Tourette's syndrome, reducing the number of "ticks" while not altering their neuropsychological performance. Dose regulation issues have been documented with the use of Marinol® as discrepancies in peak plasma concentrations suggest variable pharmacokinetics. A new oral tablet of pure THC, Namisol®, has been developed to improve pharmacokinetics with a rapid onset reaching the maximal THC concentration in blood plasma 1.5-5.5 times faster than Cesamet®, Marinol® and Savitex® (Klumpers et al., 2012). Namisol® has completed phase II trials for the treatment of dementia and chronic abdominal pain duet to pancreatitis (https://www.clinicaltrials.gov/ct2/home).

GW pharmaceuticals combined THC and cannabidiol into a sublingual spray called Savitex®. Savitex® has been tested to treat the spasmodic side effects of multiple sclerosis and spinal cord injury. The studies concluded that cannabinoids produce a slight improvement in the spasticity of these patients as well as a slight improvement in motor

capacity and quality of life (Ben Amar, 2006). Savitex® has also been proven to treat allodynia associated with neuropathic pain improving the intensity of pain by at least 30% in 26% of the patients tested. Similarly to Savitex®, Marinol®, THC extracts, intravenous THC, and 3 synthetic analogues: CT-3 (oral), benzopyranoperidine (oral) and levonantradol (intramuscular); have all shown through clinical trials to be effective in the relief of various pain states: cancerous, neuropathic, postoperative and experimental pain (Ben Amar, 2006).

Despite numerous clinical trials finding positive outcomes of the use of cannabinoids in medicine, dronabinol is only registered in the United States and Germany and nabilone is registered in the US, Mexico, United Kingdom, Austria and Canada (Klumpers et al., 2012). Savitex® has the largest distribution being approved as a treatment for multiple sclerosis spasticity in 27 countries (http://www.gwpharm.com/FAQ.aspx). Further worldwide acceptance has been hindered by a number of negative side effects including: dizziness, drowsiness, hallucinations, dry mouth, euphoria, sleep disorders, disorientation, vertigo, hypotension and mood disorders (Ben Amar, 2006). Adverse side effects were reported in 91% of patients administered Savitex® for treatment of neuropathic pain. The most prevalent side effects presented in the central nervous system (paranoia and stress) and the gastrointestinal (nausea, vomiting diarrhoea and constipation) but most of the effects were considered mild (Nurmikko et al., 2007). Nevertheless, many patients find relief with cannabinoid products for various ailments, but with the limited ability and most times inability for patients to obtain these preparations for treatment has led to an exponential increase in the incidence of self-medication.

1.3.2 Self-Medication with Cannabis

Self-medication, at its most basic definition, is defined as "any use of non-prescribed drugs or alternative medicines to treat a diagnosed or undiagnosed condition". By this

definition, "medicine" can range from alcohol and cigarettes to dietary supplements and comfort food. Therefore, a drug is anything to alleviate the symptoms of the person's perceived ailment. Khantzian hypothesized there was another definition of self-medication, directing his focus at addiction and substance abuse. This definition states that a person will choose their drug of choice, often illicit drugs, subconsciously based upon the psychological need to achieve emotional stability (Khantzian, 1974). Essentially saying an attempt to "self-medicate" the underlying problem is what drives addiction. The differences between the two definitions highlights the true crux of legitimizing cannabis; the clinical use to alleviate symptoms versus self-medication which runs the potential to result in the abuse of the substance.

Self-experimentation dates all the way back to the 1830's when Aubert Roche first determined the potential benefit of medicinal cannabis for its neurotrophic effects in treating the plague (Russo, 2007). The adoption of the 1961 Single Convention of Narcotic Drugs ruling that cannabis and all of its products had a "high potential for abuse with no accepted medicinal value," made accessing cannabis and related cannabinoids difficult for scientific researchers to acquire let alone medical professionals with intent of prescribing (R. Pertwee, 2014). Despite being illegal, through means of self-experimentation, many people found cannabis to relieve a number of different ailments. This resulted in a push for the right to access cannabis for medicinal purposes in countries such as Canada, Finland, Germany and some states within the United States (Access, 2012). To date, only Canada (2001) and the Netherlands (2003) have government run programs controlling the quality and distribution of the supply of medicinal cannabis. Israel and the Czech Republic are modelling similar programs after these countries where others such as Finland, Germany and Italy are purchasing their medical cannabis from the companies run by the Dutch program (Hazekamp, Ware, Muller-Vahl, Abrams, & Grotenhermen, 2013). Difficulty in assuring

quality control, a lack of useful clinical trial data (dosage, preparation) and societal stigma have all contributed to the admonishment of legalizing cannabis and increased the prevalence of illegally obtained cannabis for self-use.

There are over 700 strains of herbal cannabis products available from legitimate and illegitimate retailers. Therefore, even within medically prescribed cannabis, without prudent quality control measures, it is hard to regulate consistent dosing regimens. The various plant compositions combined with multiple modes of administration (inhalation, vaporization, teas, edibles and extract tablets) has given self-medicators the advantage over prescribed patients. They are able to test by trial and error what strain of cannabis/method of consumption best alleviates their personal ailment as opposed to a "one size fits all" treatment. Many clinical trials were actually launched because of positive accounts of self-medication but have been inferior due to the limited sources of research-grade cannabis, usually too low of dosage to prevent overdosing and usually only oral preparations (Hazekamp et al., 2013; R. Pertwee, 2014).

The largest cross-sectional survey, conducted by the International Association of Cannabinoid Medicine (IACM), was completed to determine the preference of synthetic preparations of cannabis vs. herbal product in 953 patients. The patients involved were using cannabis, under the observation of a physician, to treat chronic pain (29%), anxiety (18.3%), loss of appetite or weight loss (10.7%), depression (5.2%), or insomnia or sleep disorder (5.1%). This study found that patients only preferred the oral preparation because of convenience (could take in a public place without judgment, etc.) but overall preferred the herbal preparations instead. This could be due to the beneficial effects of other phytocannabinoids such as CBD, tetrahydrocannabivarian (THCV) and tetrahydrocannabinolic acid (THCA) that are not in synthetic preparations (R. Pertwee, 2014). There were negative feelings toward the lack of convenient and reliable standardized

forms, so many preferred to grow their cannabis at home (Hazekamp et al., 2013). Home growing and self-medicating are more than just preference; many users could not afford cannabis otherwise with medical cannabis being almost double the price of quality cannabis on the black market. Spain and the Netherlands are the only two countries that cannabis, for certain ailments, can be claimed for insurance purposes.

Although there have been estimated around 177 million frequent cannabis users worldwide (last statistical analysis available from 2012 as documented by the United Nations Office on Drugs and Crime (UNODC), there has not been a study to determine what number of these users are recreational vs. medicinal. One Canadian study suggests that only 10% of the cannabis-using population is using it for medicinal purposes, leaving 90% of users seeking out cannabis use for recreational purposes with a growing prevalence of related substance abuse (Ogborne, Smart, Weber, & Birchmore-Timney, 2000). The UNODC report shows that cannabis use is still globally increasing from year to year which could be attributed to the decriminalization and legalization that has occurred in many countries (Crime, 2014).

1.3.3 Cannabis: A Drug of Abuse

Psychoactive drug consumption is well known throughout the existence of the human population, so, why has the consumption of mind altering substances stood the test of time? Some experts state that all human beings are wired to seek drugs because there is a biological need to alter our conscious state. From a statistical, clinical and socio-cultural standpoint, psychoactive drug use can be considered a "normal" behaviour (Nicholson, Duncan, & White, 2002). Cannabis use, especially in the age range of 16-24 year olds, has been shown to be a normative behaviour with over 50% of Europeans in this age range

having used cannabis for its desired effects of dreaminess, disinhibition and heightened awareness of sensation (R. Pertwee, 2014). In a survey ranking the desired effects of cannabis against other recreational compounds, it was ranked the highest in enjoyment and amongst the top drugs for relaxation, stress relief, sleep aid, mood and socializing.

David F. Duncan developed the "Duncan Model of Drug Dependence as Self Medication" on the basis of his experience with addicts and their behaviour. This model relies on the distinction between drug use and abuse (Duncan, 1974). Duncan defines drug use as the consumption of a drug enough to get desired effects but with minimal hazard to one's self. Drug abuse is therefore defined as the consumption of a drug to such extent that the effects put the individual in danger or prevents them from being capable of maintaining general life functioning (Nicholson et al., 2002). By this definition, most users of illegal drugs do not meet the criteria for dependence or substance abuse and are able to function within normal parameters with occasional drug use. Therefore, this model focuses on the minority of drug users who do experience the negative health consequences of illicit drugs developing dependency and substance abuse (Nicholson et al., 2002) where dependence is defined by the DSM-IV as developing tolerance as well as withdrawal to cannabis use (Coffey et al., 2002). This distinction is important, especially in terms of cannabis consumption because the majority of users can partake in its use without developing the negative side effects. But due to the minority still being about 10-20% of users, one cannot overlook cannabis as a drug of abuse.

The 2014 report from the UNODC states that 2/3 of reporting countries have stated cannabis as their number one drug of abuse (Crime, 2014). THC analysis that was performed on individuals with so-called cannabis seizures showed an increase in the level of THC from 8.7 percent in 2007 to 11.9 percent in 2011 (Crime, 2014). There is a positive correlation between the higher potency cannabis and the increase in hospitalizations and

rehab enrolment, but causal data has not yet been confirmed. The increase of hospitalization and dependence has been noted across the world of recreational cannabis users, one in nine will develop a clinical dependency that equates to around 16-17 million people worldwide (Crime, 2014). This in part is due to the fact many users have no serious side effects from cannabis, creating a positive reinforcement of its use. This tends to lead to more frequent use with daily users being most at risk for dependency. Unfortunately, there is no effective pharmacological treatment for cannabis dependency (R. Pertwee, 2014).

Cannabis dependency often goes hand in hand with more severe conditions such as psychosis, depression and anxiety and learning and memory impairment. The comorbidity of these events is often linked to the age of the user, being more detrimental to juvenile users. With psychosis, evidence continues to grow relating heavy cannabis use to earlier onset of psychosis though this relationship has yet to be proven as causative. Some argue, that juvenile users with a genetic predisposition for vulnerablity to mental illness usually present symptoms sooner if they smoke cannabis than non users but not that cannabis use causes the presentation of the illness (Lloyd, 1998). There is also evidence to link the endocannabinoid system with mood regulation where heavy cannabis use could disrupt this system. Depression and anxiety are linked to heavy cannabis use, only depression seems to be a short-term effect where anxiety increases by nearly double in long-term studies (Degenhardt et al., 2013). Looking back at Khantzian's definition of self-medication, it could be that people are drawn to using cannabis because they are predisposed to have issues with anxiety and depression (Khantzian, 1974). Finally, as previously discussed, the endocannabinoid system is detrimental to synaptic plasticity that is a necessity to long term memory. It has been proven that even acute cannabis use can cause cognitive impairment affecting both episodic and working memory. In animals, long term use can even change the shape of the hippocampus irreversibly altering its functioning (Scallet, 1991).

Cannabis consumption has also been linked to nonpsychological adverse side effects. Minor effects being eye reddening, dry mouth, constipation, vomiting, reduced attention, altered perception of time and tachycardia. The more detrimental effects being reduced sperm count, increased risk of cirrhosis, shorter duration of pregnancy with low birthweight, decreased immune function, heart attack and stroke (R. Pertwee, 2014). Due to the severity of the negatives versus the positives, cannabis use for recreational purposes is still tightly controlled.

1.3.4 **Legal Status Present Day: Decriminalization**

Although the Single Convention of 1961 made cannabis universally illegal, the language used when writing the treaty left many loopholes for debate. This "loophole language" is the basis for countries such as Canada to legalize their medical cannabis practices. Many countries have now started to lessen the penalty for possession of cannabis for personal consumption with few first-time offenders seeing jail time (R. Pertwee, 2014). This does not include people in possession of large amounts of cannabis with intent to sell, who are still highly prosecuted. This lessening of penalty is called "decriminalization." Within the United States four states have decriminalized cannabis possession laws, 4 have completely legalized cannabis for any purpose, 9 have legalized medicinal cannabis, and 10 have decriminalized possession and legalized medical cannabis.

The only three countries cannabis is completely legal are North Korea, the Netherlands and Uruguay, but all have limitations on where you can purchase and what quantity (R. Pertwee, 2014). Even though tolerance for cannabis use has increased worldwide in the past two decades, there are still many countries that have a no tolerance

policy. This eventually led to the emergence of "legal highs" and the introduction of synthetic cannabis to the international market.

1.4 THE RISE OF CANNABINOID DESIGNER DRUGS

Synthetic cannabinoids, more appropriately called cannabinoid designer drugs (CDDs), are defined by *The Handbook of Cannabis* as "clandestinely synthesized structures that function as agonists at the cannabinoid receptors and are used to produce marijuana-like intoxication" (R. Pertwee, 2014). This distinction is important because not all synthetic cannabinoids are being used as designer drugs, but they tend to be lumped together under the term SC. SCs were originally designed as therapeutic targets, but some have thence made it to the streets for intoxicating purposes, whereas the current cannabinoid designer drugs are being synthesized for the sole purpose of intoxication. Similarly, the drug of abuse monitoring system has placed them in the class of "new psychoactive substances (NPS)" when in reality the drugs are not new they are just being used in new ways (Gurney, Scott, Kacinko, Presley, & Logan, 2014).

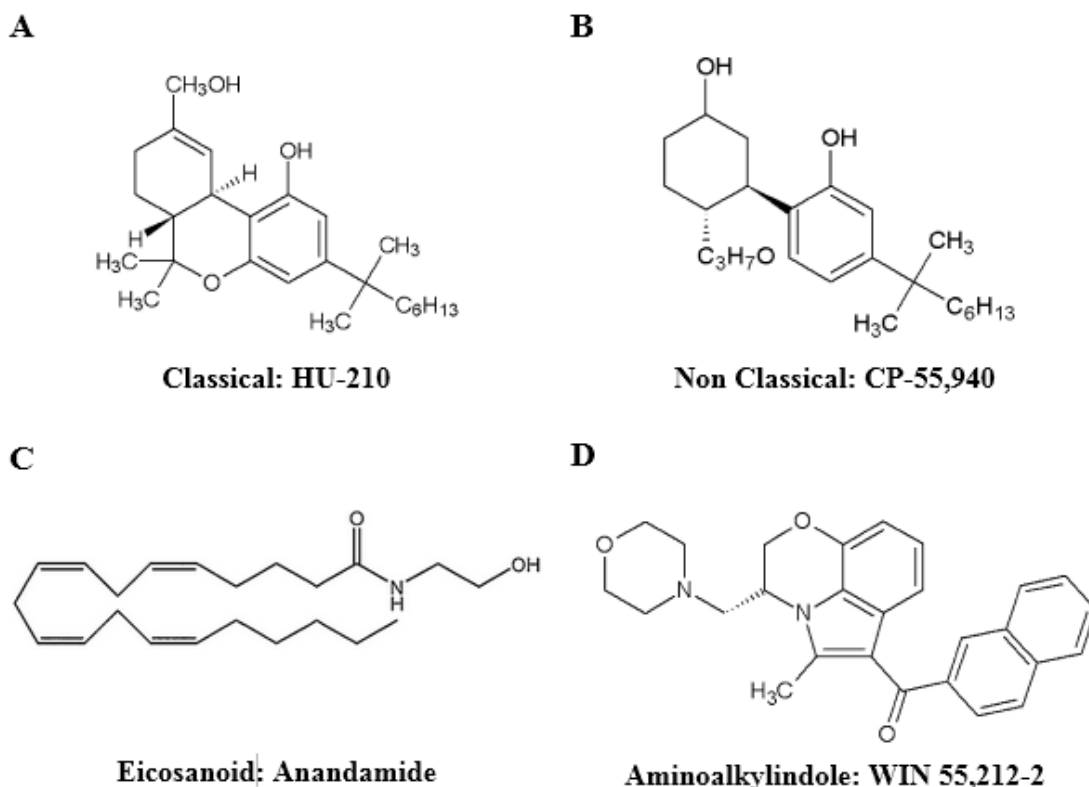### 1.4.1 Structural classes of Synthetic Cannabinoids

Synthetic cannabinoids originally were classified into four main structural groups (Figure 4): classical, nonclassical, eicosanoids, and aminoalkylindoles. Classical, defined by the dibenzopyran scaffold, includes Δ^9-THC, HU-210 and Nabilone. Non-classical, as invented by Pfizer, includes the CP family that have a cyclohexylphenol group lacking a pyran moiety in common. Used to describe the endocannabinoids AEA, 2-AG and their

analogues, eicosanoids are derived from a fatty acid attached to a long carbon chain. Finally, the aminoakylindoles, whose name is directly descriptive of its chemical scaffold, include most famously WIN 55,212-2 (WIN) and a series of compounds synthesized by John W. Huffman best known as the JWH family (Seely, Prather, James, & Moran, 2011).

Using the principles of rational drug design based on a model pharmacore of CB_1 receptor agonists, a number of clandestine laboratory chemists have driven the evolution of the structures, and are continuing to push the evolution further and further from the original four. The various degrees of evolution have made it difficult to divide the new structures into such rigid subclasses. Therefore, Figure 5 shows the six main structural scaffolds common between all SCs found in the market today. The common features between all groups are: a heterocyclic core being an indole or an indazole; a substituent at the 1-position ($-R^1$) which may be: an alkyl, alicyclic, or aromatic group; a functional group at the 3-position ($-R^2$) which may be acyl, carboxamide, or carboxylate, and which contains a substiuent that is: aromatic, alicyclic, amino acid or others. Many of the new structures have been derived from the aminoakylindole scaffold (Figure 5A) leading to the various akylindole carboxamides and carboxylates (Figure 5: B-C) which will be the primary backbone of compounds tested in the following chapters. Figure 5: D-F shows the completely novel indazole scaffold that was taken from a 2009 patent by Pfizer and modified (Buchler et al., 2011).

A

CH₃OH

Classical: HU-210

B

Non Classical: CP-55,940

C

Eicosanoid: Anandamide

D

Aminoalkylindole: WIN 55,212-2

Figure 4: Chemical Structures of the Four Main Cannabinoid Structural Groups. A.) Chemical structure of HU-210 as an example of the classical cannabinoid structure subtype identified by derivations of a dibenzopyran B.) Chemical structure of CP 55,940 representing the nonclassical cannabinoid structure subtype identified by a cyclohexylphenol group lacking a pyran. C.) Chemical structure of AEA as an example of the eicosanoid structure consisting of a fatty acid attached to a long carbon chain D.) Chemical structure of WIN as an example of the aminoalkylindole structure subtype. Chemical structures were drawn using Chemdraw Professional 15.
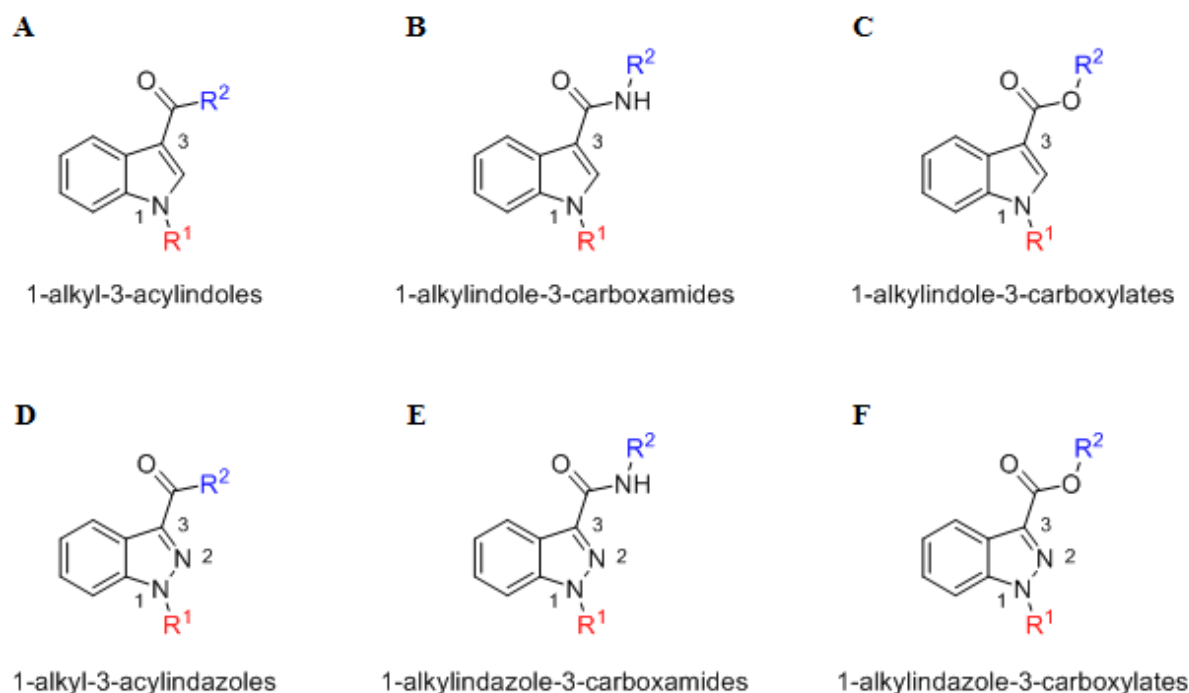
Figure 5: Chemical Structures of the Six Chemical Scaffolds from which SCs are Designed. This figure represents the six most common SC scaffolds. Each of them contain the following 1) one of two heterocyclic cores (indole or indazole) 2) a substituent at the 1-position (-R^1) which may be: alkyl (e.g. pentyl, 5-fluoropentyl, etc.); alicyclic (e.g. (cyclohexyl)methyl, etc.); aromatic (e.g. 4-fluorobenzyl) 3) a functional group at the 3-position (-R^2) which may be acyl, carboxamide, or carboxylate, and which contains a substituent that is: aromatic (e.g. naphthalene, phenyl, benzyl, quinolinyl, etc.); alicyclic (e.g. adamantane, etramethylcyclopropyl, etc.); amino acid (valinamide, tert-leucinamide, etc.) and others. Common examples: -R^1 = pentyl, 5-fluoropentyl, 4-fluorobenzyl, (cyclohexyl)methyl, etc.   -R^2 = 1-naphthyl, phenyl, benzyl, 1-adamantyl, 2,2,3,3-tetramethylcyclopropyl, 8-quinolinyl, etc. This figure was made by Sam Banister using CambridgeSoft ChemBioDraw Ultra version 12.0

1.4.2 Synthetic Cannabinoids as Therapeutic Agents

Many of the first generation synthetic cannabinoids were synthesized for their

potential therapeutic value, yet only a few made it to clinical testing. The nonclassical

cannabinoid, CP 50,556-1 (levonantradol), an analogue of Pfizer's CP-55,940, had

promising clinical trial results for its anti-emetic effect in chemotherapy patients. Due to adverse side effects, mainly strong psychoactive effects like hallucination or extreme paranoia, it was never approved by the FDA (Joss et al., 1982; Seely et al., 2011). The aminoakylindole, Pravadoline, was originally developed by Sterling Drug Company as an analgesic to replace nonsteroidal anti-inflammatory agents (Seely et al., 2011; Wiley et al., 1998). It was found to have little anti-inflammatory properties but did produce a CB_1 mediated antinociception in rats. WIN, a structural analogue to pravadoline, exhibited similar antinociceptive properties in mice and rats (Compton, Gold, Ward, Balster, & Martin, 1992; Haubrich et al., 1990) Finally, Dexanabinol, an analogue of HU-210 but with no psychotropic effects, was tested for its neuroprotective properties in brain trauma models resulting in no significant changes to brain trauma but confirmed to be safe (when administered up to 200 mg) for use in humans (Maas et al., 2006). Dexanabinol is also currently in Phase I clinical trial at University of California San Diego evaluating its penetration of the brain barrier with hopes for future trials in brain cancer treatment.

1.4.3 Emergence of "Spice"

In 2004, the product Spice began being sold in European markets. In the beginning, it was mainly sold online, most commonly under the names Spice Silver, Spice Gold and Spice Diamond. The manufacturer was linked back to a company out of Northern UK called "The Psyche Deli" (Schifano et al., 2009). Richard Creswell and Paul Galbraith were documented by Financial Times magazine as being the directors and only shareholders of the company. Their refusal to ship internationally contained the spread of the product to within Europe for a short time but eventually a similar product named K2 made its way to

the United States and Kronic to Australia and New Zealand. Upon the government's investigation into the safety of these drugs, the directors of "The Psyche Deli," which had made almost a 1 million pound profit within one year (2006-2007), sold their company to a company in the Netherlands. They chose the Netherlands due to the leniency of cannabinoid sales, and eventually moved there themselves (Jack, 2009).

So what is Spice? Spice is a product containing a synthetic cannabinoid enhanced plant matter that is packaged and sold as an herbal incense and labeled "not for human consumption". These products, whose popularity spread by word of mouth and drug user blogs, were producing similar highs to that of cannabis and were being smoked as a legal substitute. As their popularity increased, they began to emerge in head shops and gas stations. The packaging listed only natural ingredients of up to 14 different types of plant matter. Only 2 of the 14 types of plant matter listed have potential psychoactive effects, *Pedicularis densiflora* (a.k.a. Indian warrior) and *Leonotis leonurus* (aka Lion's ear, lion's tail, wild dagga) (Seely et al., 2011). The powerful high users were documenting upon consumption were more intense than what could be expected from these two plants. This led researchers to investigate these products in search of the real psychoactive ingredient/s. In 2008, Germany and Austria detected JWH-018 as the main active ingredient. This subsequently led to it being the first synthetic cannabinoid to be placed by the European Monitoring Center for Drug and Drug Abuse (EMCDDA) into their Early Warning System (EWS) (EMCDDA, 2009a). The synthetic cannabinoids were thought to be dissolved in a volatile liquid such as acetone or alcohol, then either soaked or sprayed onto the plant matter and evaporated; leaving the plant matter fully coated with the synthetic compound (Schneir, Cullen, & Ly, 2011). The packaging had no mention of the synthetic products let alone a concentration or dose to give the user some indication of the potency. Some packages were found to not even contain the synthetic compounds. The variance in

contents, labeling and packaging, creates one of the biggest, if not the biggest, issue when trying to manage and regulate these products.

At the beginning of 2009, CP 47,497 and three other CP analogues were detected in spice products. This led to Germany, Austria, France, Poland and Luxembourg using various versions of legislation to amend their drug laws to make JWH-018 and the CP analogues illegal (EMCDDA, 2009a). Ironically, the attempt to limit these compounds for the safety of its users only triggered manufacturers to produce a wide range of structurally diverse analogues. Attempts to avoid legislation led to compounds whose activity has been shown to be stronger and more dangerous. By the end of 2009, 27 new smoking blends came onto the market as an alternative to spice with the main active ingredient switching from JWH-018 to JWH-073. This trend is the essence of the entire synthetic cannabinoid pandemic currently being battled today.

1.4.4 Epidemiology

To date, there have been ten studies completed to determine the main demographic of SC users (Castaneto et al., 2014; Palamar & Acosta, 2015). Of the ten studies, two were worldwide surveys, and the rest were single country surveys. A trend developed across the surveys stating that the most common characteristics displayed by the average SC user were: an average age of 26 years (range usually 18-40), single, Caucasian (potentially skewed by countries that responded to the survey), male and with at least a high school education. Many of these users also stated that they were regular cannabis and alcohol users (usually concurrent use) (Vandrey, Dunn, Fry, & Girling, 2012; Winstock & Barratt, 2013). A field-based study including 1,740 adults was administered in New York City nightclubs in 2012 which found that 8.2% had used SCs in the past year and that of that portion 41.2%

were heterosexual men and 17.4% were lesbian or bisexual women (Castaneto et al., 2014; Kelly et al., 2013).

As the number of high school users increased from 2011 onward, the Monitoring the Future program put out a survey to 50,000 high school students across the US to gauge how many had used SC between 2011-2013. This survey found that in that time, cannabis use went up from 24.7% to 25.8% while the prevalence of SC use went down from 8% to 6.4%. 23.5% of high school seniors also had the perception that SC were less harmful than other drugs, including cannabis (O'Malley, Meich, Bachman, & Shulenberg, 2014). Though the prevalence of use seemed to decrease, a 2015 survey found that one in ten (n=11,863) high school students had tried SC in the past year (Palamar & Acosta, 2015). Cannabis use was the highest proponent of synthetic use but alcohol, cigarettes, number of nights spent going out for fun (4-7) and other illicit drug use highly increased the probability of use. This study did find that only 3% of users tried SCs six times or more showing that many people just experiment and do not seek continued use. Illicit drug use is the greatest factor that correlates with extended SC use. Interestingly, this study found that being religious seemed to be a protective property except the "legal" status of the SC drugs actually made religious students more likely to try these drugs rather than other drugs (Palamar & Acosta, 2015).

The "legal" status combined with the fact synthetic cannabinoids did not show up in a standard drug test saw increased use in military personnel, people on parole and athletes. The United States Army banned the use of SC in 2010 but in 2012, 1148 urine samples were obtained and tested specifically for SCs with 78% being found positive for their use. In another army study, 10,000 randomly selected urine samples that had tested negative for drugs were rescreened for SCs and 2.5% came back positive. SCs are now included in the routine army screening but upon looking at which compounds they screen for, granted the information was limited, seemed to be only a few of the first generation JWH and CP

compounds. The World Anti-Doping Agency (WADA) also placed SCs on the prohibited list and extended their drug test screening to include specific compounds in 2012 (Castaneto et al., 2014). Therefore, many of the newest SC compounds, whose metabolism pathways and metabolites have yet to be elucidated, will still produce a negative test result increasing their desirability for people undergoing drug testing.

1.4.5 Products Available on the Market

The EMCDDA listed 101 new psychoactive substances reported in 2014 and of these 30 were new SCs. This brings the total number of SCs monitored by the EWS to 134 compounds (as of the end of 2014). Though some surveys seem to convey that usage has gone down since 2012, the number of seizures still taking place has had a 200-fold increase from 2008-2013. In 2013, there were over 21,000 SC seizures (in the European market alone) totalling just under 1.6 tonnes of product seized. Roughly 40% of this total was seized in powder form whereas the rest was plant matter. 90% of the powder consisted of 10 compounds, and the other 10% was made up of 39 other compounds. The most abundant compounds seized were AM-2201, XLR-11, and 5F-AKB48 (EMCDDA, 2015). Figure 6 breaks down the 1.6 tonnes into the structural groups seized by percentage.
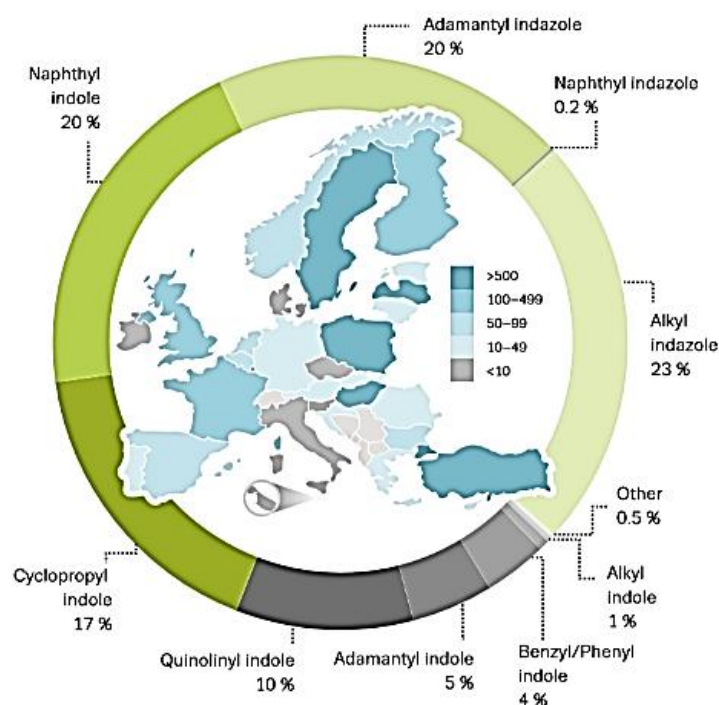
Figure 6: Quantity of SCs by structure type and by country seized in 2013. This figure, published in the EMCDDA 2015 update of the Early Warning System report, represents the percentage of seizures by sub-category of structural groups in pie graph form and the number of seizures per country in the inner map of Europe in 2013.

In a documentary by Hamilton Morris named "The Synthetic Drug Revolution" (https://mail.google.com/mail/u/0/#search/sam/14cc3877c701e279?projector=1), they fly to Shanghai, China to some of the clandestine laboratories making these products. In the video, it shows the sheer scope of mass production. These labs work on an industrial level of synthesis with chemical equipment capable of making kilograms of product at one time, and anyone can come to the chemist with money and a new chemical structure and get that product synthesized regardless of its intended use. The chemist they interview describes the business as growing not declining. These chemicals are tested to make sure they are analytically the chemical purchased but have no tests done regarding reactivity, and there are no standards of cleanliness or purity. The documentary goes on to say that there are

160,000 of these labs in China alone, and those are just the ones that are known. These laboratories then go on to ship these compounds to "middle men" manufacturers who package them and resell them at a higher cost. That isn't to say that a person could not just order straight from the Chinese suppliers because there are websites out there that do get product directly from China.

Once it is packaged, there are hundreds of different brand names with which it could be packaged. One news report named over 400 SC brand names that had been banned in the state of Georgia alone (Stucka, 2012). At one retailer website they had empty packages with brand names such as Scooby Snax, Mind-Trip and Geeked up, some saying right on the package "does not contain JWH-018 or AM-2201." Since they are sold empty, it is possible and probable that someone could order any compound from China, even the ones specifically listed as not in the product and package these themselves to resell. There are many websites giving you exact recipes of how to make synthetic cannabis from the powder form. A simple Google search revealed many hits but this website was the most thorough -- http://slashcannabis.com/make-your-own-synthetic-cannabinoid-blend/ -- which gives you a step by step guide with pictures on how to add synthetic cannabis to plant matter. With all these different variables, the number of compounds, the number of brand names and the number of manufacturers and retailers; the synthetic cannabinoid problem has proven to be nearly impossible to control.

1.4.6 Motivations

What makes these drugs so appealing? From a manufacturer standpoint, SCs are much cheaper to produce, when ordered from China in bulk, than growing natural cannabis. Also, the quantity that can be produced at one time is much greater than natural cannabis.

The documentary mentioned earlier stated that these drugs are also easier to transport internationally and get through customs checks as dogs are not as well trained to detect the synthetic products, as well as natural cannabis.

From a consumer standpoint, a survey conducted across 13 countries including 391 participants, many cited curiosity as the main reason for trying the drugs. There are thousands of online drug forums citing the strong effects of the spice products. Many claiming the high is "more intense" than normal cannabis. 58% of the surveyed population cited "favouring drug effects" as their reason for use. The ease with which one was able to purchase it, though more expensive than normal cannabis, was a driving factor for many. As previously stated, many of these drugs are not detected in standard drug testing making them popular among people on probation for drug offenses and military. The legal perception (as many of these products have now become illegal which will be discussed in depth later) has also increased their incidence of use as people feel like they avoid the "drug taker" label if they smoke these as opposed to normal cannabis (Palamar & Acosta, 2015). Surveys have shown that many people discontinue use after a few attempts, mainly citing the negative side effects as the reason. Though data is limited in patients with long term use, there has been evidence showing that SC consumption can lead to dependence and withdrawal, leading to the continued use by these users (Gunderson, Haughey, Ait-Daoud, Joshi, & Hart, 2012; Nacca et al., 2013).

1.4.7 **Negative Health Effects**

Cannabis use has been known to cause short and long term side effects. The common short term side effects of cannabis are paranoia, panic, anxiety, lack of

coordination, distortions in time, fatigue, increased appetite, depression and increased heart rate. Long-term side effects can range from suppressed immune system, reduced male sex hormones, permanent memory damage, lack of motivation, cognitive deficits, personality and mood changes and destruction of lung and brain fibers (R. Pertwee, 2014). SCs have similar short term effects with the most common recorded being anxiety, irritation, anger and paranoia (Gurney et al., 2014). Although many of the mild adverse side effects between smoking regular cannabis and SCs are the same, synthetic users claim that the high they get from consuming SCs is "more intense" which has been interconnected with more dramatic and sometimes life-threatening side effects. The number of emergency room visits for adverse reactions to SCs are on the rise since the beginning of 2015, updated statistics are not available, but the New York Times posted an article stating the in the first 3 weeks of April, 2015 there were 1,000 cases reported which is more than the first 3 months combined. The American Association for Poison Control Centers also stated that SC cases have been reported four times more than in 2014 already this year(AAPCC, 2015). Many of the SC brands contain mixtures a few different compounds making pinpointing what compound is causing what reaction difficult. For a review on specific effects per compound see Gurney et al., but only general adverse effects will be described in detail.

1.4.7.1   *Effects on the Central Nervous System*

The most common side effect mentioned in almost all blog entries is paranoia and anxiety. Many of these users were also users of cannabis and have stated that the paranoia and anxiety experienced after smoking SC is far beyond anything they ever experienced with natural cannabis (drug-forums.com). Many of the blog posts seem to be describing symptoms more congruent with mania or psychosis. Mania being defined as an elevated state of arousal and psychosis being a mental disorder where all sense of reality is lost. Given the inability to confirm the veracity of blog posts, one must look to case studies

presented. Many case studies have confirmed that mania and psychosis are in fact side effects of SC use but given the small number of case studies published it minimizes the scale of their presentation compared to that of the blogosphere. There were a few case studies analyzing the urine of users who were disoriented, presenting paranoia and hallucinations after smoking SC that after further testing were found to be JWH-018 and JWH-073. Hallucinations, delirium, confusion and suicidal thoughts were also confirmed after the ingestion of JWH-112, JWH-250, JWH-210 or AM-694. (Gurney et al., 2014). The stronger psychotic effects have been hypothesized, at least in the case of JWH-018, to be linked to the full agonist activity at CB_1, which is a common theme that will be seen throughout the following chapters. Cases of paranoia in cannabis use are mainly linked to strains that have higher concentrations of THC. Strains with higher THC would therefore, have more effect on the CB_1 receptor as well as have a higher concentration of CBD which has been thought to contribute neuroprotective effects that may negate some of the THC effects. The lack of CBD in SC preparations could be linked to the higher increase in psychological effects (Every-Palmer, 2011). The lack of CBD, which has been shown to have anticonvulsant properties in mice may contribute to the occurrence of seizures following the consumption of JWH-018, Am-2201, JWH-122 and JWH-210. The mechanism for the lowering of the seizure threshold has yet to be determined (Gurney et al., 2014).

Mild neurological short-term side effects have been reported such as drowsiness, dizziness, headache, dilated pupils, droopy eyelids, and slow speech. More severe cognitive impairments have been listed such as memory loss, unresponsiveness, loss of consciousness/coma and even temporary paralysis (Gurney et al., 2014). The debilitating effects of these cognitive impairments have been studied in relation to driving. There have been a number of case studies where people have been pulled over for impaired driving

and the officer has noted swaying, slurred speech, dilated pupils, inability to cross eyes, instability and slow reaction time (Yeakel & Logan, 2013). In incidents where impairment led to accidents, JWH-018, AM-2201, JWH-210 and JWH-122 were all found in the driver's system ranging from 0.1ng/mL to 9.9ng/mL (Gurney et al., 2014). There have been a number of car accidents resulting in a driver under the influence of SCs either killing themselves or killing others but only some of these are verified accounts from news articles the others are found in blogs meant to memorialize victims of SCs and victims of SC users (http://tothemaximusblog.org/?page_id=560).

1.4.7.2   Peripheral Effects

Tachycardia, elevated heart rate, is a common side effect of cannabis use. Many of the SCs has been found to produce the same response (JWH-018, JWH-122, JWH-073, JWH-015, JWH-081, MAM-2201 and UR-144). In singular (separate) cases, bradycardia, myocardial infarction and an increase of troponin (a protein that is released when the heart has been damaged) were recorded after consumption of SCs but the specific identity of compound was not verified. There have been reports of both hyper- and hypotension found after the consumption of SCs but it is unclear if this response is compound dependent or a function of time elapsed before tested (Gurney et al., 2014).

Within the pulmonary system, SC use has mild symptoms such as shortness of breath, coughing and chest pain. The most severe of the pulmonary symptoms is the development of fluid into the lungs. One case of a male ingesting SC for at least a four month period, found having AM-2201, JWH-122 and JWH-210 in his system, developed diffuse pulmonary infiltrates. Another young girl developed alveolar infiltrates, or fluid filling the alveoli sacs. Two cases of pneumonia were also reported after the consumption of ADB-PINACA (Gurney et al., 2014).

Nausea, vomiting and abdominal pain are some of the most prominent complaints of people seeking medical treatment for SC use. This could be due to the SC acting directly on the gastrointestinal system or could be in conjunction with acute kidney injury (AKI) which has similar symptoms. AKI is diagnosed by increased urinary creatinine that was has been documented in over ten cases with the majority of kidney issues being linked to XLR-11 and its metabolite UR-144 N-pentanoic acid. It should be noted that these compounds were consumed at the time of testing but because the patients had prior SC use before seeking medical attention and it cannot be said with certainty that these compounds were the cause (Gurney et al., 2014). Many of the JWH (018, 810, 250, 122) compounds have also been found to decrease the regulation of body temperature and electrolytes/fluids, which can be linked but are not necessarily caused by kidney malfunctions (Hermanns-Clausen, Kneisel, Szabo, & Auwarter, 2013). JWH-018 and AM-2201 increased the level of blood nitrogen urea in at least one patient which also signifies that the kidneys are not working properly. ADB-PINACA was also linked to elevated levels of potassium in the blood, which again signifies renal insufficiency. Hyperkalaemia can also lead to heart arrhythmias which have also been documented in a few case studies (Gurney et al., 2014; Hermanns-Clausen et al., 2013).

Other side effects, varying in severity, which have been documented are pallor, redness or itchy skin, increased acidity of the blood, incontinence, sustained muscle contractions, hot flashes, burning eyes, deafness, blindness, haemorrhage and increased white blood cell count (Gurney et al., 2014).

1.4.7.3 Death

The actual number of deaths resulting from SC consumption has not been accurately documented. In some cases, SCs were consumed but could not be determined if they were the cause of death or not, just that they were present in the system. Other

deaths, such as deaths of victims of SC impaired drivers are not considered in the death toll. 5F-PB-22 has been implicated in the death of at least four individual and its parent analogue PB-22 has been implicated in 3 deaths (Behonick et al., 2014; Gerostamoulos, Drummer, & Woodford, 2015). MAM-2201 has been confirmed to be the cause of death at a concentration of 12.9 ng/mL (Gurney et al., 2014). 5-fluoro-ADB-PINACA was also found to be the cause of death, but it was in conjunction with one of the most recently identified new SCs, MAB-CHMINACA (Hasegawa et al., 2015). "*The Guardian*" reported that since the introduction of MAB-CHMINACA and AB-CHMINACA in the United States, in the last month, two people have died in Mississippi, and one in Virginia ("Synthetic marijuana-related hospitalizations skyrocket in US," 2015). The "K2" brand of spice, without identification of active compounds or a post-mortem toxicology report, was linked to the death of one individual by cardiac infarction and another individual who committed suicide after its consumption (Mir, Obafemi, Young, & Kane, 2011). Scanning news articles showed synthetic cannabinoids were thought to be responsible for the deaths of 11 people in Alabama (B. Brown, 2013; Robinson, 2015), 3 deaths in Colorado (J. Wilson, 2013), 6 deaths Queensland, Australia (Chamberlin, 2015; Murray, 2013) and 40 across Russia ("ФСКН: от отравления спайсами в российских регионах погибли более 40 человек," 2014) in the past year, but specific compounds were not stated. In most instances, even if SCs are tested for post mortem, which many times is not the case, examiners are either lacking the analytical equipment needed or they do not know what compounds or metabolites to screen for as many have not yet been identified. This makes identifying cause of death due to SCs very difficult and sometimes impossible.

1.4.8 **Governmental Control and Scheduling**

Since the Single Convention of 1961 and the UN Convention of 1971, which are still the main rulings for international drug scheduling, did not have regulations in place regarding structural analogues of scheduled drugs, many of the first spice products remained legal for many years after their introduction. Each country has had to use various forms of legislative manipulation to try and halt the spread and use of the ever evolving generations of these products. Some European countries have placed a ban on these substances under food regulation laws (Switzerland), while others have tried to ban the plant matter Leonotis leonurus (Poland and Latvia) and Nymphaea caerulea (Romania). Many others have banned "spice" the product regardless of its contents while others have only banned specific compounds leaving them vulnerable to the new structural versions of spice.

In July, 2012, the United States enacted the Food and Drug Administration Safety and Innovation Act, which added a provision that placed any substance that acted as a CB_1 agonist in Schedule I and, therefore, was illegal. It goes on to list 5 of the structural scaffolds with provisions like "further substitution on… to any extent" to try and pre-emptively schedule analogues that have yet to be made. Unfortunately, there is a clause stating that if the structure falls outside the bounds of the structural groups listed, there must be published binding assay data proving that it is a CB_1 agonist for it to fall under Schedule I control (*Food and Drug Administration Safety and Innovation Act*). This highlights the need for a high-throughput binding assay to try and minimize the time the new analogues are considered legal in the market.

In 2013, Australia enacted a 3 month "interim" ban on the sale or possession of any synthetic product and multiple spice brands in an attempt to slow down the rate of consumption as 1.2% of the population had used SCs over the previous 23 months (Welfare, 2013). As of today, there has not been a more permanent ban on Australia nationwide as the

interim ban expired October 2013. New South Wales did pass a bill that made any drug with psychoactive properties illegal. It is the first "blanket" legislation put in place worldwide. New Zealand shortly after followed, banning all "legal highs" as of May 2014.

Although nearly all countries with a prevalence of SC use have attempted to add legislation to prevent its sale and use, there are still many loopholes present. Without a more strict "catch-all" type legislation, there will continue to be an incentive for manufacturers to produce structurally altered and novel synthetic drugs.

1.4.9 Issues That Remain Regarding the Synthetic Cannabinoid Problem

Even with the legislative attempts, there are still a variety of issues that need to be addressed before there is a resolution to the SC problem. From a medical standpoint, more research is needed to understand the mechanisms of action of these compounds to be able to come up with treatments for the overwhelming instances of overdoses. From an identification standpoint, better analytical techniques are needed to be able to identify new derivatives. At the present moment, analytical techniques can identify compounds but only if they are the compounds being sought. A way to screen for the multiple unknown compounds present will need to be developed in order to keep up with the rate of compounds emerging.

Due to the fact these products are manufactured and sold illegally, there is nothing that can be done in terms of regulating the contents or purity of the compounds that reach consumers. For users, this means there is no guarantee that within the same brand that there will be the same compound/s that were previously in that package. There are no rules on what compounds are mixed and at what concentrations with which they are present. K2 has

even been found to be laced with the drug phencyclidine (PCP) a dissociative hallucinogenic (Kersten & McLaughlin, 2014). This meaning that the brands that have been around for years containing various SCs now could contain a completely different type of drug. From a governmental standpoint, the discrepancy in packaging makes being able to determine which packages contain the illegal compounds nearly impossible unless every package is tested. This is an unreasonable and essentially impossible task. Until there is a way to detect, limit or completely prevent the sale and import of these drugs from China and other clandestine laboratories, this problem is bound to get worse before it gets better.

1.5 AIMS

The main aim of this body of work was to build pharmacological profiles for many of the most prevalent SCs, their analogues and some predicted structures thought to be potentially in the next generation of compounds to reach the market. The building of these profiles was under the assumption that the compounds being studied were desgined to be cannabimetic and mimic Δ^9-THC. Therefore, we tested the hypothesis that structural differences would alter signalling and that the differences in signalling would reflect in potency and toxicity at the cannabinoid receptors and off target pathways. "Off target pathways" was used to describe any receptor other than the cannabinoid receptors tested but it was in no way assumed that the targets tested were comprehensive of the potential off target pathways.

Aim 1: Determine the validity of a high throughput membrane potential assay for SCs on AtT20 cells and determine their functional activity at CB_1 and CB_2 receptors.

Aim 2: Examine the validity of a high throughput assay that measured changes in intracellular calcium and determine if any of these SCs had off target pathway activation potentially illuminating possible modes of toxicity.

Aim 3: Determine if there were any structural activity relationships within structural subsets relating to specific receptor activation and potency and efficacy at those receptors.

Aim 4: Develop a lipid extraction and high performance liquid chromatography and tandem mass spectrometry protocol to determine if the application of potent agonists to these receptor systems had an effect on the endocannabinoid system by measuring the changes in endocannabinoids.

CHAPTER 2: MATERIALS AND METHODS

2 MATERIALS AND METHODS

2.1 CELL CULTURE

All cells were cultivated in Dulbecco's Modified Eagle's Medium (DMEM) supplemented with 10% fetal bovine serum (FBS), and penicillin/streptomycin (100 U/100 µg mL^{-1}) (P/S). They were grown in 75 mm^2 flasks and incubated in 5% CO_2 at 37°C. They were passaged at approximately 90% confluency and were only used in experiments within 20 passages post defrosting from liquid nitrogen. To passage, all additive solutions were warmed to 37°C. The cells were first washed with 5mL phosphate-buffered saline (PBS) immediately followed by 2 mL of Trypsin for approximately 2 minutes or until cells detached from the flask with little force. 5 mL of DMEM was added to the flask to stop the effects of trypsin. The DMEM/trypsin solution was then transferred to a 15 mL Falcon tube and centrifuged for 5 minutes at 1000 rpm. The supernatant was removed, and the remaining pellet was resuspended into supplemented DMEM (with specific selection antibiotics later described per cell type). A few drops (5-10) of the re-suspension was then added to a new T-75 flask with 10 mL of supplemented DMEM and placed in the incubator.

2.1.1 AtT20 Wild Type (AtT20-WT)

Mus musculus pituitary tumour AtT20 wild type (CCL-89 or CRL-1795) cells were purchased from ATCC (Manassas, VA, USA). No selection antibiotics were used.

2.1.2 AtT20 Rat Cannabinoid Receptor 1 (AtT20-rCB1)

AtT20 cells were stably transfected with a single HA-tagged rat CB_1 (Mackie et al., 1995) and gifted to the lab of Mark Connor by Ken Mackie from Indiana University. The selection antibiotic added to the supplemented DMEM for these cells was G418 (400 μg/mL).

2.1.3 AtT20 Human Cannabinoid Receptor 1 (AtT20-hCB1)

The three hemeagglutinin (3HA) hCB_1 plasmids were purchased in vector pcDNA3.1(+) (Invitrogen, Carlsbad, CA, USA) and stably transfected into mus musculus pituitary tumour AtT20 cells (Grimsey, Graham, Dragunow, & Glass) by Natasha Grimsey at The University of Auckland. They were a gift from Michelle Glass. The selection antibiotic added to the supplemented DMEM for the maintenance of these cells was Zeocin (250 μg/mL).

2.1.4 AtT20 Human Cannabinoid Receptor 2 (AtT20-hCB2)

A pcDNA3.1 vector encoding human CB_2 with 3HA tags at the receptor N-terminus was purchased from the Missouri S&T cDNA Resource Center (www.cdna.org; #CNR020TN00) and stably transfected into mus musculus pituitary tumour AtT20 cells also completed by Natasha Grimsey and gifted by Michelle Glass (Grimsey, Goodfellow, Dragunow, & Glass). The selection antibiotic added to the supplemented DMEM was for these cells was G418 (200 μg/mL).

2.1.5 Human Embryonic Kidney (HEK) 293 Human Transient Receptor Potential Vanilloid 1 (hTRPV1)

Flp-In TRex HEK 293 cells were stably transfected with human TRPV1 and were gifted by Peter McIntyre from RMIT University in Melbourne, Australia. The selection antibiotics added to the supplemented DMEM were Hygromycin (100 µg/mL) and Blasticidin (50 µg/mL).

2.1.6 HEK 293 Human Transient Receptor Potential Ankyrin 1 (hTRPA1)

Flp-In TRex HEK 293 (Life Technologies, Mulgrave, Victoria, Australia) cells were stably transfected with human TRPA1 as described in Redmond et al. (Redmond et al., 2014). The cells were cultivated with the selection antibiotics Hygromycin (100 µg/mL) and Blasticidin (50 µg/mL) added to the supplemented DMEM.

2.2 MEMBRANE POTENTIAL ASSAY

Cells were grown to 90% confluency and resuspended in L15 medium (supplemented with 1% FBS, 1% P/S, and 15 mM glucose) and were plated (90 µL/well) into a black, clear-bottomed, poly-D-lysine coated (10 µg/mL per well) 96 well plates (Corning, Castle Hill, NSW, Australia). The cells were incubated overnight at 37°C in an incubator containing humidified room air. The next day, 90 µL of blue membrane potential dye, which had been diluted to 50% with low potassium (K^+) Hanks Balanced Salt Solution (HBSS) which consisted of (mM): NaCl 140, $CaCL_2$ 1.3, $MgCl_2$ 0.5, HEPES 22, Na_2HPO_4 0.338, $NaHC0_3$ 4.17, KH_2PO_4 0.44, $MgSO_4$ 0.4 and glucose 10 (pH 7.4, osmolarity= 315 ± 15 mosmol). The diluted dye was then added to each well and incubated at 37°C between 1 and 1.5 hours. Using a FLEX Station 3 Microplate reader (Molecular Devices, Sunnyvale, CA, USA) set to 37°C, fluorescence readings were measured every 2 seconds (λexcitaion=

530 nM, λemission= 565 nM). All drugs were made up in dimethyl sulfoxide (DMSO), with the exception of somatostatin which was made up in distilled water, and diluted in the low K^+ HBSS buffer with a final DMSO concentration of 0.05-0.1% (0.01% max per well). Drugs were added after a 2 minute baseline recording and each drug was run in duplicate measurements. If the experiment called for one drug addition 20 µL of drug was added to each well, whereas if it required two drug additions a 20 µL addition was followed by a 22 µL drug addition.

Data were analysed using Microsoft Excel (2010) and GraphPad Prism (Version 6). Excel was used to determine the maximum decrease in fluorescence after the subtraction of the DMSO blank. This was done by finding the percentage change over the baseline average for the 30 seconds immediately prior to drug addition. GraphPad Prism was then used to calculate concentration-effect by fitting data to a four-parameter logistic Hill equation (bottom constrained to equal 0% change in RFU) to derive the EC_{50}, pEC_{50} and Hill slope.

2.2.1 Membrane Potential Assay: Agonist Activity (n= 4-12)

AtT20-hCB1 and AtT20-hCB2 were the cell types tested to determine if the SCs had agonist activity. All drugs were screened at 10 µM concentrations. If a drug had agonist activity, as demonstrated by a hyperpolarization of the cell, a concentration response curve was completed to determine the potency of the drug. Concentrations varied between 1 pM and 30 µM depending on the potency and solubility of the drug. Drugs were added after a 120 second base line reading and the total run time was 300 seconds. Concentration-response data was then normalized to the maximum response of the efficacious synthetic cannabinoids WIN (1-3 µM) or CP 55,940, as noted. In experiments where CP 55,940 was used to normalize the responses, compounds were also diluted into low K^+ HBSS supplemented with 0.01-0.1% bovine serum albumin (BSA) (Sigma-Aldrich, St. Louis,

MO).

2.2.2 Membrane Potential Assay: Pertussis Toxin (PTX) Pretreatment (n= 3)

AtT20-hCB1 or AtT20-hCB2 cells were plated at 81 µL in even rows and 90 µL in odd rows of a 96 well plate. 9 µL of 2 µg/mL PTX (List Biological Laboratories, Campbell, California, USA) was added to each well in the even rows making the final concentration of PTX 200 ng/mL per well. The plates were then incubated for 24 hours at 37°C before experimentation. 10 µM additions of each drug were then tested in duplicate (meaning the same drug was tested on two rows). Therefore, the drugs were tested on both PTX treated and non-treated cells to be sure a lack of signal was a result of the PTX treatment. An example trace is shown in Figure 7 for clarity.
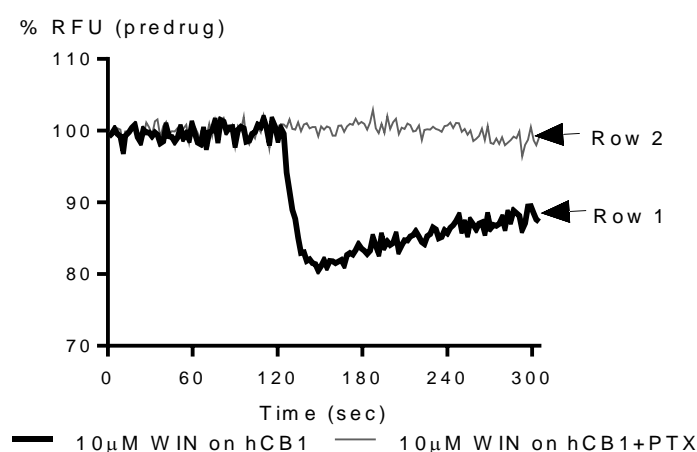
Figure 7: Traces of the response of WIN at AtT20-hCB1 with and without the pretreatment of PTX. This figure illustrates the response of 3 µM WIN added to AtT20-hCB1 cells that had been both treated and non-treated with 200 ng/mL of PTX. This shows a test duplicate from the same plate where drugs were taken from the same drug plate 5 minutes apart from each other. Row 1 was non-treated with PTX to show that the cells were fully functional and to confirm the lack of response in Row 2 was definitely caused by the pretreatment of PTX.

2.2.3 Somatostatin (SRIF) Effect on AtT20-WT cells (n=5)

10 μM concentrations of the each drug were added after a 120 second baseline reading. 100 nM of SRIF was added at 420 seconds for a total run time of 600 seconds. The maximum decrease in fluorescence was calculated after both the first and the second additions. The first was to determine if there were any nonspecific effects represented by a hyperpolarization. The second to see if there was any receptor competition shown by a decrease the maximum effect of SRIF. The data were calculated after the subtraction of a DMSO/DMSO blank and normalized to the maximum SRIF response (DMSO/100 nM SRIF) per plate. Individual traces for each drug can be found in Appendix A (pg. 246-304).

2.3 CHANGES IN INTRACELLULAR CALCIUM ASSAY

Cells were grown to 90% confluency and resuspended in L15 medium supplemented with 1% P/S and plated (80 μL/well) into a black, clear bottomed 96 well plate. The cells were incubated overnight as previously described in Section 2.2. 20 μL of tetracyclin (1 μg/mL) was added to each well and incubated between 4.5-5 hours before the experiment. Calcium 5 dye was prepared by adding a 1:10 dilution of high K^+ HBSS buffer (mM: NaCl 140, $CaCL_2$ 1.3, $MgCl_2$ 0.5, HEPES 22, Na_2HPO_4 0.338, $NaHCO_3$ 4.17, KH_2PO_4 0.44, $MgSO_4$ 0.4, KCl 5.33 and glucose 10 (pH 7.4, osmolarity= 315 ± 15 mosmol)), 100 μL of probenecid per 5 mL of dye, and made to pH 7.4. 1.5 hours before the experiment, 80 μL of calcium 5 dye was added to each well and incubated at 37°C. The FlexStation 3 was used to take fluorescence measurements every 2 seconds (λexcitaion= 485 nM, λemission= 565 nM). All drugs were made up in DMSO, with the exception of capsaicin which was made up in ethanol, and diluted in the low K^+ HBSS buffer with a final DMSO concentration of 0.05-0.3% (max per well 0.03%) They were added after a 120 second baseline recording. If the experiment called for one drug addition, 20 μL of drug was added to each well.

Whereas, if it was a two drug addition, 20 µL addition was followed by a 22 µL drug addition.

Data were analysed using Microsoft excel (2010) and GraphPad Prism (Version 6). Excel was used to determine the maximum increase in fluorescence by finding the percentage change over the baseline average for the 30 seconds immediately prior to drug addition with a DMSO blank subtracted. GraphPad Prism was then used to calculate concentration-effect by fitting data to a four-parameter logistic Hill equation (bottom constrained to equal 0% change in RFU) to derive the EC_{50}, pEC_{50} and Hill slope.

2.3.1 Changes in intracellular Calcium Assay: Agonist Activity (n=5-10)

This experiment was done on both HEK293 hTRPA1 and hTRPV1. All drugs were scanned at 30 µM concentrations which were recorded after a 120 second baseline with a total run time of 780 seconds. Agonist activity was determined by an increase in cytosolic calcium resulting in an increase in fluorescence. If the drug had agonist activity over 30% of the maximum increase of fluorescence of hTRPA1 (CIN 300 µM) or hTRPV1 agonist (CAP 10 µM), a dose response curve was completed to determine the potency of the drug. Individual traces for each drug can be found in Appendix A (pg. 246-304).

2.3.2 Changes in intracellular Calcium Assay: Antagonist Activity (n=5)

Due to the lack of substantial agonist activity at hTRPV1, the drugs were tested for their antagonist activity. 30 µM of each drug was added after a 120 second baseline reading. 300 nM capsaicin (a high efficacy TRPV1 agonist) was added at 420 seconds and allowed to run until 780 seconds. A blank, where DMSO was added instead of the drug in

both the first and second addition, was subtracted and data was compared to the maximum fluorescence increase of a DMSO/ 300 nM capsaicin addition. The data was then presented as the percent decrease from maximum capsaicin response. If a drug inhibited the increase of capsaicin by 50% it was considered and antagonist and a dose response curve for the inhibition of capsaicin was completed. Individual traces for each drug can be found in Appendix A (pg. 246-304).

2.4 LIPID EXTRACTION (N= 4-10)

This protocol was adapted from Stuart et al., 2013 . Cells were grown to 90% confluency in T-125 cm^2 flasks. Drugs were diluted into warmed (37°C) serum free DMEM. Prior to the drug addition, the media the cells were grown in was aspirated off. 3.5 mL of each drug (enough to coat the entire surface of the plate evenly) was added to each flask for 5 minutes except when including the antagonist. In this case, the antagonist was added 10 minutes prior, aspirated off, then followed by the agonist addition for 5 minutes. After the 5 minutes, 7.5 mL of 100% high performance liquid chromatography (HPLC) grade methanol (MeOH) was added to each flask. Using a cell scraper, the cells were scraped off and the cell/methanol solution was pipetted into a 15 mL centrifuge tube. 20 µL of 1 µM deuterium labelled anandamide (d$_4$-AEA) was then added to each centrifuge tube (weights previously recorded) to act as an internal standard. 20 µL of 1 µM d$_4$AEA was also added to an autosampler vial containing 1.5 mL of 100% HPLC grade MeOH to use as a comparison (acting as a recovery equal to 100%) to determine the effectiveness of the extraction and to determine the percent loss of compounds of interest throughout the extraction process. The tubes were then parafilmed and left covered (to prevent degradation of the compounds due to light exposure) on ice for approximately 2 hours. The samples were then centrifuged at

19,000xG for 20 minutes at 24°C. The supernatant was then transferred to a 50 mL falcon tube and the centrifuge tube was placed upside down on paper towel to dry. This was done because the endocannabinoid levels were calculated in mols/gram tissue, therefore, the pellet remaining after centrifugation would be needed for this weight calculation as later described. HPLC-grade water was then added to make the final supernatant solution 25% organic.

A Preppy vacuum manifold (Sigma-Aldrich, St, Louis, MO, USA) was then assembled with 500 mg C18 solid phase extraction columns to isolate and partially purify the lipids of interest. The columns were conditioned with 5 mL of HPLC grade MeOH to activate the carbon chains and attract the nonpolar entities. The drip rate was set to approximately 1 drop/second. 2.5 mL of water was then added to activate the silica to bind the polar compounds, making sure at no point in the conditioning steps that the columns run dry. The 25% organic supernatant solution was then, for each sample, loaded into its corresponding column. 2.5 mL of HPLC water was then used to wash the columns, immediately followed by 2 mL of 40% MeOH and then by 2 mL of 50% MeOH were added in attempts to wash out the impurities and unwanted compounds. 1.5 mL of 60%, 70%, and 80% MeOH were then added in succession to further the purification process. The drip rate was then slowed to 1 drop/ 2 seconds. 1.5 mL of 100% HPLC grade MeOH was then added to elute the ethanolamides which was collected in autosampler vials. The autosampler vials were then stored in the -80°C freezer until mass spectrometer analysis. After a few days, ensuring all of the liquid remaining in the pellet at the bottom of the centrifuge tube had evaporated to prevent inflated weights, centrifuge tube + pellet were weighed. The original weight of the centrifuge tube previously recorded was then subtracted to leave the weight of the pellet itself.

2.5 HPLC/MS/MS QUANTIFICATION

Samples were brought to room temperature and vortexed for approximately one minute before being put in the autosampler for analysis. The autosampler was held at 24°C. 20 μL injections of each sample were rapidly separated using a C8 Zorbax guard column in conjunction with a C18 Zorbax reverse-phased analytical column to separate the compounds if interest before they were shot into the mass spec for quantification. The aqueous mobile phase (mobile phase A) was made up with 20% ultrapure HPLC grade MeOH, 80% filtered HPLC grade water, and 1 mM ammonium acetate. The organic mobile phase (mobile phase B) was made with 100% ultrapure HPLC grade MeOH and 1 mM Ammonium Acetate. Two Shimadzu 8030 pumps (Rydalmere, NSW, Australia) were then used to create a pressurized gradient elution (200 μL/min). A Shimadzu 8030 triple quadrupole mass spectrometer was used to ionize the sample using positive electrospray ionization (ESI) through a multiple reaction monitoring (MRM) method. Synthetic standards of anandamide (AEA), Palmitoyl ethanolamide (PEA), Oleoyl Ethanolamide (OEA), Linoleoyl ethanolamide (LEA), 2-Arachidonoyl Glycerol (2AG) and d^4-AEA were used to generate optimized MRM^+ methods, while also providing a reference for retention time and identifying the specific precursor ion and fragment ion for each analyte.

LabSolutions software (Shimadzu, Rydalmere, NSW, Australia) was utilized to quantify the amount of each compound in a sample. Synthetic standards were used to make calibration curves to determine the concentration of the analytes in the unknown samples. The internal standard, representing 100% recovery, was then used to determine the effectiveness of the isolation and purification process. The concentration of each analyte was then converted to moles per gram tissue (using the weights obtained). Statistical analysis using a one-way ANOVA with post hoc Fisher's LSD with a 95% confidence interval ($p \leq 0.05$) were used to determine variations of the standard means compared to the

control groups (GraphPad Prism 6),

2.6 MATERIALS AND REAGENTS

2.6.1 Cell Culture

Tissue culture media was either purchased from Sigma-Aldrich (St. Louis, MO, USA) or Life Technologies (Carlsbad, CA, USA). Selection antibiotics were purchased from Invivogen (San Diego, CA, USA). Plastic ware was purchased from Corning (Corning, NY, USA).

2.6.2 Synthetic Cannabinoids and Standards

All synthetics unless otherwise stated were synthesized by Sam Banister or Shane Wilkerson at Sydney University in the lab of Michael Kassiou. WIN 55,212-2, CP 55,940, AEA and 2-AG were purchased from Cayman Chemical (Ann Arbor, MI, USA). CBD, AM-2201 and JWH-018 were purchased from National Measurement Institute (Sydney, NSW, Australia). Cinnamaldehyde and Δ^9-THC were purchased from Sigma-Aldrich (St. Louis, MO, USA). Capsaicin was purchased from Ascent Scientific (Cambridge, UK).

2.6.3 Membrane Potential and Changes in intracellular Calcium Assays

The membrane potential dye kits, calcium 5 dye kits, and black pipet tips specific for the Flexstation 3 were purchased from Molecular Devices (Sunnyvale, CA, USA). Drug plates were purchased from Greiner Bio One (Kremsmünster, Austria). GraphPad Prism (Version 6, GraphPad Software, Inc., La Jolla, CA, USA) was used for all analyses.

2.6.4 Lipid Extraction and Mass Spectrometer Consumables

HPLC grade and ultra-pure HPLC grade methanol were purchased from Merck Millipore (Bayswater, VIC, Australia). AEA, PEA, OEA, LEA, and 2AG were purchased from Cayman Chemical (Ann Arbor, MI). D_4-AEA was purchased from Tocris Bioscience (St. Louis, MO). Ammonium Acetate was purchased from Sigma-Aldrich (St. Louis, MO). The C18 solid phase extraction columns, the C8 guard column, and C18 Zorbax reverse-phase analytical column were purchased from Agilent Technologies (Santa Clara, CA).

CHAPTER 3: VALIDATING THE USE OF A FLUORESCENCE-BASED PLATE READER ASSAY USING REFERENCE COMPOUNDS

3 VALIDATING THE USE OF A FLUORESCENCE-BASED PLATE READER ASSAY USING REFERENCE COMPOUNDS

3.1 SUMMARY

Many of the synthetic cannabinoids being abused at present date are based on the same pharmacophore as that of Δ^9-THC but are of a new structural class. With a lack of published pharmacological and toxicological data for many of the new SCs, there was a need for a high-throughput assay to generate pharmacological data at a pace that could match the rapidity of the evolving drug culture. This chapter discusses the development and optimization of a functional, *in vitro* membrane potential and intracellular calcium measurement assay on various cell types. This was done using well-studied phyto-, endo- and synthetic cannabinoids that will be used as references in later chapters for comparison with the newer, less studied synthetic cannabinoids.

3.2 INTRODUCTION

A number of different bioassays have been developed to test the pharmacological actions of cannabinoid receptor/ligand interactions. Some of the most used *in vivo* assays to test cannabinoid activity include dog static ataxia, overt behavior in monkeys, rat and monkey drug discrimination and the mouse tetrad model (A. C. Howlett et al., 2002). Although *in vivo* assays are important in assessing the behavioural effects of synthetic cannabinoid activation, it can be difficult to determine unequivocally which molecular targets or likely targets are activated to cause the displayed effects. From an ethics perspective, the use of animals, though necessary, should be minimized if an in vitro method can be used in its place. Finally, animal models are time consuming, costly, and their findings are not always translatable to humans (Perez-Reyes et al., 1973). Part of the scientific and governmental battle against the SC pandemic has been trying to produce

pharmacological data at a pace that can be beneficial to legislation. This presented the need for a high-throughput *in vitro* assay.
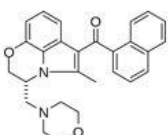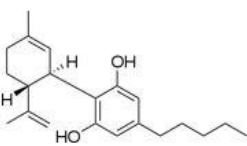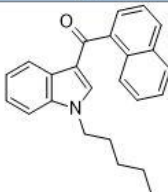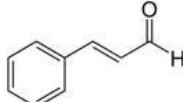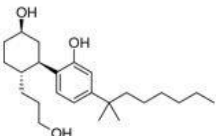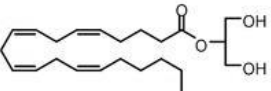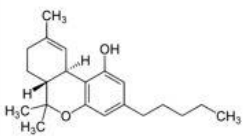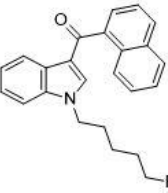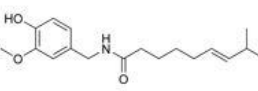
In vitro, there are three main methodologies to screen for receptor interaction: interactions between ligand and receptor, the production of secondary messengers or functional response (de Jong, Uges, Franke, & Bischoff, 2005). Radioligand binding assays use a radio labeled agonist, with high affinity for the specific receptor of interest, to determine the binding affinity. An unknown drug is added to the receptor with the prebound radiolabeled agonist, and the binding affinity is determined by the amount the unknown drug displaces the radiolabelled compound from the receptor. Although this assay is useful in determining receptor affinity, it does little to provide information on intrinsic activity (de Jong et al., 2005). Second messenger assays, such as the measurement of AC activity (through changes in cAMP), are valuable in studying $G\alpha_s$ and $G\alpha_{i/o}$ interactions. They are highly sensitive and have high throughput capabilities but are relatively expensive, some (but not all) involve radioactive material and can be subject to signal amplification due to their location further down the signalling cascade (A. C. Howlett et al., 2002; Thomsen, Frazer, & Unett, 2005). GPCR-mediated guanine nucleotide exchange measures the agonist-stimulated $[^{35}S]GTP\gamma S$ binding to plasma membranes expressing CB_1 or CB_2. This assay is advantageous as it represents an event proximal to receptor activation and, therefore, its signal is less influenced by downstream effects. Some limitations of this assay are that it is dependent on and influenced by the abundance of G proteins present and therefore, usually signals through $G\alpha_{i/o}$ making studying other $G\alpha$ subunits difficult. It requires a filtration step to separate free from bound $[^{35}S]GTP\gamma S$ and therefore is usually a low throughput assay, though one lab has adapted it to a high throughput model (Johnson et al., 2008). Also, it is less sensitive to compounds with low efficacy and/or partial agonists (A. C. Howlett et al.,

2002; Strange, 2010). Therefore, a plate reader based functional bioassay was chosen to develop the pharmacological profiles for the SCs.

Unlike the previous membrane potential dyes, DiBAC$_4$, Molecular Devices developed a proprietary indicator dye that is lipophilic, anionic and bis-oxonol that partitions across the cytoplasmic membrane of live cells depending upon the membrane potential. As the membrane potential decreases, i.e. due to an outflux of potassium, the cell membrane becomes hyperpolarized and the dye will flow out of the cell resulting in a decrease in fluorescence (Devices). Knapman et al. developed a minimally invasive protocol utilizing Molecular Device's "Membrane Potential Assay Kit" and a Flexsation 3 plate reader to examine agonist activity at AtT20 pituitary tumor cells stably transfected with FLAG epitope-tagged mouse μ–opioid receptor (Knapman et al., 2013). As the μ–opioid receptor is also a GPCR, Cawston et al. were able to adapt this protocol to test the functional activity of AtT20 cells stably transfected with cDNA of rat CB$_1$ (Cawston et al., 2013).

Molecular devices also produces a dye to measure changes in intracellular calcium to look specifically at Gα_q coupled pathways and ion channel targets with Ca^{2+} permeability, called Calcium 5 dye. Ca^{2+} 5 dye consists of a calcium fluorophore that upon addition to the cell is taken into the cytoplasm. In the presence of an agonist, there will be an influx of calcium into the cytoplasm. The Ca^{2+} then binds to the dye that results in an increase in fluorescence. The Ca^{2+} 5 version of this dye also contains masking technology that remains outside the cell and inhibits background fluorescence which increases the signal window and improves assay performance (Devices). TRPA1 and TRPV1, calcium permable cation channels, upon activation produce influx of calcium into the cell (Luo, Zhu, Zhu, & Hu, 2011). Therefore, making it possible to study agonist/antagonist activity at these ion channels using a FlexStation 3 plate reader.

Aminoalkylindoles/ Non Classical	Endocannabinoids	Classical	First Generation SC	TRPA1/ TRPV1 Agonists
WIN 55,212-2	AEA	CBD	JWH-018	Cinnamaldehyde
CP 55,940	2-AG	Δ^9-THC	AM-2201	Capsaicin

Figure 8: Chemical structures of Compounds Tested in Chapter 3. This table shows the chemical structures of the compounds tested in this chapter drawn by Chemdraw Professional 15. They are separated by structure class.

3.3 RESULTS

3.3.1 GIRK Activation in AtT20-rCB1, AtT20-hCB1 and AtT20-hCB2 by WIN 55,212-2 (WIN) measured using a Membrane Potential Sensitive dye

An fluorescence-based plate reader assay using membrane potential sensitive dye was completed using a FlexStation 3, as described in Section 2.2, to assess the feasibility of this technique in studying receptor activation in three different AtT20 receptor systems (rCB$_1$, hCB$_1$ and hCB$_2$). WIN, a nonselective agonist at both the CB$_1$ and CB$_2$ receptor, was used as a positive control for receptor activation (Florek-Luszczki, Wlaz, Kondrat-Wrobel, Tutka, & Luszczki, 2014). A maximally effective concentration of WIN (3 μM) hyperpolarized AtT20-rCB1, AtT20-hCB1 and AtT20-hCB2 with maximum decreases in fluorescence equal to $33 \pm 2\%$, $29 \pm 2\%$, and $28 \pm 1\%$ respectively. Hyperpolarization of the cell is consistent with the receptor activation being coupled to GIRK channels. An overnight pretreatment of 200 ng/well of PTX, a Gα$_{i/o}$ inhibitor, completely blocked the

agonist response for each receptor confirming that this response was $G\alpha_{i/o}$ coupled, further

implicating GIRK mediation (Figure 9).
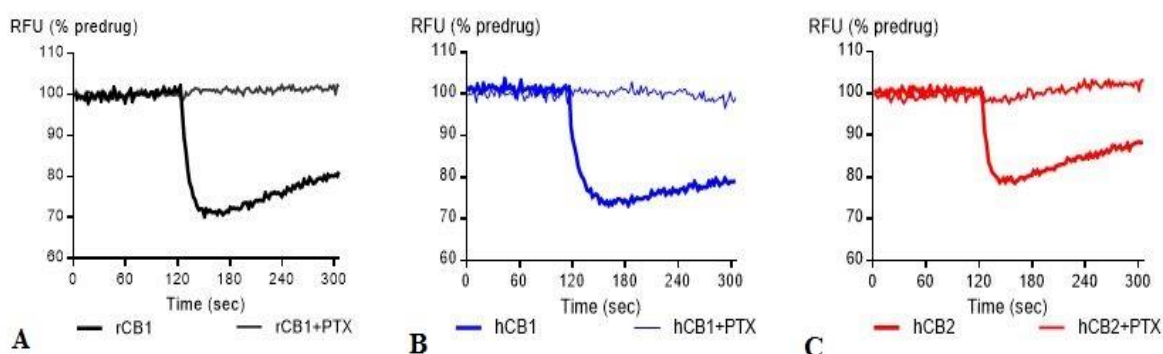
Figure 9: Traces produced by the addition of WIN to cells containing cannabinoid receptors with and without the pretreatment of PTX. This figure illustrates the response of 3 μM WIN (n=1) on A) AtT20-rCB1 B) AtT20-hCB1 and C) AtT20-hCB2. The pretreatment of PTX showed a completed abolished the response of WIN at all three receptor types signifying $G\alpha_{i/o}$ coupling.

3.3.2 **TRPV1 Activation in HEK293 T-TRex Cells by Capsaicin, measured using calcium sensitive dye**

An assay measuring the changes in intracellular calcium was performed using a Flex

Station 3, as described in Section 2.3, to test agonistic activity of a tetracycline-inducible

HEK293 TRex hTRPV1 system. Capsaicin (CAP), a high efficacy agonist at hTRPV1, was

used as a positive control to confirm the functionality of this assay. HEK293-hTRPV1 cells

were induced for 4 hours with 50 μg/well tetracycline. The responses to various

concentrations were used to calculate a pEC_{50} value of 7.4 ± 0.1 as represented by the

concentration repsonse curve shown in Figure 10(b). The maximal fluorescence increase

was determined by the response at 10 μM capsaicin with an E_{max} of $200 \pm 2\%$, shown by

Figure 10(a). This data confirmed that this assay is suitable for studying agonist activity at

hTRPV1. The maximum increase in fluorescence produced by CAP was then used as a

standard to normalize between different experiment days and between drugs. Any

compounds with a maximal fluorescence increase greater than 30% of the CAP max response had concentration response curves generated and a pEC_{50} calculated. Data will be presented as "% CAP Max" in the following chapters.
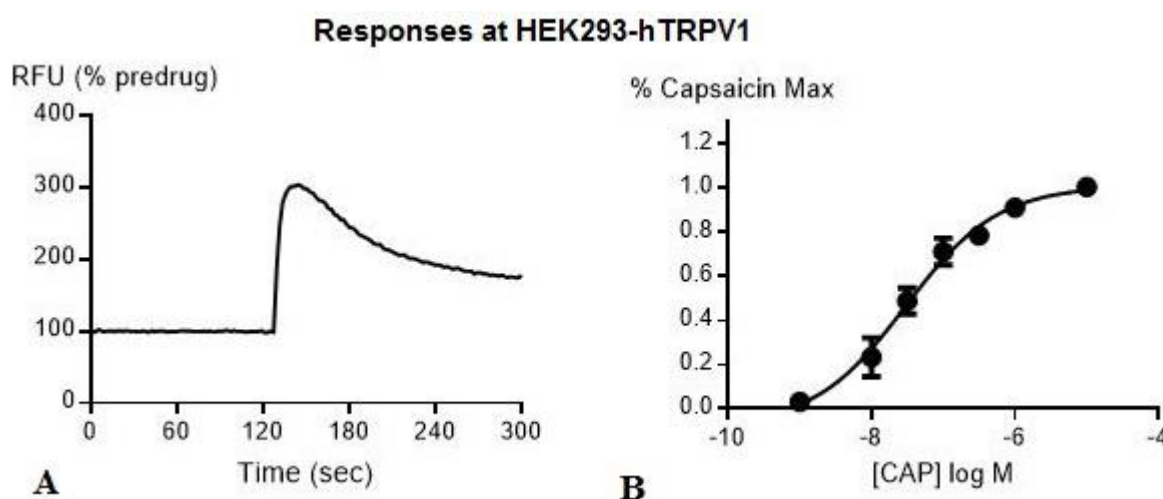
Figure 10: Agonist Activity of CAP at hTRPV1. A) Shows the trace of the r**esponse of 10 μM** CAP **in hTRPV1** (n=1) **B)** Shows the **concentration response curve** for CAP **in hTRPV**1. Data represent mean values ± SEM from 7 experiments each run in duplicate.

3.3.3 Optimization of Assay Measuring the Changes of Intracellular Calcium on HEK293 T-TRex hTRPA1 using Cinnamaldehyde

Cinnamaldehyde (CIN), a high efficacy agonist at hTRPA1, was used as a positive control to confirm the functionality of the fluorescence-based plate reader assay used to measure the changes in intracellular calcium at this receptor. HEK293-hTRPA1 cells were induced for 4 hours with 50 μg/well tetracycline. The responses to various concentrations were used to calculate a pEC_{50} value of 5.21 ± 0.04 (Figure 11(b)). The maximal fluorescence increase was determined by the response to 300 μM cinnamaldehyde, which produced an E_{max} of $452 \pm 3\%$, shown by Figure 11(a). This data confirmed that this assay

is suitable for studying agonist activity at hTRPA1. The increase in fluoresence produced by 300 μM CIN was used as a standard to normalize between experiments and between drugs. Any compounds with a maximal fluorescence increase greater than 30% of the CIN max had concentration response curves generated and a pEC_{50} calculated. Data will be presented as "% CIN Max" in the following chapters.
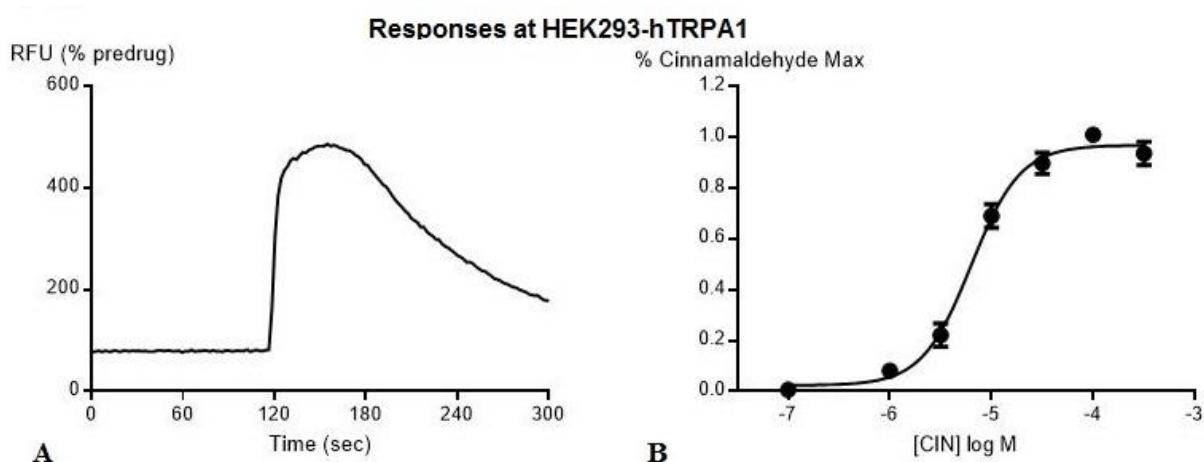
Figure 11: Agonist Activity of CIN at hTRPA1. A) Shows the trace of the increase in intracellular calcium when 300 μM CIN was added to hTRPA1 B) Shows the concentration response curve for CIN in hTRPA1. Data represent mean values ± SEM from 5 experiments each run in duplicate.

3.3.4 Functional activity of Normalization Standards: WIN 55,212-2 and CP 55,940

3.3.4.1 Membrane Potential

After agonist activity had been confirmed at the cannabinoid receptors, concentration response curves were generated for each receptor (rCB_1, hCB_1, hCB_2). The maximum change in fluorescence produced by WIN in each cell line was then used as a standard to normalize between assays and between drugs. The pEC_{50} concentrations were then determined from the normalized concentration response curves. WIN concentration

response curves (Figure 12) show that WIN is an efficacious agonist at all three receptors with pEC_{50} values of 6.55 ± 0.06 (rCB_1), 7.21 ± 0.09 (hCB_1), 4.89 ± 0.15 (hCB_2). All the data following for AtT20-rCB1, AtT20-hCB1 and AtT20-hCB2 throughout chapters 4-7 will be presented as "% of WIN Max".

After confirmation that the agonist response of WIN was G-protein mediated, the same membrane potential assay was completed on AtT20-WT cells to be sure that the response shown was due to cannabinoid receptor activation and not due to any nonspecific effects. A maximal concentration of WIN (3 μM) was added to AtT20-WT cells and then after five minutes, as a positive control, the cells were challenged with 100 nM SRIF (Appendix A pg. 304). It should be noted that at the highest concentration tested, 10 μM WIN, there was a small decrease in fluorescence in AtT20-WT cells (<10% WIN max). Though the nonspecific effect was minimal, the concentration of WIN used to normalize the remaining data was dropped to 3 μM, a concentration that has similar maximal efficacy but where the nonspecific effects were not seen.

CP 55,940, a nonselective high efficacy agonist at both CB_1 and CB_2, had no nonspecific effects at 10 μM in AtT20-WT (Appendix A pg. 305) (Felder et al., 1995). Because it is more potent than WIN, and has been reported to have fewer direct effects on ion channels, we switched to CP 55,940 for experiments in Chapter 6 where compounds were compared to the maximal decrease in fluorescence produced by CP 55,940, which was found to be $29 \pm 1\%$ at hCB_1 and $21 \pm 2\%$ at hCB_2. Figure 12, shows the concentration response curves for CP 55,940 with respect to % max WIN with pEC_{50} values of 7.6 ± 0.1 at hCB_1 and 7.8 ± 0.1 at hCB_2.
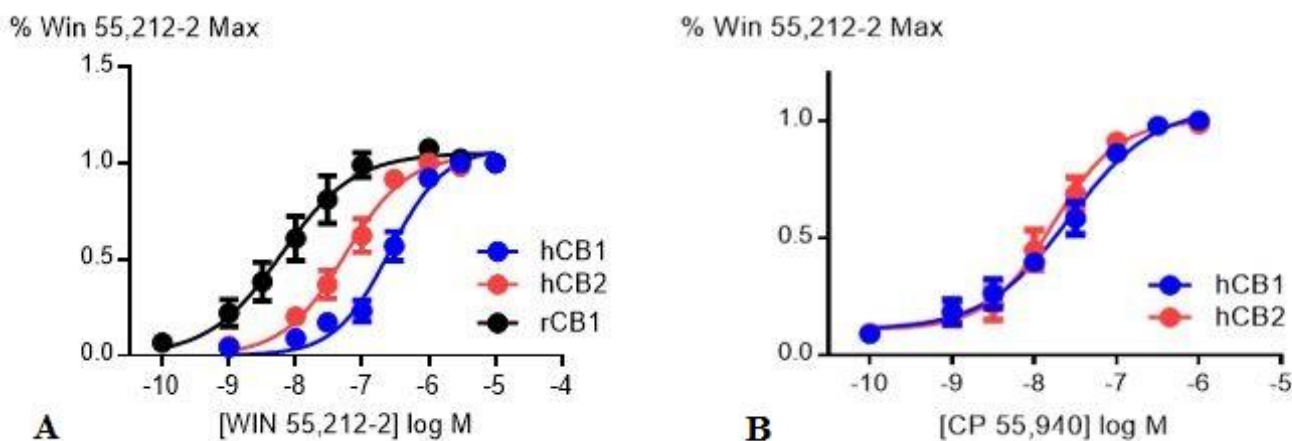
Figure 12: Concentration response curves for reference compounds WIN and CP 55,940 at cannabinoid receptors. **This figure illustrates** A) **C**oncentration response curves for WIN at rCB_1, hCB_1 and hCB_2 presented as a percentage of the maximal WIN response at 3 μM B) **C**oncentration response curve**s** for CP 55,940 at hCB_1 and hCB_2 as presented as a percentage of the maximum WIN response at 3 μM. Data represent mean values ± SEM from between 6-9 experiments each run in duplicate.

3.3.4.1 *Changes in Intracellular Calcium*

Neither WIN nor CP 55,940 had any agonist or antagonist effects at hTRPV1. At 30 μM CP 55,940 had low efficacy at hTRPA1 with a maximum fluorescence increase of 25 ± 3% with respect CIN max. WIN displayed partial agonist activity with a % CIN max of 57 ± 5% and a pEC_{50} of 4.89 ± 0.15. Since the highest concentration tested (30 μM) did not reach a maximum response, represented by the lack of plateau at the top of the usual sigmoidal curve, the nonlinear regression fit was constrained to the maximum of CIN to determine the notional pEC_{50} (Figure 13).
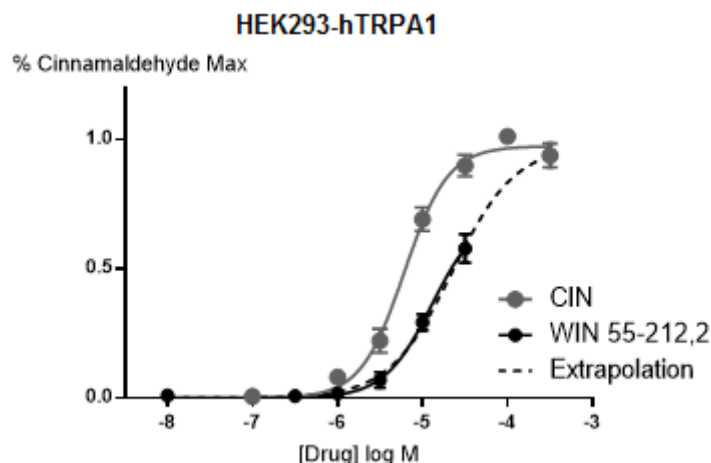
Figure 13: Validation of pEC_{50} extrapolation for hTRPA1 solubility constrained agonists. Shows the concentration-response curve for WIN on hTRPA1 (black) and the concentration-response curve for CIN (dark grey). The dashed black line represents an extrapolated WIN curve extended up to the maximum CIN response to validate constraining the top of the nonlinear regression to 1 to determine the pEC_{50} in cases where higher concentration values are restricted by solubility. Data represent mean values ± SEM from 5 experiments each run in duplicate.

3.3.5 Functional activity of Reference Compounds for Comparison: Classical, Endocannabinoids and First Generation SC

Two well-studied compounds from each of the remaining three original cannabinoid structural groups were tested to compare the results of fluorescence-base plate reader assays with values generated using other bioassays found in the literature. Also, as "first generation" compounds, their reactivity can be thought of as a "baseline" with which to compare the newer SCs. Table 2 summarizes the functional activity and binding of these compounds between a FlexStation 3 (FS 3) membrane potential, $[^{35}S]GTP\gamma S$ binding and radioligand binding (RLB) assays at the cannabinoid receptors and Table 3 at the TRP ion channels. Values were displayed as EC_{50} values for easier comparison against other literature EC_{50} values. It should be noted that the experiments testing these compounds were run concurrently with other SCs in later chapters to allow for a balanced comparison between the references and the SCs.

Table 2: Comparison of agonist activity values generated versus values found in literature across three bioassays at cannabinoid receptors. This table compares the EC_{50} values (±SEM) generated by the FlexStation 3 membrane potential assay with data found in literature for the EC_{50} values (±SEM) of $[^{35}S]GTP\gamma S$ binding assays and the K_i (±SEM) values of radioligand binding assays on cells containing rat and human CB_1 and human CB_2.

	Rat CB1			Human CB1			Human CB2		
	FS 3 EC_{50} (nM)	GTPγS EC_{50} (nM)	RLB Ki (nM)	FS 3 EC_{50} (nM)	GTPγS EC_{50} (nM)	RLB Ki (nM)	FS 3 EC_{50} (nM)	GTPγS EC_{50} (nM)	RLB Ki (nM)
WIN 55,212-2	6.1 ± 0.1	120§	10Ө	256.9 ± 0.1	40.73±1£	1.9 ± 0.09¥	55.2 ± 0.1	5.62±1£	0.28±0.16†
CP 55,940	N.T.	31 ± 5ǂ	0.5 ±0.1ǂ	26.5 ± 0.1	0.16±0.3£	0.58±0.07†	16.6 ± 0.1	3.89±0.3£	0.69±0.02†
Δ -THC	58.1 ± 0.1	>10μM§	208.9±0.5£	292.3 ± 0.1	A.F.L	41 ± 2†	3982 ± 1	23.44±1£	36.4 ± 10¥
CBD	N.T.	δ	A.F.L	S.E. at 10μM	A.F.L	4350±380¥	S.E. at 10μM	δ	2860±1230¥
AEA	N.T.	276 ± 53ǂ	71.7 ± 7.3ǂ	870 ± 0.2	631 ± 1ɸ	89 ±10¥	5036 ± 2	S.E. at 10μM ₸	279 ± 58ǂ
2-AG	N.T.	125.3€	200Ө	273.5 ±0.1	A.F.L	A.F.L	320.9 ±0.1	122 ± 17 ₸	371 ± 102¥*
JWH-018	N.T.	36†	9.0± 5.0†	103.0 ±0.1	A.F.L	9.5 ± 5¥	133.2± 0.1	A.F.L	2.9±2.6†*
AM-2201	N.T.	24.4†	1†	37.4 ± 0.1	A.F.L	A.F.L	58.4 ±0.1	A.F.L	2.6†*

N.T= not tested   A.F.L.= absent from literature   S.E. Slight Effect

*rat CB2 was used for this

δ reviewed in discussion

† taken from the review (Gurney et al., 2014)

¥ values from (Showalter, Compton, Martin, & Abood, 1996)

§ values from (Sim, Hampson, Deadwyler, & Childers, 1996)

ǂ values from (Hillard et al., 1999)

ɸ values taken from (Martin et al., 2002)

£ values from (Govaerts, Hermans, & Lambert, 2004)

Ө values from (A. C. Howlett, 2002)

€ values from (Luk et al., 2004)

₸ values from (Gonsiorek et al., 2000)

Table 3: Comparison of activity at the TRP channels of data generated versus values found in literature. This table compares the agonist activity values generated using the FS 3 assay measuring the changes in intracellular calcium with data found in the literature that measure calcium changes on HEK293 containing human TRPA1 or TRPV1 cation channels.

	FS 3 $[Ca^{2+}]_i$ hTRPA1 Max response at 30μM (% CIN max)	hTRPA1 Literature $[Ca^{2+}]_i$ EC_{50}	FS 3 $[Ca^{2+}]_i$ hTRPV1 Max response at 30μM (% CAP max)	hTRPV1 Literature Value EC_{50}
WIN 55,212-2	58 ± 5	δ	N.A.	δ
CP 55,940	25 ± 3	S.E. at 100 μM[2]	N.A.	N.E[2]
Δ -THC	57 ± 3	12 μM[1]	N.A.	N.E[2]
CBD	77 ± 5	81.4 μM[2]	N.A.	3.5 μM[2]
AEA	<2	4.9 μM[2]	46 ± 2	1.15 μM[2]
2-AG	53 ± 10	A.F.L.	N.A.	N.E.[2]
JWH-018	<10	A.F.L.	N.A.	A.F.L.
AM-2201	<10	A.F.L.	N.A.	A.F.L.
	EC_{50}		EC_{50}	
Cinnamaldehyde	6.32 ± 0.05 μM	11 μM[3]	N.E.	N.E.[1]
Capsaicin	N.E.	N.E.[1]	36.5 ± 0.1 nM	0.04-1 μM[1]

$[Ca^{2+}]_I$ = changes in intracellular calcium assay   (±SEM)

N.E.= No Effect   S.E.= Slight effect   A.F.L.= absent from literature

δ reviewed in discussion

[1] values from (Islam, 2011)

[2] values from (R. G. Pertwee et al., 2010)

[3] values from (Redmond et al., 2014)

3.4 DISCUSSION

The fluorescence-based plate reader system was chosen to undertake the building of pharmacological profiles of SCs for a number of reasons. First, it is a whole cell functional assay that provides more information than just receptor affinity as one would see with a radioligand binding assay. The ability to add multiple additions to the same well allowed for both agonist and antagonist reactivity to be tested at the same time. Second, it can be high throughput which was desired in trying to produce pharmacological data at a pace that could attempt to keep up with the rate structural evolution seen in SCs. As well as being high throughput, it has the benefits of being a real-time assay and therefore desensitization can be monitored and readings taken before it occurs. In contrast, a GTPγS binding assay is a

longer experiment (around 60 minutes) where the data represents a single point snapshot of a cumulative signal. Finally, plate reader based fluorescent assays have the ability to look at more than just G-protein coupled receptors which provided the ability to look into off-target cation channels.

As Mackie et al. has previously shown that AtT20 cells stably transfected with cDNA of rat CB_1 couple to GIRK channels (Mackie et al., 1995), Cawston et al. were able to use the fluorescence based plate reader membrane potential assay to test for allosteric modulators at this receptor (Cawston et al., 2013). AtT20-rCB1 were then used to verify the use of a fluorescence-based plate reader assay as a method to assess coupling consistent with GIRK channel activation by SCs. This was done by adding the non-selective CB_1/CB_2 receptor agonist WIN as a positive control on rCB_1. WIN showed a PTX sensitive hyperpolarization of $33 \pm 2\%$ with an EC_{50} of 6.1 ± 0.1 nM. Table 2 shows that WIN is 20 times more potent using this technique than compared to the $GTP\gamma S$ binding assay. GTPyS binding does not usually have spare receptors, whereas the activation of GIRK channels might. Therefore, receptor expression, which we did not measure, could contribute to this difference, although as noted, the assay conditions are quite different between GTPyS and fluorescence based assays.

Felder et al. tested signalling transduction pathways of human cannabinoid receptors CB_1 and CB_2 in AtT20 cells. They found that AtT20-hCB1 mediated the activation of GIRK channels, but not AtT20-hCB2 (Felder et al., 1995). In another study, human CB_1, expressed in Xe*nopus laevis* oocytes, co-injected with GIRK1 or GIRK1/4 showed an inwardly rectifying potassium current upon the addition of WIN. In the same study, human CB_2 was shown to not efficiently couple to GIRK channels having inconsistent responses to WIN even at increased concentrations of receptor (McAllister, Griffin, Satin, & Abood, 1999). Using the same cell type Ho et al. showed that both human CB_1 and CB_2 were

coupled to GIRK channels (B. Y. Ho et al., 1999). Given the discrepancy, specifically at hCB$_2$, the fluorescence-based membrane potential assay was used to test presumptive coupling to native GIRK channels present in AtT20 pituitary tumor cells for human cannabinoid receptors. Like with rCB1, WIN was used as a positive control for both receptors due to its nonselective high efficacy agonist activity. Both AtT20-hCB1 and AtT20-hCB2 showed a PTX sensitive hyperpolarization of the cell with similar maximums ($29 \pm 2\%$, and $28 \pm 1\%$ respectively). As AtT20 cells have native GIRK, WIN was tested on AtT20-WT to be sure that the hyperpolarization was hCB$_1$ and hCB$_2$ mediated GIRK activation. A maximally effective concentration of WIN (3 µM) showed no response in AtT20-WT cells, therefore confirming that the hCB$_1$ and hCB$_2$ activation was consistent with GIRK coupling and validated the use of this assay to test for functional reactivity of the cannabinoid receptors.

At the beginning of this project, we performed all preliminary experiments on AtT20-rCB1. Subsequently, we obtained both AtT20-hCB1 and AtT20-hCB2 as a generous gift from Michelle Glass, therefore, compounds that had previously been run on AtT20-rCB1 were then analysed in these expression systems. WIN and Δ^9-THC, as shown in Table 2, had potency differences 20 and 5 times greater at rCB$_1$ than hCB$_1$ respectively. Straiker et al. showed that human and rat CB$_1$ differ from each other at 13 different residues and that their signaling is quantitatively different. He also states that this could be due to receptor expression differences (Straiker, Wager‑Miller, Hutchens, & Mackie, 2012).

WIN was shown to be more potent at hCB$_2$ than hCB$_1$, which has also been shown with GTPγS binding assays (Govaerts et al., 2004), wherein, WIN showed a 5 fold selectivity towards the hCB$_2$ receptor over the hCB$_1$ receptor. CP 55,940 was found to be more potent than WIN at both hCB$_1$ and hCB$_2$. It showed a 2-fold selectivity for the hCB$_2$ receptor. Govaerts et al. showed CP 55,940 to have the opposite effect being more potent at

hCB$_1$ than hCB$_2$. They reported that the expression of CHO-hCB1 was higher than CHO-hCB2 in their experiments potentially explaining this discrepancy (Govaerts et al., 2004).

The classical cannabinoid, CBD showed a maximum decrease in hyperpolarization of less than 10% that of %WIN max in both AtT20-hCB1 and AtT20-hCB2 cells. Our results are consistent with previously published results which have shown that CBD has a very low binding affinity at both receptors. However, Thomas et al, found CBD to be an antagonist at mouse CB$_1$ receptors and to show inverse agonism/ antagonism at hCB$_2$ (Thomas et al., 2007). Δ^9-THC was found to be a partial agonist at the hCB$_1$ receptor having a maximum hyperpolarization of around 60% that of %WIN max. Although it is less efficacious than WIN, it is relatively close in potency with an approximate EC$_{50}$ of 292 and 256 nM respectively highlighting that potency is not directly related to efficacy (or affinity). Δ^9-THC has been reported as a partial agonist (Bayewitch et al., 1995), an inverse agonist (Govaerts et al., 2004), and an antagonist (Bayewitch et al., 1996) throughout the literature for the hCB$_2$ receptor. Δ^9-THC had little to no activity (<30 μM) with a maximum of 22% that of %WIN max in AtT20-hCB2 cells in the fluorescence-based plate reader membrane potential assay. Consistent with this finding, Govaerts also found that although Δ^9-THC could act as an agonist at CB$_1$ (mouse) it was only able to induce a modest inhibition of adenylyl cyclase at CHO-hCB2 (Govaerts et al., 2004). In AtT20-WT cells neither CBD nor Δ^9-THC had an agonist effect, but Δ^9-THC did inhibit the maximum response of 100 nM SRIF by approximately 23% that of the SRIF max. This could be happening for three possible reasons. The first, is that Δ^9-THC is acting as an antagonist at SRIF receptors. Future experiments will need to test if this is the cause by completing full concentration response curves for the inhibition of SRIF and seeing if Δ^9-THC shifts it in a competitive manner. The second, Δ^9-THC may be interfering with G-protein coupling. Future studies to test this would be to administer Δ^9-THC to different receptor types such as the μ-opioid receptor or serotonin

receptors to see if it also blocked those responses. Or thirdly, it could be blocking GIRK directly which could be tested for by using a direct activiator of GIRK, such as SCH-28080, and see if Δ^9-THC blocks that response as well (Walsh, 2011).

2-AG is known to bind to both CB_1 and CB_2 with potencies similar to Δ^9-THC and at higher potencies and efficacies than that of AEA at both receptors (Raphael Mechoulam et al., 2014). 2-AG was confirmed having a similar potency of 274 vs. 292 nM of Δ^9-THC at hCB_1. However, its potency at hCB_2 differed significantly at 330 nM vs. 3.8 μM Δ^9-THC. 2-AG was, however, more efficacious and potent than AEA at both receptors and AEA was more potent and efficacious at hCB_1 than hCB_2 corroborating the previous literature (Gonsiorek et al., 2000; Martin et al., 2002; Showalter et al., 1996).

JWH-018 was of the first SCs to be identified in "Spice" and, therefore, has the most published data both *in vitro* and *in vivo* making it a good reference with which to compare the newer SCs. AM-2201, its fluorinated analogue on the aliphatic side chain, is actually considered a second generation SC but is presented with JWH-018 to establish a reference for halogenated analogues, as this has become a common modification seen in structural evolution after it was reported that AM-2201 possesses psychoactivity at submilligram doses in humans (S. D. Banister et al., 2015). JWH-018 was found to have similar efficacies at both hCB_1 and hCB_2. It is roughly twice as potent as Δ^9-THC at hCB_1, and almost 30 times more potent than Δ^9-THC at hCB_2 though its potencies between the receptors are nearly identical (103 nM, 133 nM). It has been argued that the full agonist activity at the CB_1 receptor, as opposed to partial agonism of Δ^9-THC, may potentially cause the negative psychological side effects linked to the consumption of JWH-018 (Every-Palmer, 2011). Which, therefore, would infer that there would be worse side effects from consuming AM-2201 as it is more potent and efficacious at both hCB_1 and hCB_2 (37 nM, 58 nM). In the case studies presented AM-2201 was usually mixed with JWH-018 or other SCs. Therefore,

it cannot be determined if it does, in fact, have more psychological effects due to a higher potency at hCB_1 (Gurney et al., 2014). Full agonist activity at CB_2, more importantly CB_2 selectivity, may have been present in synthetic compounds like WIN, but WIN was never consumed by humans in clincial trials of any kind and it is unknown what implications CB_2 agonism will have in relation to toxicity and negative health consequences and anything presented will be speculative.

Due to the toxic effects seen among users of SCs, which have been quoted as "more severe and unusual than THC," off target pathways were tested to see if SC promiscuity was contributing to their toxicity (Gurney et al., 2014). TRPV1 and TRPA1, known to be activated by different phyto- and endocannabinoids, have recently been shown to play a role in communication between neurons and in synaptic plasticity in the CNS (Edwards, 2014). They have also been implicated in both the cardiovascular system, pulmonary system and the gastrointestinal system (Fernandes, Fernandes, & Keeble, 2012; Peng & Li, 2010). As these are some of the main areas having detrimental side effects after SC use, TRP channels may be mediating some of the toxic effects.

Positive controls of CAP (TRPV1) and CIN (TRPA1) were performed to verify that using the fluorescence-based plate reader assay to measure the changes in intracellular calcium was a feasible method for testing cation channel activation. Both agonists, in their respective assays, caused an increase of cytosolic calcium, depolarizing the cells. Ionomycin (3 μM), an ionophore which elevates intercellular calcium, was tested on both cell types to determine if dye saturation was occurring. The maximum CIN response was only 63% of the maximum response of ionomycin in hTRPA1 and the CAP maximum was only 35% the of the maximum ionomycin response showing that neither system was undergoing dye saturation (data not shown).

The reference compounds at hTRPA1 have similar reactivity patterns of other assays measuring changes in calcium from the literature. WIN, Δ^9-THC, CBD and 2-AG all showed partial agonism with EC_{50} values in the low micromolar range. In electrophysiological assays of native mouse TRPA1, WIN had an EC_{50} of 25 µM. Similarly, in rat TRPV1 26 µM generated 70-80% response to that of capsaicin in an electrophysiology model (Akopian, Ruparel, Patwardhan, & Hargreaves, 2008). The responses of TRPV1 in our assay was more consistent with the literature in the lack of effect with most of the reference drugs seen at 30-100 µM concentrations. CBD was found to have an effect by Bisogno et al. but this was not replicated in our assay. They used HEK 293 cells with highly expressed TRPV1, which could have more receptor than with the inducible HEK293 line. Similarly, Smart et al. found AEA to be a full agonist at hTRPV1 using a FLIPR assay where it was only a partial agonist in the current study. They too used a stably transfected cell line which discrepancies could again be receptor expression variations (Smart et al., 2000).

The main purpose of this chapter was to verify the use of fluorescence-based plate reader bioassays by showing their validity with positive and negative controls, while also comparing the generated data to literature values. The assays in this chapter will be used in the following chapters to test the reactivity of various structural classes of the "harmful" SCs and their analogues. The compounds in this chapter will be references with which to compare the following data and help in building structural activity relationships profiles.

CHAPTER 4: CANNABIMIMETIC ACTIVITY OF AB-001, SDB-001, AND STRUCTURAL DERIVATIVES

4 CANNABIMIMETIC ACTIVITY OF AB-001, SDB-001 AND STRUCTURAL DERIVATIVES

4.1 SUMMARY

Structure activity relationships (SAR) of published cannabimimetic agonists are thought to be the driving force of the SC rational drug design. Indole and pyrrole-derived cannabinoids, being among the most studied and published, have also had the highest number of derivatives present in SC products. From 2010, adamantane derivatives were identified in drug seizures and several have now been reported present in herbal smoking blends. Pharmacological assessment was done to build systematic SARs to determine the effect on cannabinoid and off-target reactivity by aromatic side chains of various sizes.

4.2 INTRODUCTION

A common trend in the SC revolution are chemical structures that have had their structural core taken from scientific journals or pharmaceutical industry patents (Gurney et al., 2014; Wiley, Marusich, Huffman, Balster, & Thomas, 2011). The patents include cannabinoid receptor binding, activity and sometimes selectivity (Makriyannis & Deng, 2007). It is assumed, by the compounds that actually make it into herbal blend packets, that the clandestine chemists take the backbone of active compounds from these journal articles or patents and add (or remove) components, slightly modifying the structure but hoping to keep the cannabimimetic activity intact. Therefore, novel compounds have been identified in seizures that have yet to have any pharmacological data presented in the literature. Many governments require published proof of cannabimimetic activity before they can schedule these compounds making it important that their pharmacology is evaluated (Food and Drug Administration Safety and Innovation Act).

In 2007, Makriyannis and Deng placed a patent on receptor selective cannabimimetic aminoalkylindoles (Makriyannis & Deng, 2007). Within this patent was the compound AM-1248 (1-((1-methylpiperidin-2-yl)methyl)-1H-indol-3-yl (adamantyl)methanone)), a structure where the naphthalene group of the parent aminoalkylindole was replaced with an adamantane group (Figure 14), showed cannabimimetic activity at both CB_1 and CB_2 with a strong preference for CB_2 (Frost et al., 2010).
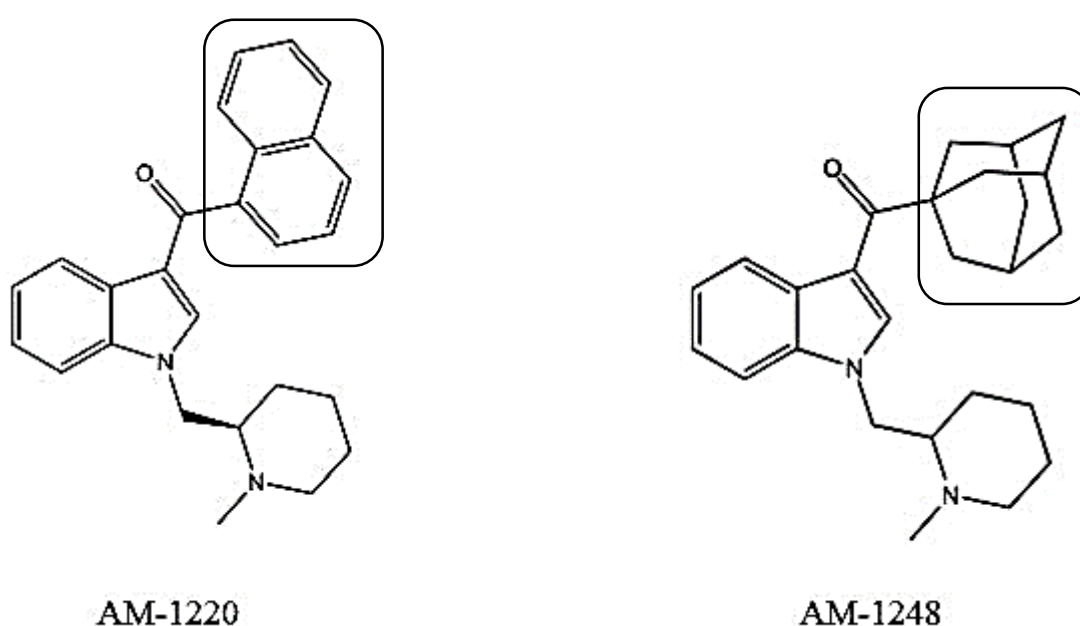
AM-1220   AM-1248

Figure 14: Chemical structures of the AM-1220 and AM-1248. This figure illustrates the structural difference between analogues AM-1220 and AM-1248 where the naphthoyl group (AM-1220) has been replaced with an adamantyl group (AM-1248). AM-1248, therefore, resembles some of the structures investigated in this chapter with the difference being at the $-R^1$ position. Chemical structures were drawn using Chemdraw Professional 15.

In 2010, a derivative of this compound, 3-[(adamantan-1-yl)carbonyl]-1-pentylindole named AB-001, was isolated from the spice brand "Atomic Bomb" (Grigoryev, Kavanagh, & Melnik, 2012). AB-001 was also identified in bulk powders that were seized by the authorities at a Hungarian international airport being transported under the guise of calcium stearate and malic acid. Though it was thought to originate in Ireland,

around the same time, German authorities reported AB-001 to the EMCDDA EWS, thus demonstrating the breadth of its distribution (Jankovics et al., 2012). Little is known about the adverse effects of this drug as the only documented case of consumption was by the scientists identifying the metabolites in their urine. They reported no physiological effects (Grigoryev et al., 2012).

In 2012, another adamantane containing structure referred to as either SB-001, SDB-001, or APICA (N-(adaman-1-yl)-1-pentyl-1H-indole-3-carboxamide) was identified by the National Institute of Health Sciences in Japan (Uchiyama, Kawamura, Kikura-Hanajiri, & Goda, 2012). This compound also shared a similar core (as seen in Table 4 "Backbone") to some compounds found in patents by Makriyannis (Makriyannis & Deng, 2007). SB-001 too had no pharmacological data published until the data presented in this chapter was published by Banister et al. (Appendix B, pg. 305) (S. D. Banister et al., 2013). The synthesis of each compound as well as preliminary data for biotelemetry in mice is presented as well as the some of the pharmacological data presented here. In addition to what was published, data for AtT20-hCB1, HEK293-hTRPV1 and HEK293-hTRPA1 will be presented along with new structural adamantyl, cyclohexyl and phenyl containing analogues to further investigate SAR interactions. Some of these analogues have not yet been identified in the literature and were made using rational drug design by Sam Banister, at the University of Sydney. Drugs that have been published are therefore called by their literature names, whereas any that were synthesized by Sam have the qualifier "SDB". Unpublished analogues were synthesized with the intention of generating pharmacological data for publication, to help further legislation before these new structures have a chance to reach the market as well as to determine more in-depth SAR analysis. All full chemical structures can be found in Appendix A (pg. 254-273), whereas structures are presented in this chapter by backbone and -R groups.
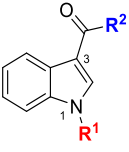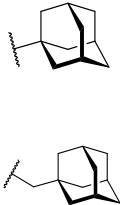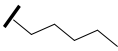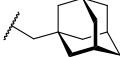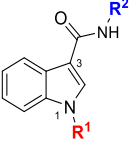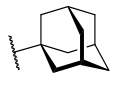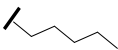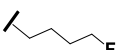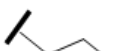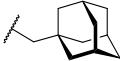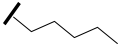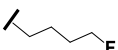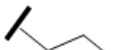
4.3 RESULTS

4.3.1 Cannabimimetic activity at rCB_1, hCB_1 and hCB_2

Using the fluorescence-based plate reader membrane potential assay described in Chapter 2 and verified in Chapter 3, 21 derivatives were tested for their cannabimimetic activity using AtT20-rCB1, AtT20-hCB1 and AtT20-hCB2; 9 adamantane, 6 cyclohexane, and 6 phenyl derivatives. The concentration response curves and control experiments for compounds that are not illustrated within this chapter can be found in Appendix A (pg. 254-273). None of the SCs displayed agonist activity when they were added to AtT20-WT cells. At 10 μM, SDB-007-9 and SDB-011-12 inhibited the maximum response of SRIF (100 nM) between 20-27% SRIF max. The rest of the compounds had a maximum inhibition of ≤18% SRIF max. As outlined in Chapter 3, these drugs are potentially decreasing the SRIF response due to: weak antagonist activity at the SRIF receptors, interference with G-coupling, or a direct blockage of the GIRK channel; but further experiments are needed to determine the exact cause.
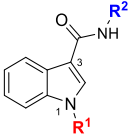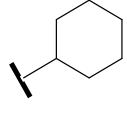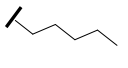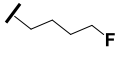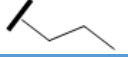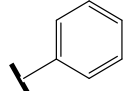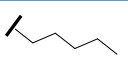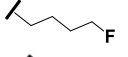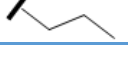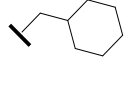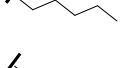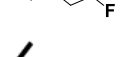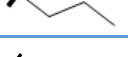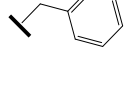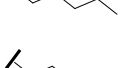
Table 4 shows a comparison of the functional data as listed by adamantane linker and R-group at the 1-indole position. Table 5 shows a comparison of the functional data as listed by cyclohexane or phenyl linker and R-group at the 1-indole position Selectivity was calculated in terms of potency by a ratio of pEC_{50} values and presented as whichever ratio CB_1 vs. CB_2 had a value higher than 1.

Table 4: Functional agonist activity of adamantyl derivatives at the cannabinoid receptors. This table compares the agonist activity of the adamantyl derivatives at CB_1 receptors (both rat and human) and hCB_2. They are separated by similarities in functional groups $-R^1$ and $-R^2$ for easier comparison. Data represent mean values $\pm$ SEM from 4-7 experiments each run in duplicate.

Backbone	R2	R1	NAME	AtT20-rCB1		AtT20-hCB1		AtT20-hCB2		SEL.
				pEC_{50}	E_{Max} (%WIN)	pEC_{50}	E_{Max} (%WIN)	pEC_{50}	E_{Max} (%WIN)	human
			AB-001	7.5 ± 0.1	92 ± 5	6.8 ± 0.1	100 ± 8	7.83 ±0.16	85 ± 5	CB₂ 10.4
			AB-002	7.0 ± 0.1	91 ± 6	6.1 ± 0.1	89 ± 7	7.4 ± 0.1	82 ± 7	CB₂ 8.5
			SDB-001	7.42 ±0.06	97 ± 7	6.89 ±0.06	100 ± 5	7.50 ±0.05	90 ± 10	CB₂ 4
			STS-135	N.T.	N.T.	7.29 ±0.12	123 ± 8	7.88 ±0.26	114 ± 12	CB₂ 3.9
			SDB-013	7.2 ± 0.2	84 ± 7	6.4 ± 0.2	97 ± 8	7.5 ± 0.2	68 ± 1	CB₂ 14.4
		CH₃	SDB-107	N.T.	N.T.	6.8 ± 1.7	21 ± 12	7.0 ± 0.1	86 ± 7	CB₂ 1.6
			SDB-002	7.54 ± 0.1	84 ± 6	6.65 ±0.09	54 ± 4	7.2 ± 0.3	23 ± 4	CB₂ 3.7
			SDB-008	N.T.	N.T.	6.56 ±0.16	87 ± 8	6.69 ±0.12	39 ± 3	CB₂ 1.3
			SDB-014	6.12 ±0.21	33 ± 5	8.5± 0.6	17 ± 3	6.2± 2.6	33 ± 3	CB₁ 21

N.T. = Not Tested

Table 5: Functional agonist activity of phenyl and cyclohexyl derivatives at the cannabinoid receptors. This table compares the agonist activity of the phenyl and cyclohexyl derivatives at CB_1 receptors (both rat and human) and hCB_2. They are separated by similarities in functional groups $-R^1$ and $-R^2$ for easier comparison. Data represent mean values $\pm$ SEM from 4-7 experiments each run in duplicate.

Backbone	R2	R1	NAME	AtT20-rCB1		AtT20-hCB1		AtT20-hCB2		SEL
				pEC_{50}	E_{Max} (%WIN)	pEC_{50}	E_{Max} (%WIN)	pEC_{50}	E_{Max} (%WIN)	human
	(cyclohexyl)		SDB-003	7.42 ±0.15	93 ± 7	6.82 ±0.06	83 ± 3	6.98 ±0.08	95 ± 5	CB$_2$ 1.4
			SDB-009	N.T.	N.T.	7.1 ± 0.1	104 ± 7	7.53 ±0.06	84 ± 3	CB$_2$ 2.5
			SDB-015	6.04 ± 0.4	79 ± 2	5.66 ± 2.2	22 ± 2	6.93 ±0.01	115.5 ± 10	CB$_2$ 18.7
	(phenyl)		SDB-005	7.7 ± 0.1	99 ± 6	6.98 ±0.07	100 ± 4	6.8 ± 0.01	74 ± 6	CB$_1$ 1.4
			SDB-011	N.T.	N.T.	6.83 ±0.13	92 ± 7	6.87 ±0.09	67 ± 4	CB$_2$ 1.1
			SDB-017	>10 μM	12 ± 8 at 10 μM	>10 μM	17 ± 2 at 10 μM	6.5 ± 0.7	47 ± 15	CB$_2$
	(cyclohexylmethyl)		SDB-004	7.8 ± 0.2	93 ± 9	6.73 ±0.06	106 ± 4	6.65 ±0.09	71 ± 4	CB$_1$ 1.2
			SDB-010	N.T.	N.T.	7.39 ±0.06	104 ± 4	7.20 ±0.12	84 ± 4	CB$_1$ 1.5
			SDB-016	6.53 ±0.08	50 ± 3	4.53±0.06*	40 ± 1	7.00± 0.13	65 ± 5	CB$_2$ 38
	(benzyl)		SDB-006	7.7 ± 0.1	84 ± 5	7.0 ± 0.09	97± 6	6.9 ± 0.2	68 ± 9	CB$_1$ 1.4
			SDB-012	N.T.	N.T.	7.30 ±0.09	87 ± 4	6.9 ± 0.1	61 ± 4	CB$_1$ 2.4
			SDB-018	6.8 ± 0.3	20 ± 4	7.1 ± 0.8	29 ±12	6.8 ± 0.4	46 ± 10	CB$_1$ 2

N. T. = Not Tested

4.3.1.1 Differences between AtT20 rat and human CB1

Only a portion of the structures tested in this chapter had their interactions in AtT20-rCB1 and AtT20-hCB2 published in Banister et al. (Appendix B, pg. 305) (S. D. Banister et al., 2013). AtT20-hCB1 values in later papers had the nonlinear regression fit constrained to zero. Therefore, to allow direct comparison with AtT20-rCB1 data, the AtT20-rCB1 data was reanalysed and constrained to zero. This accounts for the small variance seen between the numbers presented here and the numbers presented in that paper. All compounds tested for both receptors showed a difference in potency and most in efficacy between rCB$_1$ and

hCB$_1$. The compounds with the same efficacies for both receptors were AB-002, SDB-001, SDB-005 and SDB-017. Rank orders were determined for both potency and efficacy to highlight the differences in their reactivity.

AtT20-rCB1 Rank order for potency:

SDB-004≥SDB-005=SDB-006≥SDB-002>AB-001≥SDB-003=SDB-001>SDB-013>AB-002≥SDB-018>SDB-016>SDB-014≥SDB-015>SDB-017

AtT20-hCB1 Rank order for potency:

SDB-014>SDB-018=SDB-006=SDB-005≥SDB-001=SDB-003=AB-001≥SDB-004=SDB-002≥SDB-013>AB-002>SDB-015>SDB-016>SDB-017

AtT20-rCB1 Rank order for efficacy:

SDB-005=SDB-001≥SDB-003=SDB-004=AB-001=AB-002>SDB-006=SDB-002=SDB-013≥SDB-015>SDB-016>SDB-014≥SDB-018>SDB-017

AtT20-hCB1 Rank order for efficacy:

SDB-004≥SDB-005=SDB-001=AB-001=SDB-006=SDB-013>AB-002=SDB-003>SDB-002>SDB-016>SDB-018=SDB-015≥SDB-014=SDB017

All compounds tested for both CB$_1$ receptors were less potent at rCB$_1$ than WIN (pEC$_{50}$ = 8.2 ± 0.1). With the exception of AB-002, SDB-013, SDB-015, SDB-016 and SDB-017, the rest of the compounds tested were more potent than WIN (pEC$_{50}$ = 6.55 ± 0.06) at hCB$_1$. The main similarity between the compounds less potent than WIN at hCB$_1$, excepting AB-002, was an N-propyl group in the -R^1 position. Figure 15 shows select examples of concentration response curves highlighting the differences in potency between the two receptors. Six compounds had a similar efficacy to WIN at rCB$_1$: AB-001, AB-002, SDB-001, SDB-003, SDB-004 and SDB-005. At hCB$_1$, four compounds (STS-135, SDB-004, SDB-009, and SDB-

010) exceeded the maximum efficacy of WIN with STS-135 (10 μM) having a 23% greater maximal response. SDB-001, SDB-005 and SDB-011 also had similar efficacies to that of WIN at hCB_1 with the rest showing partial agonist activity.
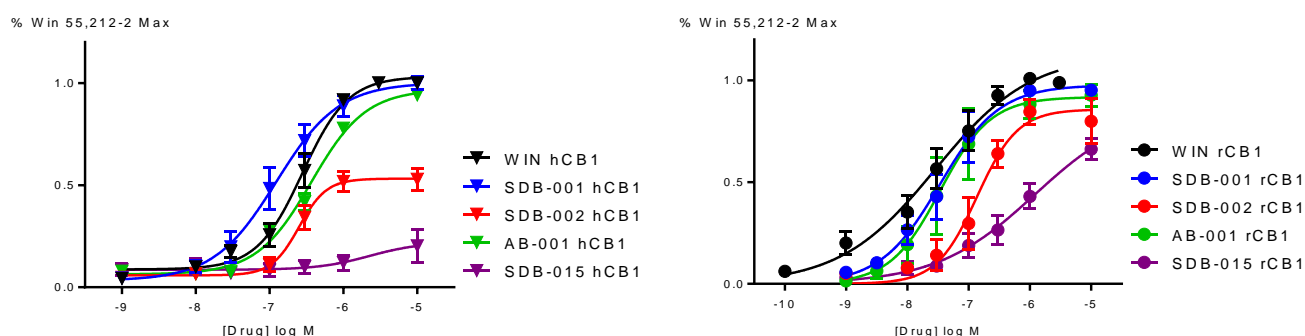
Figure 15: Comparison of concentration responses for WIN, SDB-001, SDB-002, AB-001 and SDB-015. This figure illustrates the concentration response curves of select compounds that showed differences in activity between the rCB_1 (left) and the hCB_1 (right) receptors. Data represent mean values ± SEM from 4-7 experiments each run in duplicate.

4.3.1.2 Comparison of agonist activity at hCB_1 and hCB_2

All 21 compounds showed agonist activity at hCB_2 and, with the exception of SDB-017, hCB_1. SDB-004, SDB-005, SDB-006, SDB-010, SDB-012, SDB-014 and SDB-018 were more potent at hCB_1 and, therefore, hCB_1 selective. The majority of this group, excluding SDB-014 and SDB-018, contain a pentyl or 5-fluoropentyl chain as the $-R^1$ group. They also contain, in all but SDB-005, a nitrogen containing, 4 bond length linker from the 3 carbon on the indole group. The remaining compounds all showed hCB_2 selectivity ranging from 1.1 to 38. This is similar to other aminoalkylindole SCs, WIN and JWH-018 with a CB_2 selectivity of 4.7 and 1.3 respectively. SDB-014, SDB-015, SDB-016,

SDB-017, SDB-018 and SDB-107 all showed low efficacy at hCB_1 with efficacies less than or equal to 40% the maximum response of WIN. All of these CB_2 selective compounds contain an *N*-propyl or *N*-methyl substituent on the indole ring as the -R^1 group. Although SDB-107 had low efficacy at hCB_1, it was a potent and efficacious agonist at hCB_2 which is represented in Figure 16. SDB-002, SDB-008 and SDB-014 showed low efficacy at hCB_2 with efficacies less than or equal to 40% the maximum response of WIN, and all contain the adamantane group extended further from the indole ring than SDB-001, for example, by a methylene spacer. By contrast, AB-002 is comprised of an adamantane group at a distance from the indole ring that is equal to SDB-001 and its R^1-modified analogues, whereas AB-001 contains the adamantane group even closer to the indole 3-position. It is likely that both the nature of the 3-indole linker, length of -R^1 substituent, and the protrusion of the -R^2 group are important determinants of hCB_2 efficacy.
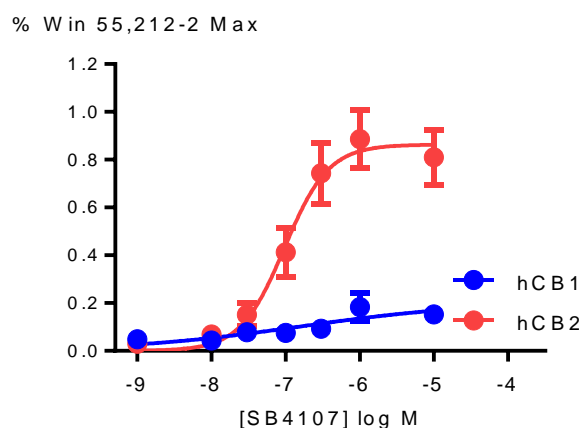
Figure 16: Concentration response curves of SDB-107. The figure illustrates the concentration response curves for SDB-107 shown as the percent of the maximum response of WIN at hCB_1 (blue) and hCB_2 (red). Data represent mean values ± SEM from 4-6 experiments each run in duplicate.

4.3.1.2.1 *How distance between indole 3-position and -R² group affected potency and efficacy*

Within the different structural derivatives, the connection between the indole 3-position and the -R^2 group is either an acyl (C=O), carboxamide (C(=O)NH), or carboxylate (C(=O)O) linker with a distance of either 2 or 4 bond lengths. A trend appeared in the structures with an adamantane in the -R^2 position. Adamantane derivatives showed reduced efficacy at both hCB_1 and hCB_2 when there was a methylene spacer between the carboxamide and the polycycle, as seen in structures SDB-002, SDB-008, SDB-014, when compared to the *N*-adamantyl carboxamides SDB-001, STS-135, SDB-013 and SDB-107. Figure 17 demonstrates this relationship in AtT20-hCB2. The potency also decreases almost 10-fold at hCB_2 between the methylene-spaced and non-spaced carboxamide analogues. This trend was not seen within the cyclohexane or phenyl -R^2 groups as their efficacy and potency remained reasonably consistent. Of the highest potency drugs at hCB_1, most (with the exception of fluorinated compounds) all contained a methylene-spaced carboxamide. Dissimilarly, all the highest potency drugs at hCB_2 had a non-spaced pendant group.
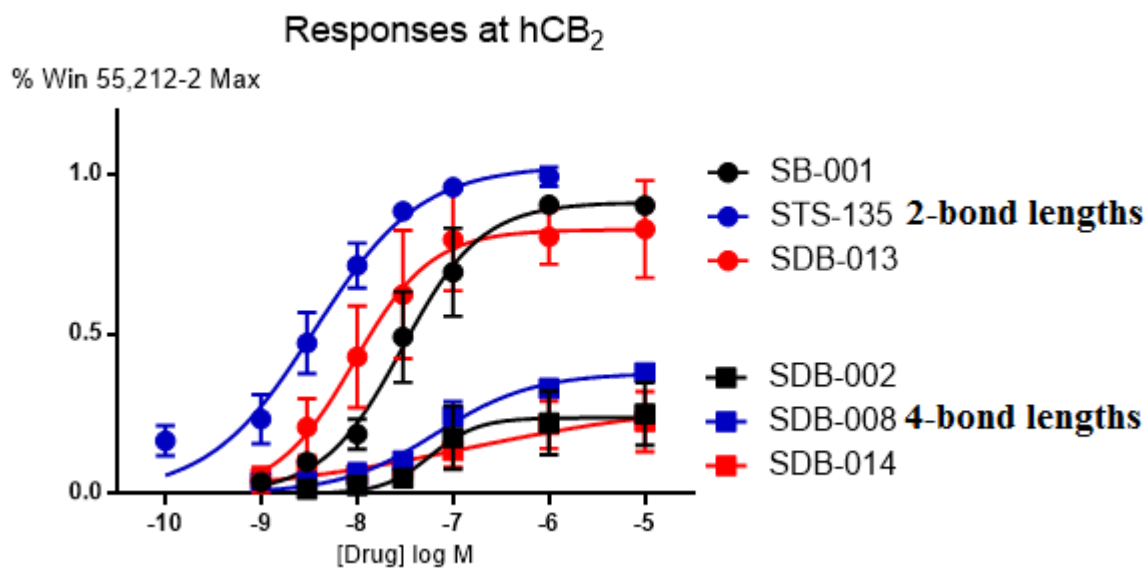
Figure 17: Concentration response curves for SDB-001, STS-135, SDB-013, SDB-002, SDB-008 and SDB-014 at hCB$_2$. It illustrates the efficacy decrease at hCB$_2$ **exhibited by compounds with** that have the $-R^2$ substituent at a distance of 4 bond lengths away from **the 3-indole carbon and the adamantane group compared with the compounds** with a 2 bond length distance. Data represent mean values ± SEM from 4-6 experiments each run in duplicate.

4.3.1.2.2   How the length of the -R^1 alkyl group affected potency and efficacy

The effect caused by varying lengths of the -R^1 group did not have consistent trends across receptor types having more of an apparent effect on potency and efficacy at hCB$_1$. SDB-107, seen in Figure 16, loses almost all hCB$_1$ efficacy when the alkane chain is truncated to a methyl group with a maximum 22% when compared to % WIN max. All structures, with the exception of SDB-013, had a greater efficacy at hCB$_1$ when the -R^1 group was a pentyl chain. This trend was not seen with potency as the highest potency derivative, SDB-014, had an *N*-propyl -R^1 group even though it was the second least efficacious ligand. At hCB$_2$, there were no consistent trends in either potency or efficacy. Four of the five most potent and efficacious compounds at hCB$_2$ had a pentyl -R^1 group.

4.3.1.2.3   *How the size of the -R^2 sgroup affected potency and efficacy*

The steric bulk of the pendant -R^2 group had no effect on activity at either hCB$_1$ or hCB$_2$ as all derivatives retained cannabimimetic activity. The four most potent compounds at hCB$_2$ (AB-001, STS-135, SDB-001 and SDB-013) did contain an adamantane group. Three of the four most efficacious compounds at hCB$_1$ contained a cyclohexane group (SDB-004, SDB-009 and SDB-010). There were no other clear trends based on -R^2 size alone.

4.3.1.2.4   *How fluorination of the -R^1 alkyl group affected potency and efficacy*

The addition of a terminal fluorine to the end of the -R^1 pentyl chain, as seen with STS-135 and SDB-008–SDB-012, had similar effects in both AtT20-hCB1 and AtT20-hCB2. Potency remained constant, meaning no significant difference (≤0.3 change in pEC$_{50}$) between the fluorinated compound and the corresponding des-fluoro analogue, with SDB-008 and SDB-011 at hCB$_1$. SDB-011, as well as SDB-010 and SDB-012, also remained constant in efficacy (≤10% change) at hCB$_1$. The rest of the compounds had an increase in both potency and efficacy at hCB$_1$. Similarly, at hCB$_2$, SDB-012 remained constant in potency and efficacy as well as SDB-009 and SDB-011 in only efficacy. The rest had an increase in both potency and efficacy, with the exception of SDB-008 which decreased in potency by 5-fold when the *N*-pentyl chain was fluorinated. The increase in potency and efficacy that was seen in most of the compounds tested is a similar effect to that seen with JWH-018 and its fluorinated analogue AM-2201 (shown in Chapter 3).

4.3.2 Activity at TRP Channels

A fluorescence-based plate reader assay was used measure the change in intracellular calcium as described in Chapter 2 and verified in Chapter 3. Two of the 21 compounds had weak agonist activity at hTRPV1, SDB-008 and SDB-010. They had a maximum increase at 30 µM of 18 and 11% respectively to that of %CAP max. Compounds SDB-004, SDB-005, SDB-008, SDB-010, SDB-011 and SDB-016 had weak antagonist activity shown by inhibition of the response of 300 nM CAP by between 11 and 20% that of %CAP max. No activity, agonist or antagonist, was substantial enough to warrant further experiments.

Eleven of the 21 compounds had at least partial agonist activity at the highest concentration tested (30 µM) at hTRPA1, shown in Table 6. Three compounds, SDB-004, SDB-005 and SDB-010; showed high efficacy similar to that of cinnamaldehyde (Figure 18 A). SDB-006, SDB-009, SDB-013, SDB-016 and STS-135 showed mid-range efficacy (50%-80% that of % CIN max) as shown in Figure 18 (B). SDB-001, SDB-003 and SDB-014 showed low efficacy at less than 45% that of CIN max response as seen in Figure 18 (C).
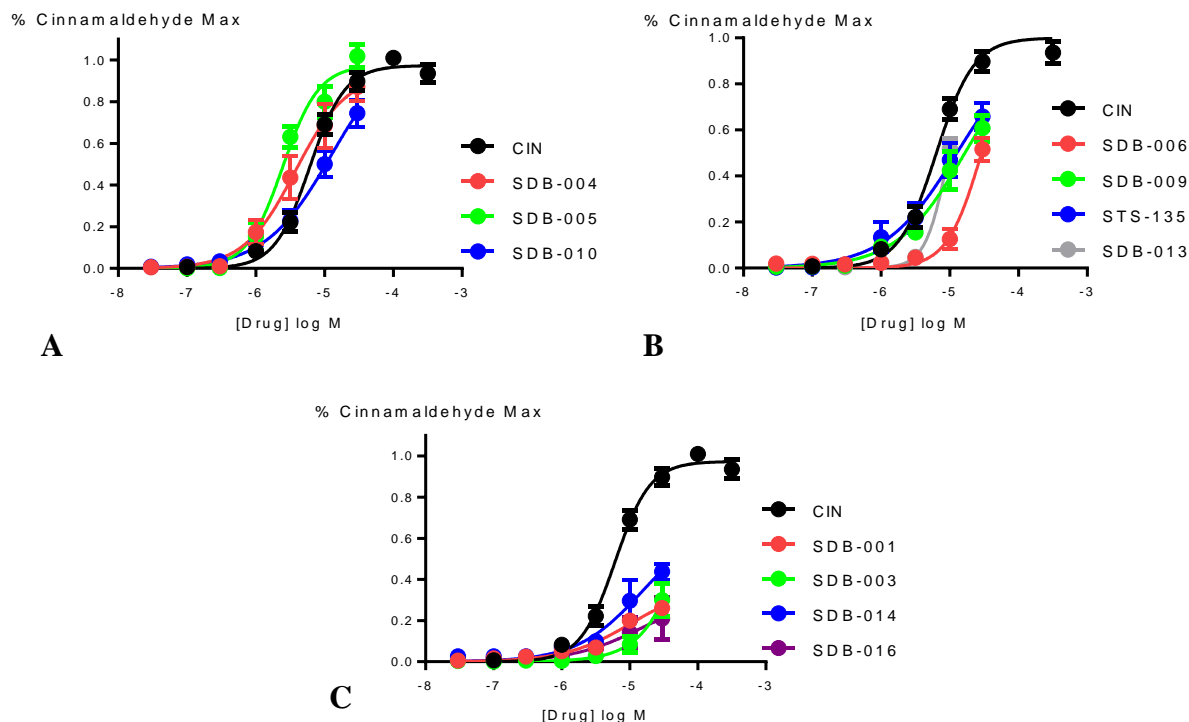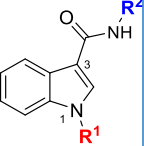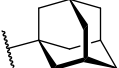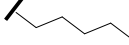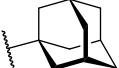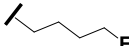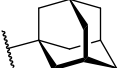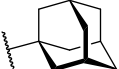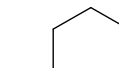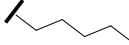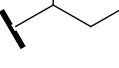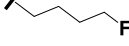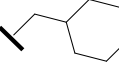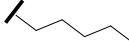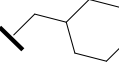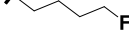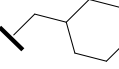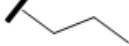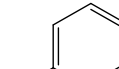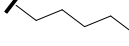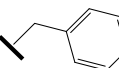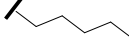
Figure 18: Concentration response curves for all compounds with agonist activity at hTRPA1. This figure illustrates the concentration response curves of compounds showing substantial agonist activity at hTRPA1 compared to CIN. A.) Shows compounds with similar efficacy to that of CIN (95-100% that of CIN max) B.) Shows compounds with modest agonist activity (50-80% that of CIN max) and C.) Shows low efficacy agonists (≤45% that of CIN max). Data represent mean values ± SEM from 6-10 experiments each run in duplicate.

Agonist efficacy ranged from approximately 30% to 110% that of the CIN max. SDB-013 due to poor solubility could only be tested to 10 μM. The rest were constrained to 30 μM by solubility. Potency and efficacy values for compounds with agonist activity are presented in Table 6.

Table 6: Functional agonist activity at hTRPA1. This table shows compounds that had substantial agonist/partial agonist activity at hTRPA1. They are separated by similarities in functional groups $-R^1$ and $-R^2$ for easier comparison. Maximum agonist/antagonist data for hTRPV1 has been provided where applicable. Data represent mean values $\pm$ SEM from 6-10 experiments each run in duplicate.
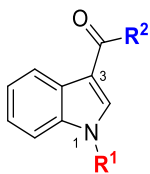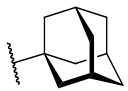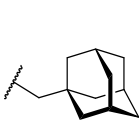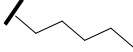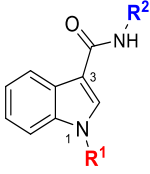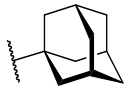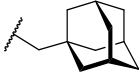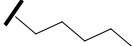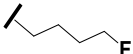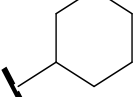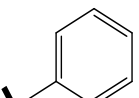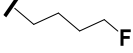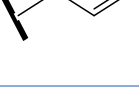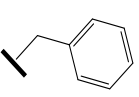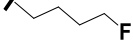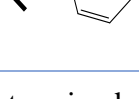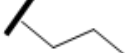
Backbone	R2	R1	NAME	HEK293-hTRPV1		HEK293-hTRPA1	
				Max Response at 30 µM (%CAP)	Max Inhibition of 300 nM CAP (%CAP)	pEC_{50}	Max Response at 30 µM (%CIN)
			SDB-001	<10	N.D.	4.0 ± 0.1*	31 ± 10
			STS-135	<10	≤10	4.92 ± 0.07*	66 ± 7
			SDB-013	<10	<5	5.0 ± 0.01*	55 ± 13
			SDB-014	<1	≤10	4.32 ± 0.14*	44 ± 4
			SDB-003	<5	<5	4.2 ± 0.1*	30 ± 10
			SDB-009	<10	<5	5.1 ± 0.2	77 ± 17
			SDB-004	<5	20%	5.61 ± 0.06	98 ± 5
			SDB-010	12 ± 1	12%	4.9 ± 0.3	109 ± 3
			SDB-016	<1	15%	4.55 ± 0.05*	53 ± 10
			SDB-005	<5	20%	5.42 ± 0.16	94 ± 5
			SDB-006	<1	<10	4.54 ± 0.02*	52 ± 6

*pEC_{50} assuming that the maximum is equivalent to the maximum of CIN

Agonist potency ranged from pEC_{50} 4 – 5.6 (2.4-30 µM) compared to that of CIN (pEC_{50} = 5.21 $\pm$ 0.04). SDB-004 and SDB-005 had higher potencies with pEC_{50} values of 5.61 $\pm$ 0.06 and 5.42 $\pm$ 0.04 respectively. Therefore, they are the only two compounds with similar

reactivity profiles as CIN being both potent and efficacious agonists. The rest of the compounds tested showed little to no activity at 30 µM on hTRPA1 as shown in Table 7.

Table 7: Maximum Responses of compounds with very weak or no agonist activity at hTRPA1. This table shows the compounds that had either no agonist activity at 30 µM or weak agonist activity that was too low to warrant full concentration response curves to be generated. Data represent mean values ± SEM from 6-10 experiments each run in duplicate.

Backbone	R2	R1	NAME	HEK293-hTRPV1		HEK293-hTRPA1	
				Max Response at 30 µM (%CAP)	Max Inhibition of 300 nM CAP (%CAP)	pEC_{50}	E_{Max} (%CIN)
(indole-3-acyl backbone with O, R2, N-R1)	*(adamantyl)*	*(hexyl chain)*	AB-001	<10	<10	N.D.	<5
	(adamantyl-methylene)		AB-002	<10	N.C.	N.D.	<5
(indole-3-carboxamide backbone with O, NH-R2, N-R1)	*(adamantyl)*	CH_3	SDB-107	<5	≤10	N.D.	<5
	(adamantyl-methylene)	*(hexyl chain)*	SDB-002	<1	N.C.	>30µM	18 ± 3
		(fluoropentyl chain, F)	SDB-008	18 ± 1	13	>30µM	11 ± 10
	(cyclohexyl-methylene)	*(pentyl chain)*	SDB-015	<1	<10	N.D.	<10
	(benzyl/phenyl-methylene)	*(fluoropentyl chain, F)*	SDB-011	<10	11	N.D.	<10
		(butyl chain)	SDB-017	<1	≤10	N.D.	<5
	(phenethyl-methylene)	*(fluoropentyl chain, F)*	SDB-012	<5	N.C.	N.D.	<10
		(pentyl chain)	SDB-018	<1	≤5	N.D.	<5

N.D. = Not Determined   N.C. = No Change

Of the derivatives that showed agonist activity, the carboxamide linker seems to be necessary but not sufficient. The distance between the pendant amide group and the indole ring seems to be irrelevant in terms of potency and efficacy, as compounds containing both linker lengths were strong agonists, though the majority of the agonists (7 of 11) had non-methylene spaced amide substituents. Pentyl -R^1 groups showed increased potency and efficacy, but this subunit was not a necessity for binding. Propyl, pentyl, and fluoropentyl -R^1 groups and variously sized -R^2 groups were also tolerated. A terminal fluorine atom was found in 3 of the 5 most efficacious, and 2 of 5 most potent, agonists. Not all fluorine containing compounds had activity, suggesting that fluorine may enhance efficacy in cases where the des-fluoropentyl analogue is already active.

4.4 DISCUSSION

The implications of adding an adamantane group to the indole structure of known SCs, as was found in several compounds reported to the EWS of the EMCDDA (AB-001 and SDB-001) had yet to be fully explored. In this chapter, AB-001, SDB-001, and seven other adamantane derivatives were tested on AtT20-rCB1, AtT20-hCB1 and AtT20-hCB2 to determine their cannabimimetic activity. To further evaluate the effect of having a bulky -R^2 group (like adamantane) on activity, derivatives containing smaller alicyclic (cyclohexane) or aromatic (phenyl) groups were synthesized and tested on the same receptors for comparison. The 21 compounds, in total, were then tested on hTRPV1 and hTRPA1 to determine off-target effects.

Due to genetic similarity, availability and to provide a comparison between *in vitro* and *in vivo* experiments, the rat CB_1 receptor has been used to test cannabinoid activity since it was cloned in 1990. The human and rat cannabinoid receptor only differ from each

other by 2.7% (13 residues out of 473) (Matsuda et al., 1990). Although they differ by a small percentage, it has been proven that altering a receptor by even one residue can vastly change how ligands bind and as a result how the receptor signals (Song, Slowey, Hurst, & Reggio, 1999). Many studies have confirmed that these cells are functional and have "grossly similar" signalling properties (Felder et al., 1995; Guo & Ikeda, 2004; Straiker et al., 2012). When comparing receptors with similar signalling profiles, a difference in response could be due to differences in receptor expression. This would mean if one receptor is expressed less than the other, there would be less "spare receptors" available for binding and the response profile would decrease proportionally (Straiker et al., 2012). In section 4.3.1.1, rank orders were established for both efficacy and potency at rCB_1 and hCB_1. Half of the compounds (9/18) were ranked differently in terms of potency whereas 11 were ranked differently in terms of efficacy. This suggests that these compounds are binding differently to the human versus rat CB_1 receptor. A result that supports the finding of Straiker et al. that signaling between hCB_1 and rCB_1 is quantitatively very different (Straiker et al., 2012). Additional testing is needed to further confirm binding differences by assessing their secondary messenger systems.

How a ligand interacts with a receptor is a combination of both chemical and geometric interactions. These interactions include electrostatic, such as hydrogen bonds and π-π aromatic interactions, as well as mutual spatial complementarity exhibited by van der Waals forces. In G-protein coupled receptor interactions, the ligand has to be transferred from the extracellular aqueous environment to the binding site crevice in the transmembrane domain. This differs from water soluble proteins as this interaction occurs apart from bulk water. Due to this difference, hydrophobic effects and desolvation penalties become important for ligand-receptor interactions and, in the case of transmembrane proteins like G-protein coupled receptors, transport proteins or ion channels; ligands must be almost

entirely desolvated before they can enter the binding site crevice (González et al., 2011). The hydrophobic effect describes how hydrophobic entities, when placed in a polar environment, decrease entropy by creating stronger bonds between the polar molecules as they reform to encompass the hydrophobic molecule. Hydrophobic entities aggregate, therefore, reducing the amount of energy disruptions. This is contributed to the polar solvent encompassing a smaller surface area than if it encompassed each individual hydrophobic molecule (Bissantz, Kuhn, & Stahl, 2010). Desolvation is the enthalpy penalty associated with the amount of energy it takes to break the bonds between polar ligand and their aqueous environments so new interactions can form with the receptor. A favourable interaction enthalpy, therefore, means the energy lost when breaking the polar bonds is less than the energy it takes to form a new bond. Desolvation entropy, on the other hand, is increased when water molecules are released as both the drug and the binding cavity are desolvated mainly seen in interactions with hydrophobic groups (Freire, 2008).

Cannabinoid receptors 1 and 2 both exhibit enthalpy-entropy compensation, meaning a change in one is balanced by a change in the other, and that their binding equilibrium is enthalpy driven for antagonists and entropy driven for agonists (Merighi, Simioni, Gessi, Varani, & Borea, 2010). In line with the principles of hydrophobicity, desolvation and energy compensation, for a cannabinoid to have optimal binding, it would not only be in a conformation that has a good "fit" for the receptor binding site, but it would also have sufficient numbers of hydrophobic substituents to offset the desolvation penalty associated with the polar compounds present. 3D-QSAR studies for CB_1 and molecular modelling for CB_2 have shown that at least two hydrogen bonds (in the case of classical cannabinoids) are needed for an agonist to have significant affinity, though the residues with which the ligand forms the hydrogen bonds are different at each receptor (Feng et al., 2014; Mella-Raipan et al.). Mutation models have also shown that cannabimimetic indoles

bind to residues within the receptor binding site that differ from those binding classical cannabinoids, relying more on aromatic-aromatic interactions than hydrogen bonding (J. W. Huffman & Padgett, 2005). The CB_2 receptor also has an additional aromatic residue when compared to CB_1, potentially contributing to the CB_2 selectivity often demonstrated by aminoalkylindoles (R.G. Pertwee, 2006; Song & Bonner, 1996). This means that polar entities are not essential for indole binding, but may suggest that polar compounds within some indole SC structures are potentially tolerated due to the additional side groups with high hydrophobicity and aromatic character, both of which are essential to CB_1 and CB_2 binding (Mella-Raipan et al.; Stern et al., 2006). Adamantane, cyclohexane and phenyl groups are all highly hydrophobic (Stern et al., 2006). Their presence as $-R^2$ groups may have allowed for tolerance of the addition of the polar carboxamide by reducing desolvation while also contributing aromatic-aromatic interactions (in the case of the phenyl derivatives).

In determining the effect of the size of the $-R^2$ side group, steric bulk seemed to have little effect on the cannabimimetic activity since all compounds containing an adamantane unit were agonists at both hCB_1 and hCB_2, with comparable potencies to the highly efficacious and potent WIN. Substituting the bulky adamantane group for smaller alicyclic and aromatic groups was also tolerated at hCB_1, with the potencies and efficacies of these analogues similar to those of WIN and the adamantane derivatives. The only decreases in potency in compounds with smaller $-R^2$ groups included a truncated $-R^1$ side chain. At hCB_2, potency remained constant between the adamantane and smaller $-R^2$ groups, though there was an overall decrease in efficacy in the compounds with smaller $-R^2$ groups.

A study on cannabimimetic activity of biphenylic carboxamides by Bertini et al. showed that a cyclohexane group attached to a carboxamide perfectly fills the hydrophobic

pocket of the CB$_2$ receptor when in conjunction with a n-butyl group off the biphenyl group (in the same orientation as the indole *N*-alkyl group) therefore, many of these compounds showed CB$_2$ selectivity (Bertini et al., 2015). Similarly, the highest efficacy compound at hCB$_2$, SDB-015, contains a methylene-spaced cyclohexyl carboxamide group with an *n*-butyl -R^1 chain. Cyclohexane as an -R^2 group also showed a trend for CB$_2$ preference, except for SDB-004 and SDB-010, which were only slightly more CB$_1$ selective. Their pEC$_{50}$ values only differing by 0.8 and 0.19 respectively between hCB$_1$ and hCB$_2$.

Huffman et al. has also determined cannabimimetic activity for 3-phenylacetyl indoles, only differing from the derivatives tested that contained an -R^2 phenyl group by replacement of the carboxamide linker with an acetyl linker. Huffman et al. found that in contrast to many of the cannabimimetic indoles that show CB$_2$ selectivity, these compounds showed a 5-fold CB$_1$ selectivity (J. W. Huffman et al., 2005). With the exception of SDB-011, whose potency between hCB$_1$ and hCB2 only differed by a pEC$_{50}$ of 0.04, the rest of the compounds with a phenyl -R^2 group were CB$_1$ selective. SDB-017 showed little cannabimimetic activity at hCB$_1$ but this may be due to its truncated -R^1 group more than the phenyl side chain.

Seven of the nine most potent compounds at hCB$_2$ were adamantane derivatives. In previous experiments done by Lu et al., adamantane groups have been substituted for the alkane side chain seen on classical cannabinoids like Δ^8-THC (Lu et al., 2005). Lu et al. confirmed that the presence of an adamantane side group was tolerated by both CB$_1$ and CB$_2$ but that receptor selectivity was dependent on the orientation of the adamantane group with respect to the tricyclic component of the classical cannabinoid on the basis of the allowable conformational space of each substituent (Lu et al., 2005). They found that both the carbon at which the adamantane is attached and the ability for rotation about the linker

had significant effects on binding and selectivity. Attaching the adamantane at the 1-carbon had CB_1 selectivity whereas an adamantane attached at the 2-carbon was CB_2 selective (Lu et al., 2005). This difference in adamantane attachment is present between AB-001 (1-carbon) and AB-002 (2-carbon) but the trend was not reproduced with the indole core SCs as both compounds were CB_2 selective. Interestingly, all nine of the adamantane derivatives were hCB_2 preferring. Frost et al. has shown that 3-cycloalkyl-ketones with adamantane substituents are high affinity and highly selective CB_2 agonists which was confirmed with both binding and FLIPR assays in HEK293 cells with the human CB_2 receptor (Frost et al., 2010).

Frost et al. also confirmed what Huffman et al. had previously established; that an *N*-propyl substituent at the 1-indole position confers CB_2 selectivity, as opposed to an *N*-pentyl chain which optimizes selectivity for CB_1 (Frost et al., 2010; John W Huffman, Dai, Martin, & Compton, 1994). Rat *in vivo* studies showing that a four to six carbon chain at the 1-indole position was also optimal for CB_1-mediated hypothermic and bradycardic activity (Wiley et al., 1998). This trend is also corroborated by this data set. All compounds, except for SDB-013, that contained an *N*-butyl group had an efficacy less than 40% that of WIN max at the hCB_1 receptor. Activity at hCB_2 had less dependence on the length of the R^1 side chain having strong potency and efficacy at all lengths. Reducing the *N*-propyl to an *N*-methyl also created a highly CB_2 selective agonist with little to no activity at hCB_1 or off target pathways. This could have implications for medicinal chemistry as potent highly selective CB_2 agonists are sought out for their potential uses in the treatment of pain, cancer and regulation of nociception (Whiteside, Lee, & Valenzano, 2007).

As previously stated, Lu et al. found that rotation around the linker bond decreased binding affinity at both CB_1 and CB_2 because it allowed the adamantane to interact with

multiple conformational spaces. When the linker bond was held rigid with a double bond the adamantane derivatives showed strong CB_2 binding affinity (Lu et al., 2005). The carboxamide linker creates a double bond character between the C-N on the carbonyl restricting its rotation. This is the case with all carboxamide compounds lacking a methylene spacer in the $-R^2$ group, with the exception of SDB-005. Incorporation of a methylene spacer adds a rotatable C-C bond between the carboxamide and the $-R^2$ group, allowing greater conformational freedom about that bond. If these SCs are interacting similar to classical cannabinoids, there would be a decrease in binding at both receptors due to the ability of a given compound to occupy a larger range of conformational states. Although the adamantane groups with a methylene spacer all remained CB_2 preferring, which may be due to hydrophobicity, they did show decreased efficacy at hCB_2. SDB-016 was the only compound that contained both a smaller $-R^2$ group and a methylene spacer, and was CB_2 preferring, but its pEC_{50} only differed by 0.18 between CB_1 and CB_2.

Terminal fluorination of the pentyl chain of nonclassical cannabinoids, as seen with AM-2201, has been applied to many SCs of abuse (covered in Chapter 6) and improves binding affinity for both CB_1 and CB_2 (Choi, Heo, Kim, et al., 2013). STS-135 and SDB-008-12, in comparison with their non-fluorinated counterparts, had potencies and efficacies that remained constant between hCB_1 and hCB_2 or greatly increased. It has been hypothesized that fluorine may increase in surface area due to electron shielding putting it at a more favorable distance to interact with the receptor. This increase in size also has been shown to disrupt its interactions with water, increasing the hydrophobicity of the carbon chain that is known to interact with a hydrophobic pocket, therefore, its presence would increase affinity (Dalvi & Rossky, 2010).

Terminal fluorination may also contribute to, but does not always play a role in, hTRPA1 activation as three of the six fluorinated compounds were agonists. The TRPA1 mechanism of action differs from that of other chemoreceptors by agonist activity depending less on structural similarities and more on the chemical reactivity of the compounds. Compounds that are electrophilic in nature are able to covalently bond to the cysteine residues in the N-terminus of the intracellular membrane (Hinman et al., 2006). Due to their physiochemical profile, it is unlikely that the SCs showing TRPA1 activity are doing so through covalent binding, as they lack electrophilic functional groups. Δ^9-THC and other non-reactive compounds, such as menthol and arachidonoic acid, bind to TRPA1 non-covalently suggesting a more traditional binding pocket (Obata et al., 2005; Redmond et al., 2014). Besides the similarity of an amide linker, no structural trends were apparent as all -R^1 and -R^2 groups were present among the hTRPA1 ligands showing agonist activity. Aromatic character has been implicated in TRPA1 activation (Haynes et al., 2008). The hydrophobicity of these structures potentially increases their ability to enter the lipid membrane may contribute to their activity. The most efficacious of the agonists, showing efficacies similar to or higher than CIN, did have smaller -R^2 groups, which suggests steric interactions may play a role in efficacy. Therefore, further conclusions cannot be made on why these specific compounds are showing agonist activity.

With few studies reporting physiological or psychological effects of the drugs examined here published, it is hard to translate how these compounds are functioning in the body. Adamantanes are known for their use in brain delivery drugs, such as the AIDs treatment AZT, due to their high hydrophobicity and lipophilicity (Mansoori, George, Assoufid, & Zhang, 2007). Therefore, being strong agonists at both CB_1 and CB_2 and having the ability to easily cross the blood brain barrier and enter lipophilic membranes, could have detrimental effects in the CNS. (Mansoori et al., 2007).

CHAPTER 5: RCS-4 REGIOISOMERS, C4-HOMOLOGUES, AND CARBOXAMIDE REGIOISOMER DERIVATIVES

5 RCS-4 REGIOISOMERS, C4-HOMOLOGUES, AND CARBOXAMIDE REGIOISOMER DERIVATIVES

5.1 SUMMARY

N-alkylated (methoxybenzoyl)indoles, a new class of SCs thought to be the product of rational drug design, were discovered in 2010. The use of RCS-4, the most common of this class to be identified in herbal blends, soon spread worldwide. Methoxy regioisomers and N-butyl homologues of RCS-4 have also been identified in government seizures. A pharmacological profile has only been determined for RCS-4 and its regioisomer RCS-2, therefore, a pharmacological assessment was completed on the remaining RCS analogues to determine how the position of the directing group affects the cannabinoid and off-target reactivity. Carboxamide derivatives of the RCS analogues were also synthesized to further compare how an amide linker compared to a ketone affects activity (as seen in Chapter 4). Finally, the effect on reactivity was determined when methoxymethane substituent was replaced with a fluorine group.

5.2 INTRODUCTION

In 2010, Hungarian police alerted the EMCDDA EWS of the first of the benzoylindoles class, RCS-4 (EMCDDA, 2010). RCS-4, (4-methoxyphenyl)(1-pentyl-1H-indol-3-yl)methanone, has also been sold under the names OBT-199, SR-19, BTM-4 and Eric-4, later shortened to E-4 (Pierce Kavanagh, Grigoryev, Melnik, & Simonov, 2012). Although it was reported to the EWS, there had been no publications detailing the identification, isolation or quantification of this compound from herbal products. January, 2011 it was reported by Nakajima et al. at the Tokyo Metropolitan Institute of Public Health (Nakajima, Takahashi, Seto, et al., 2011). Within the packages tested, Nakajima found that RCS-4 was present at varying concentrations ranging from 1.7-18 mg/package (Nakajima,

Takahashi, Seto, et al., 2011). In 2011, Nakajima then isolated the 2-methoxy regioisomer of RCS-4, named RCS-2, and determined their cannabimimetic affinity at rat CB1 using [^{35}S]GTPγS binding. Nakajima et al. determined that RCS-4 and RCS-2 both had agonist activity at rCB$_1$ with EC$_{50}$ values of 199 nM and 166 nM and E$_{max}$ of 72 and 58% respectively (Nakajima, Takahashi, Nonaka, et al., 2011). This study also showed that RCS-4 and RCS-2 were present together with JWH-122 and AM-2201, within one herbal blend package (net weight 3.04 grams), at concentrations of 33.9 and 31.1 mg/pack respectively. A German study in 2011 also tested the contents of seven different herbal blend packages and found that one package contained a mixture of RCS-4 and its C1-homologue, RCS-4-(N-Me), at concentrations as high as of 157 and 19 mg/gram respectively. The discrepancies in concentrations of RCS-4 (and other SCs) present in each package essentially confirms, what has already been assumed, that manufacturers are preparing these compounds without regard to dose, activity or quality control to assure drug is distributed throughout the product evenly. Though no cannabimimetic activity for RCS-4-(N-Me) was determined in this study and this compound was not tested in this chapter, Simolka et al. suggested that the C1-homologue would likely not have activity due to its truncated indole, but the similarly truncated compound SDB-107 (presented in Chapter 4) showed high agonist activity at hCB$_2$. This further exemplifies how cannabimimetic profiles need to be generated for each compound as not all SCs follow SAR principles.

In determining the active ingredients of the Kronic brand being sold in Auckland, New Zealand, Couch et al. isolated RCS-4 and its novel N-butyl homologue (RCS-4-C4) (Couch & Madhavaram, 2012). Shortly after the identification of RCS-4-C4, the National Forensic Service of South Korea discovered the N-butyl homologue of RCS-2 (RCS-2-C4) in seized SC products (Choi, Heo, Kim, et al., 2013). Although four RCS analogues have an identification and quantification method available for herbal preparations, only RCS-4 and

its determined metabolites (Pierce Kavanagh et al., 2012) have had a method developed for biological samples such as hair, urine, serum and oral fluid (Hermanns-Clausen et al., 2013; Hutter, Kneisel, Auwärter, & Neukamm, 2012; Kneisel, Auwärter, & Kempf, 2013; Sundström et al., 2013). Ammann et al., therefore, developed a method using an HPLC/MS/MS to screen for RCS-4, RCS-4-C4, RCS-2 and RCS-3 (otherwise absent in the literature) in whole blood to broaden the range of SCs that are able to be tested at one time (Ammann, McLaren, Gerostamoulos, & Beyer, 2012). Being able to screen for a larger array of SCs in blood will help to accurately determine which SCs are present in patients presenting SC intoxication.

The popularity of the use of RCS-4 as an active ingredient in herbal blends has been documented worldwide as seen by its appearance in governmental seizures in the Hungary, Japan, New Zealand, South Korea, United States (Logan, Reinhold, Xu, & Diamond, 2012), Belgium (El Kouzi & Siddiqui, 2015), Ireland (Pierce Kavanagh et al., 2012), and Poland (Zuba & Byrska, 2013). Despite its prevalence, there is very little known about its effects in humans. The urine samples Kavanagh et al. used to isolate RCS-4 were from users that had gone to the emergency room presenting drug intoxication but specific symptoms were not listed (Pierce Kavanagh et al., 2012). The only other human data presented was by the US Poison Control Center that received an estimated total of 2,977 reports of synthetic cannabinoids in 2010 and RCS-4 was reported in 16 (0.54%) of those cases. Specific side effects were not listed with the calls to poison control (Administration, 2011).

The pharmacological data for the RCS analogues, including RCS-3-C4, a compound that was synthesized for comparison against other C4-homologues although it has yet to be isolated from herbal products, at hCB_1 and hCB_2 was recently published in *Forensic Toxicology* (S. Banister et al., 2015), Appendix B (pg. 305). Therefore, all synthesis information is presented in that work. This chapter will present that data while also

presenting activity at the TRP channels hTRPA1 and hTRPV1. It will also investigate how the carboxamide linker, as seen in Chapter 4, affects activity, as well as, if activity is dependent on the position of the methoxymethane group seen within the RCS analogues.
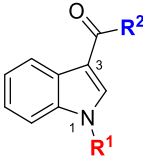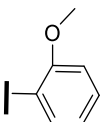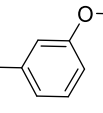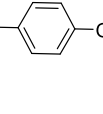
5.3 RESULTS

5.3.1 Cannabimimetic activity at hCB$_1$ and hCB$_2$
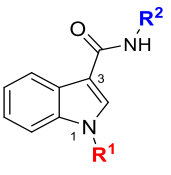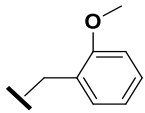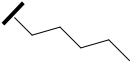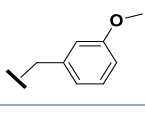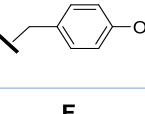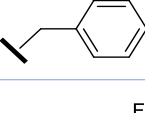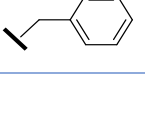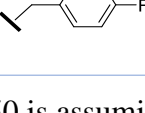
Using the plate reader based membrane potential assay described in Chapter 2 and validated in Chapter 3, six regioisomeric and homologueous 1-alkyl-3-(methoxybenzoyl)indoles (RCS-2-C4, RCS-3-C4, RCS-4-C4, RCS-2, RCS-3, RCS-4), three regioisomeric *N*-(methoxybenzyl)-1-pentylindole-3-carboxamides (SDB-022, SDB-023, SDB-024), and three regioisomeric *N*-(fluorobenzyl)-1-pentylindole-3-carboxamides (SDB-019, SDB-020, SDB-021) were tested for their cannabimimetic activity in AtT20-hCB1 and AtT20-hCB2 cells. All concentration response curves and control experiments for each compound that are not illustrated within this chapter can be found in Appendix A (pg. 274-286). Table 8 shows a comparison of the functional data for 1-alkyl-3-(methoxybenzoyl)indoles listed by methoxylphenyl position (2-, 3-, or 4-isomer) as well as the length of the 1-alkyl (R^1 group) chain (butyl or pentyl homologues). Table 9 shows a comparison of the functional data for the *N*-(methoxybenzyl)-1-pentylindole-3-carboxamides, also listed by methoxybenzyl isomerism (2-, 3-, or 4-position). Table 9 also compares the substitution of methoxy substituent for fluorine in the latter series to give the corresponding *N*-(fluorobenzyl)-1-pentylindole-3-carboxamides. Some compounds reached saturation of assay media below 10 μM, and several below 1 μM, with the resultant precipitation limiting the maximum concentrations that could be tested. The pEC$_{50}$ values of all compounds were calculated similarly to the response of WIN at hTRPA1 in Figure 13 Section 3.3.2., and were compared to the maximum response of WIN. Selectivity was

calculated in terms of potency by the ratio of EC_{50} values, and presented as whichever ratio

of CB_1 and CB_2 had a value higher than 1.

Table 8: **Comparison of functional agonist activity of *1-alkyl-3-(methoxybenzoyl)indoles* (RCS derivatives) at hCB1 and hCB2.** Data is listed by -R^2 group (2-, 3-, or 4-methoxybenzoyl regiosiomerism) and -R^1 group (length of alkyl chain at the 1-indole position). Data represent mean values ± SEM from 5-7 experiments each run in duplicate.

Backbone	R2	R1	NAME	AtT20-hCB1		AtT20-hCB2		SEL
				pEC_{50}	E_{Max} (%WIN)	pEC_{50}	E_{Max} (%WIN)	human
		(C5)	**RCS-2**	7.27±0.09	93 ± 6	8.16±0.04	98 ± 3	CB_2 7.8
		(C4)	**RCS-2-C4**	6.75±0.13	81 ± 8	8.35±0.05	102 ± 3	CB_2 39.6
		(C5)	**RCS-3**	6.95±0.05	99 ± 3	7.46±0.06	97 ± 4	CB_2 3.2
		(C4)	**RCS-3-C4**	6.48±0.05	70 ± 3	7.97±0.05	97 ± 2	CB_2 31.2
		(C5)	**RCS-4**	6.84±0.06	88 ± 4	7.34±0.09	87 ± 4	CB_2 3.2
		(C4)	**RCS-4-C4**	6.24±0.08	71 ± 4	7.87±0.04	96 ± 2	CB_2 42.2

Table 9: Agonist activity of *N-(methoxybenzyl)-* and *N-(fluorobenzyl)-1H-indole-3-carboxamide derivatives at hCB₁ and hCB₂. Data is listed by $-R^2$ group (2-, 3-, or 4-methoxybenzyl or fluorobenzyl regiosiomerism), with $-R^1$ group as a pentyl chain in all cases (substituent at 1-indole position). Data represent mean values ± SEM from 5-7 experiments each run in duplicate.

Backbone	R2	R1	NAME	AtT20-hCB1		AtT20-hCB2		SEL
				pEC_{50}	E_{Max} (%WIN)	pEC_{50}	E_{Max} (%WIN)	human
			SDB-022	6.0 ±0.2**	76 ± 5	6.93 ± 0.1	41 ± 3	CB₂ 28.8
			SDB-023	6.41 ±0.12	69 ± 7	6.8 ± 0.2	34 ± 4	CB₂ 2.5
			SDB-024	2.3 ±0.6**	22 ± 2	6.5 ± 0.1	24 ± 4	CB₂
			SDB-019	6.78 ±0.09	103 ± 6	6.70 ± 0.08	69 ± 3	CB₁ 1.2
			SDB-020	5.64±0.9**	73 ±4	6.24 ± 0.3	59 ± 13	CB₂ 2.5
			SDB-021	5.4 ± 0.2**	61 ± 5	6.6 ± 0.3	52 ± 7	CB₂ 6.4

**pEC50 is assuming the maximum is the equivalent to the maximum of WIN

5.3.1.1 Comparison of agonist activity at hCB₁ and hCB₂

Methoxylation and fluorination of the $-R^2$ phenyl and benzyl group was tolerated in AtT20-hCB1 and AtT20-hCB2 for all regioisomers and both acyl and amide linkers. All compounds, with the exception of SDB-019 whose pEC_{50} was the same for both receptors, were more potent at the hCB₂ receptor, and therefore were CB₂ preferring. RCS-2, RCS-2-C4, RCS-3, RCS-4 and SDB-019 were the only compounds that were more potent than WIN at hCB₁. All RCS analogues were of greater potency than WIN at hCB₂, but all of the

methoxybenzyl-substituted carboxamides (SDB-022, SDB-023, SDB-024) had a lower potency than that of WIN.

Of the RCS analogues, all six had either no difference in efficacy or higher efficacy at AtT20-hCB2. SDB-022, -023, and -024, differing from RCS-2, -3, and -4 by a methylene-spaced carboxamide linker in place of the ketone linker of the latter, had roughly half the maximal efficacy at hCB_2 compared to maximal efficacy at hCB_1, except for SDB-024 which had low efficacy at both receptors (~20% WIN max). SDB-019, 20 and 21, the corresponding fluorinated analogues of SDB-022, 23 and 24, also had a consistent decrease in potency at hCB_2. RCS-2 and RCS-3 had similar efficacies to WIN at both receptor types. SDB-019 only had similar efficacy to WIN at hCB_1, whereas RCS-2-C4, 3-C4, and 4-C4 all had similar efficacies to WIN at hCB_2.

5.3.1.1.1 *How the length of the $-R^1$ alkane group affected potency and efficacy*

Of the compounds described in this chapter, variation of $-R^1$ group was only investigated for the series of RCS analogues. Figure 19, shows the concentration response curves for butyl and pentyl homologues of a given methoxybenzoyl regioisomer of an RCS compound. In the name of each compound, the numeral after RCS refers to the methoxy position on the benozyl ring, and compounds containing the 1-butyl chain at $-R^1$ have the C4 suffix in their name. Compared to the 1-pentyl analogues RCS-2, -3, and -4, truncation of the alkyl chain by a single carbon to give the corresponding homologues RCS-2-C4, -3-C4, and -4-C4 decreases the efficacy and potency of the compounds at hCB_1. This is consistent with data presented in Chapter 4, and prior literature, which showed that CB_1 activity is optimal for a pentyl chain at the 1-indole position. Truncation of the 1-indole substituent greatly increased CB_2 selectivity of the compounds, increasing their potency by

up to 50-fold. This too was similar to data presented in Chapter 4, which showed the

truncated 1-propyl group conferred higher CB_2 activity and selectivity. The maximum

difference, as seen between RCS-2-C4, was a 160-fold greater potency at hCB_2 than hCB_1.
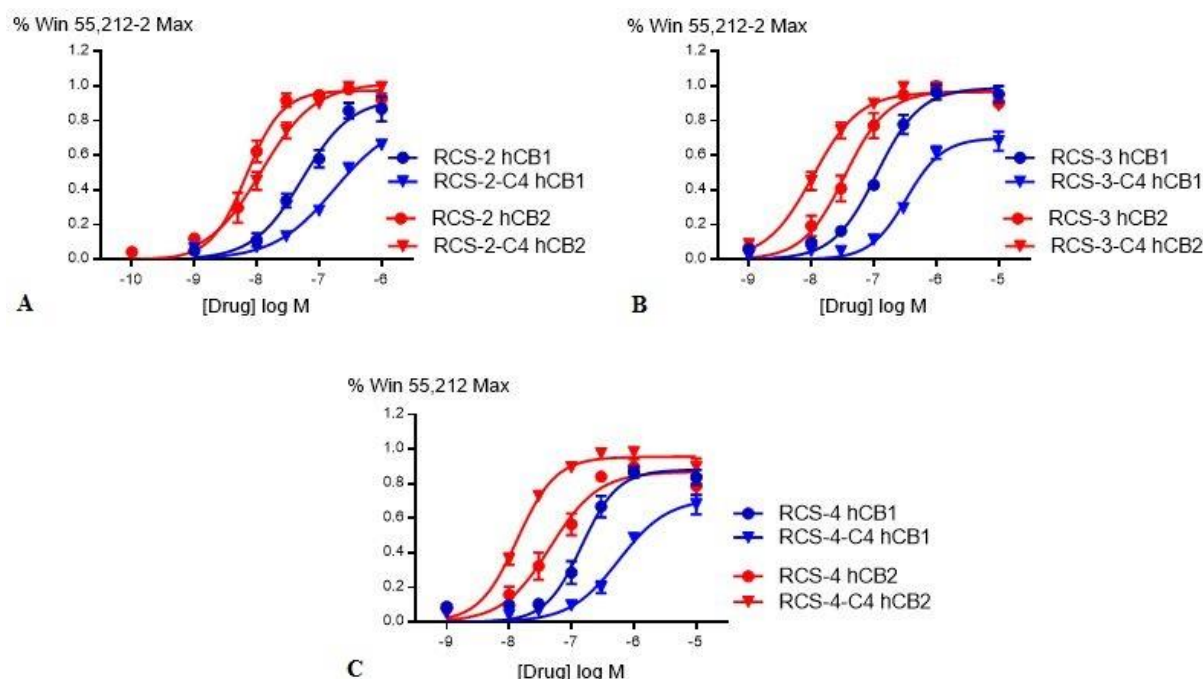
Figure 19: Concentration response curves comparing molecules with different 1-indole alkane hCB1 (blue) and hCB2 (red). A.) shows RCS-2 and RCS-2-C4. B.) RCS-3 vs. RCS-3-C4 C.) RCS-4 vs. RCS-4-C4. Data represent mean values ± SEM from 5-7 experiments each run in duplicate.

5.3.1.1.2 *How the position of the ring substituent of the -R² group affected potency and efficacy*

All positions were tolerated at both hCB_1 and hCB_2 for methoxy and fluoro

substituent groups. Trends were seen when compounds were separated by regioisomer, at

hCB_1, potency was highest when the methoxy or fluorine group were in the 2-position,

followed by the 3- and 4-positions. This was seen in all but SDB-022 and SDB-023, which

had a higher potency when the methoxy group was in the 3-position as opposed to the 2-

position. This observation did not hold for efficacy where no trends were apparent. At

hCB$_2$, the same trend was observed, excepting SDB-021 which had the fluorine group in the 4-position and showed higher potency than the 3-fluoro analogue SDB-020. For the acyl-linked RCS series, efficacy at hCB$_2$ decreased as the methoxy group was moved from the 2-, to 3-, to 4-position. The same trend followed with the next highest efficacy after this group was that of the fluorobenzyl carboxamides, followed by the methoxybenzyl carboxamides.

5.3.1.1.3 *How the methoxylation or fluorination of the -R^2 group affected potency and efficacy*

To determine how a fluorine atom differed from a methoxy group as a substituent on the -R^2 benzyl ring, SDB-019, 20 and 21 were compared to SDB-022, 23 and 24. The fluorinated carboxamides were consistently higher in efficacy than the methoxylated carboxamides at both receptors regardless of the substituent position (see Figure 20. Potency at hCB$_1$ also followed this trend, with the exception of SDB-020 and SDB-023; analogues containing substituents in the 3-position. For these compounds, the 3-methoxybenzyl carboxamide conferred a higher potency than the 3-fluorobenzyl carboxamide. At hCB$_2$, the methoxybenzyl analogues had greater potency than the fluorobenzyl congeners for all regioisomers except the 4-substituted compounds (SDB-021 and SDB-024).
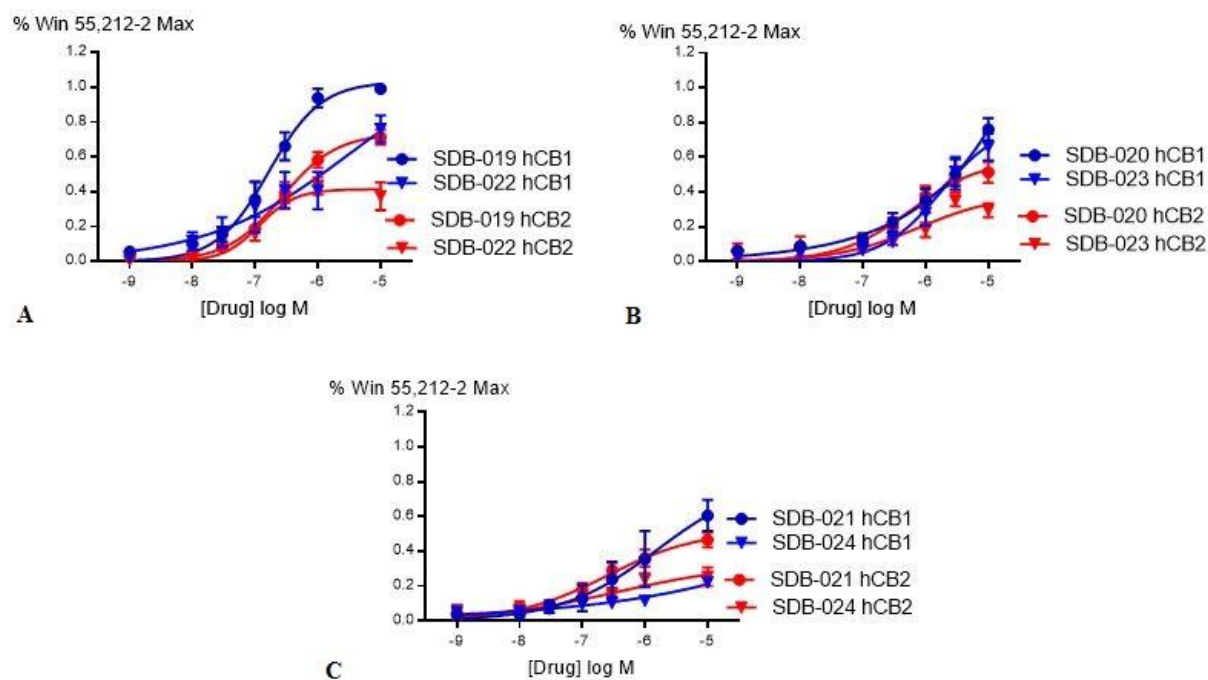
Figure 20: Concentration response curves for analogues with fluorinated or methoxylated substituents on the phenyl group of –R^2. Activity at hCB$_1$ (blue) and hCB$_2$ (red) for fluoro (circles) or methoxy (triangles) substituents. Carboxamids with substituents in the A.) 2- (SDB-019 and 22) B.) 3- (SDB-020 and 23) and C.) 4-positions (SDB-021 and 24). Data represent mean values ± SEM from 5-7 experiments each run in duplicate.

5.3.1.1.4 *How the difference in linker between the 3-indole carbon and -R^2 side affected potency and efficacy*

To determine the difference in ketone versus carboxamide linker activity, RCS-2, -3 and -4 (ketone linker) were compared to SDB-022, -023 and -024 (carboxamide linker). The ketone linker compounds showed higher potency and efficacy at both hCB$_1$ and hCB$_2$. This result is consistent with the data presented in Chapter 4 which showed lower activity for extended, methylene-spaced acyl substituents.

5.3.2 Activity at TRP Channels
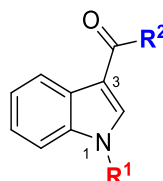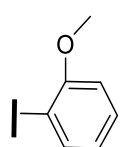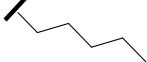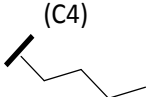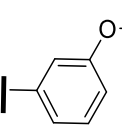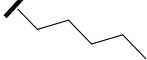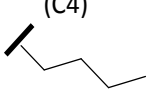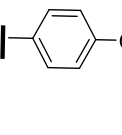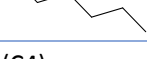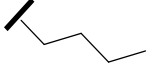
A fluorescence-based plate reader assay was used to measure the change in intracellular calcium as described in Chapter 2 and verified in Chapter 3. Two compounds,
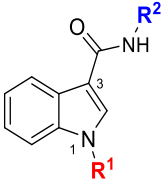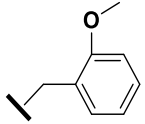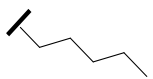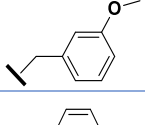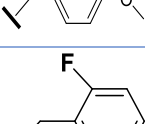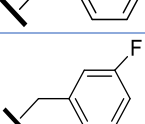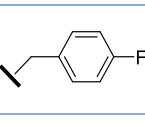
RCS-3-C4 and RCS-4-C4, showed weak agonist activity with a maximum response at 10 μM that was 15% that of %CAP max (Appendix A, pg. 274-286). All RCS analogues and SDB-019 showed weak antagonist activity inhibiting the max response of CAP (300 nM) between 16-25%. All twelve of the compounds tested in this chapter had agonist activity at hTRPA1. With the exception of RCS-4, having a maximum response of 50% that of CIN max, all of the RCS analogues had efficacy similar to that of CIN max (90-107%), as shown in Table 10. The potencies for all six substituted *N*-benzyl carboxamide analogues were also similar to CIN (EC_{50}= 6μM) and to each other having EC_{50} values ranging from 6.75-12μM (see Table 11).

Table 10: Functional agonist activity at hTRPA1 of RCS-analogues. This table shows which of the RCS-analogues had substantial agonist/partial agonist activity at hTRPA1. They are separated by similarities in functional groups $-R^1$ and $-R^2$ for easier comparison. Data represent mean values $\pm$ SEM from 5-8 experiments each run in duplicate.

Backbone	R2	R1	NAME	HEK293-hTRPV1		HEK293-hTRPA1	
				Max Response at 30 μM (%CAP)	Max Inhibition of 300 nM CAP (%CAP)	pEC$_{50}$	Max Response at 30 μM (%CIN)
	(o-methoxyphenyl)	(C5)	**RCS-2**	<1	24%	5.08 ± 0.03	96 ± 4
		(C4)	**RCS-2-C4**	<5	20%	5.17 ± 0.06	90 ± 6
	(m-methoxyphenyl)	(C5)	**RCS-3**	<10	25%	4.93 ± 0.11	97 ± 18
		(C4)	**RCS-3-C4**	15 ± 2	24%	5.09 ± 0.03	107 ± 5
	(p-methoxyphenyl)	(C5)	**RCS-4**	<5	16%	4.92 ± 0.13	50 ± 10
		(C4)	**RCS-4-C4**	15 ± 2	17%	4.94 ± 0.12	92 ± 20

The fluorinated and methoxylated carboxamides were not as efficacious as the RCS analogues with the highest efficacy compounds SDB-022 and 024 having a maximal response being only 80% of CIN max. SDB-019 and 23 had mid-range efficacy of around 60% that of CIN max. SDB-020 and 21 were low efficacious agonists with a max response $\leq$45% CIN max (Table 11).

Table 11: Functional activity at hTRPA1 of methoxylated and fluorinated carboxamide analogues. This table shows which of the fluorinated and methylated analogues had substantial agonist/partial agonist activity at hTRPA1. They are separated by $-R^2$ side groups, specifically the position of the directing group. Data represent mean values ± SEM from 5-8 experiments each run in duplicate.

Backbone	R2	R1	NAME	HEK293-hTRPV1		HEK293-hTRPA1	
				Max Response at 30 μM (%CAP)	Max Inhibition of 300 nM CAP (%CAP)	pEC$_{50}$	Max Response at 30 μM (%CIN)
			SDB-022	<10	<5	5.32 ±0.08	80 ± 3
			SDB-023	<5	<10	5.02 ±0.04	63 ± 4
			SDB-024	12 ± 1	<5	5.23 ±0.07	83 ± 6
			SDB-019	<10	25%	5.10 ±0.13	66 ± 10
			SDB-020	<5	≤5	>30μM	21 ± 6 at 30μM
			SDB-021	<5	<5	5.07 ±0.06	45 ± 4

5.3.2.1.1 SAR analysis of hTRPA1 activity

The length of the 1-alkyl chain of the indole ring had no bearing on the potency or efficacy of these compounds at hTRPA1, and butyl and pentyl chains both resulted in agonists with high potency and efficacy. Ketone and amide linkers were also tolerated, although the five most efficacious (RCS-2, RCS-2-C4, RCS-3, RCS-3-C4 and RCS-4-C) compounds contained the ketone linker. The linker type was not the key determinant of potency as the top six most potent analogues were comprised of an equal number with ketone or amide linkers. Methoxybenzyl carboxamides were more potent and efficacious

than their fluorinated counterparts at each respective substituent position. The most efficacious compounds, RCS-3 and RCS-3-C4, both had the methoxy group in the 3-position. No other trends could be determined from directing group position.

5.4 DISCUSSION

Although RCS-4 and RCS-2 were previously shown to have cannabimimetic activity at rat CB_1, pharmacological assessments still needed to be completed at the human cannabinoid receptors as well as off-target activities for all of the RCS analogues (Nakajima, Takahashi, Nonaka, et al., 2011). Structure-activity relationships were generated (to expand the SARs developed in Chapter 4) by preparing and pharmacologically characterising all regioisomers of several methoxybenzoyl, methoxybenzyl, and fluorobenzyl-substituted indole-type cannabinoids.

John W. Huffman, the originator of the JWH family of SC compounds, has developed SAR profiles regarding the addition of a methoxy group, at various position, to both naphthoyl and benzoyl cannabimimetic indoles. Methoxylation on various carbons of the naphthalene group of parent structure JWH-018 resulted in regioisomers JWH-081 (4-methoxy) and JWH-267 (2-methoxy). He found that the 4-methoxy group retained agonist activity at both rat CB_1 and human CB_2 receptors, and conferred a preference for CB_1. The 2-methoxy derivative showed a different binding profile, having little affinity for rCB_1 but high affinity for hCB_2. Receptor docking studies showed that the attenuation of rCB_1 affinity in JWH-267 was due to steric obstruction of key aromatic stacking interactions which are essential for indole binding at cannabinoid receptors. The same docking study showed that a variety of substituents at the C4' carbon of the naphthalene group were tolerated at rCB1 due to the generous size of the lipophilic binding pocket (J. W. Huffman & Padgett, 2005).

In another Huffman et al. study, systematic methoxylation of the phenyl group of 1-pentyl-3-phenylacetylindole gave three regioisomers: JWH-250 (2-methoxy), JWH-302 (3-methoxy) and JWH-201 (4-methoxyl), entirely analogues to RCS-2, -3 and -4 respectively, but with an additional methylene spacer. Structurally, this difference is analogueous to that seen when comparing AB-001 and AB-002. Binding affinity for rCB_1 and hCB_2 was highest for these phenylacetylindoles when the methoxy group was in the 2-position, followed by the 3- and then 4-positions, with the latter both showing low binding affinity for both CB receptors. A methoxy group in the 2- and 3-positions showed CB_1 selectivity, with the 3-methoxy analogue being 5 times more selective for CB_1 than CB_2. Comparing activity between methoxylated naphthoyl and benzoyl indoles at rCB1, Huffman suggested that the aromatic-aromatic interactions of the naphthalene group with the hydrophobic binding pocket, showing increased potency compared to benzoyl, was due to its geometry within the receptor and not due to its extra aromatic ring (J. W. Huffman et al., 2005).

RCS-2, -3 and -4 differ from the methoxylated naphthoylindoles by the lack of a second aromatic ring, and the methoxylated phenylacetylindoles by one less carbon-carbon bond length in the ketone linker between the indole 3-position and the phenyl ring. Despite such small changes to the CB_1-preferring JWH compounds, all RCS analogues showed a preference hCB_2. Since RCS-2, -3 and -4 were all more potent and had similar efficacies (88-99% that of WIN max) to that of WIN at hCB_1, it can be argued that the decrease in the linker by one bond length and the lack of a second aromatic moiety did not affect the geometry or aromatic stacking at the hCB_1 receptor. Although they are different structures, and therefore not guaranteed to have the same trends in activity, there is a possibility that the discrepancy in the selectivity of the 2- and 3-methoxy analogues could be due to the use of rat versus human CB_1 receptors. [^{35}S]GTPγS binding was done at both rCB_1 and hCB_2 for JWH-302 (3-methoxyphenylacetylindole) resulting in EC_{50} values of 29 and 24 nM

respectively (J. W. Huffman et al., 2005). RCS-3, the analogue of JWH-302 lacking a methylene spacer, had EC_{50} values of 114 and 34 nM respectively. Alternatively, Chapter 4 data suggests that greater CB_2 activity is seen in SCs with a shorter linker between the 3-indole carbon and the R^2 substituent. The greatest potency being exhibited by AB-001, which contains the same linker type and length as that of the RCS compounds. Five out of the six highest efficacy compounds also contained a short amide linker.

The influence of the $-R^2$ group linker can further be assessed by comparing the difference in reactivity between RCS-2, -3 and -4 to SDB-022, -023 and -024. Changing the linker to an amide and increasing the distance between the indole and the phenyl ring introduced a uniform decrease in potency and efficacy at both hCB_1 and hCB_2, with more dramatic differences at CB_2. This finding is consistent with Chapter 4 results, which suggested that the extended methylene-spacer between amide and $-R^2$ pendant group has rotational freedom about the C-C bond directly attached to the $-R^2$ pendant group, allowing for conformational changes that could disrupting aromatic stacking in the hydrophobic binding pocket. The influence of the length of the $-R^1$ chain on cannabimimetic activity also remained consistent with previous SAR trends in the literature and in Chapter 4. RCS-2-C4, RCS-3-C4 and RCS-4-C4 showed a decrease in CB_1 activity and an increase in CB_2 activity due to the truncation of their 1-indole substituent from a *n*-pentyl to a *n*-butyl chain (Wiley et al., 1998).

The difference in the position of the methoxy group between regioisomers showed trends in potency and efficacy, with few exceptions, consistent with those displayed by the JWH 1-pentyl-3-phenylacetylindole derivatives. Within structures only differing by the placement of the directing group, such as RCS-2, -3 and -4, the compound with the methoxy group in the 2-position was always more potent than the corresponding 3-methoxy analogue, which was more potent than the respective 4-substituted congener, at both hCB_1

and hCB_2. The exception to this trend was the lower potency of SDB-022 (3-methoxy) relative to SDB-023 (4-methoxy) at hCB_1. There was a similar trend in efficacy at hCB_2 but not at hCB_1 where no trends were apparent.

Many of the new compounds being isolated from SC products contain bioisosteric fluorine atoms in place of various hydrogen atoms (typically at the terminal carbon) of the 1-alkyl chain of the indole nitrogen. SDB-019-021 were synthesized to see how fluorination of the $-R^2$ group affected cannabimimetic activity. Huffman et al. also reported cannabimimetic activity for regioisomers of the core 1-pentyl-3-(fluorophenylacetyl)indoles, which differ from SDB-019-021 by an acyl rather than amide linker, and by having the phenyl ring one bond length closer to the indole ring. He found a similar trend to the amide-linked methoxy regioisomers that activity decreases the farther away the fluorine group moves from the ketone linker. This trend was also seen in both efficacy and potency at both hCB_1 and hCB_2, with the exception of SDB-020 and -021 showing higher potency for the 4-fluoro than the 3-fluoro examples at CB_2. The fluorinated species showed an increase in efficacy at both hCB_1 and hCB_2 when compared their methoxylated counterparts.

Capsaicin, an efficacious agonist at TRPV1, contains a terminal amide-linked aromatic group not unlike that found at the 3-indole position of SDB-022, -023 and -024, however, the capsaicin amide has the reverse connectivity to the amide linker found in the SDB analogues. At hTRPV1, RCS-3-C4 and RCS-4-C4 showed weak agonist activity with maximum elevations of intracellular calcium at 10 μM of around 15% that of CAP max. RCS analogues and SDB-019 showed weak antagonist activity with a maximum inhibition of the capsaicin response (300 nM) of around 25% in each case. This suggests that these compounds share sufficient structural similarities to TRPV1 agonists to display slight competitive inhibition at the receptor binding site without enough structural specificity to

bind to the receptor. Although weak agonist/antagonist activity was shown at the highest concentrations tested, the potency was not sufficient to justify further utilization of any of the compounds assayed as lead structures for further TRPV1 ligand development.

All twelve compounds tested in this chapter had agonist activity at hTRPA1. The results of Chapter 4 suggested that the amide linker between the indole 3-position and the -R^2 group, regardless of intergroup distance, may be essential for hTRPA1 activation. These results did not confirm this trend, since all RCS analogues, devoid of an amide linker, were potent and efficacious at hTRPA1, with five of the six showing efficacies similar to that of CIN. As these compounds lack the electrophilic groups necessary for binding with N-terminal cysteine residues, this data further suggests a more traditional binding site for the SCs at TRPA1. Additional trends in activity due to structural similarities were not apparent.

CHAPTER 6: PHARMACOLOGICAL PROFILES OF CANNABIMIMETIC INDAZOLES

6   PHARMACOLOGICAL PROFILES OF CANNABIMIMETIC INDAZOLES

6.1   SUMMARY

As legislation tightened and more 1-indole derivatives were regulated, an entirely new structural scaffold containing an indazole group rather than an indole as the core structure and either an L-valinamide or L-*tert*-leucinamide subunit instead of an aromatic substituent appeared within herbal smoking blends. Since their first isolation in 2012, the number of structures containing an indazole core has been consistently growing, with two new compounds (AB-CHIMIMACA and MAB-CHIMIMACA) being discovered even within the last few months. The American Association of Poison Control Centers published that in April and May of this year there were 2,721 cases of SC related illness reported. This was approximately 1,800 more cases than in the first three months of 2015 and more than all of the cases reported in 2013 (AAPCC, 2015). There has been speculation that this sudden spike is related to the simultaneous appearance of MAB-CHMINACA in herbal smoking blends (News, 2015). Aside from isolation, these compounds are relatively absent within the scientific literature making the pharmacological implications of the indazole scaffold unknown. Therefore, nine compounds of this new structural class, previously documented in the literature, were synthesized along with four novel indole analogues to be used for pharmacological assessment of their functional activity at the cannabinoid receptors and off-target TRP channels. This data was then used to develop relevant SAR, where applicable, to determine which, if any, of the heteroaromatic core, amino acid side chains and/or the alkyl substituents are the main contributors to their activity.

6.2 INTRODUCTION

The use of an indazole heteroaromatic substructure in rational drug design was first published by the Eli Lilly research group as a bioiostere of an indole moiety for the development of new serotonin receptor (5-HT_3) antagonists in 1987. In 2007, Janssen Pharmaceutical patented a number of tetrahydro-2H-indazole pyrazole derivatives synthesized to be both CB_1 and CB_2 receptor agonists (Liotta, Lu, Wachter, & Xia, 2010). This was followed by a Pfizer patent in 2009 that had synthesized and assessed the activity of 728 indazoles which were invented to be used in "treatments of disease conditions mediated by CB_1 receptor binding activity,"(Buchler et al., 2011).

Since 2009, The National Institute of Health Sciences, led by Nahoko Uchiyama, has been astutely monitoring the composition of designer drug products that are sold in Japan and therefore they have been an integral part of the isolation and identification of at least a dozen novel SCs. In 2012, they identified the first of the indazole core derivative to be found in herbal products, AKB48 (APINACA) alongside of its indole counterpart, SDB-001 (assessed in Chapter 4) (Uchiyama et al., 2012). In 2013, the same group found two new indazole derivatives, AB-PINACA and AB-FUBINACA, novel in both the indazole scaffold but also the use of an amino acid side chain, L-valinamide. Later in the year, they found structural analogues of these two compounds, ADB-PICA and ADB-FUBINACA, which only differ by substitution of the L-valinamide to an L-*tert*-leucinamide (Uchiyama, Matsuda, Kawamura, Kikura-Hanajiri, & Goda, 2013). After their isolation, it was later realized that the structures for AB-FUBINACA and ADB-FUBINACA were listed in the 2009 Pfizer patent (Buchler et al., 2011). As the patent stated the CB_1 binding affinity to be strong and in the low nanomolar range, it strengthened the claim that the clandestine chemists were referencing the scientific literature for rational drug design (Uchiyama et al., 2012). Following the trend of N-pentyl chain fluorination, 5F-AB- PINACA and 5F-ADB-

PINACA were also identified in Japan (Uchiyama, Shimokawa, Kawamura, Kikura-Hanajiri, & Hakamatsuka, 2014; Wurita et al., 2015). Although Japan was on the forefront of this wave of SCs, they have also been found in seizures in Australia, Belgium, Turkey, Germany, Sweden, the United States and the United Kingdom (EMCDDA, 2014).

Metabolic profiles have recently been established for ADB-FUBINACA, AB-FUBINACA, AB-PINACA, and 5F-AB-PINACA making it possible for their identification as it relates to toxic events (Takayama et al., 2014). Even with the metabolic profiles established, that does not always mean that the technology is readily available for health care professionals. Therefore, physiological implications of the indazole scaffold and the addition of an amino acid side chain to the SCs structure remains unclear. Of the instances where indazoles have been implicated, ADB-PINACA and 5F-ADB-PICA were reported to be the cause of neurotoxicity and cardiotoxicity in the former and in "non-fatal intoxications" in the latter (Control & Prevention, 2013b; EMCDDA, 2014; Monte et al., 2014). Fatal intoxications have been reported for 5F-ADB-PINACA, it was found to be ingested at the same time as a newer indazole derivative, MAB-CHMINACA (Hasegawa et al., 2015). This has resulted in AB-FUBICA, AB-FUBINACA, AB-PINACA, ADB-PINACA, 5F-AB-PINACA and ADB-PICA being reported to the EMCDDA EWS and their temporary regulation under the Controlled Substances Act in the United States (Drug Enforcement Administration, 2014; EMCDDA, 2014).

Outside of the original human CB_1 binding assay in the Pfizer patent, which found both AB-FUBINACA and ADB-FUBINACA to have affinities to the human CB_1 receptor in the sub/nanomolar range, there has been no pharmacological data reported for this class of compounds. A review of the current literature also revealed a lack of SAR information regarding the indazole core and the amino acid side chain. Therefore, Sam Banister from Sydney University, synthesized the relevant indazole structures from the published literature

as well as their indole counterparts. That way direct influences contributed by indazole and the amino acid chain could be determined individually. Using fluorescent-based plate reader assays, pharmacological assessments were made on hCB_1 and hCB_2 as well as the off-target TRP channels. Trends in reactivity profiles were then compared and SARs were determined. The hCB_1 and hCB_2 data found in this chapter has already been submitted to the journal of *ACS chemical neuroscience* and is in the process of revision (Appendix B, pg. 305) (S. D. Banister, Moir, Michael, Stuart, Jordyn, Wood, Kate, Kevin, Richard, Beniat, Corinne, Wilkinson, Shane, Buchanan, Alexandra, Glass, Michelle, Connor, Mark, McGregor, Iain, Kassiou, Michael, 2015).

6.3 RESULTS

6.3.1 Cannabimimetic activity at hCB_1 and hCB_2

Using a fluorescence-based plate reader membrane potential assay described in Chapter 2 verified in Chapter 3, 13 derivatives of the new indazole scaffold were tested for their cannabimimetic activity at the hCB_1 and hCB_2 receptors. The previous compounds presented were given to us at various times and structure families were not necessarily synthesized simultaneously. Therefore, any alterations to the experimental design were not possible to still be able to compare values between structural groups. Conversely, the indazole compounds were given to us at the same time and as they were the last ones tested, came at a time with enough of a natural break for alterations to be made to the protocol for testing.
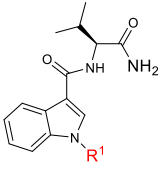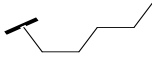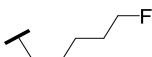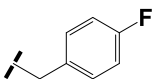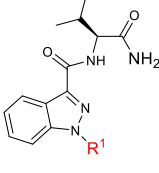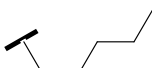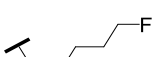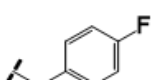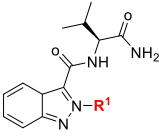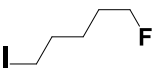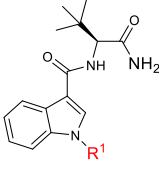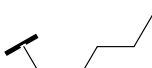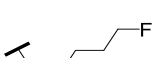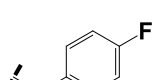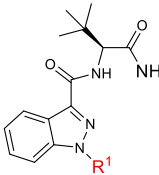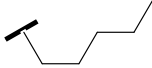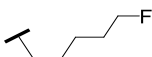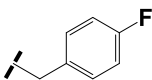
First, the reference compound used for normalization between drugs and assays was changed to CP 55,940. This was done for a few reasons: 1) potential non-specific effects seen with 10 μM WIN in AtT20-WT cells (which led to the decrease of WIN max to

be lowered to 3 μM) where CP 55,940 had no such effects at maximal concentrations 2) CP 55,940 is more potent than WIN and in hCB$_1$ more efficacious. On principle of having the reference compound being a "full agonist" that would mean using the one with the greater response 3) it has been reported to have fewer direct effects on ion channels. Second, bovine serum albumin (BSA) was added to buffers (0.01%) used in the fluorescence-based membrane potential assay. This was adopted by our lab for all techniques using cannabinoids as they have been known to stick to glassware and plastic. BSA was not added to any buffers used for measuring intracellular calcium as BSA has been shown to interfere with hTRPV1 activation (Luciano De Petrocellis, Davis, & Di Marzo, 2001).

Table 12 lists the functional agonist activity at hCB$_1$ and hCB$_2$ as separated out by backbone structure and by –R^1 group. Selectivity was calculated in terms of potency by a ratio of EC$_{50}$ values and presented as whichever ratio CB$_1$ vs. CB$_2$ had a value higher than 1. All concentration response curves and control experiments for each compound that are not illustrated within this chapter can be found in Appendix A (pg. 292-304). None of the SCs displayed agonist activity when they were added to AtT20-WT cells. At 10 μM, ADB-PICA and ADB-PINACA inhibited the maximum response of SRIF (100 nM) by approximately 20% SRIF max. The rest of the compounds had a maximum inhibition of ≤13% SRIF max. As outlined in Chapter 3, these drugs are potentially decreasing the SRIF response due to: weak antagonist activity at the SRIF receptors, interference with G-coupling, or a direct blockage of the GIRK channel.

Table 12: Functional Activity of indazole derivatives. This table lists the values for agonist activity at hCB_1 and hCB_2 as separated out by differences in backbone structure: 1-alkyl-3-acylindazole, 1-alkylindazole-3-carboxamide, and 1-alkylindazole-3-carboxylate and by $-R^1$ functional groups: N-pentyl, N-fluoropentyl, and 4-fluorobenzolic. Data represent mean values ± SEM from 5-11 experiments each run in duplicate.

Backbone	R1	NAME	AtT20-hCB1		AtT20-hCB2		Selectivity
			pEC_{50}	E_{Max} (%WIN)	pEC_{50}	E_{Max} (%WIN)	human
		AB-PICA	7.92 ±0.07	99 ± 3	7.92 ±0.21	94 ± 9	CB_1 1.0
		5F-AB-PICA	8.28 ±0.21	123± 13	8.05 ±0.53	121 ± 24	CB_1 1.7
		AB-FUBICA	7.67 ±0.14	115 ± 7	7.84 ±0.27	99 ± 10	CB_2 1.5
		AB-PINACA	8.91 ±0.09	103 ± 4	8.60 ±0.16	104 ± 8	CB_1 2.1
		5F-AB PINACA	9.32± 0.10	94 ± 6	8.59 ±0.25	110 ± 13	CB_1 5.4
		AB-FUBINACA	8.76± 0.10	108 ± 7	8.50 ±0.20	95 ± 12	CB_1 1.8
		5F-AB-2PINACA	7.92 ±0.46	106 ± 8	8.38 ±0.35	83 ± 10	CB_2 2.9
		ADB-PICA	9.16 ±0.16	98 ± 7	8.75 ±0.18	94 ± 7	CB_1 2.6
		5F-ADB-PICA	9.12 ±0.14	110 ± 7	8.91 ±0.14	92 ± 6	CB_1 1.6
		ADB-FUBICA	8.58 ±0.15	113 ± 8	8.52 ±0.16	96 ± 7	CB_1 1.2
		ADB-PINACA	9.28 ±0.08	117 ± 6	9.06 ±0.31	107 ± 16	CB_1 1.7
		5F-ADB-PINACA	9.61 ±0.19	91 ± 7	8.68 ±0.11	94 ± 5	CB_1 8.8
		ADB-FUBINACA	8.92 ±0.16	152 ± 11	8.46 ±0.13	104 ± 7	CB_1 2.9

6.3.1 Agonist activity at hCB_1 and hCB_2 of Indazole Derivatives

All 13 indazole derivatives were very potent and very efficacious agonists at hCB_1 and hCB_2. At hCB_1 potencies ranged from 0.25-21 nM with E_{Max} values ranging from 91-152% of CP 55,940 max. With sub-nanomolar potencies at hCB_1, 5F-AB-PINACA, ADB-PICA, 5F-ADB-PICA, ADB-PINACA and 5F-ADB-PINACA are of the most potent SCs to ever be reported. Similarly at hCB_2, ADB-PINACA had a sub-nanomolar potency and all but AB-PICA, 5F-AB-PICA and AB-FUBICA had potencies less than or equal to 5nM. Δ^9-THC, when using CP 55,940 to normalize the experiments, had an EC_{50} of 235 nM at hCB_1. Therefore, even the weakest compound is 11 times more potent than that of the active ingredient in cannabis. 5F-ADB-PINACA, the strongest agonist, had a potency 1000 times that of Δ^9-THC. All of the compounds, with the exception of 5F-AB-2PINACA and AB-FUBICA, were hCB_1 preferring but many had very similar potencies between the two receptors.

6.3.2 SAR for cannabimimetic activity

6.3.2.1 Influences of the heteroaromatic core: indole vs. indazole

Both the indole and indazole were well tolerated at hCB_1 and hCB_2. To look specifically at the influence of the indole versus the indazole at the resulting effect on activity, the compounds were paired like so: AB-PICA—AB-PINACA, 5F-AB-PICA—5F-AB-PINACA, AB-FUBICA—B-FUBINACA, ADB-PICA—ADB-PINACA, 5F-ADB-PICA—5F-ADB-PINACA, and ADB-FUBICA—ADB-FUBINACA. At hCB_1, all of the indazole compounds were more potent than their indole counterparts. Efficacy had the opposite trend having a lower efficacy in the indazole group, with the exception of ADB-

FUBINACA and ADB-PINACA which both displayed significant increases in efficacy than their indole counterparts.

At hCB$_2$, the indazole derivatives were more potent than their indole counterparts with the exceptions of ADB-FUBINACA, whose potency was the same as its indole counterpart, and 5F-ADB-PINACA, whose potency was significantly less than its indole derivative. There were no clear trends in terms of efficacy at hCB$_2$ as many of the indoles and indazole had similar efficacies, with the exception of 5F-AB-PICA whose E$_{Max}$ was 30% of CP 55,940 max higher than its indole counterpart, 5F-ADB-PICA.

6.3.2.2 Influences of the amino acid side chain: L-valinamide vs. L-*tert*-leucinamide

The only difference between the L-valinamide and the L-*tert*-leucinamide amino acid side chains is an extra methyl turning it from an isopropyl into a tertbutyl pendant. The addition of this extra methyl increased the potency of all of the compounds compared to their L-valinamide counterparts at both hCB$_1$ and hCB$_2$. This trend was not seen in terms of efficacy as many of the analogues had the same efficacy regardless of the amino acid substituent. An exception was a major increase in efficacy of the L-*tert*-leucinamide containing derivative ADB-FUBINACA by approximately 45% of CP 55,940 max compared to the L-valinamide, AB-FUBINACA, at hCB$_1$. The opposite being shown with an increase in E$_{Max}$ (~30% CP 55,940 max) of the L-valinamide containing 5F-AB-PICA at hCB$_2$ compared to its L-*tert*-leucinamide counterpart, 5F-ADB-PICA.

6.3.2.3 Influences of the N1 alkyl side chain: N-pentyl, N-fluoropentyl and 4-fluorobenzoyl

At hCB$_1$, the 4-fluorobenzoyl was consistently the lowest in potency compared to the other N1 side groups sharing the same backbone. There were no trends in efficacy

between all of the N1 groups, but at hCB_1, the highest efficacy compound, ADB-

FUBINACA, contained a 4-fluorobenozyl side group. Figure 21 shows a comprehensive

comparison of the compounds separated out by their substituent differences at hCB_1 and

hCB_2 which is shown in Figure 22.
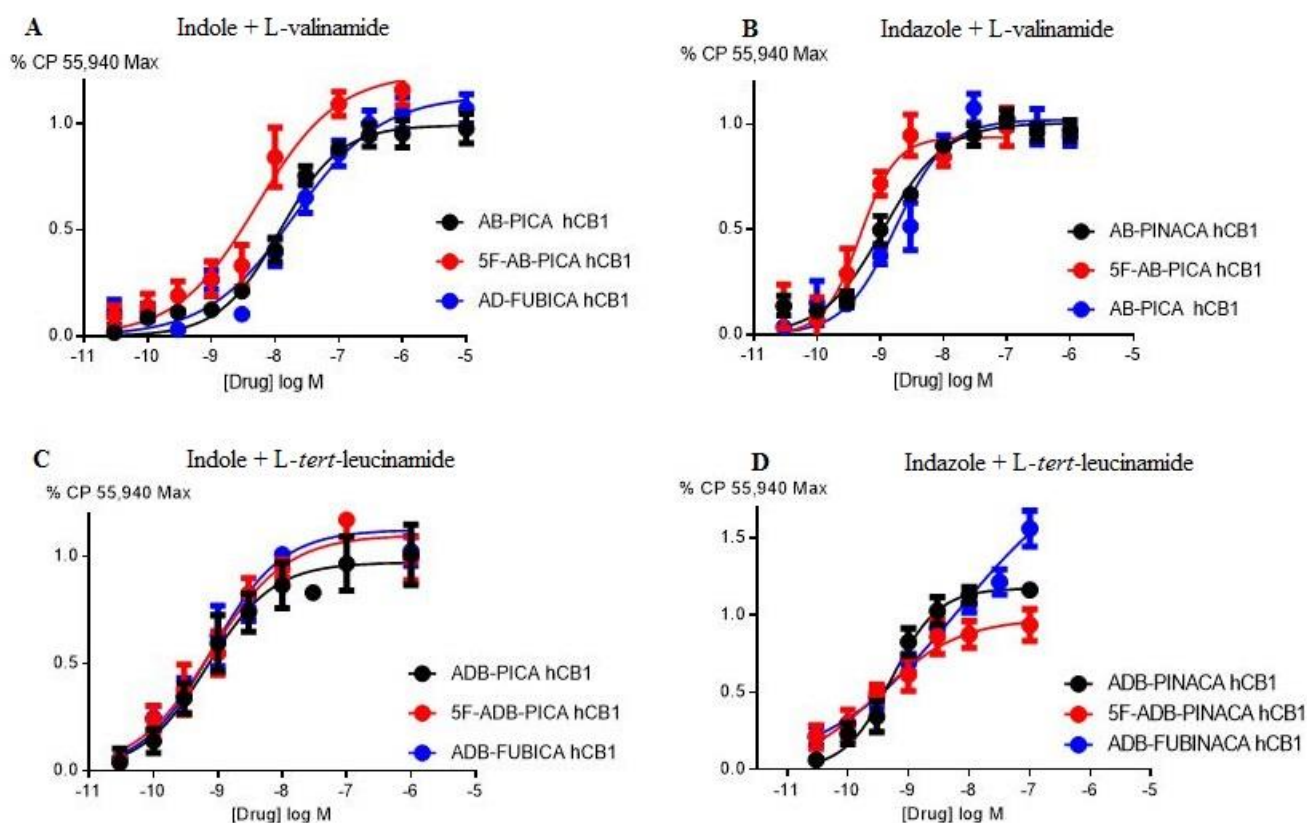
Figure 21: Comprehensive comparison of differences in activity at hCB_1 by indazole/indole derivatives as separated by their structural differences. This figure illustrates the concentration response curves of agonist activity at hCB_1 by all the indazole/indole derivatives, with exception of 5F-AB-2PINACA. Color differences represent the differences in N1 side chains. Red = N-fluoropentyl, Blue = 4-fluorobenzoyl and Black = N-pentyl. They are then further separated by indole (graphs A and C) and indazole (graphs B and D). L-valinamide structures are in graphs A and B while L-tert-leucinamide derivatives are in graphs C and D. Data represent mean values ± SEM from 5-11 experiments each run in duplicate.
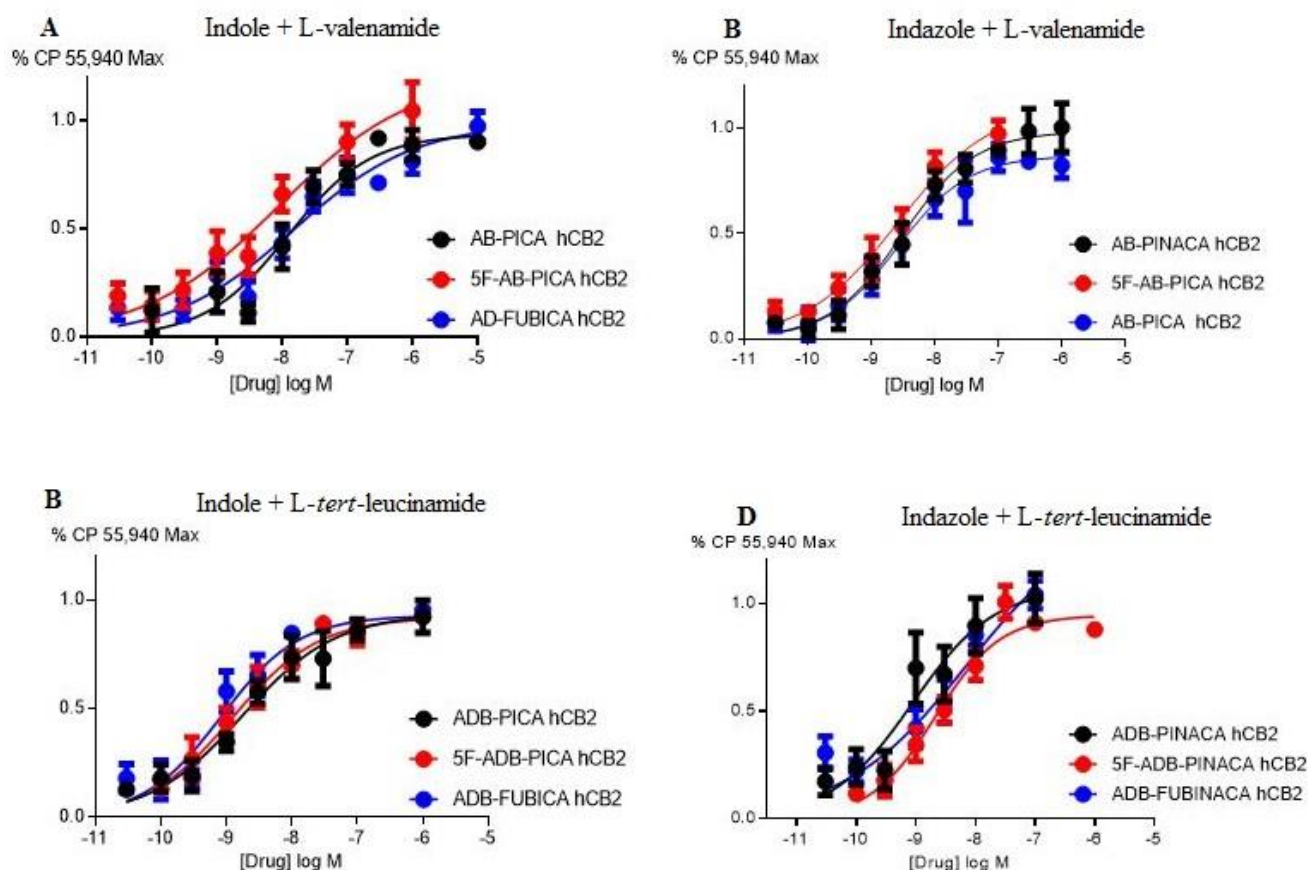
Figure 22: Comprehensive comparison of differences in activity at hCB₂ by indazole/indole compounds as separated by their structural differences. This figure illustrates the concentration response curves of agonist activity at hCB₂ by all the indazole/indole derivatives, with exception of 5F-AB-2PINACA. Color differences represent the differences in N1 side chains. Red = N-fluoropentyl, Blue = 4-fluorobenzoyl and Black = N-pentyl. They are then further separated by indole (graphs A and C) and indazole (graphs B and D). L-valinamide structures are in graphs A and B while L-tert-leucinamide derivatives are in graphs C and D. Data represent mean values ± SEM from 5-11 experiments each run in duplicate.

6.3.2.1 N2 side group instead of N1

There was only one analogue that had the side chain substituent on the N2 nitrogen of the indazole group instead of the N1 nitrogen as seen between 5F-AB-PINACA and 5F-AB-2PINACA. When the N-fluoropentyl was on the N1 nitrogen, it was 25 times more potent at hCB₁ than when it was on the N2. At hCB₂ the N1 position was still more potent but it was only 2 fold different. There were no significant differences in efficacy at hCB₁ or
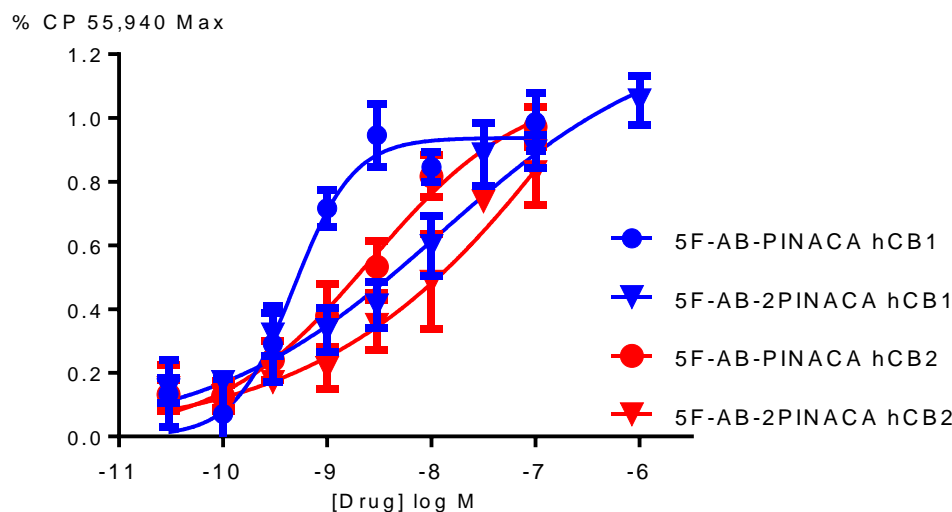
Figure 23: Concentration response curves for 5F-AB-PINACA and 5F-AB-2PINACA at hCB$_1$ and hCB$_2$. This figure illustrates the differences in the concentration response curves at hCB$_1$ and hCB$_2$ when the N-fluoropentyl side chain is on the N1 nitrogen (5F-AB-PINACA) and when it is on the N2 nitrogen (5F-AB-2PINACA). Data represent mean values ± SEM from 5-11 experiments each run in duplicate.

6.3.1 Activity at TRP channels

As shown in Table 13, of the indazole derivatives, only two had partial agonist activity at hTRPA1, ADB-PICA and ADB-FUBICA. They had a maximum response at 30 μM of 32 ± 1 and 38 ± 1% of CIN max. The only structural similarities shared between the two compounds was an indole core and the L-*tert*-leucinamide amino acid side chain, though the N-fluoropentyl N1 side chain of this common backbone had no activity. At TRPV1, none of the compounds had agonist activity at the maximum concentration tested (30 μM) but most of them showed weak antagonist activity inhibiting the maximum response of 300 nM CAP by 10-28%. Three of the four compounds with inhibition of ≥20% had a common N-pentyl N1 side chain. No other structural similarities were present.

Table 13: Functional Activity of indazole/indole derivatives at TRP Channels.
This table lists the values for agonist activity at hTRPA1 and agonist/antagonist activity at hTRPV1 as separated out by differences in backbone structure: 1-alkyl-3-acylindazole, 1-alkylindazole-3-carboxamide, and 1-alkylindazole-3-carboxylate and by $-R^1$ functional groups: N-pentyl, N-fluoropentyl, and 4-fluorobenzolic. Data represent mean values $\pm$ SEM from 5-7 experiments each run in duplicate.

Backbone	R1	NAME	HEK293-hTRPV1		HEK293-hTRPA1	
			Max Response at 30 µM (%CAP)	Max Inhibition of 300 nM CAP (%CAP)	pEC$_{50}$	Max Response at 30 µM (%CIN)
		AB-PICA	<5	12	--	<5
		5F-AB-PICA	<10	17	--	<1
		AB-FUBICA	<10	17	--	<5
		AB-PINACA	<5	25	---	<5
		5F-AB PINACA	<5	<5	--	<5
		AB-FUBINACA	<10	21	--	<5
		5F-AB-2PINACA	<10	13	--	<5
		ADB-PICA	<10	25%	4.35±0.02*	38± 1
		5F-ADB-PICA	<10	12%	--	<5
		ADB-FUBICA	<10	<10	4.27±0.03*	32 ± 1
		ADB-PINACA	<5	28	--	<5
		5F-ADB-PINACA	<10	10	--	<10
		ADB-FUBINACA	<10	16	--	<5

6.4 DISCUSSION

The indazole scaffold, as well as the amino acid side chain/s found within the –ICA/ -INACA class of compounds, was found to not only be tolerated at hCB_1, as it was originally published, but also tolerated at hCB_2 with high efficacies and potencies at each receptor. The original Pfizer patent used a $[^{35}S]GTP\gamma S$ binding assay to show that AB-FUBINACA and ADB-FUBINACA had EC_{50} values of 23.2 and 0.98 nM respectively in hCB_1 (Buchler et al., 2011). The fluorescence-based plate reader membrane potential assay utilized in this chapter generated EC_{50} values for these compounds to be 2 nM and 1.2 nM respectively, AB-FUBINACA showing a significantly more potent response in this assay. Despite this discrepancy, both models still showed the indazole scaffold derivatives and their indole counterparts to be some of the strongest SCs to date. At hCB_1, even the derivative with the weakest response (AB-FUBICA) was 11 times more potent than Δ^9-THC. 5F-ADB-PINACA, notably the only compound to be linked with a fatality, was shown to have the highest potency for hCB_1 being approximately 1000 times more potent than Δ^9-THC.

SAR trends were determined by comparing the reactivity of the compounds tested with similarities in their functional groups. The indazole scaffold proved to have higher potency than its indole counterpart at hCB_1. Potency at the hCB_2 receptor seemed to favour the indole scaffold except in the case of 5F-AB-PINACA whose indazole structure had a potency that was significantly higher. There were no real trends in efficacy at either receptor based on indole versus indazole comparisons alone. The amino acid side chain showed a preference at both receptors for the L-*tert*-leucinamide group, resulting in an increase in potency compared to the L-valinamide groups in all instances. This could potentially be due to an increase in hydrophobicity or the steric hindrance caused by the tertbutyl group may alter the conformation of the structure optimally. Again, efficacies were similar between

both groups and therefore no trends could be determined. Finally, the influence of the N1 side chain seemed to favour the N-fluoropentyl moiety. It has been shown that a terminal fluorine can increasing binding at both receptors (S. D. Banister et al., 2015), which is consistent with these compounds at hCB_1, but not at hCB_2, where the N-pentyl and N-fluoropentyl side chains had similar reactivity. The 4-fluorobenzyl moiety had consistently the lowest potency at both receptors, yet at hCB_1 it had the highest efficacy of all the side chains. Finally, the placement of the N-fluoropentyl chain from the N1 nitrogen to the N2 nitrogen showed a significant decrease in potency at both hCB_1 and hCB_2. CB_1 activity has been proven to rely on the length of the N1 chain (J. W. Huffman & Padgett, 2005; Wiley et al., 1998). It can be assumed that by changing the side chain to the N2 nitrogen that it would be located at a further distance from the hydrophobic pocket with which it usually binds. As CB_2 activity is less dependent on the length of N1 side chain, it would make sense that 5F-AB-2PINACA would have less of a reactivity difference at hCB_2 than at hCB_1 compared to 5F-AB-PINACA. This is assuming that these compounds are interacting within the binding pocket of the receptors in the same way as classical or indole based cannabinoids.

As previously discussed, both hCB_1 and hCB_2 rely on hydrophobicity and aromatic-aromatic interactions for binding (J. W. Huffman & Padgett, 2005). The addition of the amino acid side chain completely removes the aromatic character that had previously been thought to be necessary for a ligand interaction to take place at the cannabinoid receptors. On the contrary, the high potency and efficacy shown by these compounds proves that an aromatic entity connected to the 3 carbon of the indole/indazole is not essential. In fact, the indoles tested in this chapter have higher potencies than any other indole tested in this body of work suggesting that the amino acid side chain, more so than the indazole, is causing the increase in reactivity. As it has it was proven that indoles bind to different residues in the binding pocket of the cannabinoid receptors than classical cannabinoids (Song & Bonner,

1996), the lack of aromatic character linked with the increases in potency and efficacy may suggest that these compounds are also binding in a unique way. Docking studies will need to be completed to determine what specifically about these compounds is making them highly reactive.

At hTRPV1, almost all of the compounds had weak antagonist activity but none were substantial enough to continue evaluating. There were two derivatives that had partial agonist activity at hTRPA1, ADB-PICA and ADB-FUBICA. As neither are electrophilic in character, it corroborated previous chapter conclusions that activity at this receptor is probably through a more traditional binding site than through covalent bonding of the N-terminus.

It has been previously hypothesized that full agonist activity of SCs at CB_1, specifically JWH-018, is what leads to stronger psychotic and deleterious effects on the CNS (Every-Palmer, 2011). Therefore, the negative neurotoxic effects linked with this specific class of drugs could be a direct correlation to the potency of these drugs at the hCB_1 receptor. This is supported by the most potent drug of the compounds tested, 5F-ADB-PINACA, being the only compound associated with a fatality. Although it is probably a cause for the toxicity, it is more than likely just a contributing factor to the overall picture of toxicity. One theory, which will be discussed more extensively in the following chapter, is the concept of pro-drugs. A pro-drug is a biochemically inactive compound that does not convert into its active form until it has come in contact with specific physiological barriers. This technique has been used in pharmacology to make target specific drugs that are activated when they come in contact with specific enzymes (Mitra, Lee, & Cheng, 2013). Easily cleavable linkers, such as esters or amides, can then be utilized to improve the drug by adding on side chains to increase solubility, add more stability or prolong metabolism (Mitra et al., 2013). Many of the SCs that have been tested within this body of work have

structural characteristics that would place them into this pro-drug category. When looking at the patent submitted by Pfizer it specifically states that pro-drugs fall under the category of their invention, meaning any structural modification made to one of the drugs in their patent to enhance its reactivity is essentially still their intellectual property, and that some of the drugs present may already be in the pro-drug form. This suggests that as these drugs metabolize, their metabolites may also be cannabimimetically active.

The metabolism of JWH-018 and Δ^9-THC has already been established, as most of their phase I and II metabolites have had their cannabimimetic activity assessed at CB_1 and some at CB_2 (Fantegrossi, Moran, Radominska-Pandya, & Prather, 2014; Su, Seely, Moran, & Hoffman, 2015). Both JWH-018 and Δ^9-THC undergo oxidative metabolism resulting in various hydroxylated metabolites (S. D. Banister et al., 2015). Some of JWH-018 metabolites have even been shown to be more potent than JWH-018 itself at both cannabinoid receptors (Rajasekaran, Brents, Franks, Moran, & Prather, 2013). Metabolic profiles have been determined for AB-PINACA and 5F-AB-PINACA which show similar metabolic pathways. Through hydrolysis, AB-PINACA was metabolized primarily to AB-PINACA carboxylic acid, carbonyl-AB-PINACA, and (4)-hydroxypentyl AB-PINACA, whereas, 5F-AB-PINACA underwent oxidative defluorination to produce AB-PINACA pentanoic acid and 5-hydroxypentyl-AB-PINACA (A. Wohlfarth et al., 2015). If the hydroxylated metabolites of these compounds react in a similar manner to JWH-018 and AM-2201 hydroxylated metabolites, then their potencies could be even higher than the already astoundingly high potencies in their unaltered form. Pharmacological profiles will need to be established to determine if active metabolites play a role in the toxicity of these compounds.

CHAPTER 7: REACTIVITY OF HIGH TOXICITY SCS: PB-22, 5F-PB-22, UR-144, 5-OH-UR-144 AND XLR-11

7 REACTIVITY OF HIGH TOXICITY SCS: PB-22, 5F-PB-22, UR-144, 5-OH-UR-144, AND XLR-11

7.1 SUMMARY

Two new classes of SCs structures have been produced by altering the 3-(1-naphthoyl)indole core: tetramethylcyclopropyl derivatives (UR-144, XLR-11 and 5-OH-UR-144) and methoxyquinolinyl derivatives (PB-22 and 5F-PB-22). Consumption of these compounds has been associated with some of the most toxic effects presented in SC cases including AKI and death. No pharmacological information has been presented for PB-22 and 5F-PB-22 but initial pharmacological assessments have been made for UR-144 and its fluorinated counterpart, XLR-11, at the cannabinoid receptors. Therefore, pharmacological profiles were determined at the hCB_1 and hCB_2 and, when relevant, compared to the previous findings in the literature. These compounds were also tested at the TRP channels to determine if off-target activity could potentially contribute to their relatively high toxicity. Finally, 5-OH-UR-144, a mutual metabolite of UR-144 and XLR-11 was tested at the cannabinoid receptors and TRP channels to assess whether SC metabolites, themselves, show cannabimimetic activity.

7.2 INTRODUCTION

As SCs have have gone through numerous iterations of structural derivatives, two new additions to the 3-(1-naphthoyl)indole core have been isolated in smoking blends and are notorious for having toxic side effects when consumed. 3-(tetramethylcyclopropylmethanoyl)indole derivatives, were originally synthesized by Frost et al. at Abbott Laboratories as CB_2 selective ligands for their potential therapeutic value

(Frost et al., 2008). In 2010, during the development of the SAR for N1 groups on the new 3(tetramethylcyclopropylmethanoyl)indole derivatives, UR-144 was developed and subsequently sold on the internet as a "research chemical" (Frost et al., 2010; Sobolevsky, Prasolov, & Rodchenkov, 2012). UR-144 was first reported in herbal blends in Europe by the UNDOC International Collaborative Exercises (ICE) program in their 2010-2011 report (Hammond, 2012). In 2012, an N-fluoropentyl analogue of UR-144 which had been absent from the scientific literature, referred to as 5F-UR-144 or XLR-11, was also isolated in herbal blends in South Korea (Choi, Heo, Choe, et al., 2013; P. Kavanagh, Grigoryev, Savchuk, Mikhura, & Formanovsky, 2013). Within one year, XLR-11 became the most abundant of the South Korean SCs seized and tested (Chung, Choi, Heo, Kim, & Lee, 2014). Soon UR-144 and XLR-11 could be found worldwide with reports of their isolation from governmental seizures in Russia, Japan, Europe and the United States (Ariane Wohlfarth et al., 2013). Due to adverse effects of XLR-11 and the prevalence of its consumption in the United States, in May 2013, XLR-11 and similar analogue UR-144 were placed under Schedule I of the Controlled Substances Act to temporarily regulate the use of these compounds until a more permanent solution could be enacted (Administration, 2011).

After the regulation of XLR-11 and UR-144, the United States saw an increase in the presence of two novel SCs, PB-22 and 5F-PB-22. These are the first of the indole derivative SCs to have an ester linker between the 3 carbon of the indole and the side substituent (Ariane Wohlfarth et al., 2014a). The side substituent, a quinoline substructure, has been previously found in compounds that had been made with the intention of being CB_2 selective agonists. In these, the quinoline was within the core structure, as opposed to a side group and therefore, resembled the structure of the aminoalkylindole WIN (Baraldi et al., 2012). PB-22 was first isolated in Japan and shortly after in Russia (Shevyrin, Melkozerov, Nevero, Eltsov, & Shafran, 2013; Uchiyama et al., 2013). It was also in Japan

that the N-fluoropentyl analogue of PB-22, 5F-PB-22 was isolated in late 2013 (Uchiyama, Matsuda, Kawamura, Kikura-Hanajiri, & Goda, 2014). By January of 2014, the United States had also added these compounds to Schedule I, due to their threat on public health and safety (Drug Enforcement Administration, 2014).

Of the SCs that have been identified and linked to adverse effects in humans, XLR-11, PB-22 and 5F-PB-22 seem to have the most inherent toxicity. In four clinical case studies implicating the ingestion of SCs to AKI, 30 patients spanning the United States presented symptoms of nausea, vomiting, flank pain and high creatine levels (associated with AKI). 16 patients were able to provide biological samples (either serum, urine and/or biopsy tissue) for analysis. In seven cases, the packets of herbal incense that were consumed (or assumed to be the product consumed) were tested concurrent with the biological samples and in two cases they were tested in lieu of biological samples. Of the 16 biological samples that were sufficient enough for analysis (2 were not), seven showed the presence of XLR-11 or its metabolites. In two cases UR-144 was found in combination with XLR-11. Patients claimed that the onset of symptoms was between 30 minutes to 24 hours after consumption. The hospitals reported that all of the patients' creatine levels eventually returned to normal, but the time it took was variable and lasted on average three days, though one man was reported as still having elevated creatine after 23 days without recurrent use. All of the patients lived, but some had to be placed on haemodialysis (Bhanushali, Jain, Fatima, Leisch, & Thornley-Brown, 2012; Buser et al., 2014; Control & Prevention, 2013a; Thornton, Wood, Friesen, & Gerona, 2013). No long term effects of these instances of AKI have been reported but it has been shown that an episode of AKI increases the likelihood of chronic kidney disease by almost 9-fold and end-stage renal disease by 3 fold (Buser et al., 2014). In an unrelated case study, a man presented cerebral ischemia shortly after smoking

XLR-11 but no other case studies with similar occurrences have been reported (Takematsu et al., 2014).

Due to the negative health effects and the prevalence of use, in this chapter, XLR-11 and UR-144 were tested for their cannabimimetic activity at AtT20-hCB1 and AtT20-hCB2. They were also tested at the off-target TRP channels to determine if their activity is limited to hCB_1 and hCB_2 and if their pharmacological profiles differed from other SCs highlighting potential areas of toxicity. During the investigation into these compounds, Wiley et al. published the first pharmacological data on XLR-11 and UR-144 by testing their cannabimimetic activity using a radioligand binding and a $[^{35}S]GTP\gamma S$ binding assay in HEK293 cells expressing human CB_1 and CB_2 receptors. She also compared the *in vitro* activity to *in vivo* activity with a mouse tetrad model and a drug discrimination model (Wiley et al., 2013). The results were that both XLR-11 and UR-144 had high affinity to both cannabinoid receptors and that their abuse potential and psychoactive profile were similar to that of Δ^9-THC and other SCs. These results were then compared to the results generated by the fluorescent-based membrane potential assay.

PB-22 and 5F-PB-22 were implicated in a case study where SC use was followed by repetitive delayed-onset seizures, although, JWH-122, AM-2233 and BB-22 were also present in the serum sample (Schep, Slaughter, Hudson, Place, & Watts, 2014). In another case study, seizures were presented by both a man and his dog after the consumption of PB-22 mixed with UR-144. The man became incoherent followed by a high enough agitation state that he needed to be restrained (Gugelmann et al., 2014). PB-22 was also linked to the death to three people in Victoria, Australia though autopsies did not elucidate the biological cause of these deaths (Gerostamoulos et al., 2015). 5F-PB-22 consumption has also been described as including seizures, as well as, migraines and panic at high doses (over a milligram) (Ariane Wohlfarth et al., 2014a). Unfortunately, the main adverse effect linked

to 5F-PB-22 is death. The Iowa poison control center confirmed 5F-PB-22 was in the systems of three young teens who died after its consumption but they say "it is difficult to prove the sole cause of death" (Leys, 2014).

Alternatively, a case study that tested the post mortem tissues of four fatalities from 5F-PB-22 overdose reported the probable biological causes of the deaths through autopsy analysis. Knowing the cause of death could help shed light on which of the physiological systems the SCs are having the most toxic effect. All four fatalities had similar 5F-PB-22 concentrations within their blood serum of 1.1 - 1.5 ng/mL. Three of the four, died suddenly, whereas the exception had escalating symptoms that could not be treated by health care professionals. One of the fatalities was described as having trouble breathing and though attempts of resuscitation were made, he died shortly after the onset of symptoms. It was hypothesized that a rapid onset of heart dysrhythmias or a seizure could have been the cause of death. The other two sudden fatalities had similarities in their symptoms such as swelling of the visceral organs and fluid in the lungs which is suggestive of heart failure. Finally, the patient with the slow onset of symptoms had acute kidney and liver injuries upon his arrival to the emergency room. As time progressed, his symptoms worsened to severe liver injury, the inability to clot blood, AKI, and acute respiratory failure which in turn caused low levels of oxygen and increased lactic acid in the blood stream. He was revived from cardiac arrest only to deteriorate into an all physiological systems failure. The cause of death as determined by autopsy was ultimately liver failure (Behonick et al., 2014).

Originally in this patient, 5F-PB-22 was not discernible in ante-mortem blood samples that were taken, but high concentrations of the Δ^9-THC metabolite, 11-nor-9-Carboxy-Δ^9-THC (176-246 ng/mL), were present. It was not until the next day that 5F-PB-22 (1.3 ng/mL) could be detected in his blood. This could suggest a different time course

between the metabolism or potential storage of Δ^9-THC and 5F-PB-22 (Behonick et al., 2014). Due to the ability of Δ^9-THC to be stored in adipose tissue and undergo enterohepatic circulation, short term cannabis intoxication can last up to 24 hours but it has been shown to reside in the body of chronic users for up to 4 weeks even after abstaining from use (Greydanus, Hawver, Greydanus, & Merrick, 2013). Some SCs, JWH-210 and JWH-122, have also been shown to be stored in adipose tissue but at higher concentrations than Δ^9-THC for up to 2 weeks in a rat model (Schaefer et al., 2014) Before the influence that metabolism and storage have on 5F-PB-22 activity can be assessed, functional data for PB-22 and 5F-PB-22 needs to be determined as there has been no pharmacological data presented for either compound at CB_1 or CB_2. Therefore, a fluorescence-based plate reader membrane potential assay will be used to determine the cannabimimetic activity of the novel structural group. Activity at the TRP channels will also be determined to see if off-target pathways could potentially contribute to the toxic effects associated with these compounds.

Finally, the detection of the Δ^9-THC metabolite, 11-nor-9-Carboxy-Δ^9-THC, found in the blood sample of the deceased case study patient, highlights the importance of metabolite assessment described in Chapter 6. The metabolism of Δ^9-THC has already been established and of its phase I and II metabolites, only 11-nor-9-hydroxy-Δ^9-THC has cannabimimetic activity at CB_1 (Fantegrossi et al., 2014; Su et al., 2015). Alternatively, the hydroxylated metabolites of JWH-018 have been shown to be more potent than JWH-018 at both cannabinoid receptors (Rajasekaran et al., 2013). Through oxidative defluorination, AM-2201 metabolizes to have the same metabolite 1-(5-hydroxypentyl)-1H-indol-3-yl)(naphthalen-1-yl)methanone as JWH-018. This metabolite showed high levels of activation with high affinity and high efficacy at CB_1 (Brents et al., 2011). A metabolic profile completed by Wohlfarth et al., found UR-144 to metabolize via oxidation and XLR-

11 to metabolize via oxidative defluorination resulting in the mutual metabolite, 5-OH-UR-144 (Ariane Wohlfarth et al., 2013). Although this metabolic profile was not elucidated until 2013, the N-5-hydroxylpentyl $-R^1$ side chain of 5-OH-UR-144 was one of the substituents Frost et al. used when developing the SAR for the 1N on the tetramethylcyclopropyl derivatives (Frost et al., 2010). Therefore, binding affinity data at hCB_1 and hCB_2, FLIPR agonist activity at hCB_2 and inhibition of AC at both hCB_1 and hCB_2 have already been determined. Functional data for 5-OH-UR-144 at the cannabinoid receptors will be completed for comparison purposes and TRP will also be tested to see if they are targets for biological metabolites. The data presented in this chapter for the activity at hCB_1 and hCB_2 has already been published in *ACS Chemical Neuroscience* as listed in Appendix B (pg. 305) (S. D. Banister et al., 2015).
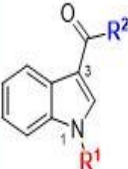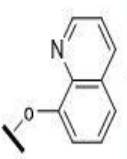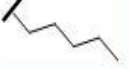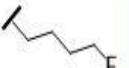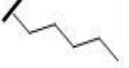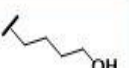
7.3 RESULTS

7.3.1 Cannabimimetic activity in AtT20-hCB1 and AtT20-hCB2 cell types

Using the fluorescence-based plate reader membrane potential assay described in Chapter 2 and verified in Chapter 3, PB-22 and UR-144, their fluorinated counterparts (5F-PB-22 and XLR-11), and the mutual metabolite of XLR-11 and UR-144 (5-OH-UR-144) were tested for their cannabimimetic activity at hCB_1 and hCB_2. All concentration response curves and control experiments for each compound that are not illustrated within this chapter can be found in Appendix A (pg. 292-304). No agonist activity was detected in AtT20-WT cells and the inhibition of SRIF hyperpolarization was $\leq 15\%$ for all compounds. Table 14 shows the functional data for the activity at hCB_1 and hCB_2 as listed by differences in side groups. Selectivity was calculated in terms of potency by a ratio of

drugs were efficacious agonists at CB$_1$ and CB$_2$ receptors.

Table 14: Functional agonist activity at the cannabinoid receptors hCB$_1$ and hCB$_2$ of derivatives as separated by similar functional groups. The functional activity of compounds PB-22, 5F-PB-22, UR-144, XLR-11 and 5-OH-UR-144 are listed by their common functional groups: -R^1 N-pentyl, N-5-fluoropentyl and N-5-hydroxyl; and –R^2 groups: methoxyquinolinyl and tetramethylcyclopropyl. Data represent mean values ± SEM from 5-8 experiments each run in duplicate.

Backbone	R2	R1	NAME	AtT20-hCB1		AtT20-hCB2		Selectivity
				pEC$_{50}$	E$_{Max}$ (%WIN)	pEC$_{50}$	E$_{Max}$ (%WIN)	human
			PB-22	8.30±0.06	114 ± 3	7.43±0.08	101 ± 5	CB$_1$ 7.3
			5F-PB-22	8.55±0.10	108 ± 5	7.97±0.07	101 ± 3	CB$_1$ 3.9
			UR-144	6.38±0.06	94 ± 4	7.15±0.05	104 ± 3	CB$_2$ 5.8
			XLR-11	7.01±0.07	110 ± 4	7.08±0.15	117 ± 10	CB$_2$ 1.2
			5-OH-UR-144	5.71±0.12	159± 11	8.18±0.11	102 ± 5	CB$_2$ 301

7.3.1 Comparison of Agonist activity at hCB$_1$ and hCB$_2$

7.3.1.1 Methoxyquinolinyl derivatives

Having a methoxyquinolinyl –R^2 side group, as seen in PB-22 and 5F-PB-22, was tolerated at both hCB$_1$ and hCB$_2$ receptors as both compounds were highly efficacious and highly potent agonists. Both compounds were hCB$_1$ selective with the highest potencies

shown by SCs next to the indazole/indole derivatives. Their potencies ranged from 50-90 times more potent than WIN and 12-23 times more potent than Δ^9-THC at hCB$_1$ (Figure 24 A). At hCB$_2$, potencies and efficacies were similar to that of WIN (Figure 24 B). The fluorination of the N-pentyl side chain did not show a significant difference in potency at hCB$_1$ or hCB$_2$ as potencies differed less than 2-fold between PB-22 and 5F-PB-22.
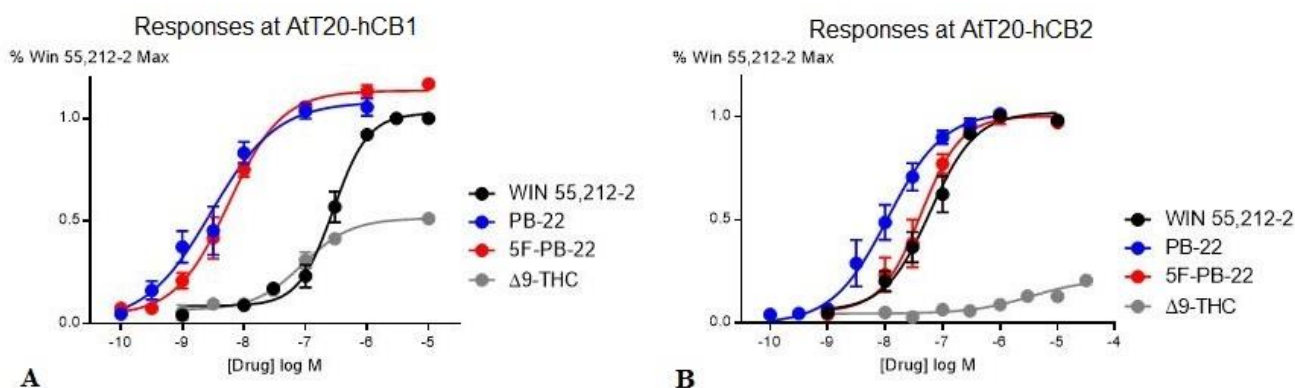
Figure 24: Concentration response curves for WIN, PB-22, 5F-PB-22 and Δ^9-THC at hCB$_1$ and hCB$_2$. A.) Illustrates the increase in potency and efficacy displayed by PB-22 and 5F-PB-22 compared to WIN and Δ^9-THC at hCB$_1$. B.) Illustrates an increase in potencies and efficacies for PB-22 and 5F-PB-22 compared to WIN and Δ^9-THC at hCB$_2$. This highlights the degree of hCB$_1$ selectivity displayed by both compounds. Data represent mean values $\pm$ SEM from 5-8 experiments each run in duplicate.

7.3.1.1 Tetramethylcyclopropyl derivatives

Both XLR-11 and UR-144 were potent and efficacious at both hCB$_1$ and hCB$_2$, confirming findings previously reported in the literature. UR-144 had similar reactivity at both hCB$_1$ and hCB$_2$ but was slightly less potent than WIN at hCB$_1$. XLR-11 had efficacies greater than the maximum WIN response at both hCB$_1$ and hCB$_2$. Its potency was similar to that of WIN at hCB$_2$, but was 5 times more potent than WIN at hCB$_1$. A comparison of their concentration response curves at hCB$_1$ (A) and hCB$_2$ (B) can be seen in Figure 25. The fluorination of the N-pentyl side chain had a more significant effect at hCB$_1$ within this –R^2 side group as XLR-11 was approximately 4 times more potent than its non-fluorinated

counterpart. There was no effect on potency between the fluorinated and non-fluorinated compounds at hCB$_2$ as they both had EC$_{50}$ values of 72 nM. Efficacy had no significant differences between the compounds at either receptor.
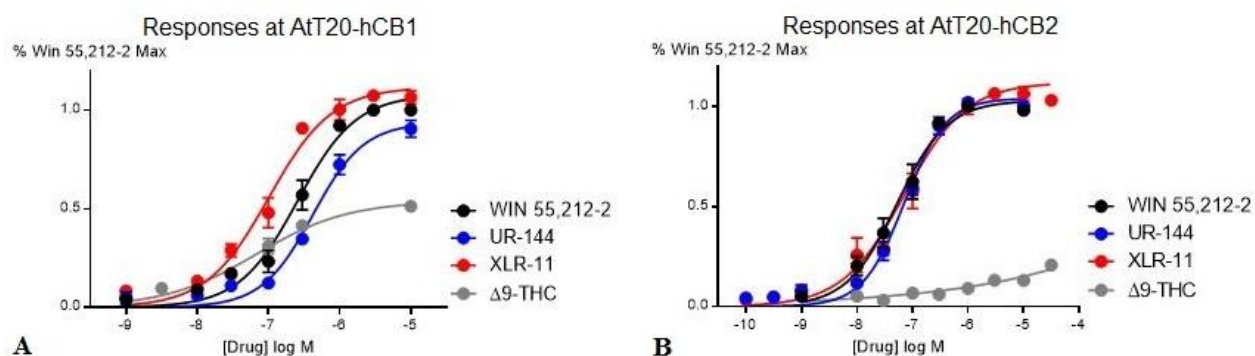
Figure 25: Concentration response curves for WIN, UR-144, XLR-11 and Δ^9-THC at hCB$_1$ and hCB$_2$. A.) Illustrates the increase in potency and efficacy displayed by XLR-11 compared to WIN and Δ^9-THC. It also illustrates the decrease in potency and efficacy of UR-144 compared to WIN and a decrease in potency but an increase in efficacy compared to Δ^9-THC at hCB$_1$. B.) Illustrates the slight increase in efficacies of UR-144 and XLR-11 compared to WIN (large increase compared to Δ^{9-}THC) but that potencies remained similar to WIN at hCB$_2$. Data represent mean values ± SEM from 5-8 experiments each run in duplicate.

7.3.1.1.1 *Hydroxylated Mutual Metabolite*

The hydroxylated mutual metabolite of XLR-11 and UR-144 was also a potent and efficacious agonist at both hCB$_1$ and hCB$_2$. Though its potency was approximately 7 times less than both WIN and Δ^9-THC at hCB$_1$, the highest recorded response at 30 μM exceeded the E$_{Max}$ of WIN by approximately 50% of WIN max. Due to the constraints of solubility, this compound could not be tested over 30 μM, but as seen in Figure 26, an E$_{Max}$ was not yet achieved and therefore, its efficacy could be even greater. 5-OH-UR-144 was also highly hCB$_2$ selective with its potency being 300 times greater at hCB$_2$ than hCB$_1$. Its efficacy was similar to that of WIN but it was 40 times more potent than WIN at hCB$_2$.
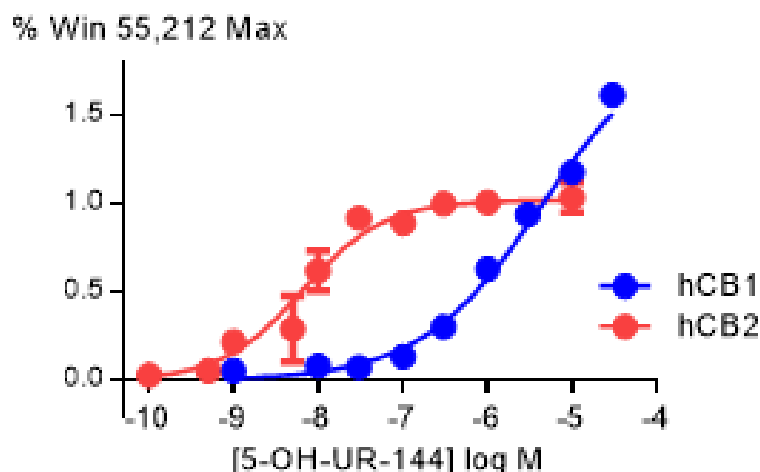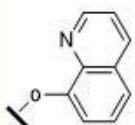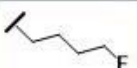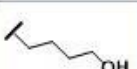
Figure 26: Concentration response curves for 5-OH-UR-144 at hCB$_1$ and hCB$_2$.
This highlights the magnitude of the potency differences between hCB$_1$ and hCB$_2$ of the highly hCB$_2$ selective metabolite, 5-OH-UR-144. It also illustrates that an E$_{Max}$ was not reached at hCB$_1$ at the highest concentration tested (30 μM). Data represent mean values ± SEM from 5-8 experiments each run in duplicate.

7.3.1 Activity at TRP Channels

A fluorescence-based plate reader assay was used to measure the change in intracellular calcium as described in Chapter 2 and verified in Chapter 3. All compounds were tested for their agonist activity at hTRPV1 and hTRPA1. All compounds except for 5F-PB-22 showed agonist/partial agonist activity at hTRPA1. Agonist/Antagonist activity was tested at hTRPV1 and only 5-OH-UR-144 showed partial agonist/antagonist activity. UR-144 and XLR-11 had weak antagonist activity. Maximum responses for agonist/antagonist activity at both receptors is listed in Table 15, as well as, pEC$_{50}$ values where applicable.

Table 15: Functional agonist activity at hTRPA1 and agonist/antagonist activity at hTRPV1 as separated by similarities in functional groups. The functional activity of compounds PB-22, 5F-PB-22, UR-144, XLR-11 and 5-OH-UR-144 are listed by their common functional groups: $-R^1$ N-pentyl, N-5-fluoropentyl and N-5-hydroxyl; and $-R^2$ groups: methoxyquinolinyl and tetramethylcyclopropyl. Data represent mean values $\pm$ SEM from 5-6 experiments each run in duplicate.

Backbone	R2	R1	NAME	hTRPV1			hTRPA1	
				Max Response at 30 μM (%CAP)	Max Inhibition of 300 nM CAP (%CAP)	pEC50	Max Response at 30 μM (%CIN)	
			PB-22	<10	<10	4.31 ± 0.03*	35 ± 2	
			5F-PB-22	<10	<5	N.D.	<10	
			UR-144	<5	12%	3.91 ± 0.22*	38 ± 2	
			XLR-11	<1	30%	3.91 ± 0.2*	89 ± 2	
			5-OH-UR-144	37 ± 2	60%	4.6 ± 0.2	100 ± 5	

*pEC50 assuming that the maximum is equivalent to the maximum of cinnamaldehyde
N.D. = Not Detected at 30 μM

7.3.1.1 Methoxyquinolinyl derivatives

Neither PB-22 nor 5F-PB-22 showed either antagonist or agonist activity at hTRPV1. PB-22 did have weak agonist activity at hTRPA1. Due to solubility PB-22 could not be tested higher than 30 μM, at this concentration it had a maximum response of 35% of CIN max.

7.3.1.2 Tetramethylcyclopropyl derivatives

Both UR-144 and XLR-11 had agonist activity at hTRPA1. Similar to that of PB-22, neither UR-144 nor XLR-11 reached an E_{Max} at the highest concentration tested (30 μM). Although it did not reach a clear plateau, XLR-11 still had similar response at the maximum concentration tested (89% of CIN max at 30 μM) to the E_{Max} of CIN. UR-144 had a

maximum response of approximately half of that of its fluorinated counterpart (38% of CIN max). This was the opposite of the methoxyquinolinyl derivatives where the fluorinated analogue had no activity at hTRPA1. Both XLR-11 and UR-144 were also weak antagonists at hTRPV1 with maximum decreases in the response of 300 nM CAP being 30 and 12% of CAP max respectively.

7.3.1.2.1   *Hydroxylated Mutual Metabolite*

5-OH-UR-144 showed agonist activity at both hTRPV1 and hTRPA1. At hTRPA1, 5-OH-UR-144 was five times less potent than CIN ($pEC_{50} = 5.22 \pm 0.04$) with a pEC_{50} value of 4.7 ± 0.4, but had a maximal response at 30 μM that was 100% of CIN max even though it did not reach a clear plateau (Figure 27).
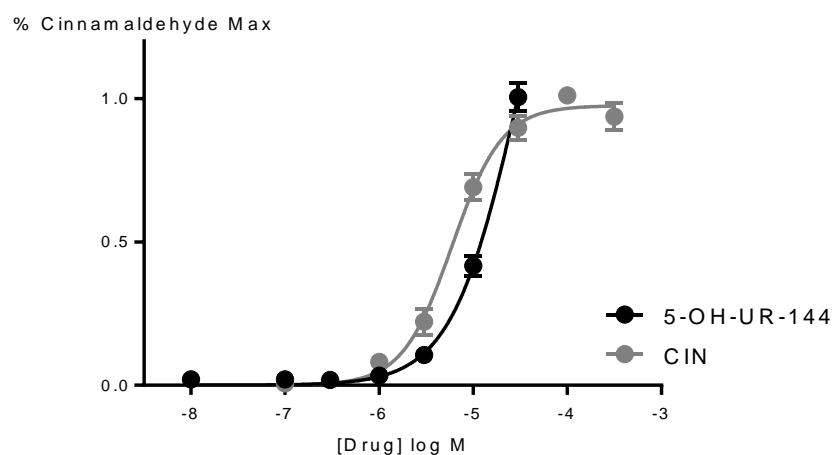
Figure 27: Agonist activity of 5-OH-UR-144 at hTRPA1. This illustrates the concentration response curves for 5-OH-UR-144 compared to that of CIN. It highlights that 5-OH-UR-144 has the same maximal response at 30 μM as the E_{Max} of CIN even though that has not reached an E_{Max} itself. Data represent mean values ± SEM from 5-6 experiments each run in duplicate.

At hTRPV1, 5-OH-UR-144 had partial agonist activity with its maximal response at

30 μM being 38% of CAP max (Figure 28 B). However, when 30 μM 5-OH-UR-144 was

challenged with 300nM CAP after 10 minutes, it inhibited the maximum response of CAP

by 60% (Figure 28 A). Due to the non-proportional agonist/antagonist effect, a

concentration response curve for the antagonism of 300 nM CAP was completed and IC_{50}

was calculated to be 3.0 ± 0.2 μM (Figure 28 C).
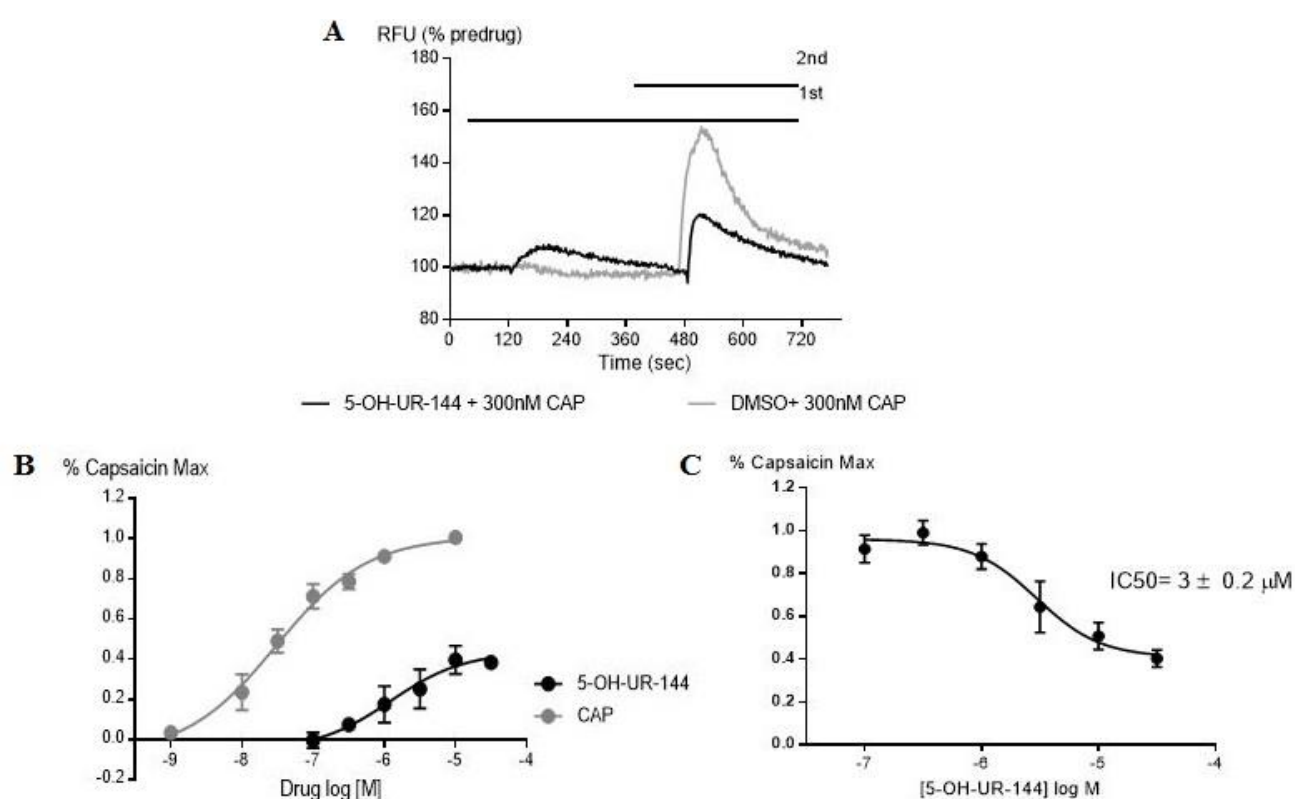
Figure 28: Partial Agonist/Antagonist Activity of 5-OH-UR-44 at hTRPV1. This
figure illustrates A) a trace of the response of 30 μM 5-OH-UR-144 (10 mins)
followed by the addition of 300 nM CAP compare to a DMSO blank (10 mins)
followed by the addition of 300 nM CAP. Both agonist and antagonist effects are
visible. B) concentration response curves for CAP and 5-OH-UR-144 to highlight the
partial agonist activity as shown by the decreased efficacy of 5-OH-UR-144
compared to CAP C) the concentration response curve for the inhibition of 300 nM
CAP response by 5-OH-UR-144 with IC_{50} value of 3.0 ± 0.2 μM. Data represent
mean values $\pm$ SEM from 4-5 experiments each run in duplicate.

7.4 DISCUSSION

Some pharmacological data has previously been reported for the tetramethylcyclopropyl derivatives. Our findings about the potency and efficacy of UR-144, XLR-11 and 5-OH-UR-144 largely corroborated previous findings. Using a FLIPR calcium mobilization assay at hCB_2, Frost reported the EC_{50} values of UR-144 and 5-OH-UR-144 to be within the ranges 29-44 nM and 8-23 nM with E_{Max} values of 93% and 105% of CP 55,940max respectively (Frost et al., 2010). To compare to the fluorescence-based plate reader membrane potential assay at hCB_2, UR-144 and 5-OH-UR-144 exhibited EC_{50} values of 71 nM and 10 nM with E_{Max} of 104% and 117% of WIN max respectively. These results are similar given the differences in the cell lines used (HEK293 and AtT20), differences in normalizations standards and differences between calcium and membrane potential measurements.

Frost et al. also measured the inhibition of adenylate cyclase in hCB_1 and hCB_2 cells and reported that the EC_{50} values for 5-OH-UR-144 were within the range 1881-3383 nM with an E_{Max} of 98% at hCB_1 and 2.1-2.2 nM with an E_{Max} of 100% at hCB_2 (Frost et al., 2010). This indicates that 5-OH-UR-144 is highly CB_2 selective, which would be expected as its creation was developed using SAR knowledge to generate compounds that were structurally predicted to be highly CB_2 selective. Using the fluorescence-based membrane potential assay, 5-OH-UR-144 was found to have EC_{50} values at hCB_1 and hCB_2 of 1949 nM and 6 nM with E_{Max} of 159% and 102% of WIN max. Potencies are similar between the different assays, but the efficacies are significantly different at hCB_1. This is a product of the assay design. By principle the efficacy cannot exceed the 100% maximum in an adenylate cyclase assay as E_{Max} is determined by the displacement of a fixed amount of radiolabeled cAMP that optimally fills all receptor sites and therefore, has a definitive maximum effect that can be attained. In the membrane potential assay, the 100% maximum

response value is determined by the maximum response of the reference compound so in this case, WIN. Reference compounds are chosen for a specific assay by their ability to produce a maximum effect within the bounds of the experimental design. WIN is considered as being a "full agonist", but efficacy is relative, and an agonist displaying "Full" agonism in one system can show reduced relative activity in another because of differences in receptor reserve or signalling bias. Whether WIN is biased to cAMP signalling over GIRK activation compared with 5-OH UR144, or whether there were significant differences in the receptor reserve in the cell lines expressing AC or GIRK remains to be established.

Wiley et al., tested the activity of XLR-11 and UR-144 using [^{35}S] GTPγS binding and found the EC_{50} values for UR-144 and XLR-11 to be 98 nM and 159 nM at hCB_1 and 334 and 145 nM at hCB_2 respectively. Although UR-144 has a lower potency at hCB_1, it had a lower affinity at hCB_2 (< 30 nM) in a radioligand binding assay (Wiley et al., 2013). Therefore, their results validate the tetramethylcyclopropyl derivatives are CB_2 selective which is in agreement with the findings presented here as well as by Frost et al. Our membrane potential assay had EC_{50} values of XLR-11 at hCB_1 and hCB_2 of 97 nM and 83 nM which are 1.5 -2 times more potent than the values generated by Wiley et al, which could reflect the type of assay or relative receptor expression between the 2 cell lines..

Differences in the N1 group (N-pentyl, N-fluoropentyl, N-hydroxypentyl), were consistent with previous findings that the addition of a fluorine to the end of a pentyl chain increases activity at both receptors. XLR-11 had increased potency at both receptors but no change in efficacy. This is the same trend exhibited by JWH-018 and its fluorinated analogue, AM-2201. The hydroxylation that occurs on the N1 substituent through either oxidative defluorination of XLR-11 or oxidative metabolism of UR-144, the N-hydroxypentyl side chain that remains decreases potency significantly at the hCB_1 receptor

yet increases efficacy by approximately 50% of WIN max compared to the N-pentyl or N-fluoropentyl side chains. At hCB$_2$, the N-hydroxypentyl side chain had a potency 17 times greater than that of XLR-11 and 70 times greater than that of UR-144. Similar to that of JWH-018 and AM-2201, the hydroxylated mutual metabolite remains active at both receptors which could be a mode for toxicity.

XLR-11 and 5-OH-UR-144 were also as efficacious at the hTRPA1 receptor as CIN whereas UR-144 only had partial agonist activity. The previous chapters have implicated a more traditional binding site for hTRPA1 which is supported by the lack of electrophilic character in agonist structures. The addition of the terminal fluorine on the N-pentyl in this case seems to increase the amount of activity at hTRPA1. This trend was not seen within PB-22 and 5F-PB-22 as the fluorinated compound had no activity at hTRPA1 where the non-fluorinated showed partial agonist activity. Previous chapters have also shown that the addition of the terminal fluorine only has hTRPA1 activation in specific cases. Therefore, this suggests that the –R^2 side group is more of the determining factor in hTRPA1 activation, though further SAR experiments will need to be done to determine which –R^2 characters have the most influence on hTRPA1 binding. The metabolite 5-OH-UR-144 had the highest activity at hTRPA1 despite it being the most nucleophilic. Though it did not reach an E$_{Max}$, it still had a response similar to CIN max at the highest concentration tested. The fact both parent and metabolite are having strong agonist activity at the off-target pathway could have implications in the toxic effects seen with UR-144 and XLR-11, as TRPA1 acts on sensory nerve endings within the lung, bladder, or other visceral and vascular organs to produce inflammation, vasodilation, and edema (Diana M. Bautista et al., 2006).

The metabolite 5-OH-UR-144 was the only compound to have partial agonist activity as well as significant antagonist activity at hTRPV1. The antagonist activity

displayed is most likely due to 5-OH-UR-144 filling the receptors and therefore blocking

CAP from the binding site. AEA and capsaicin have been shown to bind to the same

TRPV1 binding site as AEA shows partial agonist activity that also decreases the CAP

response when they are co-superfused in mouse TRPV1 (Roberts et al., 2002). This is

similar to the AEA response in the fluorescent-based assay measuring intracellular calcium

saw AEA with a 46% of CAP max response as an agonist and a the partial 42% reduction in

the response of CAP 300 nM at 30 μM. The proportional activation/blocking effect seen by

AEA in this experiment is not mirrored by 5-OH-UR-144 as it has an increase of 38% of

CAP max and a decrease in 300 nM CAP of 60% of CAP max. This may show that though

it does not have a higher intrinsic response at hTRPV1 it may have a higher receptor

occupancy which would explain the higher antagonistic effect seen at 30 μM.

Although PB-22 and 5F-PB-22 are novel SCs in terms of designer drugs of abuse,

quinoline substructures have been used as cannabimimetic agonists since 2006. Instead of

using an indole, Stern et al. used a quinoline structure as the cannabimimetic core in such an

orientation that the nitrogen of the quinoline was in the same location as the N1 position of

an indole. Due to the placement of the quinoline, the structure had a level of "rigidity" that

seemed to increase the binding for the CB_2 receptor, a concept that was covered in Chapter

4 with the rotation of the adamantane moiety (Stern et al., 2006). Unlike these original

cannabimimetic quinolines, PB-22 and 5F-PB-22 have the quinoline structure as a bulky

side group. Huffman et al. has suggested that the aromatic-aromatic interactions of a

naphthalene group with the hydrophobic binding pocket relies on the geometry of its 3-6

carbons (J. W. Huffman et al., 2005). Therefore, the addition of a polar entity into the exact

location where the geometry has been shown to be essential for the formation of aromatic-

aromatic interactions with the binding pocket, would in theory suggest that these

compounds would have decreased activity at the cannabinoid receptors. This was not the

case as PB-22 and 5F-PB-22 were highly potent and efficacious agonists. They were highly CB$_1$ selective, unlike their structural ancestors, with potencies that were 50- 90 times more potent than WIN and 12-23 times more potent than Δ^9-THC. Their efficacies also exceeded the maximum response of WIN at both receptors. Alternatively to other fluorinated/non-fluorinated pairs, the N-fluoropentyl group did not show an increase in receptor activity as the efficacies for both receptors and the potency at hCB$_1$ remained constant with the addition of a terminal fluorine on the $-R^1$ side chain. At hCB$_2$, the potency actually decreased with fluorination.

Another structural difference that has made PB-22 and 5F-PB-22 unique is the connection of the indole group to its $-R^2$ side chain by an ester linker, a common linker used in pro-drug formation, which is susceptible to hydrolysis by nonspecific esterases making the compounds relatively unstable (Mitra et al., 2013). A metabolic profile constructed by Wohlfarth et al. showed PB-22 and 5F-PB-22 primarily undergo ester hydrolysis to form a wide variety of (5-fluoro)pentylindole-3-carboxylic acid metabolites. They still underwent oxidation and oxidative defluorination to make a 5-hydroxylpentyl metabolite similar to other non-fluorinated/fluorinated SCs but this metabolic pathway was secondary to that of the ester hydrolysis (Ariane Wohlfarth et al., 2014b). Glucuronidation was the most common phase II metabolic pathway which is the same primary pathway for the metabolism of paracetamol which could lead to toxicity in the liver. With lower doses of paracetamol, it is metabolized by cytochrome P-450 enzymes to make NAPQI (*N*-acetyl-*p*-benzoquinone imine), a toxic intermediate that is deactivated by the conjugation with a glutathione and safely passed into the urine (Miner & Kissinger, 1979). In a paracetamol overdose, there is not enough glutathione to deactivate the NAPQI causing it to build up resulting in reactions with hepatocellular proteins and nucleic acids. The analytical conditions used to determine the metabolic profile of PB-22 and 5F-PB-22 was not able to see quinoline metabolites due

to their small size and polarity but there is potential the quinoline structure or another metabolite is forming a similar toxic structure to that of NAPQI (Behonick et al., 2014; Ariane Wohlfarth et al., 2014b) . There is evidence for this as acetylcysteine, which is used to replenish the supply of glutathione in the liver, successfully reversed the symptoms presented by SC intoxication (Sheikh, Lukšič, Ferstenberg, & Culpepper-Morgan, 2014).

As necessary as it is to develop pharmacological profiles of the new SCs that are being developed, this data set corroborates the increasing evidence that metabolism of these compounds is an integral factor in the presentation of their physiological effects. The increase in activity at the off-target TRP channels of 5-OH-UR-144 compared to its parent compounds shows metabolites could potentially have more deleterious actions as they are targeting more pathways. With many SCs undergoing similar metabolic pathways, it is important that metabolite profiling continues to be assessed.

CHAPTER 8: DEVELOPMENT OF LIPIDOMICS METHODS TO QUANTIFY ENDOCANNABINOID PRODUCTION AFTER DRUG TREATMENT

8 DEVELOPMENT OF LIPIDOMICS METHODS TO QUANTIFY ENDOCANNABINOID PRODUCTION AFTER DRUG TREATMENT

8.1 SUMMARY

Case studies of patients presenting with SC adverse effects have reported that many complain of severe agitation, paranoia and hallucinations, which would be a side effect consistent with CB_1 activation. Other, less predictable adverse effects are that of the peripheral pain, cardiac arrest, edema and inflammation of organs (Behonick et al., 2014). Endocannabinoids (EC) have been implicated in the modulation of behavioural responses to pain and inflammation (Cravatt & Lichtman, 2004). There is a potential that SCs are having further off-target effects, invoking the EC system, which could mean their actions could be cannabinoid receptor mediated both directly and indirectly (Van der Stelt et al., 2005). As some activate the TRP channels which would result in an influx of calcium, it can be presumed that AEA and 2-AG may be made "on demand" as a result (Raphael Mechoulam et al., 2014). These ECs have potential to then further activate cannabinoid receptors adding another layer to the already complicated SC story. Therefore, to determine if the exposure to SCs was having off-target effects involving EC generation, a lipidomics method was adapted from previous work and used to determine the endocannabinoid changes after drug stimulation. Preliminary data will be presented on the levels of the endocannabinoids: AEA, 2-AG, PEA, OEA and LEA; in HEK293-WT, HEK293-hTRPV1, HEK293-hTRPA1, AtT20-hCB1 and AtT20-hCB2 cell lines. Although this was a preliminary study and therefore, much work is still to be done, the success in method development and intriguing preliminary results demonstrates the value of looking at the endocannabinoid system for off-target effects that could be potential modes for SC toxicity.

8.2 INTRODUCTION

The endocannabinoid system is responsible for a myriad of processes both in the central nervous system and throughout the periphery. CB_1 receptors in the CNS are located presynaptically and have a primary purpose of regulating the release of neurotransmitters through the inhibition of glutamatergic, GABAergic, glycinergic, cholinergic, noradrenergic and serotonergic neurotransmission by endogenous or exogenous cannabinoids (Szabo & Schlicker, 2005). In the periphery, activation of CB_1 receptors can inhibit the release of noradrenaline and/or ATP which elicits its overall inhibitory effect on responses in the heart, inmesenteric and renal blood vessels and in the vas deferens. This can induce hypotension and bradycardia by depression of the vagal nerve stimulation (R.G. Pertwee, 2006). Of the adverse side effects reported after SC consumption, tachycardia and bradycardia, necrotizing granulomatous inflammation, pulmonary edema, and congestion of viscera have all been reported (Behonick et al., 2014; Harris & Brown, 2013). As many of these side effects seen had cross over with endocannabinoid-associated effects, a method was developed to determine if the SCs had an effect on endocannabinoid production. This was done by utilizing a lipid extraction technique found in Stuart et al, and adapting it to and in-flask cellular based extraction (Stuart et al., 2013). Originally, HEK293-hTRPV1 cells were used to explore the vitality of this method.. Liao et al. had previously shown that capsaicin mediates anti-nociception by the activation of presynaptic TRPV1 channels resulting in the release of glutamate, which could then activate the postsynaptic metabotropic glutamate receptor 5 ($mGlu_5$) causing the production of 2-AG which could then be used for retrograde signaling at CB_1. They proved 2-AG release by blocking the capsaicin induced effect with MAG lipase but did not actually measure 2-AG levels (Liao, Lee, Ho, & Chiou, 2011).

Therefore, capsaicin was added to HEK293-hTRPV1 cells to determine if A) endocannabinoid levels could be determined from cells in general 2) that capsaicin would cause an increase in 2-AG. The same experimental conditions were then used in HEK293-WT cells as a negative control. At the time of MS/MS analysis, SCs had not been shown to have significant effects on hTRPV1 in the fluorescent-based plate reader assays that measured the changes in intracellular calcium, therefore, SCs were not tested on this cell line. AtT20-hCB1, AtT20-hCB2 and HEK293-hTRPA1 cells were then tested to determine if a five minute stimulation with the maximal concentration used the in the fluorescent-based membrane potential assay would cause a change in the levels of endocannabinoids at these receptors. Of the SCs, XLR-11 and 5-OH-UR-144 were tested for their agonist activity at all three receptor types. Due to the concurrent fluorescent-based plate reader assays, when partial agonist activity was determined for 5-OH-UR-144 on HEK293-hTRPV1, time precluded the ability to test this drug at this receptor type. This experiment as well as further antagonist and wild type negative controls will be first priority in future studies.

8.3 RESULTS

The specific methods used in this chapter are covered in Chapter 2 sections 2.4 and 2.5. First mass spectrometic methods had to be developed to determine if it was possible to isolate endocannabinoids from cell extracts. Iain McGregor graciously allowed the use of his Shimadzu high performance liquid chromatography machine in tandem with a Shimadzu triple quadrupole mass spectrometer for use in the following experiments. Using electrospray ionization (ESI), preliminary product ion scans (PSI) were run to determine the optimal fragmentation (and specific collision energies) of the endocannabinoids: AEA, 2-

AG, PEA, OEA, LEA and d$_4$-AEA which were then compared and validated against the fragmentation profile used in previous mass spectrometer experiments (Stuart et al., 2013). Using the final fragmentation profile (parent ion/ daughter fragment) as shown in Table 16, a multiple reaction monitoring method in the positive mode (MRM$^+$) was used to scan for the endocannabinoids simultaneously. Figure 29 shows chromatograms for a 10 μL injection of a 1 nM standard solution. A representative chromatogram of biological sample versus standard peaks are shown in Appendix C (pg. 308-314).

Table 16: Spectrometry Properties of Standards. This table represents the fragmentation profile of the standard compounds. It also shows the retention time (RT) relative to an 8 minute runtime.

	D$_4$AEA	AEA	2-AG	PEA	OEA	LEA
M/Z	352.0/66.0	348.0/62.2	379.2/287.1	300.2/62.2	326.0/62.2	324.0/62.0
RT (MINS)	3.982	3.986	3.979	4.153	4.201	3.891
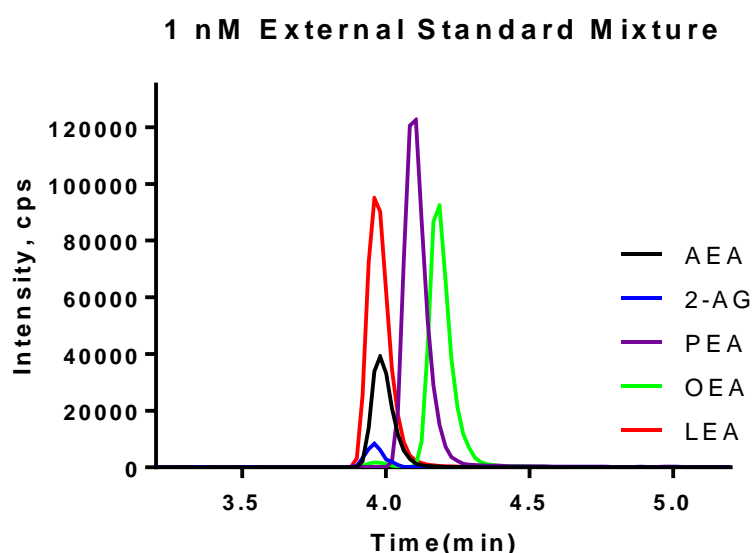
Figure 29: Chromatograms for Endocannabinoid Standards. This figure illustrates the chromatograms of a 10 μL injection of a 1 nM standard to establish that clear separation was occurring and that all compounds were able to be identified.

8.3.1 **Drug stimulations on HEK293-hTRPV1**

A DMSO control (0.01%), 10 μM capsazepine (CAPZ) and 1 μM CAP concentrations were added to HEK293-hTRPV1 cells that had been induced with tetracyclin (1 μg/mL) for 4 hours. The DMSO, capsazepine, and capsaicin additions were administered for 5 minutes. 100% HPLC MeOH was added to each reaction flask, killing the cells and therefore stopping further endocannabinoid production. In the antagonist challenged experiment, capsazepine was added for 10 minutes and aspirated off before the addition of capsaicin which was allowed to incubate for 5 minutes before the addition of MeOH. Reverse phase column chromatography was used to isolate and purify the compounds of interest and HPLC/MS/MS was used to quantify the level of endocannabinoids. Recoveries were calculated by a comparison of the amount of d_4AEA left in the biological sample (originally added to the sample pre lipid extraction) compared to a recovery standard that is representative of 100% recovery, meaning the amount of d_4AEA that should have been present in the sample had no compound been lost. This value represents the effectiveness of the extraction process and therefore, final mean values (n= 4-9) of the amount of compound present was adjusted to compensate for this loss. Appendix C (pg. 308-314) has a graphic representation of all of the endocannabinoid levels present by cell type and drug condition as well as tables for statistical p values to determine significant differences. Only significant changes compared to the DMSO control, as determined by a one-way ANOVA with post hoc Fisher's LSD with a 95% confidence interval for the mean (GraphPad Prism 6), will be presented in a graphic representation in this chapter. Figure 30 shows the only significant change in the HEK293-hTRPV1 stimulation experiment was an increase in 2-AG as stimulated by CAP. Table 17 shows the rest of the values of endocannabinoids present per drug condition as presented in moles/gram tissue.
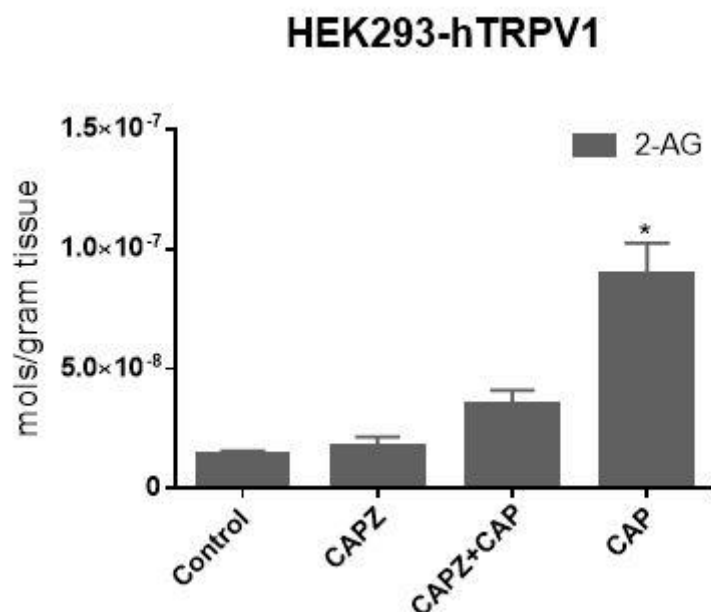
HEK293-hTRPV1

Figure 30: 2-AG levels in HEK293-hTRPV1 after drug treatment (n=6-8). This figure illustrates the significant increase in 2-AG levels of the CAP stimulation group compared to that of the DMSO control group as determined by a one-way ANOVA with post hoc Fisher's LSD with a 95% confidence interval (* = p < 0.0001).

Table 17: Levels of endocannabinoids after drug stimulation in HEK293-hTRPV1. This table shows the values of each endocannabinoid per drug treatment in HEK293-hTRPV1 (n=6-8). The values are represented as moles per gram tissue ± SEM. The average recovery value of d_4AEA with which the values were adjusted is also represented as a percentage. Significant changes are highlighted in bold as determined by a one-way ANOVA with post hoc Fisher's LSD with a 95% confidence interval for the mean using SPSS software (P≤0.05).

	AEA (mols/gram tissue) ± SEM	2-AG (mols/gram tissue) ± SEM	PEA (mols/gram tissue) ± SEM	OEA (mols/gram tissue) ± SEM	LEA (mols/gram tissue) ± SEM	Average Recovery (%)
Control	$1.0 \text{ E}^{-11} \pm$ 1.7 E^{-12}	$1.4 \text{ E}^{-9} \pm$ 1.0 E^{-9}	$3.0 \text{ E}^{-10} \pm$ 3.8 E^{-11}	$1.1 \text{ E}^{-9} \pm$ 1.3 E^{-10}	$6.3 \text{ E}^{-11} \pm$ 1.9 E^{-11}	
CAPZ	$8.5 \text{ E}^{-12} \pm$ 1.7 E^{-13}	$1.7 \text{ E}^{-9} \pm$ 4.6 E^{-10}	$3.2 \text{ E}^{-10} \pm$ 1.9 E^{-11}	$1.1 \text{ E}^{-9} \pm$ 1.2 E^{-10}	$5.7 \text{ E}^{-11} \pm$ 4.7 E^{-12}	57
CAPZ + CAP	$1.6 \text{ E}^{-11} \pm$ 1.7 E^{-12}	$3.5 \text{ E}^{-9} \pm$ 7.6 E^{-10}	$4.6 \text{ E}^{-10} \pm$ 1.3 E^{-10}	$1.5 \text{ E}^{-9} \pm$ 3.7 E^{-10}	$9.1 \text{ E}^{-11} \pm$ 2.9 E^{-11}	
CAP	$1.1 \text{ E}^{-11} \pm$ 1.8 E^{-12}	**$8.9 \text{ E}^{-9} \pm$ 1.3 E^{-9}**	$3.4 \text{ E}^{-10} \pm$ 4.0 E^{-11}	$1.1 \text{ E}^{-9} \pm$ 1.1 E^{-10}	$5.7 \text{E}^{-11} \pm$ 1.2E^{-11}	

8.3.2 Drug stimulations on HEK293-WT

To determine if the 2-AG increase seen post CAP stimulation was a result of the hTRPV1 receptor, HEK293-WT cells were tested under the same conditions as HEK293-hTRPV1. There was a significant increase in 2-AG and AEA in the antagonist + agonist test group as seen in Figure 31. There was not, however, the same increase in 2-AG that was seen with CAP in the hTRPV1 cells. Table 18 shows the rest of the values of endocannabinoids present per drug condition as presented in moles/gram tissue.
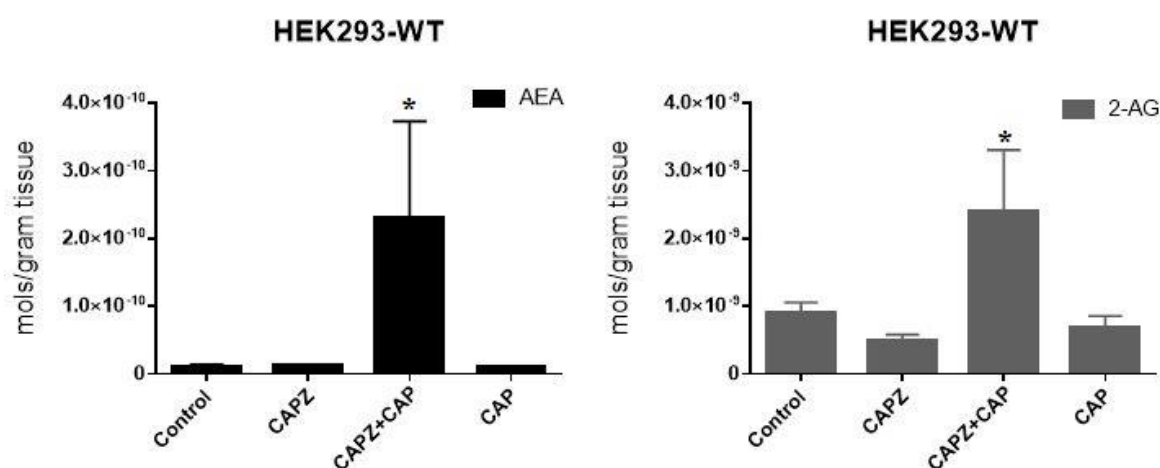
Figure 31: AEA and 2-AG levels in HEK293-WT after drug treatment (n=4-7). This figure illustrates the significant increase in AEA and 2-AG levels of the capsazepine + capsaicin stimulation group compared to that of the DMSO control group as determined by a one-way ANOVA with post hoc Fisher's LSD with a 95% confidence interval (* = $p < 0.0121$ and 0.0197 respectively).

Table 18: Levels of endocannabinoids after drug stimulation in HEK293-WT.
This table shows the values of each endocannabinoid per drug treatment in HEK293-WT(n=4-7). The values are represented as moles per gram tissue ± SEM. The average recovery value of d_4AEA with which the values were adjusted is also represented as a percentage. Significant changes are highlighted in bold as determined by a one-way ANOVA with post hoc Fisher's LSD with a 95% confidence interval for the mean using SPSS software (P≤0.05).

	AEA (mols/gram tissue) ± SEM	2-AG (mols/gram tissue) ± SEM	PEA (mols/gram tissue) ± SEM	OEA (mols/gram tissue) ± SEM	LEA (mols/gram tissue) ± SEM	Average Recovery (%)
Control	$1.2\,E^{-11} \pm 2.7\,E^{-12}$	$9.0\,E^{-10} \pm 1.8\,E^{-10}$	$4.4\,E^{-10} \pm 8.0\,E^{-11}$	$1.7\,E^{-9} \pm 4.4\,E^{-10}$	$1.1\,E^{-10} \pm 1.9\,E^{-11}$	
CAPZ	$1.3\,E^{-11} \pm 1.3\,E^{-12}$	$5.0\,E^{-10} \pm 9.6\,E^{-11}$	$4.4\,E^{-10} \pm 4.4\,E^{-10}$	$1.6\,E^{-9} \pm 4.5\,E^{-10}$	$1.1\,E^{-10} \pm 4.7\,E^{-11}$	
CAPZ + CAP	$\mathbf{2.3\,E^{-10} \pm 1.7\,E^{-10}}$	$\mathbf{2.1\,E^{-9} \pm 8.2\,E^{-10}}$	$8.7\,E^{-10} \pm 4.3\,E^{-10}$	$2.5\,E^{-9} \pm 1.2\,E^{-9}$	$2.2\,E^{-10} \pm 2.9\,E^{-10}$	51
CAP	$1.0\,E^{-11} \pm 1.7\,E^{-12}$	$6.8\,E^{-10} \pm 2.0\,E^{-10}$	$4.0\,E^{-10} \pm 9.3\,E^{-11}$	$1.2\,E^{-9} \pm 2.7\,E^{-10}$	$5.3\,E^{-11} \pm 1.2E^{-11}$	

8.3.3 Drug stimulations on AtT20-hCB1

To determine if SCs were having an effect on the endocannabinoid system, AtT20-hCB1 were used to directly compare endocannabinoid production to agonist activity generated with the fluorescent-based membrane potential assay. A DMSO control (0.01%), 1 μM SR141617A, 1 μM CP 55,940, 10 μM XLR-11 and 10 μM 5-OH-UR-144 concentrations were added to AtT20-hCB1 cells. All drugs were administered for five minutes except for the SR141617A + CP 55,940 which had a 10 minute stimulation of SR141617A that was aspirated off before a five minute addition of CP 55,940. There was only one significant change in one endocannabinoid level in one drug test group and that was an increase in PEA after stimulation with XLR-11 compared to the DMSO control as seen in Figure 32. Table 19 shows the rest of the values of endocannabinoids present per drug condition as presented in moles/gram tissue.
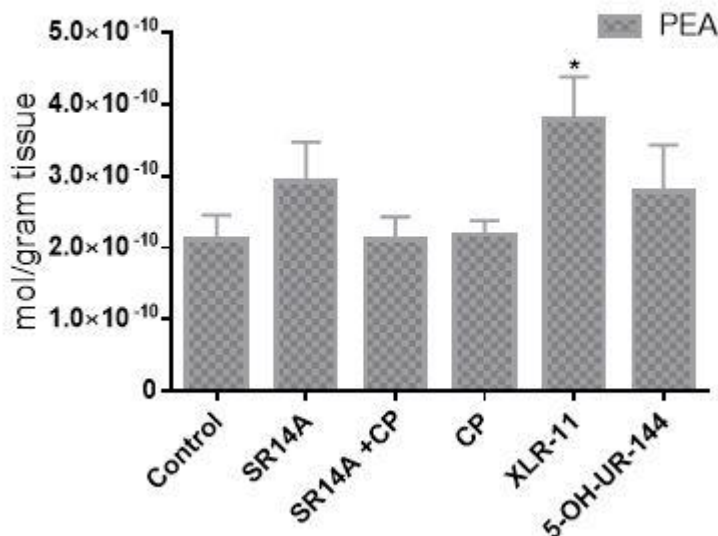
Figure 32: PEA levels in AtT20-hCB1 after drug treatment (n=6). This figure illustrates the significant increase in PEA levels of the XLR-11 stimulation group compared to that of the DMSO control group as determined by a one-way ANOVA with post hoc Fisher's LSD with a 95% confidence interval (* = $p < 0.031$).

Table 19: Levels of endocannabinoids after drug stimulation in AtT20-hCB1. This table shows the values of each endocannabinoid per drug treatment in AtT20-hCB1 (n=6). The values are represented as moles per gram tissue ± SEM. The average recovery value of d_4AEA with which the values were adjusted is also represented as a percentage. Significant changes are highlighted in bold as determined by a one-way ANOVA with post hoc Fisher's LSD with a 95% confidence interval for the mean using SPSS software (P≤0.05).

	AEA (mols/gram tissue) ± SEM	2-AG (mols/gram tissue) ± SEM	PEA (mols/gram tissue) ± SEM	OEA (mols/gram tissue) ± SEM	LEA (mols/gram tissue) ± SEM	Average Recovery (%)
Control	$2.2\,E^{-11} \pm 1.3\,E^{-11}$	$2.1\,E^{-9} \pm 1.5\,E^{-10}$	$2.1\,E^{-10} \pm 4.0\,E^{-11}$	$5.6\,E^{-10} \pm 1.7\,E^{-10}$	$4.9\,E^{-11} \pm 1.5\,E^{-11}$	
SR14A	$2.1\,E^{-11} \pm 5.9\,E^{-12}$	$2.0\,E^{-9} \pm 3.4\,E^{-10}$	$2.8\,E^{-10} \pm 6.5\,E^{-11}$	$5.9\,E^{-10} \pm 1.5\,E^{-10}$	$4.8\,E^{-11} \pm 9.7\,E^{-12}$	
SR14A + CP 55,940	$1.7\,E^{-11} \pm 3.8\,E^{-12}$	$1.6\,E^{-9} \pm 5.1\,E^{-10}$	$2.2\,E^{-10} \pm 3.6\,E^{-11}$	$5.5\,E^{-10} \pm 8.0\,E^{-11}$	$5.0\,E^{-11} \pm 7.4\,E^{-12}$	46
CP 55,940	$2.2\,E^{-11} \pm 7.9\,E^{-12}$	$1.1\,E^{-9} \pm 2.5\,E^{-10}$	$2.2\,E^{-10} \pm 2.4\,E^{-11}$	$5.6\,E^{-10} \pm 8.8\,E^{-11}$	$3.8\,E^{-11} \pm 7.7\,E^{-12}$	
XLR-11	$1.2\,E^{-11} \pm 6.3\,E^{-12}$	$2.3\,E^{-9} \pm 2.5\,E^{-10}$	**$2.8\,E^{-10} \pm 7.5\,E^{-11}$**	$5.7\,E^{-10} \pm 1.6\,E^{-10}$	$5.0\,E^{-11} \pm 2.0\,E^{-11}$	
5-OH-UR-144	$3.9\,E^{-11} \pm 2.9\,E^{-12}$	$1.9\,E^{-9} \pm 5.0\,E^{-10}$	$3.8\,E^{-10} \pm 7.4\,E^{-11}$	$8.6\,E^{-10} \pm 3.2\,E^{-10}$	$5.7\,E^{-11} \pm 1.5\,E^{-11}$	

8.3.4 **Drug stimulations on AtT20-hCB2**

To determine if SCs were having an effect on the endocannabinoid system at AtT20-hCB2, cells were tested to directly compare endocannabinoid production to agonist activity generated with the fluorescent-based membrane potential assay. A DMSO control (0.01%), 10 μM AM630, 1 μM CP 55,940, 10 μM XLR-11 and 10 μM 5-OH-UR-144 concentrations were added to AtT20-hCB2 cells. All drugs were administered for five minutes except for the AM630 + CP 55,940 which had a 10 minute stimulation of AM630 that was aspirated off before a five minute addition of CP 55,940. There was only one significant change in one endocannabinoid level in one drug test group and that was an increase in 2-AG after stimulation with AM-630 compared to the DMSO control as seen in Figure 33. Table 20 shows the rest of the values of endocannabinoids present per drug condition as presented in moles/gram tissue.
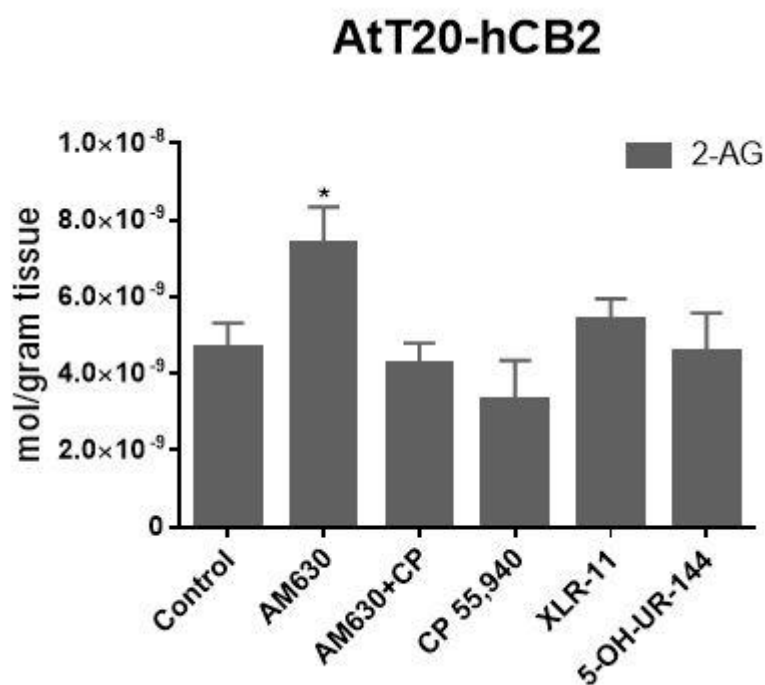
Figure 33: 2-AG levels in AtT20-hCB2 after drug treatment (n=6). This figure illustrates the significant increase in 2-AG levels of the AM630 stimulation group compared to that of the DMSO control group as determined by a one-way ANOVA with post hoc Fisher's LSD with a 95% confidence interval (* = $p < 0.035$).

Table 20: Levels of endocannabinoids after drug stimulation in AtT20-hCB2.
This table shows the values of each endocannabinoid per drug treatment in AtT20-hCB2 (n=6). The values are represented as moles per gram tissue $\pm$ SEM. The average recovery value of d_4AEA with which the values were adjusted is also represented as a percentage. Significant changes are highlighted in bold as determined by a one-way ANOVA with post hoc Fisher's LSD with a 95% confidence interval for the mean using SPSS software (P$\leq$0.05).

	AEA (mols/gram tissue) $\pm$ SEM	2-AG (mols/gram tissue) $\pm$ SEM	PEA (mols/gram tissue) $\pm$ SEM	OEA (mols/gram tissue) $\pm$ SEM	LEA (mols/gram tissue) $\pm$ SEM	Average Recovery (%)
Control	$4.5\,E^{-11} \pm 1.4\,E^{-11}$	$1.9\,E^{-10} \pm 4.8\,E^{-11}$	$4.8\,E^{-10} \pm 2.1\,E^{-11}$	$1.9\,E^{-9} \pm 4.1\,E^{-10}$	$1.9\,E^{-10} \pm 4.8\,E^{-11}$	
AM630	$4.6\,E^{-11} \pm 2.0\,E^{-11}$	$\mathbf{3.1\,E^{-10} \pm 6.8\,E^{-11}}$	$7.4\,E^{-10} \pm 1.6\,E^{-10}$	$2.3\,E^{-9} \pm 5.6\,E^{-10}$	$3.1\,E^{-10} \pm 6.8\,E^{-11}$	
AM630 + CP 55,940	$2.7\,E^{-11} \pm 9.9\,E^{-12}$	$1.5\,E^{-10} \pm 2.7\,E^{-11}$	$4.9\,E^{-10} \pm 9.2\,E^{-11}$	$1.3\,E^{-9} \pm 2.4\,E^{-10}$	$1.5\,E^{-10} \pm 2.7\,E^{-11}$	42
CP 55,940	$3.4\,E^{-11} \pm 9.8\,E^{-12}$	$1.7\,E^{-10} \pm 5.6\,E^{-11}$	$6.4\,E^{-10} \pm 1.6\,E^{-10}$	$1.7\,E^{-9} \pm 4.8\,E^{-10}$	$1.7\,E^{-10} \pm 5.6\,E^{-11}$	
XLR-11	$3.9\,E^{-11} \pm 9.4\,E^{-12}$	$6.1\,E^{-11} \pm 4.1\,E^{-11}$	$5.0\,E^{-10} \pm 9.2\,E^{-11}$	$1.3\,E^{-9} \pm 2.0\,E^{-10}$	$6.0\,E^{-11} \pm 4.1\,E^{-11}$	
5-OH-UR-144	$3.2\,E^{-11} \pm 1.2\,E^{-11}$	$1.3\,E^{-10} \pm 5.9\,E^{-11}$	$5.3\,E^{-10} \pm 1.0\,E^{-10}$	$1.5\,E^{-9} \pm 3.4\,E^{-10}$	$1.3\,E^{-10} \pm 5.9\,E^{-11}$	

8.3.5 **Drug stimulations on HEK293-hTRPA1**

To determine if SCs were having an effect on the endocannabinoid system at HEK293-hTRPA1, cells were tested to directly compare endocannabinoid production to agonist activity generated with the fluorescent-based assay measuring intracellular calcium. A DMSO control (0.01%), 300 μM CIN, 10 μM XLR-11 and 10 μM 5-OH-UR-144 concentrations were added to HEK293-hTRPA1 cells. There was only one significant change in one endocannabinoid level in one drug test group and that was an increase in 2-AG after stimulation with CIN compared to the DMSO control as seen in Figure 30. Table 19 shows the rest of the values of endocannabinoids present per drug condition as presented in moles/gram tissue. Due to time constraints, the antagonist experiments could not be conducted. A repeat of this experiment with antagonists is a first priority for future studies.

HEK293-hTRPA1
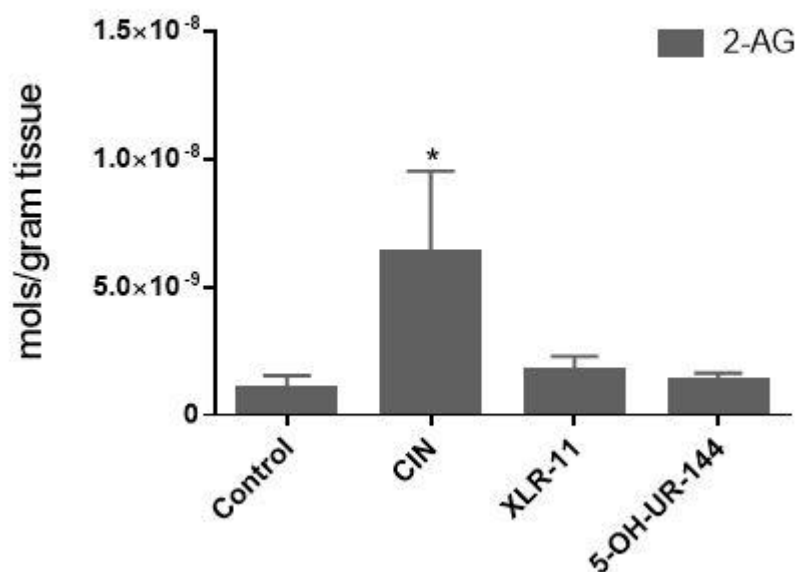
Figure 34: 2-AG levels in HEK293-hTRPA1 after drug treatment (n=6-11). This figure illustrates the significant increase in 2-AG levels of the CIN stimulation group compared to that of the DMSO control group as determined by a one-way ANOVA with post hoc Fisher's LSD with a 95% confidence interval (* = $p < 0.0056$).

Table 21: Levels of endocannabinoids after drug stimulation in HEK293-hTRPA1. This table shows the values of each endocannabinoid per drug treatment in HEK293-hTRPA1 (n=6-11). The values are represented as moles per gram tissue ± SEM. The average recovery value of d_4AEA with which the values were adjusted is also represented as a percentage. Significant changes are highlighted in bold as determined by a one-way ANOVA with post hoc Fisher's LSD with a 95% confidence interval for the mean using SPSS software (P≤0.05).

	AEA (mols/gram tissue) ± SEM	2-AG (mols/gram tissue) ± SEM	PEA (mols/gram tissue) ± SEM	OEA (mols/gram tissue) ± SEM	LEA (mols/gram tissue) ± SEM	Average Recovery (%)
Control	$8.9\,E^{-12} \pm$ $4.4\,E^{-12}$	$9.9\,E^{-10} \pm$ $5.5\,E^{-10}$	$2.9\,E^{-10} \pm$ $1.5\,E^{-10}$	$8.5\,E^{-10} \pm$ $4.5\,E^{-10}$	$7.1\,E^{-11} \pm$ $4.0\,E^{-11}$	
CIN	$2.0\,E^{-11} \pm$ $6.5\,E^{-12}$	$\mathbf{6.3\,E^{-9} \pm}$ $\mathbf{3.0\,E^{-9}}$	$5.0\,E^{-10} \pm$ $1.8\,E^{-10}$	$1.6\,E^{-9} \pm$ $6.2\,E^{-10}$	$1.4\,E^{-10} \pm$ $5.7\,E^{-11}$	60
XLR-11	$2.0\,E^{-11} \pm$ $9.4\,E^{-12}$	$1.7\,E^{-9} \pm$ $5.8\,E^{-10}$	$5.3\,E^{-10} \pm$ $2.1\,E^{-10}$	$1.8\,E^{-9} \pm$ $7.5\,E^{-10}$	$1.5\,E^{-10} \pm$ $7.9\,E^{-11}$	
5-OH-UR-144	$1.6\,E^{-11} \pm$ $4.3\,E^{-12}$	$1.4\,E^{-9} \pm$ $3.0\,E^{-10}$	$5.2\,E^{-10} \pm$ $1.7\,E^{-10}$	$1.8\,E^{-9} \pm$ $5.8\,E^{-10}$	$1.3\,E^{-11} \pm$ $4.3\,E^{-11}$	

8.4 DISCUSSION

The objective of this chapter was to develop a method wherein endocannabinoid levels could be quantified from cell lines before and after a drug stimulation. This method was ultimately successful being able to quantify endocannabinoid levels from five different cell types. This experiment also showed a significant increase in 2-AG in HEK293-hTRPV1 after a stimulation with CAP, that was not replicated in HEK293-WT cells which corroborates the hypothesis by Liao et al. that capsaicin activation of TRPV1 would lead to an increase of 2-AG (Liao et al., 2011). This is an effect that has been replicated by Heather Bradshaw using stably expressed HEK293-hTRPV1 and an Applied Biosystems/MDS Sciex API3000 triple quadrupole mass spectrometer. She presented both sets of data (hers and mine) at the International Cannabinoid Research Society (ICRS) 2014 meeting (Bradshaw, 2014).

As this is preliminary data used for method development, adaptations to original experimental design need to be made and experiments need to be repeated. For instance, AtT20-hCB1 and AtT20-hCB2 cells were used for these experiments in trying to keep a uniformity between the fluorescence-based assays and mass spectrometry assays. Both AEA and 2-AG, are known to be synthesized on demand usually in the response to an increase in intracellular calcium related to a post-synaptic event (Raphael Mechoulam et al., 2014). Therefore, in future experiments, HEK293-hCB1 and HEK293-hCB2 will need to be used to determine if the endocannabinoid system would be more affected if the receptors could $G\alpha_q$ – couple, as opposed to the AtT20 cell systems with primarily functioning through $G\alpha_{i/o}$. Another interesting finding was that if experiments were repeated on different days, the basal endocannabinoid levels seemed to decrease as the cell line aged (even within 2-3 passages). This resulted in very high error and was amended by running enough replicates of each drug condition on the same day with the same cell passage. This decreased error

significantly. As this is a lot of cells to grow and a lot of flasks, it will be best to compare one SC versus its own DMSO, antagonist and antagonist+SC controls individually instead of trying to run more than one SC versus the same control groups.

As for antagonists, the HEK293-WT cells had an unexpected finding having significant increases in 2-AG and AEA in cells that had been treated with CAPZ followed by CAP, whereas there was no increase in cells treated with CAPZ or just CAP individually. As these cells are without the hTRPV1 receptor, the usual target for these compounds, it makes this finding all the more unusual. CAP has been shown to have no increase in intracellular calcium in HEK293-WT cells (Hirota, Smart, & Lambert, 2003) as well as CAPZ had no inhibiting effect on a pH driven $[Ca^{2+}]$ influx in wild type cells (Jerman et al., 2000). As there is no evidence in the literature that would suggest CAPZ acting at endogenously found receptor systems within wild type cells, this will need to be repeated as it was only an n=5 to verify it was not an anomaly. It could also be a product of the successive drug addition, which will be tested by having a DMSO/DMSO control in the next repeat experiments. If it does appear to be true then CAPZ by itself will need to be added for 10 minutes to determine if the excess time it is added to the cells is showing the increase in these endocannabinoids compared to the five minute CAPZ addition by itself. It would be beneficial in general to run a time course experiment to determine the time point for optimal endocannabinoid production.

The AtT20-hCB2 antagonist, AM630, also showed an increase in 2-AG compared to the control group. This is opposite of what would be expected as AM630 has been shown to reduce intracellular calcium in the presence of an agonist both extracellularly and intracellularly. Brailoiu et al. showed that when 2-AG was added after a pretreatment of AM630 (1 μM) there was a decrease in the level of intracellular calcium, but a co-injection showed that it still had an increase in calcium, though it was only slightly above that of the

control. This was tested in a system where CB_2 was coupled to G_q, furthering the necessity of repeating experiments in a HEK293-hCB2 system (Brailoiu et al., 2014). In the AtT20-hCB2 system, AM630 followed by the addition of CP 55,940 did not show a significant difference in the change of 2-AG. As AM630 has been shown to be an inverse agonist, it could be that without a ligand, its activity at the receptor in its inactive state is what is causing this increase in 2-AG (Ross et al., 1999). Further testing will need to be done to further explain this result but it does highlight the difference between being receptor selective and receptor specific as being a "selective" CB_2 antagonist still showed off-target effects, proving lack of specificity.

Similar to that of HEK293-hTRPV1, the use of the known agonist CIN showed an increase in the level of 2-AG in HEK293-TRPA1 cells. TRPA1 in nerve terminals has been shown to spontaneously release L-glutamate upon activation with lidocaine (Piao et al., 2009). The increase in glutamate could then activate postsynaptic mGlu5 receptors, like that with the HEK293-hTRPV1, yielding a 2-AG increase (Liao et al., 2011). As both XLR-11 and 5-OH-UR-144 are agonists at hTRPA1, yet did not see and increase similar to that of CIN, could have been due to the use of 10 μM concentrations instead of 30 μM concentrations which had similar efficacies to that of CIN. In future experiments, the concentrations will be increased as well as the addition of antagonist experiments which have not yet been completed.

Finally, the significant increase of PEA after the stimulation of XLR-11 in AtT20-hCB1 may have physiological implications for SCs and their interaction with the EC system. This increase is important because in experimental stroke, CB_1 receptors are induced and have been reported to show an increase in PEA in the brain following ischaemic insult which is thought to be increased as a neuroprotective agent to lessen the damaging effects (Natarajan, Schmid, & Schmid, 1986). Since XLR-11 has been linked to a

case of cerebral ischemia, it could implicate CB_1 mediated action (Takematsu et al., 2014). Glutamate-induced neurotoxicity has also been shown to increase the levels of PEA resulting in cell damage and even cell death (Lambert, Vandevoorde, Jonsson, & Fowler, 2002). Therefore its increase after the stimulation of XLR-11 could potentially highlight toxicity at a cellular level. This finding also shows that the downstream effectors of the activation of receptors tested is important, and could also be a potential source of toxicity.

The AtT20 receptor systems used have been tested prior to experimentation to see if they display changes in calcium upon receptor activation which they did not (data not shown). The lack of increase in AEA and 2-AG in the $G\alpha_{i./o}$ receptor system therefore, highlights that the activation at hCB_1 and hCB_2 displayed by SCs is not a product of EC generation from any off target $G\alpha_q$ coupled receptors that could be present in these systems. For instance if SCs activated muscarinic receptors that were present endogenously in the cell type, they could thus show an increase in calcium via a $G\alpha_q$ coupled pathway, resulting in an increase in EC. The increase in AEA and 2-AG have potential to then activate hCB_1 and/or hCB_2 receptor. These interactions are complex and much research is needed to determine the likelihood of this possibility. The co-incidence of TRPV1 and CB1 receptor activation is sure to attenuate the possibility of this effect (Millns et al., 2006). As there is no increase in 2-AG or AEA it is highly unlikely that this is occurring further proving that the activation of SCs is due to receptor activation directly and not downstream effects. Although, due to functional selectivity, it is unknown whether SCs and endocannabinoids would have the same downstream effects post CB_1 activation or how they would affect other non-cannabinoid targets makes knowing if they are synthesized vital (Leach, Conigrave, Sexton, & Christopoulos, 2015).

Inflammation of peripheral tissues has also been a major adverse side effect of SC consumption. As many of the SCs are CB_2 selective agonists, CB_2 receptor activation has

been known to release anti-inflammatory agents, which would suggest a decrease in the presence of inflammation (Dhopeshwarkar & Mackie, 2014). AEA and 2-AG have been known to induce the production of arachidonate which modulates the synthesis of compounds that have opposing actions on inflammatory response, such as prostaglandin E2 from macrophages and leukotrienes from mast cells (Maccarrone, Bari, Battista, & Finazzi-Agro, 2002). Future studies will include the development of a prostaglandin E2 mass spec method which can quantify changes in its production after SC stimulation to further determine what about SC reactivity is causing inflammation.

CHAPTER 9: DISCUSSION

9 GENERAL DISCUSSION

The first aim of this body of work was to determine the validity of using a fluorescence-based plate reader assay that measures receptor activation by changes in membrane potential to build pharmacological profiles for SCs. The membrane potential assay was used to test $G\alpha_{i/o}$ coupling to native GIRK channels in AtT20 cells that had been stably transfected with rat or human CB_1 and human CB_2. As treatment with CB_1 and CB_2 non-selective agonist WIN or CP 55,940 both caused a PTX sensitive hyperpolarization of the cell membrane, with potencies and efficacies similar to that of literature values, it was determined that this was a viable technique. In building pharmacological profiles for SCs of abuse, all 60 compounds tested at the hCB_1 and hCB_2 receptors had some level of agonist activity. Similar to previous findings in the literature, rat and human CB_1 receptors had different reactivity profiles as shown by differences in rank order in both potency and efficacy of the compounds tested at both receptors. In the future, experiments will be completed to determine if they also differ in secondary messengers. Using the reactivity profiles of SCs on hCB_1 and hCB_2, similarities in reactivity in relation to structural groups was used to develop SAR. For this review, hCB_1 reactivity and physiological implications will be assessed first, then followed by hCB_2.

9.1 hCB₁ ACTIVITY

As an in-depth SAR analysis was presented in the discussions of each chapter, all structure types and their activity at hCB_1 will be compared. All compounds showed cannabimimetic activity with potencies that ranged between >10 μM to sub-nanomolar. All $-R^2$ side groups: naphthaloyl, adamantane, phenyl, cyclohexyl, methoxybenzoyl, fluorophenylacetyl, tetramethylcyclopropyl, methoxyquinolinyl, L-valinamide and L-*tert*-

leucinamide, were tolerated with at least one derivative of each side chain showing high

potency depending on its other structural components. Of the $-R^1$ side chains, all were

tolerated, but side chains containing less than 5 carbons in length showed a significant drop

in potency and SDB-107 showed very weak agonist activity when the $-R^1$ was truncated to a

methyl. Ketone, carboxamide and ester linkers at lengths between two and four bond

lengths were also tolerated. It should be reminded that the indazole structures were

normalized to a maximum of CP 55,940. The maximum response of CP 55,940 and WIN

were similarly around a 30% hyperpolarization. The potency shift for CP 55,940 normalized

to WIN and normalized to itself was only by a pEC_{50} of 0.1. As the indazole group was of

the most potent and efficacious of the compounds tested by a much larger factor than what

the discrepancies in normalization would be responsible for, they will be compared directly.

At hCB_1, both WIN and Δ^9-THC had pEC_{50} values of approximately 6.5. When compared

to a rank order of all the other SCs, there are only 14 other compounds with potencies

lower. Of the compounds with lower potency, six had a truncated $-R^1$ sidechain. In the two

instances where the $-R^1$ side chain was truncated to three carbons and the compound

retained a high potency, both had a greater distance between the indole core and the side

substituent (4 bond lengths). This suggests that with a 3 carbon length side chain, the

increase in distance between the indole and the $-R^2$ side group may compensate for the

decrease in length on $-R^1$. This is further supported by when the $-R^1$ side chain was 5

carbons long the increase in distance between the indole core and the $-R^2$ side group

showed decreases in potency compared to their shorter distance counterparts. The addition

of a terminal fluorine on the end of the $-R^1$ side chain had been thought to increase activity

at both of the cannabinoid receptors (S. D. Banister et al., 2015). Out of 13 structure pairs,

only differing by an N-pentyl or N-fluoropentyl side chain, three had the same potencies

and ten had 2 –5 fold increases in potency with the addition of the terminal fluorine. Of the

–R^2 side groups, the groups showing the highest potency were that of the compounds containing amino acids in the –R^2 position. This was an interesting finding as CB_1 reactivity was thought to be dependent on aromatic-aromatic interactions (J. W. Huffman et al., 2005; Mella-Raipan et al., 2013; Stern et al., 2006). Higher potency was observed in the L-*tert*-leucinamide group compared to the L-valinamide group suggesting that either the bulk of the extra carbon is preferable or that additional hydrophobic interactions help binding to the hydrophobic pocket of the receptor binding site. Other than the indazole derivatives, PB-22 and 5F-PB-22 showed approximately 60 and 110 fold potency increases at hCB_1 compared to WIN or Δ^9-THC, although it could not be determined if this was due to their the ester linker or the quinolinyl side group.

In terms of efficacy, the length of the –R^1 side chain was especially important. Compounds with an N-pentyl group showed efficacies similar to that of WIN which decreased to a maximal effect between 60-80% of WIN max when the side chain was truncated to 4 carbons. When the side chain was truncated to 3 carbons, no compound showed a maximal effect over 40% of WIN max. There were less trends in efficacy as over 50% of the compounds tested had maximal effects greater than or equal to 100% WIN max. There was a correlation between the distance of the –R^2 side group from the indole core, showing a lower efficacy when bulkier side chains were at a farther distance. The highest efficacy group was that of the mutual metabolite of UR-144 and XLR-11 demonstrating that not only can metabolites be cannabimimetically active even more so than their parent compounds, but also that the binding pocket known for hydrophobic interactions with the –R^1 side chain, not only tolerates a polar entity but binds with an efficacy almost 50% higher than that of WIN. Docking studies will need to be pursued to see exactly how these compounds are binding in the CB_1 receptor binding pocket to further SAR studies of SCs.

9.1.1 **Physiological Implications of hCB$_1$ Activation**

The activation of CB$_1$ receptors has been thought to be the cause of all the clinical effects of THC (Fitzgerald, Bronstein, & Newquist, 2013). It has been hypothesized that the more severe psychotic effects are a product of full agonist activity at CB$_1$. This has been supported by the cases of paranoia in cannabis use are mainly linked to strains that have higher concentrations of Δ^9-THC (Every-Palmer, 2011). The majority of SCs tested had a higher reactivity profile (both potency and efficacy) than Δ^9-THC, some even up to 1000 times more potent, therefore, the psychosis, paranoia and hallucinations that have been linked to SC consumption can be presumed to be a CB$_1$ mediated effect (Gurney et al., 2014). A bimodality seems to exist around CB$_1$ activation where it is sometimes linked to neuroprotective and sometimes neurotoxic effects (Marsicano et al., 2003). The fine line between the two events seems to also be dose and location dependent. Low doses of Δ^9-THC have been shown to cause enough of a neuronal insult to activate mechanisms that result in neuroprotection whereas at higher doses or chronic CB$_1$ receptor activation neurotoxicity is exhibited (Sarne, Asaf, Fishbein, Gafni, & Keren, 2011) and neurotoxicity has been implicated in ischemic brain trauma (Pellegrini-Giampietro, Mannaioni, & Bagetta, 2009). CB$_1$ activation has also been shown to inhibit the release of noradrenaline and/or ATP which has negative effects on the heart and vasoconstriction of blood flow (R.G. Pertwee, 2006). Within the indazole/indole derivatives, ADB-PINACA and 5F-ADB-PICA were linked to cardiotoxicity and neurotoxicity that were non-fatal. They were of some of the highest potency agonists at hCB$_1$. There were only 3 compounds that were more potent and one of them was implicated in the only documented indazole related fatality. PB-22 and 5F-PB-22 also had very strong agonist activity at hCB$_1$ and have also been linked with death. Though not causative, CB$_1$ mediated receptor activation does seem to be a large contributor to SC toxicity. Synthetic cannabinoids, at 30 μM concentrations,

have also been shown to exhibit cytotoxicity that was CB_1 receptor mediated that was not dependent on structural differences. Cytoxicity caused by SCs also showed increases in phosphatidylserine which is a known indicator of apoptosis (Tomiyama & Funada, 2014).

9.2 hCB$_2$ ACTIVITY

All compounds tested also showed agonist activity at hCB$_2$ with potencies that ranged between 631nM to 0.63nM. All $-R^2$ side groups: naphthaloyl, adamantane, phenyl, cyclohexyl, methoxybenzoyl, fluorophenylacetyl, tetramethylcyclopropyl, methoxyquinolinyl, L-valinamide and L-*tert*-leucinamide, were tolerated with at least one derivative of each side chain showing high potency depending on its other structural components. Unlike hCB$_1$, almost 50% of the compounds were less potent than WIN at hCB$_2$ which would be expected as WIN is slightly more CB$_2$ selective. It has been shown that the length of the $-R^1$ group is tolerated better at the CB$_2$ receptor which was corroborated by this data (Frost et al., 2010; John W Huffman et al., 1994). SDB-107, the only compound to have its $-R^1$ side chain shorted to a methyl group had a potency similar to that of WIN. CB$_2$ potency, as well as efficacy, seemed to rely most heavily on the distance between the indole/indazole and the $-R^2$ side group as it was almost exactly split down the middle between compounds with a distance of 2 or 3 bond lengths having higher potencies and efficacies and then a sudden decrease in both when the bond length was increased to 4 regardless of the bulkiness of the $-R^2$ side group. This was the only trend in efficacy, as all $-R^2$ side groups and $-R^1$ chains were present amongst the most efficacious of SC compounds. Potency, similar to that of hCB$_1$, was highest in compounds that had an indazole scaffold with an L-*tert*-leucinamide moiety. This was an interesting finding as CB$_2$ receptor binding has been thought to rely on more aromatic-aromatic interactions as it has an extra aromatic residue in its binding pocket, yet the compounds lacking an aromatic entity were the

compounds with the highest potency. Dissimilarly to hCB_1, the terminal fluorine effect was seconded to that of the linker length. When the linker length was 2 bond lengths the fluorine increased potency by 2 fold but when the linker length was 3 or more bond lengths, the terminal fluorine group was less reactive than that of the N-pentyl group.

9.2.1 Physiological Implications

As it is now documented, SCs are having a much higher activity at CB_2 receptors than that of Δ^9-THC. Due the doses at which these compounds are presumably being consumed (as determined by blood analysis post consumption) as well as the CB_2 activations seen by their metabolites, it is important to look at physiological implications of this level of receptor activation. Unfortunately, little is known about the consequences involved in chronic CB_2 receptor activation (Atwood, Straiker, & Mackie, 2012). In one study, WIN activated MAP kinase and recruited β arrestin, both have been established as CB_2 mediated pathways, but did not inhibit voltage-dependent calcium channels and cause receptor internalization. Although the SCs are binding to the receptor and showing coupling to GIRK channels, does not necessarily mean that they are having the same downstream effects as other CB_2 agonists. It can be therefore hypothesized that in binding to the receptor without further mediating downstream responses that SCs could be having an almost antagonist effect in vivo (Atwood et al., 2012). This could be an explanation of why CB_2, which is known for mediating and releasing anti-inflammatory agents, has sometimes been reported to mediate pro-inflammatory effects in certain assays (Oka et al., 2006).

Chronic activation of CB_2 has also been shown to cause an upregulation in the serotonin 5-HT_{2A} receptors, a receptor which has been linked to mental disorders when there is an alteration to their normal homeostasis (Papanti, Orsolini, Francesconi, & Schifano, 2014). As SCs cause a level of anxiety, paranoia and psychosis not exhibited upon

the consumption of Δ^9-THC, there is potentially cross talk between the CB_2 receptor and the 5-HT$_{2A}$ system with which the effects are mediated by CB_2 activation (Fantegrossi et al., 2014). Evidence for cross talk between CB_2 receptor activation and other pathways for illicit drugs of abuse have been exhibited in pathways of nicotine, alcohol and cocaine (Onaivi et al., 2008; Xi et al., 2011).

9.3 HCB$_1$ VERSUS HCB$_2$

In the instances where the theory behind the new structural designs could be linked back to patents or scientific literature, many of the studies were attempting to design compounds with therapeutic potential that had high CB_2 selectivity with little to no activity at CB_1 (Frost et al., 2008; John W Huffman et al., 1994; J. W. Huffman et al., 2005; Makriyannis & Deng, 2005, 2007). Therefore, it is not surprising that many of the compounds were hCB$_2$ selective. Of the cannabimimetic indoles, all of the compounds with $-R^2$ side groups that contained adamantane, tetramethylcyclopropyl and methoxymethane (RCS analogues + SDB-022-24) were hCB$_2$ selective regardless of linker length, type or $-R^1$ side group. Of the $-R^2$ side groups that were hCB$_1$ selective, the quinolinyl derivatives as well as the $-$ICA/-INACA families (with the exception of 5F-AB-2PINACA which was hCB$_2$ selective). The cyclohexane, phenyl and fluorobenzyl derivatives were less consistent depending on linker length, directing group position and $-R^1$ side chain moieties to determine their selectivity yet there were no trends in selectivity other than truncated $-R^1$ being hCB$_2$ selective.

9.4 TRP CHANNELS

The second aim of this project was to determine the validity of using a fluorescence-based plate reader assay to measure changes in intracellular calcium upon activation of the receptor. This was done by the application of the agonist CIN to hTRPA1 (a response that did not show an increase in calcium when added to non-induced cells or to HEK293-hTRPV1, data not shown), as well as, testing CAP on hTRPV1 (similarly not having activity in non-induced cells or hTRPA1). The changes in intracellular calcium were similar to that of previously published literature values (Islam, 2011; Redmond et al., 2014). Ionomycin was also used to be sure that the dye was not fully saturating within the experiments. After proving the validity of this technique, it was used to show that SCs are having off-target pathway effects at the cannabimimetically relevant TRP receptors. Pharmacological profiles were determined and any relevant SAR were noted.

9.4.1 hTRPA1 Activity

The TRPA1 receptor has most commonly been shown to bind to electrophilic ligands through covalent binding at cysteine residues within the N-terminus (Hinman et al., 2006). It has also been shown to bind some compounds in a more traditional manner with implications of at least one receptor binding pocket (Redmond et al., 2014). The pharmacological profiles of the SCs supports the second notion as all of the SCs that showed binding activity at hTRPA1 lacked electrophilic character which would be necessary for binding. Therefore, like traditional binding, the structural relationships between compounds that showed activity were assessed though trends were limited. One whole structure family, the RCS analogues and their structurally similar carboxamide methoxymethane and fluorobenzyl derivatives (at all directing groups) all had hTRPA1 activity with relatively high potency similar to that of CIN. The ortho- and meta- positions of the methoxymethane derivatives also had high efficacy at their highest concentration

similar to that of CIN max. All linker lengths and types were tolerated as well as all $-R^1$ lengths except for the methyl group of SDB-107. Of the $-R^2$ side groups, all showed activity except for the L-valinamide which had no activity with any $-R^1$ side group. This may be due to its lacking of aromatic character has been implicated in TRPA1 activity as it may help ligands cross the cellular membrane to increase activity (Haynes et al., 2008). The indazole scaffold was also absent from activity. In relation to efficacy, a $-R^2$ group at a shorter distance (2 bond lengths) seemed preferable to that of 4 bond lengths suggesting that sterics may play a part in TRPA1 activation. No further SAR could be determined as the there was a wide variety of activation profiles which is consistent with the wide variety of structurally different compounds that have been known to activate TRPA1.

9.4.2 hTRPV1 Activity

There was limited activity at hTRPV1. Many compounds had weak agonist and antagonist activity but were not substantial enough for further exploration into their reactivity profiles. Only one compound showed significant partial agonist activity which was the mutual metabolite of XLR-11 and UR-144, 5-OH-UR-144. The data suggest that 5-OH-UR-144 is competitively blocking CAP from the binding site with a higher receptor occupancy that that of its intrinsic response at hTRPV1. The increase in activity at the off-target TRP channels of 5-OH-UR-144 compared to its parent compounds shows metabolites could potentially have more deleterious actions as they are targeting more pathways. This metabolite interaction specifically highlights that it is important to keep profiling metabolites as many SCs have similar metabolic pathways.

9.4.3 Physiological implications

TRPV1 and TRPA1 have been shown to be co-expressed in most DRG neurons, and both modulate key mediators, such as calcitonin gene-related peptide (CGRP), involved in nociceptive signalling (Chen & Hackos, 2015). The off target actions of SC on TRPA1 could potentially play a role in the inflammation, vasodilation and edema that have been reported as side effects after SC consumption. TRPA1 has been known to be the target of environmental irritants, such as unsaturated aldehydes present in smoke or produced by drug metabolism, which elicit pain syndromes associated with these adverse side effects (Diana M. Bautista et al., 2006). TRPA1 is widely dispersed in the lung making it plausible that negative side effects in the lung could be TRPA1 mediated. Another factor to consider is that the most common form of ingestion is through smoking. This means that pyrolysis products that are immediately synthesized by the heating of the compounds reach the lungs first, therefore activation at this receptor may play a crucial role in toxicity. As for TRPV1, and adverse side effect linked to TRPV1 activation is hypothermia. One case of SC related death was due to hypothermia. As the metabolite 5-OH-UR-144 was the only compound to be a partial agonist, it suggests that TRPV1 activation may be a delayed effect (Kronstrand, Roman, Andersson, & Eklund, 2013). The same fatality also showed signs of lung edema suggesting the activations of the TRP channels are linked, which could be due to the production of ECs upon activation (Liao et al., 2011). TRPV1 and TRPA1 are also found within the brain but their role is still highly unknown. This could implicate the TRP receptors in negative effects of the CNS as well.

9.5 ENDOCANNABINOID LIPID PROFILING

The final aim of this body of work was to develop a method to be able to quantify the level of endocannabinoids from cell lines as well as measure the change in

endocannabinoid production after a drug stimulation. This was done using reverse phase-column chromatography lipid extractions followed by analysis using HPLC/MS/MS. Although there is much work left to be done in this area of the project, the basic method development has been solidified. As endocannabinoids are known to be made "on demand" usually to a change in intracellular calcium (Maccarrone et al., 2002), the protocol was successful in measuring an increase in 2-AG in both HEK293-hTRPA1 and HEK293-hTRPV1 after stimulation with an agonist corroborating the results found by Liao et el. (Liao et al., 2011).

Other interesting findings were that the activation of cannabinoid receptors by SCs was likely mediated by direct receptor activation and not downstream effects of EC production as shown by the lack of increase in AEA and 2-AG after SC stimulation. It was also demonstrated that increases in endocannabinoids could be seen in systems that primarily couple through $G\alpha_{i/o}$ instead of $G\alpha_q$. An increase in 2-AG displayed after the stimulation of hCB_2 with the CB_2 selective inverse agonist AM630 highlights that unexpected off target effects can be demonstrated even with compounds that have been shown to be selective. Finally, a stimulation with XLR-11 showed an increase in the levels of PEA proving that SCs are having more off target effects than just at the TRP channels. As, glutamate-induced neurotoxicity has been shown to increase the levels of PEA resulting in cell damage and even cell death it implies that there is potential that SCs, specifically XLR-11 are showing toxicity at the cellular level.

Further experiments to be done within this assay are tighter control experiments including non-induced cells, as well as antagonist tests that were not already completed. Also adding a control group where two DMSO additions are added to determine if the cells are producing more endocannabinoids in antagonist+agonist experiments due to the multiple disturbances caused by drug additions. This may explain an increase in 2-AG and

AEA in the HEK293-WT atagonist + agonist control group. Higher concentrations will need to be added of SCs to see if at concentrations similar to E_{Max} of the control groups if they are having an effect on endocannabinoids. Finally, as hCB_1 and hCB_2 have been shown to couple $G\alpha_q$, testing the SCs at in receptor systems that primarily couple to $G\alpha_q$, such as HEK293, will need to be assessed.

9.6 FUTURE EXPERIMENTS

Other than experiments already outlined previously, future plans for the continuation of this project include the synthesis of more phase I and II metabolites as well as any new drugs of abuse to be isolated from herbal smoking blends to have a full pharmacological assessment on the assays outline in this body of work. To further build pharmacological profiles to develop a better understanding to how these compounds are reacting, other functional activity assays planned to be explored. More phase I and II metabolites as well as any new drugs of abuse to be isolated from herbal smoking blends will be synthesized and have a full pharmacological assessment on the assays outline in this body of work. These experiments include, $G\alpha$ modulation of AC, Gq-mediated mobilization of $[Ca]_I$ and assays measuring the activation of MAPK. Looking at specific toxicity of these compounds on hepactocytes and human proximal tublar cells to be able to determine in the most realistic in vitro assays the relative toxicity these compounds could be having in their respective organs (liver and kidney). Finally, other off target receptor pathways such as the putative cannabinoid receptors GPR119, GPR55 and GPR18 as well as potentially the serotonin receptors may be tested for their reactivity. As long as SCs are continuing to evolve in structure and the prevalence of their use remains high, further pharmacological assessment is necessary if there is hope to develop a medical intervention for their ever increasing toxic side effects.

REFERENCES

REFERENCES

AAPCC. (2015). Synthetic Marijuana. from http://www.aapcc.org/alerts/synthetic-marijuana/

Access, A. f. S. (2012). Connecticut Becomes 17th Medical Marijuana State in the Face of Ongoing Federal Intimidation Retrieved September 01, 2015 http://www.safeaccessnow.org/connecticut_becomes_17th_medical_marijuana_state_in_the_face_of_ongoing_federal_intimidation

Administration, D. E. (2011). Schedules of Controlled Substances: Temporary Placement of Five Synthetic Cannabinoids Into Schedule.

Akopian, A. N., Ruparel, N. B., Patwardhan, A., & Hargreaves, K. M. (2008). Cannabinoids desensitize capsaicin and mustard oil responses in sensory neurons via TRPA1 activation. *J Neurosci, 28*(5), 1064-1075. doi: 10.1523/jneurosci.1565-06.2008

Ammann, J., McLaren, J. M., Gerostamoulos, D., & Beyer, J. (2012). Detection and quantification of new designer drugs in human blood: part 1–synthetic cannabinoids. *Journal of Analytical Toxicology, 36*(6), 372-380.

Atwood, B. K., Straiker, A., & Mackie, K. (2012). CB 2: therapeutic target-in-waiting. *Progress in Neuro-Psychopharmacology and Biological Psychiatry, 38*(1), 16-20.

Backes, M., & Weil, A. (2014). *Cannabis Pharmacy: The Practical Guide to Medical Marijuana*: Black Dog & Leventhal Publishers, Incorporated.

Banister, S., Stuart, J., Conroy, T., Longworth, M., Manohar, M., Beinat, C., Wilkinson, S., Kevin, R., Hibbs, D., Glass, M., Connor, M., McGregor, I., & Kassiou, M. (2015). Structure–activity relationships of synthetic cannabinoid designer drug RCS-4 and its regioisomers and C4 homologues. *Forensic Toxicology*, 1-12. doi: 10.1007/s11419-015-0282-9

Banister, S. D., Moir, Michael, Stuart, Jordyn, Wood, Kate, Kevin, Richard, Beniat, Corinne, Wilkinson, Shane, Buchanan, Alexandra, Glass, Michelle, Connor, Mark, McGregor,

Iain, Kassiou, Michael. (2015). *The pharmacology of indole and indazole synthetic cannabinoid designer drugs AB-FUBINACA, ADB-FUBINACA, AB-PINACA, ADB-PINACA, 5F-AB-PINACA, ADBICA, and 5F-ADBICA*. submitted to ACS chemical neuroscience.

Banister, S. D., Stuart, J., Kevin, R. C., Edington, A., Longworth, M., Wilkinson, S. M., Beinat, C., Buchanan, A. S., Hibbs, D. E., & Glass, M. (2015). The effects of bioisosteric fluorine in synthetic cannabinoid designer drugs JWH-018, AM-2201, UR-144, XLR-11, PB-22, 5F-PB-22, APICA, and STS-135. *ACS Chemical Neuroscience*.

Banister, S. D., Wilkinson, S. M., Longworth, M., Stuart, J., Apetz, N., English, K., Brooker, L., Goebel, C., Hibbs, D. E., Glass, M., Connor, M., McGregor, I. S., & Kassiou, M. (2013). The Synthesis and Pharmacological Evaluation of Adamantane-Derived Indoles: Cannabimimetic Drugs of Abuse. *ACS Chemical Neuroscience, 4*(7), 1081-1092. doi: 10.1021/cn400035r

Baraldi, P. G., Saponaro, G., Moorman, A. R., Romagnoli, R., Preti, D., Baraldi, S., Ruggiero, E., Varani, K., Targa, M., Vincenzi, F., Borea, P. A., & Aghazadeh Tabrizi, M. (2012). 7-Oxo-[1,4]oxazino[2,3,4-ij]quinoline-6-carboxamides as selective CB(2) cannabinoid receptor ligands: structural investigations around a novel class of full agonists. *J Med Chem, 55*(14), 6608-6623. doi: 10.1021/jm300763w

Basavarajappa, B. S., Yalamanchili, R., Cooper, T. B., & Hungund, B. L. (2008). The Endocannabinoid System. In A. Lajtha & E. S. Vizi (Eds.), *Handbook of Neurochemistry and Molecular Neurobiology* (pp. 343-384): Springer US.

Basu, S., Ray, A., & Dittel, B. N. (2011). Cannabinoid receptor 2 is critical for the homing and retention of marginal zone B lineage cells and for efficient T-independent immune responses. *J Immunol, 187*(11), 5720-5732. doi: 10.4049/jimmunol.1102195

Bautista, D. M., Jordt, S.-E., Nikai, T., Tsuruda, P. R., Read, A. J., Poblete, J., Yamoah, E. N., Basbaum, A. I., & Julius, D. (2006). TRPA1 Mediates the Inflammatory Actions of Environmental Irritants and Proalgesic Agents. *Cell, 124*(6), 1269-1282. doi: http://dx.doi.org/10.1016/j.cell.2006.02.023

Bautista, D. M., Pellegrino, M., & Tsunozaki, M. (2013). TRPA1: A gatekeeper for inflammation. *Annu Rev Physiol, 75*, 181-200. doi: 10.1146/annurev-physiol-030212-183811

Bayewitch, M., Avidor-Reiss, T., Levy, R., Barg, J., Mechoulam, R., & Vogel, Z. (1995). The peripheral cannabinoid receptor: adenylate cyclase inhibition and G protein coupling. *FEBS Letters, 375*(1-2), 143-147. doi: 10.1016/0014-5793(95)01207-U

Bayewitch, M., Rhee, M. H., Avidor-Reiss, T., Breuer, A., Mechoulam, R., & Vogel, Z. (1996). (-)-∆9-Tetrahydrocannabinol antagonizes the peripheral cannabinoid receptor-mediated inhibition of adenylyl cyclase. *Journal of Biological Chemistry, 271*(17), 9902-9905. doi: 10.1074/jbc.271.17.9902

Behonick, G., Shanks, K. G., Firchau, D. J., Mathur, G., Lynch, C. F., Nashelsky, M., Jaskierny, D. J., & Meroueh, C. (2014). Four Postmortem Case Reports with Quantitative Detection of the Synthetic Cannabinoid, 5F-PB-22. *Journal of Analytical Toxicology, 38*(8), 559-562. doi: 10.1093/jat/bku048

Ben Amar, M. (2006). Cannabinoids in medicine: A review of their therapeutic potential. *Journal of Ethnopharmacology, 105*(1–2), 1-25. doi: http://dx.doi.org/10.1016/j.jep.2006.02.001

Bertini, S., Parkkari, T., Savinainen, J. R., Arena, C., Saccomanni, G., Saguto, S., Ligresti, A., Allarà, M., Bruno, A., Marinelli, L., Di Marzo, V., Novellino, E., Manera, C., & Macchia, M. (2015). Synthesis, biological activity and molecular modeling of new biphenylic carboxamides as potent and selective CB2 receptor ligands. *European*

Journal of Medicinal Chemistry, 90(0), 526-536. doi:

http://dx.doi.org/10.1016/j.ejmech.2014.11.066

Bewley-Taylor, D., & Jelsma, M. (2011). Fifty years of the 1961 Single Convention on

Narcotic Drugs: A reinterpretation. *Series on Legislative Reform of Drug Policies*(12),

1-20.

Bhanushali, G. K., Jain, G., Fatima, H., Leisch, L. J., & Thornley-Brown, D. (2012). AKI

associated with synthetic cannabinoids: a case series. *Clinical Journal of the American

Society of Nephrology*, CJN. 05690612.

Bissantz, C., Kuhn, B., & Stahl, M. (2010). A Medicinal Chemist's Guide to Molecular

Interactions. *Journal of Medicinal Chemistry, 53*(14), 5061-5084. doi:

10.1021/jm100112j

Block, R. I., O'Leary, D. S., Hichwa, R. D., Augustinack, J. C., Ponto, L. L. B., Ghoneim, M.,

Arndt, S., Hurtig, R. R., Watkins, G. L., & Hall, J. A. (2002). Effects of frequent

marijuana use on memory-related regional cerebral blood flow. *Pharmacology

Biochemistry and Behavior, 72*(1), 237-250.

Bradshaw, H. B., Leishman, Emma, Stuart, Jordyn, Connor, Mark. (2014).

*OVEREXPRESSION OF TRPV1 IN HEK CELLS DRIVES DRAMATIC CHANGES IN

BASAL ENDOCANNABINOIDS AND RELATED LIPIDS WHICH ARE

POTENTIATED WITH STIMULATION BY CAPSAICIN*. Paper presented at the

International Cannabinoid Research Society (ICRS), Baveno, Italy.

Brailoiu, G. C., Deliu, E., Marcu, J., Hoffman, N. E., Console-Bram, L., Zhao, P., Madesh,

M., Abood, M. E., & Brailoiu, E. (2014). Differential Activation of Intracellular

versus Plasmalemmal CB2 Cannabinoid Receptors. *Biochemistry, 53*(30), 4990-4999.

doi: 10.1021/bi500632a

Brents, L. K., Reichard, E. E., Zimmerman, S. M., Moran, J. H., Fantegrossi, W. E., &
Prather, P. L. (2011). Phase I hydroxylated metabolites of the K2 synthetic
cannabinoid JWH-018 retain in vitro and in vivo cannabinoid 1 receptor affinity and
activity. *PLoS ONE, 6*(7), e21917. doi: 10.1371/journal.pone.0021917

Brown, A. J. (2007). Novel cannabinoid receptors. *British Journal of Pharmacology, 152*(5),
567-575. doi: 10.1038/sj.bjp.0707481

Brown, B. (2013). 6 Deaths Linked to Synthetic Marijuana. from
http://www.wkrg.com/story/23078114/6-deaths-linked-to-synthetic-marijuana

Buchler, I. P., Hayes, M. J., Hegde, S. G., Hockerman, S. L., Jones, D. E., Kortum, S. W.,
Rico, J. G., TenBrink, R. E., & Wu, K. K. (2011). Indazole derivatives: Google
Patents.

Buser, G., Gerona, R., Horowitz, B., Vian, K., Troxell, M., Hendrickson, R., Houghton, D.,
Rozansky, D., Su, S., & Leman, R. (2014). Acute kidney injury associated with
smoking synthetic cannabinoid. *Clinical Toxicology, 52*(7), 664-673.

Calignano, A., Katona, I., Desarnaud, F., Giuffrida, A., La Rana, G., Mackie, K., Freund, T.,
& Piomelli, D. (2000). Bidirectional control of airway responsiveness by endogenous
cannabinoids. *Nature, 408*(6808), 96-101.

Castaneto, M. S., Gorelick, D. A., Desrosiers, N. A., Hartman, R. L., Pirard, S., & Huestis, M.
A. (2014). Synthetic cannabinoids: Epidemiology, pharmacodynamics, and clinical
implications. *Drug and Alcohol Dependence, 144*(0), 12-41. doi:
http://dx.doi.org/10.1016/j.drugalcdep.2014.08.005

Caterina, M. J. (2007). Transient receptor potential ion channels as participants in
thermosensation and thermoregulation. *Am J Physiol Regul Integr Comp Physiol,
292*(1), R64-76. doi: 10.1152/ajpregu.00446.2006

Cawston, E. E., Redmond, W. J., Breen, C. M., Grimsey, N. L., Connor, M., & Glass, M. (2013). Real-time characterization of cannabinoid receptor 1 (CB1) allosteric modulators reveals novel mechanism of action. *British Journal of Pharmacology, 170*(4), 893-907. doi: 10.1111/bph.12329

Chamberlin, T., Guppy, Damon. (2015). Two men dead in Mackay after suspected poisoning from toxic batch of synthetic cannabis. *The Courier-Mail.* from http://www.couriermail.com.au/news/queensland/two-men-dead-in-mackay-after-suspected-poisoning-from-toxic-batch-of-synthetic-cannabis/story-fnn8dlfs-1227184521902

Chen, J., & Hackos, D. H. (2015). TRPA1 as a drug target--promise and challenges. *Naunyn Schmiedebergs Arch Pharmacol, 388*(4), 451-463. doi: 10.1007/s00210-015-1088-3

Cheng, Y., & Hitchcock, S. A. (2007). Targeting cannabinoid agonists for inflammatory and neuropathic pain. *Expert Opin Investig Drugs, 16*(7), 951-965. doi: 10.1517/13543784.16.7.951

Choi, H., Heo, S., Choe, S., Yang, W., Park, Y., Kim, E., Chung, H., & Lee, J. (2013). Simultaneous analysis of synthetic cannabinoids in the materials seized during drug trafficking using GC-MS. *Analytical and bioanalytical chemistry, 405*(12), 3937-3944.

Choi, H., Heo, S., Kim, E., Hwang, B., Lee, C., & Lee, J. (2013). Identification of (1-pentylindol-3-yl)-(2,2,3,3-tetramethylcyclopropyl)methanone and its 5-pentyl fluorinated analog in herbal incense seized for drug trafficking. *Forensic Toxicology, 31*(1), 86-92. doi: 10.1007/s11419-012-0170-5

Chung, H., Choi, H., Heo, S., Kim, E., & Lee, J. (2014). Synthetic cannabinoids abused in South Korea: drug identifications by the National Forensic Service from 2009 to June 2013. *Forensic Toxicology, 32*(1), 82-88. doi: 10.1007/s11419-013-0213-6

Coffey, C., Carlin, J. B., Degenhardt, L., Lynskey, M., Sanci, L., & Patton, G. C. (2002). Cannabis dependence in young adults: an Australian population study. *Addiction, 97*(2), 187-194. doi: 10.1046/j.1360-0443.2002.00029.x

Compton, D. R., Gold, L. H., Ward, S. J., Balster, R. L., & Martin, B. R. (1992). Aminoalkylindole analogs: cannabimimetic activity of a class of compounds structurally distinct from delta 9-tetrahydrocannabinol. *J Pharmacol Exp Ther, 263*(3), 1118-1126.

Condie, R., Herring, A., Koh, W. S., Lee, M., & Kaminski, N. E. (1996). Cannabinoid Inhibition of Adenylate Cyclase-mediated Signal Transduction and Interleukin 2 (IL-2) Expression in the Murine T-cell Line, EL4.IL-2. *Journal of Biological Chemistry, 271*(22), 13175-13183. doi: 10.1074/jbc.271.22.13175

Control, C. f. D., & Prevention. (2013a). Acute kidney injury associated with synthetic cannabinoid use--multiple states, 2012. *MMWR. Morbidity and mortality weekly report, 62*(6), 93.

Control, C. f. D., & Prevention. (2013b). Notes from the field: severe illness associated with reported use of synthetic marijuana-Colorado, August-September 2013. *MMWR. Morbidity and mortality weekly report, 62*(49), 1016.

Corbille, A. G., Valjent, E., Marsicano, G., Ledent, C., Lutz, B., Herve, D., & Girault, J. A. (2007). Role of cannabinoid type 1 receptors in locomotor activity and striatal signaling in response to psychostimulants. *J Neurosci, 27*(26), 6937-6947. doi: 10.1523/jneurosci.3936-06.2007

Couch, R., & Madhavaram, H. (2012). Phenazepam and cannabinomimetics sold as herbal highs in New Zealand. *Drug testing and analysis, 4*(6), 409-414.

Cravatt, B. F., & Lichtman, A. H. (2004). The endogenous cannabinoid system and its role in nociceptive behavior. *J Neurobiol, 61*(1), 149-160. doi: 10.1002/neu.20080

Crime, U. N. O. o. D. a. (2014). World Drug Report 2014 United Nations Office on Drugs and Crime

Dalton, G. D., Peterson, L. J., & Howlett, A. C. (2013). CB(1) Cannabinoid Receptors Promote Maximal FAK Catalytic Activity By Stimulating Cooperative Signaling Between Receptor Tyrosine Kinases and Integrins in Neuronal Cells. *Cellular signalling, 25*(8), 1665-1677. doi: 10.1016/j.cellsig.2013.03.020

Dalvi, V. H., & Rossky, P. J. (2010). Molecular origins of fluorocarbon hydrophobicity. *Proceedings of the National Academy of Sciences of the United States of America, 107*(31), 13603-13607. doi: 10.1073/pnas.0915169107

Dawson, W. R. (1934). Studies in the Egyptian Medical Texts: III. *The Journal of Egyptian Archaeology, 20*, 41-46.

de Jong, L. A. A., Uges, D. R. A., Franke, J. P., & Bischoff, R. (2005). Receptor–ligand binding assays: Technologies and Applications. *Journal of Chromatography B, 829*(1–2), 1-25. doi: http://dx.doi.org/10.1016/j.jchromb.2005.10.002

De Petrocellis, L., Davis, J. B., & Di Marzo, V. (2001). Palmitoylethanolamide enhances anandamide stimulation of human vanilloid VR1 receptors. *FEBS Letters, 506*(3), 253-256. doi: http://dx.doi.org/10.1016/S0014-5793(01)02934-9

De Petrocellis, L., Ligresti, A., Moriello, A. S., Allara, M., Bisogno, T., Petrosino, S., Stott, C. G., & Di Marzo, V. (2011). Effects of cannabinoids and cannabinoid-enriched Cannabis extracts on TRP channels and endocannabinoid metabolic enzymes. *Br J Pharmacol, 163*(7), 1479-1494. doi: 10.1111/j.1476-5381.2010.01166.x

De Petrocellis, L., Marini, P., Matias, I., Moriello, A. S., Starowicz, K., Cristino, L., Nigam, S., & Di Marzo, V. (2007). Mechanisms for the coupling of cannabinoid receptors to intracellular calcium mobilization in rat insulinoma beta-cells. *Exp Cell Res, 313*(14), 2993-3004. doi: 10.1016/j.yexcr.2007.05.012

De Petrocellis, L., Vellani, V., Schiano-Moriello, A., Marini, P., Magherini, P. C., Orlando, P., & Di Marzo, V. (2008). Plant-derived cannabinoids modulate the activity of transient receptor potential channels of ankyrin type-1 and melastatin type-8. *J Pharmacol Exp Ther, 325*(3), 1007-1015. doi: 10.1124/jpet.107.134809

Degenhardt, L., Coffey, C., Romaniuk, H., Swift, W., Carlin, J. B., Hall, W. D., & Patton, G. C. (2013). The persistence of the association between adolescent cannabis use and common mental disorders into young adulthood. *Addiction, 108*(1), 124-133.

Devane, W. A., Hanus, L., Breuer, A., Pertwee, R. G., Stevenson, L. A., Griffin, G., Gibson, D., Mandelbaum, A., Etinger, A., & Mechoulam, R. (1992). Isolation and structure of a brain constituent that binds to the cannabinoid receptor. *Science, 258*(5090), 1946-1949.

Devices, M. FLIPR Calcium 5 Assay Kit: A homogeneous solution for GPCR assays.

Devices, M. Measuring Membrane Potential Using the FLIPR Membrane Potential Assay Kit on Fluorometric Imaging Plate Reader (FLIPR) Systems.

Dhopeshwarkar, A., & Mackie, K. (2014). CB2 Cannabinoid Receptors as a Therapeutic Target—What Does the Future Hold? *Molecular Pharmacology, 86*(4), 430-437.

Di Marzo, V. (2004). *Cannabinoids*: Springer.

Digby, G. J., Lober, R. M., Sethi, P. R., & Lambert, N. A. (2006). Some G protein heterotrimers physically dissociate in living cells. *Proceedings of the National Academy of Sciences of the United States of America, 103*(47), 17789-17794. doi: 10.1073/pnas.0607116103

Drug Enforcement Administration, D. o. J. (2014). Schedules of controlled substances: temporary placement of four synthetic cannabinoids into Schedule I. Final order. *Federal register, 79*(27), 7577.

Duncan, D. F. (1974). Letter: Drug abuse as a coping mechanism. *Am J Psychiatry, 131*(6), 724.

Edwards, J. G. (2014). TRPV1 in the central nervous system: synaptic plasticity, function, and pharmacological implications. *Prog Drug Res, 68*, 77-104.

El Kouzi, A., & Siddiqui, F. (2015). " Spicy Strokes": Synthetic Cannabis and Strokes in Young (P7. 123). *Neurology, 84*(14 Supplement), P7. 123.

EMCDDA. (2009a). Early-Warning system. Understanding the "Spice" phenonmenon.

EMCDDA. (2010). Annex-2 — New psychoactive substances reported to the EMCDDA and Europol for the first time in 2010 under the terms of Council Decision 2005/387/JHA.

EMCDDA. (2014). EMCDDA-Europol 2013 Annual Report on the implementation of Council Decision.

EMCDDA. (2015). New Psychoactive Substances in Europe: An update from the EU Early Warning System. Retrieved from

Every-Palmer, S. (2011). Synthetic cannabinoid JWH-018 and psychosis: an explorative study. *Drug Alcohol Depend, 117*(2-3), 152-157. doi: 10.1016/j.drugalcdep.2011.01.012

Fantegrossi, W. E., Moran, J. H., Radominska-Pandya, A., & Prather, P. L. (2014). Distinct pharmacology and metabolism of K2 synthetic cannabinoids compared to Delta(9)-THC: mechanism underlying greater toxicity? *Life Sci, 97*(1), 45-54. doi: 10.1016/j.lfs.2013.09.017

Felder, C. C., Joyce, K. E., Briley, E. M., Mansouri, J., Mackie, K., Blond, O., Lai, Y., Ma, A. L., & Mitchell, R. L. (1995). Comparison of the pharmacology and signal transduction of the human cannabinoid CB1 and CB2 receptors. *Molecular Pharmacology, 48*(3), 443-450.

Feng, Z., Alqarni, M. H., Yang, P., Tong, Q., Chowdhury, A., Wang, L., & Xie, X.-Q. (2014). Modeling, Molecular Dynamics Simulation, and Mutation Validation for Structure of Cannabinoid Receptor 2 Based on Known Crystal Structures of GPCRs. *Journal of Chemical Information and Modeling, 54*(9), 2483-2499. doi: 10.1021/ci5002718

Fernandes, E. S., Fernandes, M. A., & Keeble, J. E. (2012). The functions of TRPA1 and TRPV1: moving away from sensory nerves. *British Journal of Pharmacology, 166*(2), 510-521. doi: 10.1111/j.1476-5381.2012.01851.x

Fernandez-Ruiz, J., Romero, J., Velasco, G., Tolon, R. M., Ramos, J. A., & Guzman, M. (2007). Cannabinoid CB2 receptor: a new target for controlling neural cell survival? *Trends in Pharmacological Sciences, 28*(1), 39-45. doi: 10.1016/j.tips.2006.11.001

Fitzgerald, K. T., Bronstein, A. C., & Newquist, K. L. (2013). Marijuana poisoning. *Top Companion Anim Med, 28*(1), 8-12. doi: 10.1053/j.tcam.2013.03.004

Florek-Luszczki, M., Wlaz, A., Kondrat-Wrobel, M. W., Tutka, P., & Luszczki, J. J. (2014). Effects of WIN 55,212-2 (a non-selective cannabinoid CB(1) and CB(2) receptor agonist) on the protective action of various classical antiepileptic drugs in the mouse 6 Hz psychomotor seizure model. *Journal of Neural Transmission, 121*(7), 707-715. doi: 10.1007/s00702-014-1173-7

. *Food and Drug Administration Safety and Innovation Act*. US Government Publishing Office Retrieved from https://www.govtrack.us/congress/bills/112/s3187/text.

Freire, E. (2008). Do Enthalpy and Entropy Distinguish First in Class From Best in Class? *Drug discovery today, 13*(19-20), 869-874. doi: 10.1016/j.drudis2008.07.005

Freund, T. F., Katona, I., & Piomelli, D. (2003). Role of endogenous cannabinoids in synaptic signaling. *Physiological reviews, 83*(3), 1017-1066.

Frost, J. M., Dart, M. J., Tietje, K. R., Garrison, T. R., Grayson, G. K., Daza, A. V., El-Kouhen, O. F., Miller, L. N., Li, L., Yao, B. B., Hsieh, G. C., Pai, M., Zhu, C. Z.,

Chandran, P., & Meyer, M. D. (2008). Indol-3-yl-tetramethylcyclopropyl ketones: effects of indole ring substitution on CB2 cannabinoid receptor activity. *J Med Chem, 51*(6), 1904-1912. doi: 10.1021/jm7011613

Frost, J. M., Dart, M. J., Tietje, K. R., Garrison, T. R., Grayson, G. K., Daza, A. V., El-Kouhen, O. F., Yao, B. B., Hsieh, G. C., Pai, M., Zhu, C. Z., Chandran, P., & Meyer, M. D. (2010). Indol-3-ylcycloalkyl ketones: effects of N1 substituted indole side chain variations on CB(2) cannabinoid receptor activity. *J Med Chem, 53*(1), 295-315. doi: 10.1021/jm901214q

Gaoni, Y., & Mechoulam, R. (1964). Isolation, Structure, and Partial Synthesis of an Active Constituent of Hashish. *Journal of the American Chemical Society, 86*(8), 1646-1647. doi: 10.1021/ja01062a046

Garcia-Anoveros, J., & Nagata, K. (2007). TRPA1. *Handb Exp Pharmacol*(179), 347-362. doi: 10.1007/978-3-540-34891-7_21

Garzón, J., de la Torre-Madrid, E., Rodríguez-Muñoz, M., Vicente-Sánchez, A., & Sánchez-Blázquez, P. (2009). Gz mediates the long-lasting desensitization of brain CB1 receptors and is essential for cross-tolerance with morphine. *Mol Pain, 5*(11).

Gerdeman, G. L., Partridge, J. G., Lupica, C. R., & Lovinger, D. M. (2003). It could be habit forming: drugs of abuse and striatal synaptic plasticity. *Trends in Neurosciences, 26*(4), 184-192. doi: http://dx.doi.org/10.1016/S0166-2236(03)00065-1

Gerostamoulos, D., Drummer, O. H., & Woodford, N. W. (2015). Deaths linked to synthetic cannabinoids. *Forensic science, medicine, and pathology*.

Glass, M., Faull, R. L. M., & Dragunow, M. (1997). Cannabinoid receptors in the human brain: a detailed anatomical and quantitative autoradiographic study in the fetal, neonatal and adult human brain. *Neuroscience, 77*(2), 299-318. doi: http://dx.doi.org/10.1016/S0306-4522(96)00428-9

Gonsiorek, W., Lunn, C., Fan, X., Narula, S., Lundell, D., & Hipkin, R. W. (2000).
Endocannabinoid 2-Arachidonyl Glycerol Is a Full Agonist through Human Type 2
Cannabinoid Receptor: Antagonism by Anandamide. *Molecular Pharmacology, 57*(5),
1045-1050.

González, A., Murcia, M., Benhamú, B., Campillo, M., López-Rodríguez, M. L., & Pardo, L.
(2011). The importance of solvation in the design of ligands targeting membrane
proteins. *MedChemComm, 2*(3), 160-164.

Govaerts, S. J., Hermans, E., & Lambert, D. M. (2004). Comparison of cannabinoid ligands
affinities and efficacies in murine tissues and in transfected cells expressing human
recombinant cannabinoid receptors. *European Journal of Pharmaceutical Sciences,
23*(3), 233-243. doi: http://dx.doi.org/10.1016/j.ejps.2004.07.013

Greydanus, D. E., Hawver, E. K., Greydanus, M. M., & Merrick, J. (2013). Marijuana:
Current Concepts(). *Frontiers in Public Health, 1*, 42. doi: 10.3389/fpubh.2013.00042

Grigoryev, A., Kavanagh, P., & Melnik, A. (2012). The detection of the urinary metabolites
of 3-[(adamantan-1-yl)carbonyl]-1-pentylindole (AB-001), a novel cannabimimetic,
by gas chromatography-mass spectrometry. *Drug Test Anal, 4*(6), 519-524. doi:
10.1002/dta.350

Grimsey, N. L., Goodfellow, C. E., Dragunow, M., & Glass, M. Cannabinoid receptor 2
undergoes Rab5-mediated internalization and recycles via a Rab11-dependent
pathway. *Biochimica et Biophysica Acta (BBA) - Molecular Cell Research, 1813*(8),
1554-1560. doi: http://dx.doi.org/10.1016/j.bbamcr.2011.05.010

Grimsey, N. L., Graham, E. S., Dragunow, M., & Glass, M. Cannabinoid Receptor 1
trafficking and the role of the intracellular pool: Implications for therapeutics.
Biochemical Pharmacology, 80(7), 1050-1062. doi:
http://dx.doi.org/10.1016/j.bcp.2010.06.007

Gugelmann, H., Gerona, R., Li, C., Tsutaoka, B., Olson, K. R., & Lung, D. (2014). 'Crazy Monkey' poisons man and dog: Human and canine seizures due to PB-22, a novel synthetic cannabinoid. *Clin Toxicol (Phila), 52*(6), 635-638. doi: 10.3109/15563650.2014.925562

Gunderson, E. W., Haughey, H. M., Ait-Daoud, N., Joshi, A. S., & Hart, C. L. (2012). "Spice" and "K2" Herbal Highs: A Case Series and Systematic Review of the Clinical Effects and Biopsychosocial Implications of Synthetic Cannabinoid Use in Humans. *The American Journal on Addictions, 21*(4), 320-326. doi: 10.1111/j.1521-0391.2012.00240.x

Guo, J., & Ikeda, S. R. (2004). Endocannabinoids Modulate N-Type Calcium Channels and G-Protein-Coupled Inwardly Rectifying Potassium Channels via CB1 Cannabinoid Receptors Heterologously Expressed in Mammalian Neurons. *Molecular Pharmacology, 65*(3), 665-674. doi: 10.1124/mol.65.3.665

Gurney, S. M., Scott, K., Kacinko, S., Presley, B., & Logan, B. (2014). Pharmacology, toxicology, and adverse effects of synthetic cannabinoid drugs.

Hammond, B. (2012). *New and emerging psychoactive substances–The global perspective.* Paper presented at the UNODC (United Nation Office on Drugs and Crime). Available at: http://www. unodc. org/documents/eastasiaandpacific//2012/07/smart-workshop/06_New_and_emerging_psychoactive_substances_The_global_perspective. pdf [15 September 2012].

Harris, C. R., & Brown, A. (2013). Synthetic Cannabinoid Intoxication: A Case Series and Review. *The Journal of Emergency Medicine, 44*(2), 360-366. doi: http://dx.doi.org/10.1016/j.jemermed.2012.07.061

Hasegawa, K., Wurita, A., Minakata, K., Gonmori, K., Nozawa, H., Yamagishi, I., Watanabe, K., & Suzuki, O. (2015). Postmortem distribution of MAB-CHMINACA in body

fluids and solid tissues of a human cadaver. *Forensic Toxicology*, 1-8. doi: 10.1007/s11419-015-0272-y

Haubrich, D. R., Ward, S. J., Baizman, E., Bell, M. R., Bradford, J., Ferrari, R., Miller, M., Perrone, M., Pierson, A. K., Saelens, J. K., & et al. (1990). Pharmacology of pravadoline: a new analgesic agent. *J Pharmacol Exp Ther, 255*(2), 511-522.

Haynes, W. J., Zhou, X.-L., Su, Z.-W., Loukin, S. H., Saimi, Y., & Kung, C. (2008). Indole and other aromatic compounds activate the yeast TRPY1 channel. *FEBS Letters, 582*(10), 1514-1518. doi: 10.1016/j.febslet.2008.03.046

Hazekamp, A., Ware, M. A., Muller-Vahl, K. R., Abrams, D., & Grotenhermen, F. (2013). The medicinal use of cannabis and cannabinoids--an international cross-sectional survey on administration forms. *J Psychoactive Drugs, 45*(3), 199-210. doi: 10.1080/02791072.2013.805976

Hermann, D., Sartorius, A., Welzel, H., Walter, S., Skopp, G., Ende, G., & Mann, K. (2007). Dorsolateral prefrontal cortex N-acetylaspartate/total creatine (NAA/tCr) loss in male recreational cannabis users. *Biological psychiatry, 61*(11), 1281-1289.

Hermanns-Clausen, M., Kneisel, S., Szabo, B., & Auwarter, V. (2013). Acute toxicity due to the confirmed consumption of synthetic cannabinoids: clinical and laboratory findings. *Addiction, 108*(3), 534-544. doi: 10.1111/j.1360-0443.2012.04078.x

Hézode, C., Zafrani, E. S., Roudot–Thoraval, F., Costentin, C., Hessami, A., Bouvier–Alias, M., Medkour, F., Pawlostky, J. M., Lotersztajn, S., & Mallat, A. (2008). Daily cannabis use: a novel risk factor of steatosis severity in patients with chronic hepatitis C. *Gastroenterology, 134*(2), 432-439.

Hill, S. J. (2006). G-protein-coupled receptors: past, present and future. *British Journal of Pharmacology, 147*(S1), S27-S37. doi: 10.1038/sj.bjp.0706455

Hillard, C. J., Manna, S., Greenberg, M. J., DiCamelli, R., Ross, R. A., Stevenson, L. A., Murphy, V., Pertwee, R. G., & Campbell, W. B. (1999). Synthesis and Characterization of Potent and Selective Agonists of the Neuronal Cannabinoid Receptor (CB1). *Journal of Pharmacology and Experimental Therapeutics, 289*(3), 1427-1433.

Hinman, A., Chuang, H.-h., Bautista, D. M., & Julius, D. (2006). TRP channel activation by reversible covalent modification. *Proceedings of the National Academy of Sciences of the United States of America, 103*(51), 19564-19568. doi: 10.1073/pnas.0609598103

Hirota, K., Smart, D., & Lambert, D. G. (2003). The effects of local and intravenous anesthetics on recombinant rat VR1 vanilloid receptors. *Anesth Analg, 96*(6), 1656-1660, table of contents.

Ho, B. Y., Uezono, Y., Takada, S., Takase, I., & Izumi, F. (1999). Coupling of the expressed cannabinoid CB1 and CB2 receptors to phospholipase C and G protein-coupled inwardly rectifying K+ channels. *Receptors & Channels, 6*(5), 363-374.

Ho, K. W., Ward, N. J., & Calkins, D. J. (2012). TRPV1: a stress response protein in the central nervous system. *Am J Neurodegener Dis, 1*(1), 1-14.

Ho, W. S., Barrett, D. A., & Randall, M. D. (2008). 'Entourage' effects of N-palmitoylethanolamide and N-oleoylethanolamide on vasorelaxation to anandamide occur through TRPV1 receptors. *Br J Pharmacol, 155*(6), 837-846. doi: 10.1038/bjp.2008.324

Howlett, A. C. (1984). Inhibition of neuroblastoma adenylate cyclase by cannabinoid and nantradol compounds. *Life Sci, 35*(17), 1803-1810.

Howlett, A. C. (1985). Cannabinoid inhibition of adenylate cyclase. Biochemistry of the response in neuroblastoma cell membranes. *Mol Pharmacol, 27*(4), 429-436.

Howlett, A. C. (2002). The cannabinoid receptors. *Prostaglandins Other Lipid Mediat, 68-69*, 619-631.

Howlett, A. C. (2005). Cannabinoid Receptor Signaling. In R. Pertwee (Ed.), *Cannabinoids* (Vol. 168, pp. 53-79): Springer Berlin Heidelberg.

Howlett, A. C., Barth, F., Bonner, T. I., Cabral, G., Casellas, P., Devane, W. A., Felder, C. C., Herkenham, M., Mackie, K., Martin, B. R., Mechoulam, R., & Pertwee, R. G. (2002). International Union of Pharmacology. XXVII. Classification of Cannabinoid Receptors. *Pharmacological Reviews, 54*(2), 161-202.

Howlett, A. C., Breivogel, C. S., Childers, S. R., Deadwyler, S. A., Hampson, R. E., & Porrino, L. J. (2004). Cannabinoid physiology and pharmacology: 30 years of progress. *Neuropharmacology, 47, Supplement 1*(0), 345-358. doi: http://dx.doi.org/10.1016/j.neuropharm.2004.07.030

Howlett, A. C., & Fleming, R. M. (1984). Cannabinoid inhibition of adenylate cyclase. Pharmacology of the response in neuroblastoma cell membranes. *Mol Pharmacol, 26*(3), 532-538.

https://www.clinicaltrials.gov/ct2/home.   https://www.clinicaltrials.gov/ct2/home

Huffman, J. W., Dai, D., Martin, B. R., & Compton, D. R. (1994). Design, synthesis and pharmacology of cannabimimetic indoles. *Bioorganic & Medicinal Chemistry Letters, 4*(4), 563-566.

Huffman, J. W., & Padgett, L. W. (2005). Recent Developments in the Medicinal Chemistry of Cannabimimetic Indoles, Pyrroles and Indenes. *Current Medicinal Chemistry, 12*(12), 1395-1411. doi: 10.2174/0929867054020864

Huffman, J. W., Szklennik, P. V., Almond, A., Bushell, K., Selley, D. E., He, H., Cassidy, M. P., Wiley, J. L., & Martin, B. R. (2005). 1-Pentyl-3-phenylacetylindoles, a new class

of cannabimimetic indoles. *Bioorg Med Chem Lett, 15*(18), 4110-4113. doi: 10.1016/j.bmcl.2005.06.008

Hurowitz, E. H., Melnyk, J. M., Chen, Y.-J., Kouros-Mehr, H., Simon, M. I., & Shizuya, H. (2000). Genomic Characterization of the Human Heterotrimeric G Protein α, β, and γ Subunit Genes. *DNA Research, 7*(2), 111-120. doi: 10.1093/dnares/7.2.111

Hutter, M., Kneisel, S., Auwärter, V., & Neukamm, M. A. (2012). Determination of 22 synthetic cannabinoids in human hair by liquid chromatography–tandem mass spectrometry. *Journal of Chromatography B, 903*, 95-101.

Irving, A. (2011). New blood brothers: the GPR55 and CB(2) partnership. *Cell Research, 21*(10), 1391-1392. doi: 10.1038/cr.2011.77

Ishida, T., Nishiumi, S., Tanahashi, T., Yamasaki, A., Yamazaki, A., Akashi, T., Miki, I., Kondo, Y., Inoue, J., Kawauchi, S., Azuma, T., Yoshida, M., & Mizuno, S. (2013). Linoleoyl ethanolamide reduces lipopolysaccharide-induced inflammation in macrophages and ameliorates 2,4-dinitrofluorobenzene-induced contact dermatitis in mice. *Eur J Pharmacol, 699*(1-3), 6-13. doi: 10.1016/j.ejphar.2012.11.030

Islam, S. (2011). *Transient Receptor Potential Channels*: Springer Netherlands.

Jack, A. (2009). The Story of Spice. *The Financial Times*

Jankovics, P., Varadi, A., Tolgyesi, L., Lohner, S., Nemeth-Palotas, J., & Balla, J. (2012). Detection and identification of the new potential synthetic cannabinoids 1-pentyl-3-(2-iodobenzoyl)indole and 1-pentyl-3-(1-adamantoyl)indole in seized bulk powders in Hungary. *Forensic Sci Int, 214*(1-3), 27-32. doi: 10.1016/j.forsciint.2011.07.011

Jerman, J. C., Brough, S. J., Prinjha, R., Harries, M. H., Davis, J. B., & Smart, D. (2000). Characterization using FLIPR of rat vanilloid receptor (rVR1) pharmacology. *British Journal of Pharmacology, 130*(4), 916-922. doi: 10.1038/sj.bjp.0703390

Johnson, E. N., Shi, X., Cassaday, J., Ferrer, M., Strulovici, B., & Kunapuli, P. (2008). A 1,536-well [(35)S]GTPgammaS scintillation proximity binding assay for ultra-high-throughput screening of an orphan galphai-coupled GPCR. *Assay Drug Dev Technol, 6*(3), 327-337. doi: 10.1089/adt.2007.113

Joss, R., Galeazzi, R., Bischoff, A., Do, D., Goldhirsch, A., & Brunner, K. (1982). Levonantradol, a new antiemetic with a high rate of side-effects for the prevention of nausea and vomiting in patients receiving cancer chemotherapy. *Cancer Chemotherapy and Pharmacology, 9*(1), 61-64. doi: 10.1007/BF00296765

Kavanagh, P., Grigoryev, A., Melnik, A., & Simonov, A. (2012). The Identification of the Urinary Metabolites of 3-(4-Methoxybenzoyl)-1-Pentylindole (RCS-4), a Novel Cannabimimetic, by Gas Chromatography–Mass Spectrometry. *Journal of Analytical Toxicology, 36*(5), 303-311.

Kavanagh, P., Grigoryev, A., Savchuk, S., Mikhura, I., & Formanovsky, A. (2013). UR-144 in products sold via the Internet: identification of related compounds and characterization of pyrolysis products. *Drug Test Anal, 5*(8), 683-692. doi: 10.1002/dta.1456

Kelly, B. C., Wells, B. E., Pawson, M., Leclair, A., Parsons, J. T., & Golub, S. A. (2013). Novel psychoactive drug use among younger adults involved in US nightlife scenes. *Drug and Alcohol Review, 32*(6), 588-593. doi: 10.1111/dar.12058

Kersten, B. P., & McLaughlin, M. E. (2014). Toxicology and management of novel psychoactive drugs. *Journal of pharmacy practice*, 0897190014544814.

Khantzian, E. J. (1974). Opiate addiction: A critique of theory and some implications for treatment. *American Journal of Psychotherapy*.

Klumpers, L. E., Beumer, T. L., van Hasselt, J. G., Lipplaa, A., Karger, L. B., Kleinloog, H. D., Freijer, J. I., de Kam, M. L., & van Gerven, J. M. (2012). Novel Delta(9) -

tetrahydrocannabinol formulation Namisol(R) has beneficial pharmacokinetics and promising pharmacodynamic effects. *Br J Clin Pharmacol, 74*(1), 42-53. doi: 10.1111/j.1365-2125.2012.04164.x

Knapman, A., Santiago, M., Du, Y. P., Bennallack, P. R., Christie, M. J., & Connor, M. (2013). A Continuous, Fluorescence-based Assay of μ-Opioid Receptor Activation in AtT-20 Cells. *Journal of Biomolecular Screening, 18*(3), 269-276.

Kneisel, S., Auwärter, V., & Kempf, J. (2013). Analysis of 30 synthetic cannabinoids in oral fluid using liquid chromatography‐electrospray ionization tandem mass spectrometry. *Drug testing and analysis, 5*(8), 657-669.

Kolesnick, R. (2002). The therapeutic potential of modulating the ceramide/sphingomyelin pathway. *The Journal of Clinical Investigation, 110*(1), 3-8. doi: 10.1172/JCI16127

Kostenis, E., Waelbroeck, M., & Milligan, G. (2005). Techniques: Promiscuous G α proteins in basic research and drug discovery. *Trends in Pharmacological Sciences, 26*(11), 595-602. doi: http://dx.doi.org/10.1016/j.tips.2005.09.007

Kronstrand, R., Roman, M., Andersson, M., & Eklund, A. (2013). Toxicological findings of synthetic cannabinoids in recreational users. *Journal of Analytical Toxicology, 37*(8), 534-541.

Kukkonen, J. P. (2004). Regulation of receptor-coupling to (multiple) G proteins. A challenge for basic research and drug discovery. *Receptors & Channels, 10*(5-6), 167-183.

Lambert, D. M., Vandevoorde, S., Jonsson, K.-O., & Fowler, C. J. (2002). The palmitoylethanolamide family: a new class of anti-inflammatory agents? *Current Medicinal Chemistry, 9*(6), 663-674.

Lauckner, J. E., Hille, B., & Mackie, K. (2005). The cannabinoid agonist WIN55,212-2 increases intracellular calcium via CB1 receptor coupling to Gq/11 G proteins. *Proc Natl Acad Sci U S A, 102*(52), 19144-19149. doi: 10.1073/pnas.0509588102

Law, A. S. o. I. (1913). The Second International Opium Conference. *The American Journal of International Law, 7*(4), 838-847. doi: 10.2307/2187338

Leach, K., Conigrave, A. D., Sexton, P. M., & Christopoulos, A. (2015). Towards tissue-specific pharmacology: insights from the calcium-sensing receptor as a paradigm for GPCR (patho)physiological bias. *Trends in Pharmacological Sciences, 36*(4), 215-225. doi: http://dx.doi.org/10.1016/j.tips.2015.02.004

Lee, M. A. (2012). *Smoke Signals: A Social History of Marijuana - Medical, Recreational and Scientific*: Scribner.

Leys, T. (2014). New version of synthetic marijuana linked to deaths of three young Iowans. from http://blogs.desmoinesregister.com/dmr/index.php/2014/02/18/three-iowa-deaths-blamed-on-new-type-of-synthetic-marijuana

Li, H.-L. (1973). An archaeological and historical account of cannabis in China. *Economic Botany, 28*(4), 437-448. doi: 10.1007/BF02862859

Liao, H. T., Lee, H. J., Ho, Y. C., & Chiou, L. C. (2011). Capsaicin in the periaqueductal gray induces analgesia via metabotropic glutamate receptor‐mediated endocannabinoid retrograde disinhibition. *British Journal of Pharmacology, 163*(2), 330-345.

Liotta, F., Lu, H., Wachter, M. P., & Xia, M. (2010). Tetrahydro-2H-indazole pyrazole cannabinoid modulators: Google Patents.

Lloyd, C. (1998). Risk factors for problem drug use: identifying vulnerable groups. *Drugs: education, prevention and policy, 5*(3), 217-232.

Logan, B. K., Reinhold, L. E., Xu, A., & Diamond, F. X. (2012). Identification of synthetic cannabinoids in herbal incense blends in the United States. *Journal of forensic sciences, 57*(5), 1168-1180.

Lu, D., Meng, Z., Thakur, G. A., Fan, P., Steed, J., Tartal, C. L., Hurst, D. P., Reggio, P. H., Deschamps, J. R., Parrish, D. A., George, C., Järbe, T. U. C., Lamb, R. J., &

Makriyannis, A. (2005). Adamantyl Cannabinoids: A Novel Class of Cannabinergic Ligands. *Journal of Medicinal Chemistry, 48*(14), 4576-4585. doi: 10.1021/jm058175c

Luk, T., Jin, W., Zvonok, A., Lu, D., Lin, X.-Z., Chavkin, C., Makriyannis, A., & Mackie, K. (2004). Identification of a potent and highly efficacious, yet slowly desensitizing CB1 cannabinoid receptor agonist. *British Journal of Pharmacology, 142*(3), 495-500. doi: 10.1038/sj.bjp.0705792

Luo, J., Zhu, Y., Zhu, M. X., & Hu, H. (2011). Cell-based Calcium Assay for Medium to High Throughput Screening of TRP Channel Functions using FlexStation 3. *Journal of Visualized Experiments : JoVE*(54), 3149. doi: 10.3791/3149

Maas, A. I. R., Murray, G., Henney Iii, H., Kassem, N., Legrand, V., Mangelus, M., Muizelaar, J.-P., Stocchetti, N., & Knoller, N. (2006). Efficacy and safety of dexanabinol in severe traumatic brain injury: results of a phase III randomised, placebo-controlled, clinical trial. *The Lancet Neurology, 5*(1), 38-45. doi: http://dx.doi.org/10.1016/S1474-4422(05)70253-2

Maccarrone, M., Bari, M., Battista, N., & Finazzi-Agro, A. (2002). Endocannabinoid degradation, endotoxic shock and inflammation. *Curr Drug Targets Inflamm Allergy, 1*(1), 53-63.

Mackie, K., Lai, Y., Westenbroek, R., & Mitchell, R. (1995). Cannabinoids activate an inwardly rectifying potassium conductance and inhibit Q-type calcium currents in AtT20 cells transfected with rat brain cannabinoid receptor. *The Journal of Neuroscience, 15*(10), 6552-6561.

Makriyannis, A., & Deng, H. (2005). Cannabimimetic indole derivatives: Google Patents.

Makriyannis, A., & Deng, H. (2007).

Mansoori, G. A., George, T. F., Assoufid, L., & Zhang, G. (2007). *Molecular Building Blocks for Nanotechnology: From Diamondoids to Nanoscale Materials and Applications*: Springer New York.

Marsicano, G., Goodenough, S., Monory, K., Hermann, H., Eder, M., Cannich, A., Azad, S. C., Cascio, M. G., Gutiérrez, S. O., & van der Stelt, M. (2003). CB1 cannabinoid receptors and on-demand defense against excitotoxicity. *Science, 302*(5642), 84-88.

Martin, R. S., Reynen, P. H., Calixto, J. J., Reyes, C. L., Chang, T. K., Dietrich, P. S., Bonhaus, D. W., & MacLennan, S. J. (2002). Pharmacological comparison of a recombinant CB1 cannabinoid receptor with its G(alpha 16) fusion product. *J Biomol Screen, 7*(3), 281-289. doi: 10.1089/108705702760047781

Marzo, V. D., Bifulco, M., & Petrocellis, L. D. (2004). The endocannabinoid system and its therapeutic exploitation. *Nat Rev Drug Discov, 3*(9), 771-784.

Matsuda, L. A., Lolait, S. J., Brownstein, M. J., Young, A. C., & Bonner, T. I. (1990). Structure of a cannabinoid receptor and functional expression of the cloned cDNA. *Nature*(346), 561-564.

McAllister, S. D., Griffin, G., Satin, L. S., & Abood, M. E. (1999). Cannabinoid receptors can activate and inhibit G protein-coupled inwardly rectifying potassium channels in a xenopus oocyte expression system. *J Pharmacol Exp Ther, 291*(2), 618-626.

McHugh, D., Hu, S. S., Rimmerman, N., Juknat, A., Vogel, Z., Walker, J. M., & Bradshaw, H. B. (2010). N-arachidonoyl glycine, an abundant endogenous lipid, potently drives directed cellular migration through GPR18, the putative abnormal cannabidiol receptor. *BMC neuroscience, 11*(1), 44.

Mechoulam, R., & Gaoni, Y. (1967). Recent advances in the chemistry of hashish. *Fortschr Chem Org Naturst, 25*, 175-213.

Mechoulam, R., Hanus, L. O., Pertwee, R., & Howlett, A. C. (2014). Early phytocannabinoid chemistry to endocannabinoids and beyond. *Nat Rev Neurosci, 15*(11), 757-764. doi: 10.1038/nrn3811

Meier, M. H., Caspi, A., Ambler, A., Harrington, H., Houts, R., Keefe, R. S. E., McDonald, K., Ward, A., Poulton, R., & Moffitt, T. E. Persistent cannabis users show neuropsychological decline from childhood to midlife. *Proceedings of the National Academy of Sciences of the United States of America, 109*(40), E2657-E2664. doi: 10.1073/pnas.1206820109

Mella-Raipan, J., Lagos, C., Recabarren-Gajardo, G., Espinosa-Bustos, C., Romero-Parra, J., Pessoa-Mahana, H. n., Iturriaga-VÃ¡squez, P., & Pessoa-Mahana, C. (2013). Design, Synthesis, Binding and Docking-Based 3D-QSAR Studies of 2-Pyridylbenzimidazolesâ€"A New Family of High Affinity CB1 Cannabinoid Ligands. *Molecules, 18*(4), 3972-4001.

Merighi, S., Simioni, C., Gessi, S., Varani, K., & Borea, P. A. (2010). Binding thermodynamics at the human cannabinoid CB1 and CB2 receptors. *Biochem Pharmacol, 79*(3), 471-477. doi: 10.1016/j.bcp.2009.09.009

Mikuriya, T. H. (1969). Marijuana in medicine: past, present and future. *California Medicine, 110*(1), 34-40.

Millns, P., Chimenti, M., Ali, N., Ryland, E., De Lago, E., Fernandez‐Ruiz, J., Chapman, V., & Kendall, D. (2006). Effects of inhibition of fatty acid amide hydrolase vs. the anandamide membrane transporter on TRPV1‐mediated calcium responses in adult DRG neurons; the role of CB1 receptors. *European Journal of Neuroscience, 24*(12), 3489-3495.

Mills, J. H. (2003). *Cannabis Britannica: Empire, Trade, and Prohibition, 1800-1928*: Oxford University Press.

Miner, D. J., & Kissinger, P. T. (1979). Evidence for the involvement of N-acetyl-p-quinoneimine in acetaminophen metabolism. *Biochemical Pharmacology, 28*(22), 3285-3290.

Mir, A., Obafemi, A., Young, A., & Kane, C. (2011). Myocardial Infarction Associated With Use of the Synthetic Cannabinoid K2. *Pediatrics, 128*(6), e1622-e1627. doi: 10.1542/peds.2010-3823

Mitra, A., Lee, C. H., & Cheng, K. (2013). *Advanced Drug Delivery*: Wiley.

Mittleman, M. A., Lewis, R. A., Maclure, M., Sherwood, J. B., & Muller, J. E. (2001). Triggering myocardial infarction by marijuana. *Circulation, 103*(23), 2805-2809.

Monte, A. A., Bronstein, A. C., Cao, D. J., Heard, K. J., Hoppe, J. A., Hoyte, C. O., Iwanicki, J. L., & Lavonas, E. J. (2014). An outbreak of exposure to a novel synthetic cannabinoid. *New England Journal of Medicine, 370*(4), 389-390.

Moreno, E., Andradas, C., Medrano, M., Caffarel, M. M., Pérez-Gómez, E., Blasco-Benito, S., Gómez-Cañas, M., Pazos, M. R., Irving, A. J., & Lluís, C. (2014). Targeting CB2-GPR55 receptor heteromers modulates cancer cell signaling. *Journal of Biological Chemistry, 289*(32), 21960-21972.

Munro, S., Thomas, K. L., & Abu-Shaar, M. (1993). Molecular characterization of a peripheral receptor for cannabinoids.

Murray, D. (2013). Synthetic cannabis linked to series of Queensland deaths. *THE COURIER-MAIL.* from http://www.couriermail.com.au/news/queensland/synthetic-cannabis-linked-to-series-of-queensland-deaths/story-fnihsrf2-1226663431294

Musto, D. F. (1987). The history of legislative control over opium, cocaine, and their derivatives. *Dealing With Drugs: Consequences of Government Control, Lexington*.

Nacca, N., Vatti, D., Sullivan, R., Sud, P., Su, M., & Marraffa, J. (2013). The Synthetic Cannabinoid Withdrawal Syndrome. *Journal of Addiction Medicine, 7*(4), 296-298. doi: 10.1097/ADM.0b013e31828e1881

Nakajima, J. i., Takahashi, M., Nonaka, R., Seto, T., Suzuki, J., Yoshida, M., Kanai, C., & Hamano, T. (2011). Identification and quantitation of a benzoylindole (2-methoxyphenyl)(1-pentyl-1H-indol-3-yl) methanone and a naphthoylindole 1-(5-fluoropentyl-1H-indol-3-yl)-(naphthalene-1-yl) methanone (AM-2201) found in illegal products obtained via the Internet and their cannabimimetic effects evaluated by in vitro [35S] GTP γ S binding assays. *Forensic Toxicology, 29*(2), 132-141.

Nakajima, J. i., Takahashi, M., Seto, T., Kanai, C., Suzuki, J., Yoshida, M., & Hamano, T. (2011). Identification and quantitation of two benzoylindoles AM-694 and (4-methoxyphenyl)(1-pentyl-1H-indol-3-yl) methanone, and three cannabimimetic naphthoylindoles JWH-210, JWH-122, and JWH-019 as adulterants in illegal products obtained via the Internet. *Forensic Toxicology, 29*(2), 95-110.

Natarajan, V., Schmid, P. C., & Schmid, H. H. (1986). N-acylethanolamine phospholipid metabolism in normal and ischemic rat brain. *Biochimica et Biophysica Acta (BBA)-Lipids and Lipid Metabolism, 878*(1), 32-41.

New, D. C., & Wong, Y. H. (2003). BML-190 and AM251 act as inverse agonists at the human cannabinoid CB2 receptor: signalling via cAMP and inositol phosphates. *FEBS Letters, 536*(1–3), 157-160. doi: http://dx.doi.org/10.1016/S0014-5793(03)00048-6

News, C. (2015). Synthetic marijuana leads to nationwide spike in hospitalizations. from http://www.cbsnews.com/news/synthetic-marijuana-leads-to-nationwide-spike-in-hospitalizations/

Nicholson, T., Duncan, D. F., & White, J. B. (2002). Is recreational drug use normal? *Journal of Substance Use, 7*(3), 116-123. doi: doi:10.1080/14659890209169340

Nurmikko, T. J., Serpell, M. G., Hoggart, B., Toomey, P. J., Morlion, B. J., & Haines, D.

    (2007). Sativex successfully treats neuropathic pain characterised by allodynia: A

    randomised, double-blind, placebo-controlled clinical trial. *PAIN®, 133*(1–3), 210-

    220. doi: http://dx.doi.org/10.1016/j.pain.2007.08.028

O'Malley, P. M., Meich, R. A., Bachman, J. G., & Shulenberg, J. E. (Producer). (2014,

    12/4/2015). Monitoring the Future: National Results on Adolescent Drug Use.

    Overview of Keyfinding 2013. Retrieved from

    http://www.monitoringthefuture.org/data/data.html

Obata, K., Katsura, H., Mizushima, T., Yamanaka, H., Kobayashi, K., Dai, Y., Fukuoka, T.,

    Tokunaga, A., Tominaga, M., & Noguchi, K. (2005). TRPA1 induced in sensory

    neurons contributes to cold hyperalgesia after inflammation and nerve injury. *Journal*

    of Clinical Investigation, 115(9), 2393.

Ogborne, A. C., Smart, R. G., Weber, T., & Birchmore-Timney, C. (2000). Who is using

    cannabis as a medicine and why: an exploratory study. *Journal of psychoactive drugs,*

    32(4), 435-443.

Oka, S., Wakui, J., Ikeda, S., Yanagimoto, S., Kishimoto, S., Gokoh, M., Nasui, M., &

    Sugiura, T. (2006). Involvement of the Cannabinoid CB2 Receptor and Its

    Endogenous Ligand 2-Arachidonoylglycerol in Oxazolone-Induced Contact

    Dermatitis in Mice. *The Journal of Immunology, 177*(12), 8796-8805. doi:

    10.4049/jimmunol.177.12.8796

Oleson, E. B., & Cheer, J. F. (2012). A Brain on Cannabinoids: The Role of Dopamine

    Release in Reward Seeking. *Cold Spring Harbor Perspectives in Medicine, 2*(8). doi:

    10.1101/cshperspect.a012229

Onaivi, E. S., Ishiguro, H., Gong, J.-P., Patel, S., Meozzi, P. A., Myers, L., Perchuk, A.,

    Mora, Z., Tagliaferro, P. A., & Gardner, E. (2008). Brain neuronal CB2 cannabinoid

receptors in drug abuse and depression: from mice to human subjects. *PLoS ONE, 3*(2), e1640.

Overton, H. A., Babbs, A. J., Doel, S. M., Fyfe, M. C., Gardner, L. S., Griffin, G., Jackson, H. C., Procter, M. J., Rasamison, C. M., Tang-Christensen, M., Widdowson, P. S., Williams, G. M., & Reynet, C. (2006). Deorphanization of a G protein-coupled receptor for oleoylethanolamide and its use in the discovery of small-molecule hypophagic agents. *Cell Metab, 3*(3), 167-175. doi: 10.1016/j.cmet.2006.02.004

Palamar, J. J., & Acosta, P. (2015). Synthetic cannabinoid use in a nationally representative sample of US high school seniors. *Drug and Alcohol Dependence, 149*(0), 194-202. doi: http://dx.doi.org/10.1016/j.drugalcdep.2015.01.044

Papanti, D., Orsolini, L., Francesconi, G., & Schifano, F. (2014). "Noids" in a nutshell: everything you (don't) want to know about synthetic cannabimimetics. *Advances in Dual Diagnosis, 7*(3), 137-148.

Pellegrini-Giampietro, D. E., Mannaioni, G., & Bagetta, G. (2009). Post-ischemic brain damage: the endocannabinoid system in the mechanisms of neuronal death. *FEBS Journal, 276*(1), 2-12. doi: 10.1111/j.1742-4658.2008.06765.x

Peng, J., & Li, Y. J. (2010). The vanilloid receptor TRPV1: role in cardiovascular and gastrointestinal protection. *Eur J Pharmacol, 627*(1-3), 1-7. doi: 10.1016/j.ejphar.2009.10.053

Perez-Reyes, M., Timmons, M., Davis, K. H., & Wall, E. M. (1973). A comparison of the pharmacological activity in man of intravenously administered 1368-11368-11368-1, cannabinol, and cannabidiol. *Experientia, 29*(11), 1368-1369. doi: 10.1007/BF01922823

Pertwee, R. (2014). *Handbook of Cannabis*: OUP Oxford.

Pertwee, R. G. (2006). Cannabinoid pharmacology: the first 66 years. *British Journal of Pharmacology, 147*(Suppl 1), S163-S171. doi: 10.1038/sj.bjp.0706406

Pertwee, R. G. (2006). *Cannabinoids*: Springer Berlin Heidelberg.

Pertwee, R. G., Howlett, A. C., Abood, M. E., Alexander, S. P. H., Di Marzo, V., Elphick, M. R., Greasley, P. J., Hansen, H. S., Kunos, G., Mackie, K., Mechoulam, R., & Ross, R. A. (2010). International Union of Basic and Clinical Pharmacology. LXXIX. Cannabinoid Receptors and Their Ligands: Beyond CB(1) and CB(2). *Pharmacological Reviews, 62*(4), 588-631. doi: 10.1124/pr.110.003004

Piao, L. H., Fujita, T., Jiang, C. Y., Liu, T., Yue, H. Y., Nakatsuka, T., & Kumamoto, E. (2009). TRPA1 activation by lidocaine in nerve terminals results in glutamate release increase. *Biochem Biophys Res Commun, 379*(4), 980-984. doi: 10.1016/j.bbrc.2008.12.183

Pingle, S. C., Matta, J. A., & Ahern, G. P. (2007). Capsaicin receptor: TRPV1 a promiscuous TRP channel. *Handb Exp Pharmacol*(179), 155-171. doi: 10.1007/978-3-540-34891-7_9

Rahman, I. A., Tsuboi, K., Uyama, T., & Ueda, N. (2014). New players in the fatty acyl ethanolamide metabolism. *Pharmacol Res, 86*, 1-10. doi: 10.1016/j.phrs.2014.04.001

Rajasekaran, M., Brents, L. K., Franks, L. N., Moran, J. H., & Prather, P. L. (2013). Human metabolites of synthetic cannabinoids JWH-018 and JWH-073 bind with high affinity and act as potent agonists at cannabinoid type-2 receptors. *Toxicology and applied pharmacology, 269*(2), 100-108.

Ramsey, I. S., Delling, M., & Clapham, D. E. (2006). An introduction to TRP channels. *Annu Rev Physiol, 68*, 619-647. doi: 10.1146/annurev.physiol.68.040204.100431

Re, G., Barbero, R., Miolo, A., & Di Marzo, V. (2007). Palmitoylethanolamide, endocannabinoids and related cannabimimetic compounds in protection against tissue

inflammation and pain: potential use in companion animals. *Vet J, 173*(1), 21-30. doi: 10.1016/j.tvjl.2005.10.003

Redmond, W. J., Gu, L., Camo, M., McIntyre, P., & Connor, M. (2014). Ligand determinants of fatty acid activation of the pronociceptive ion channel TRPA1. *PeerJ, 2*, e248. doi: 10.7717/peerj.248

Roberts, L. A., Christie, M. J., & Connor, M. (2002). Anandamide is a partial agonist at native vanilloid receptors in acutely isolated mouse trigeminal sensory neurons. *Br J Pharmacol, 137*(4), 421-428. doi: 10.1038/sj.bjp.0704904

Robinson, C. (2015). Spice-related illnesses, deaths soar in Alabama. from http://www.al.com/news/birmingham/index.ssf/2015/05/spice-related_illnesses_deaths.html

Ross, R. A. (2003). Anandamide and vanilloid TRPV1 receptors. *British Journal of Pharmacology, 140*(5), 790-801. doi: 10.1038/sj.bjp.0705467

Ross, R. A., Brockie, H. C., Stevenson, L. A., Murphy, V. L., Templeton, F., Makriyannis, A., & Pertwee, R. G. (1999). Agonist-inverse agonist characterization at CB1 and CB2 cannabinoid receptors of L759633, L759656 and AM630. *British Journal of Pharmacology, 126*(3), 665-672. doi: 10.1038/sj.bjp.0702351

Russo, E. B. (2007). History of Cannabis and Its Preparations in Saga, Science, and Sobriquet. *Chemistry & Biodiversity, 4*(8), 1614-1648. doi: 10.1002/cbdv.200790144

Ryberg, E., Larsson, N., Sjogren, S., Hjorth, S., Hermansson, N. O., Leonova, J., Elebring, T., Nilsson, K., Drmota, T., & Greasley, P. J. (2007). The orphan receptor GPR55 is a novel cannabinoid receptor. *Br J Pharmacol, 152*(7), 1092-1101. doi: 10.1038/sj.bjp.0707460

Sarne, Y., Asaf, F., Fishbein, M., Gafni, M., & Keren, O. (2011). The dual neuroprotective–

    neurotoxic profile of cannabinoid drugs. *British Journal of Pharmacology, 163*(7),

    1391-1401. doi: 10.1111/j.1476-5381.2011.01280.x

Scallet, A. C. (1991). Neurotoxicology of cannabis and THC: A review of chronic exposure

    studies in animals. *Pharmacology, Biochemistry and Behavior, 40*(3), 671-676. doi:

    10.1016/0091-3057(91)90380-k

Schaefer, N., Peters, B., Bregel, D., Maurer, H. H., Schmidt, P. H., & Ewald, A. H. (2014).

    Can JWH‑210 and JWH‑122 be detected in adipose tissue four weeks after single

    oral drug administration to rats? *Biomedical Chromatography, 28*(8), 1043-1047.

Schep, L., Slaughter, R., Hudson, S., Place, R., & Watts, M. (2014). Delayed seizure-like

    activity following analytically confirmed use of previously unreported synthetic

    cannabinoid analogues. *Human & experimental toxicology*, 0960327114550886.

Schifano, F., Corazza, O., Deluca, P., Davey, Z., Di Furia, L., Farre, M., Flesland, L.,

    Mannonen, M., Pagani, S., Peltoniemi, T., Pezzolesi, C., Scherbaum, N., Siemann, H.,

    Skutle, A., Torrens, M., & Van Der Kreeft, P. (2009). Psychoactive drug or mystical

    incense? Overview of the online available information on Spice products.

    International Journal of Culture and Mental Health, 2(2), 137-144. doi:

    10.1080/17542860903350888

Schmid, P. C., Wold, L. E., Krebsbach, R. J., Berdyshev, E. V., & Schmid, H. H. (2002).

    Anandamide and other N-acylethanolamines in human tumors. *Lipids, 37*(9), 907-912.

Schneir, A. B., Cullen, J., & Ly, B. T. (2011). "Spice" girls: synthetic cannabinoid

    intoxication. *J Emerg Med, 40*(3), 296-299. doi: 10.1016/j.jemermed.2010.10.014

Seely, K. A., Prather, P. L., James, L. P., & Moran, J. H. (2011). Marijuana-based Drugs:

    Innovative Therapeutics or Designer Drugs of Abuse? *Molecular Interventions, 11*(1),

    36-51. doi: 10.1124/mi.11.1.6

Shah, U. (2009). GPR119 agonists: a promising new approach for the treatment of type 2 diabetes and related metabolic disorders. *Curr Opin Drug Discov Devel, 12*(4), 519-532.

Sharir, H., & Abood, M. E. (2010). Pharmacological Characterization of GPR55, A Putative Cannabinoid Receptor. *Pharmacology & therapeutics, 126*(3), 301-313. doi: 10.1016/j.pharmthera.2010.02.004

Sheikh, I. A., Lukšič, M., Ferstenberg, R., & Culpepper-Morgan, J. A. (2014). SPICE/K2 Synthetic Marijuana-Induced Toxic Hepatitis Treated with N-Acetylcysteine. *The American Journal of Case Reports, 15*, 584-588. doi: 10.12659/AJCR.891399

Shevyrin, V., Melkozerov, V., Nevero, A., Eltsov, O., & Shafran, Y. (2013). Analytical characterization of some synthetic cannabinoids, derivatives of indole-3-carboxylic acid. *Forensic Science International, 232*(1–3), 1-10. doi: http://dx.doi.org/10.1016/j.forsciint.2013.06.011

Showalter, V. M., Compton, D. R., Martin, B. R., & Abood, M. E. (1996). Evaluation of binding in a transfected cell line expressing a peripheral cannabinoid receptor (CB2): identification of cannabinoid receptor subtype selective ligands. *Journal of Pharmacology and Experimental Therapeutics, 278*(3), 989-999.

Sibaev, A., Yüce, B., Kemmer, M., Van Nassauw, L., Broedl, U., Allescher, H. D., Göke, B., Timmermans, J.-P., & Storr, M. (2009). Cannabinoid-1 (CB1) receptors regulate colonic propulsion by acting at motor neurons within the ascending motor pathways in mouse colon. *American Journal of Physiology-Gastrointestinal and Liver Physiology, 296*(1), G119-G128.

Sim, L. J., Hampson, R. E., Deadwyler, S. A., & Childers, S. R. (1996). Effects of chronic treatment with delta9-tetrahydrocannabinol on cannabinoid-stimulated [35S]GTPgammaS autoradiography in rat brain. *J Neurosci, 16*(24), 8057-8066.

Sipe, J. C., Arbour, N., Gerber, A., & Beutler, E. (2005). Reduced endocannabinoid immune modulation by a common cannabinoid 2 (CB2) receptor gene polymorphism: possible risk for autoimmune disorders. *Journal of Leukocyte Biology, 78*(1), 231-238. doi: 10.1189/jlb.0205111

Smart, D., Gunthorpe, M. J., Jerman, J. C., Nasir, S., Gray, J., Muir, A. I., Chambers, J. K., Randall, A. D., & Davis, J. B. (2000). The endogenous lipid anandamide is a full agonist at the human vanilloid receptor (hVR1). *British Journal of Pharmacology, 129*(2), 227-230. doi: 10.1038/sj.bjp.0703050

Smith, P. B., Compton, D. R., Welch, S. P., Razdan, R. K., Mechoulam, R., & Martin, B. R. (1994). The pharmacological activity of anandamide, a putative endogenous cannabinoid, in mice. *J Pharmacol Exp Ther, 270*(1), 219-227.

Sobolevsky, T., Prasolov, I., & Rodchenkov, G. (2012). Detection of urinary metabolites of AM‐2201 and UR‐144, two novel synthetic cannabinoids. *Drug testing and analysis, 4*(10), 745-753.

Song, Z. H., & Bonner, T. I. (1996). A lysine residue of the cannabinoid receptor is critical for receptor recognition by several agonists but not WIN55212-2. *Mol Pharmacol, 49*(5), 891-896.

Song, Z. H., Slowey, C. A., Hurst, D. P., & Reggio, P. H. (1999). The difference between the CB(1) and CB(2) cannabinoid receptors at position 5.46 is crucial for the selectivity of WIN55212-2 for CB(2). *Mol Pharmacol, 56*(4), 834-840.

Ständer, S., Schmelz, M., Metze, D., Luger, T., & Rukwied, R. (2005). Distribution of cannabinoid receptor 1 (CB1) and 2 (CB2) on sensory nerve fibers and adnexal structures in human skin. *Journal of dermatological science, 38*(3), 177-188.

Staton, P. C., Hatcher, J. P., Walker, D. J., Morrison, A. D., Shapland, E. M., Hughes, J. P., Chong, E., Mander, P. K., Green, P. J., Billinton, A., Fulleylove, M., Lancaster, H. C.,

Smith, J. C., Bailey, L. T., Wise, A., Brown, A. J., Richardson, J. C., & Chessell, I. P. (2008). The putative cannabinoid receptor GPR55 plays a role in mechanical hyperalgesia associated with inflammatory and neuropathic pain. *Pain, 139*(1), 225-236. doi: 10.1016/j.pain.2008.04.006

Stern, E., Muccioli, G. G., Millet, R., Goossens, J.-F., Farce, A., Chavatte, P., Poupaert, J. H., Lambert, D. M., Depreux, P., & Hénichart, J.-P. (2006). Novel 4-Oxo-1,4-dihydroquinoline-3-carboxamide Derivatives as New CB2 Cannabinoid Receptors Agonists: Synthesis, Pharmacological Properties and Molecular Modeling. *Journal of Medicinal Chemistry, 49*(1), 70-79. doi: 10.1021/jm050467q

Straiker, A., Wager‐Miller, J., Hutchens, J., & Mackie, K. (2012). Differential signalling in human cannabinoid CB1 receptors and their splice variants in autaptic hippocampal neurones. *British Journal of Pharmacology, 165*(8), 2660-2671.

Strange, P. G. (2010). Use of the GTP γ S ([(35)S]GTP γ S and Eu-GTP γ S) binding assay for analysis of ligand potency and efficacy at G protein-coupled receptors. *British Journal of Pharmacology, 161*(6), 1238-1249. doi: 10.1111/j.1476-5381.2010.00963.x

Stuart, J. M., Paris, J. J., Frye, C., & Bradshaw, H. B. (2013). Brain Levels of Prostaglandins, Endocannabinoids, and Related Lipids Are Affected by Mating Strategies. *International Journal of Endocrinology, 2013*, 14. doi: 10.1155/2013/436252

Stucka, M. (2012). List of banned synthetic marijuana brands. from http://www.macon.com/2012/03/28/1966202_list-of-banned-synthetic-marijuana.html?rh=1

Su, M., Seely, K. A., Moran, J. H., & Hoffman, R. (2015). Metabolism of classical cannabinoids and the synthetic cannabinoid JWH‐018. *Clinical Pharmacology & Therapeutics*.

Sudbury, J. R., & Bourque, C. W. (2013). Dynamic and permissive roles of TRPV1 and
TRPV4 channels for thermosensation in mouse supraoptic magnocellular
neurosecretory neurons. *J Neurosci, 33*(43), 17160-17165. doi:
10.1523/jneurosci.1048-13.2013

Sundström, M., Pelander, A., Angerer, V., Hutter, M., Kneisel, S., & Ojanperä, I. (2013). A
high-sensitivity ultra-high performance liquid chromatography/high-resolution time-
of-flight mass spectrometry (UHPLC-HR-TOFMS) method for screening synthetic
cannabinoids and other drugs of abuse in urine. *Analytical and bioanalytical
chemistry, 405*(26), 8463-8474.

Svizenska, I., Dubovy, P., & Sulcova, A. (2008). Cannabinoid receptors 1 and 2 (CB1 and
CB2), their distribution, ligands and functional involvement in nervous system
structures â€" A short review. *Pharmacology Biochemistry and Behavior, 90*(4), 501-
511. doi: http://dx.doi.org/10.1016/j.pbb.2008.05.010

Synthetic marijuana-related hospitalizations skyrocket in US. (2015). *The Guardian.* from
http://www.theguardian.com/society/2015/may/08/synthetic-marijuana-legal-highs-
hospitalization-spice-k2

Szabo, B., & Schlicker, E. (2005). Effects of cannabinoids on neurotransmission. *Handb Exp
Pharmacol*(168), 327-365.

Takayama, T., Suzuki, M., Todoroki, K., Inoue, K., Min, J. Z., Kikura-Hanajiri, R., Goda, Y.,
& Toyo'oka, T. (2014). UPLC/ESI-MS/MS-based determination of metabolism of
several new illicit drugs, ADB-FUBINACA, AB-FUBINACA, AB-PINACA, QUPIC,
5F-QUPIC and alpha-PVT, by human liver microsome. *Biomed Chromatogr, 28*(6),
831-838. doi: 10.1002/bmc.3155

Takematsu, M., Hoffman, R. S., Nelson, L. S., Schechter, J. M., Moran, J. H., & Wiener, S.
W. (2014). A case of acute cerebral ischemia following inhalation of a synthetic

cannabinoid. *Clin Toxicol (Phila), 52*(9), 973-975. doi:
10.3109/15563650.2014.958614

Thomas, A., Baillie, G. L., Phillips, A. M., Razdan, R. K., Ross, R. A., & Pertwee, R. G.
(2007). Cannabidiol displays unexpectedly high potency as an antagonist of CB1 and
CB2 receptor agonists in vitro. *Br J Pharmacol, 150*(5), 613-623. doi:
10.1038/sj.bjp.0707133

Thomsen, W., Frazer, J., & Unett, D. (2005). Functional assays for screening GPCR targets.
Current opinion in biotechnology, 16(6), 655-665.

Thornton, S. L., Wood, C., Friesen, M. W., & Gerona, R. R. (2013). Synthetic cannabinoid
use associated with acute kidney injury*. *Clinical Toxicology, 51*(3), 189-190.

Tomiyama, K.-i., & Funada, M. (2014). Cytotoxicity of synthetic cannabinoids on primary
neuronal cells of the forebrain: the involvement of cannabinoid CB1 receptors and
apoptotic cell death. *Toxicology and applied pharmacology, 274*(1), 17-23. doi:
http://dx.doi.org/10.1016/j.taap.2013.10.028

Turu, G., & Hunyady, L. (2010). Signal transduction of the CB1 cannabinoid receptor.
Journal of Molecular Endocrinology, 44(2), 75-85. doi: 10.1677/jme-08-0190

Uchiyama, N., Kawamura, M., Kikura-Hanajiri, R., & Goda, Y. (2012). Identification of two
new-type synthetic cannabinoids, N-(1-adamantyl)-1-pentyl-1H-indole-3-carboxamide
(APICA) and N-(1-adamantyl)-1-pentyl-1H-indazole-3-carboxamide (APINACA),
and detection of five synthetic cannabinoids, AM-1220, AM-2233, AM-1241, CB-13
(CRA-13), and AM-1248, as designer drugs in illegal products. *Forensic Toxicology,
30*(2), 114-125.

Uchiyama, N., Matsuda, S., Kawamura, M., Kikura-Hanajiri, R., & Goda, Y. (2013). Two
new-type cannabimimetic quinolinyl carboxylates, QUPIC and QUCHIC, two new
cannabimimetic carboxamide derivatives, ADB-FUBINACA and ADBICA, and five

synthetic cannabinoids detected with a thiophene derivative α -PVT and an opioid

receptor agonist AH-7921 identified in illegal products. *Forensic Toxicology, 31*(2),

223-240.

Uchiyama, N., Matsuda, S., Kawamura, M., Kikura-Hanajiri, R., & Goda, Y. (2014).

Identification of two new-type designer drugs, piperazine derivative MT-45 (I-C6) and

synthetic peptide Noopept (GVS-111), with synthetic cannabinoid A-834735,

cathinone derivative 4-methoxy- α -PVP, and phenethylamine derivative 4-

methylbuphedrine from illegal products. *Forensic Toxicology, 32*(1), 9-18. doi:

10.1007/s11419-013-0194-5

Uchiyama, N., Shimokawa, Y., Kawamura, M., Kikura-Hanajiri, R., & Hakamatsuka, T.

(2014). Chemical analysis of a benzofuran derivative, 2-(2-ethylaminopropyl)

benzofuran (2-EAPB), eight synthetic cannabinoids, five cathinone derivatives, and

five other designer drugs newly detected in illegal products. *Forensic Toxicology,

32*(2), 266-281.

Van der Stelt, M., Fox, S. H., Hill, M., Crossman, A. R., Petrosino, S., Di Marzo, V., &

Brotchie, J. M. (2005). A role for endocannabinoids in the generation of parkinsonism

and levodopa-induced dyskinesia in MPTP-lesioned non-human primate models of

Parkinson's disease. *The FASEB journal, 19*(9), 1140-1142.

Vandrey, R., Dunn, K. E., Fry, J. A., & Girling, E. R. (2012). A survey study to characterize

use of Spice products (synthetic cannabinoids). *Drug and Alcohol Dependence,

120*(1–3), 238-241. doi: http://dx.doi.org/10.1016/j.drugalcdep.2011.07.011

Walsh, K. B. (2011). Targeting GIRK Channels for the Development of New Therapeutic

Agents. *Frontiers in Pharmacology, 2*, 64. doi: 10.3389/fphar.2011.00064

Welfare, A. I. o. H. a. (2013). Illicit use of drugs (NDSHS 2013 key findings). from

http://www.aihw.gov.au/alcohol-and-other-drugs/ndshs/2013/illicit-drug-use/

Wenger, T., Moldrich, G., & Furst, S. (2003). Neuromorphological background of cannabis addiction. *Brain Res Bull, 61*(2), 125-128.

Whiteside, G. T., Lee, G. P., & Valenzano, K. J. (2007). The Role of the Cannabinoid CB2 Receptor in Pain Transmission and Therapeutic Potential of Small Molecule CB2 Receptor Agonists. *Current Medicinal Chemistry, 14*(8), 917-936. doi: 10.2174/092986707780363023

Whyte, L. S., Ryberg, E., Sims, N. A., Ridge, S. A., Mackie, K., Greasley, P. J., Ross, R. A., & Rogers, M. J. (2009). The putative cannabinoid receptor GPR55 affects osteoclast function in vitro and bone mass in vivo. *Proc Natl Acad Sci U S A, 106*(38), 16511-16516. doi: 10.1073/pnas.0902743106

Wiley, J. L., Compton, D. R., Dai, D., Lainton, J. A. H., Phillips, M., Huffman, J. W., & Martin, B. R. (1998). Structure-Activity Relationships of Indole- and Pyrrole-Derived Cannabinoids. *Journal of Pharmacology and Experimental Therapeutics, 285*(3), 995-1004.

Wiley, J. L., Marusich, J. A., Huffman, J. W., Balster, R. L., & Thomas, B. F. (2011). Hijacking of Basic Research: The Case of Synthetic Cannabinoids. *Methods report (RTI Press), 2011*, 17971. doi: 10.3768/rtipress.2011.op.0007.1111

Wiley, J. L., Marusich, J. A., Lefever, T. W., Grabenauer, M., Moore, K. N., & Thomas, B. F. (2013). Cannabinoids in disguise: Δ 9-Tetrahydrocannabinol-like effects of tetramethylcyclopropyl ketone indoles. *Neuropharmacology, 75*(0), 145-154. doi: http://dx.doi.org/10.1016/j.neuropharm.2013.07.022

Willoughby, K. A., Moore, S. F., Martin, B. R., & Ellis, E. F. (1997). The Biodisposition and Metabolism of Anandamide in Mice. *Journal of Pharmacology and Experimental Therapeutics, 282*(1), 243-247.

Wilson, J. (2013). 3 deaths may be tied to Synthetic Marijuana in Colorado. from

http://edition.cnn.com/2013/09/06/health/synthetic-marijuana-denver/

Wilson, R. S., May, E. L., Martin, B. R., & Dewey, W. L. (1976). 9-Nor-9-

hydroxyhexahydrocannabinols. Synthesis, some behavioral and analgesic properties,

and comparison with the tetrahydrocannabinols. *Journal of Medicinal Chemistry,*

19(9), 1165-1167.

Winstock, A. R., & Barratt, M. J. (2013). Synthetic cannabis: A comparison of patterns of use

and effect profile with natural cannabis in a large global sample. *Drug and Alcohol*

Dependence, 131(1–2), 106-111. doi:

http://dx.doi.org/10.1016/j.drugalcdep.2012.12.011

Wohlfarth, A., Castaneto, M. S., Zhu, M., Pang, S., Scheidweiler, K. B., Kronstrand, R., &

Huestis, M. A. (2015). Pentylindole/Pentylindazole Synthetic Cannabinoids and Their

5-Fluoro Analogs Produce Different Primary Metabolites: Metabolite Profiling for

AB-PINACA and 5F-AB-PINACA. *AAPS J, 17*(3), 660-677. doi: 10.1208/s12248-

015-9721-0

Wohlfarth, A., Gandhi, A., Pang, S., Zhu, M., Scheidweiler, K., & Huestis, M. (2014a).

Metabolism of synthetic cannabinoids PB-22 and its 5-fluoro analog, 5F-PB-22, by

human hepatocyte incubation and high-resolution mass spectrometry. *Analytical and*

bioanalytical chemistry, 406(6), 1763-1780. doi: 10.1007/s00216-014-7668-0

Wohlfarth, A., Gandhi, A. S., Pang, S., Zhu, M., Scheidweiler, K. B., & Huestis, M. A.

(2014b). Metabolism of synthetic cannabinoids PB-22 and its 5-fluoro analog, 5F-PB-

22, by human hepatocyte incubation and high-resolution mass spectrometry.

Analytical and bioanalytical chemistry, 406(6), 1763-1780.

Wohlfarth, A., Pang, S., Zhu, M., Gandhi, A. S., Scheidweiler, K. B., Liu, H.-f., & Huestis,

M. A. (2013). First metabolic profile of XLR-11, a novel synthetic cannabinoid,

obtained by using human hepatocytes and high-resolution mass spectrometry. *Clinical chemistry, 59*(11), 1638-1648.

Wurita, A., Hasegawa, K., Minakata, K., Gonmori, K., Nozawa, H., Yamagishi, I., Watanabe, K., & Suzuki, O. (2015). Identification and quantitation of 5-fluoro-ADB-PINACA and MAB-CHMINACA in dubious herbal products. *Forensic Toxicology*, 1-8. doi: 10.1007/s11419-015-0264-y

Xi, Z.-X., Peng, X.-Q., Li, X., Song, R., Zhang, H.-Y., Liu, Q.-R., Yang, H.-J., Bi, G.-H., Li, J., & Gardner, E. L. (2011). Brain cannabinoid CB2 receptors modulate cocaine's actions in mice. *Nature neuroscience, 14*(9), 1160-1166.

Yeakel, J. K., & Logan, B. K. (2013). Blood synthetic cannabinoid concentrations in cases of suspected impaired driving. *J Anal Toxicol, 37*(8), 547-551. doi: 10.1093/jat/bkt065

Zlas, J., Stark, H., Seligman, J., Levy, R., Werker, E., Breuer, A., & Mechoulam, R. (1993). Early medical use of cannabis. *Nature, 363*(6426), 215-215.

Zuardi, A. W. (2006). History of cannabis as a medicine: a review. *Revista Brasileira de Psiquiatria, 28*, 153-157.

Zuba, D., & Byrska, B. (2013). Analysis of the prevalence and coexistence of synthetic cannabinoids in "herbal high" products in Poland. *Forensic Toxicology, 31*(1), 21-30.

Zygmunt, P. M., Petersson, J., Andersson, D. A., Chuang, H., Sorgard, M., Di Marzo, V., Julius, D., & Hogestatt, E. D. (1999). Vanilloid receptors on sensory nerves mediate the vasodilator action of anandamide. *Nature, 400*(6743), 452-457. doi: 10.1038/22761

. ФСКН: от отравления спайсами в российских регионах погибли более 40 человек. (2014). Moscow, Russia: ТАСС.

APPENDIX A: FLUORESCENT –BASED
PLATE READER ASSAY DATA

Figure Legend Descriptions for Appendix A

All figures will be in the same format letter A-G. Not all drugs will have all graphs as it was reactivity dependent. Following are the general descriptions for each figure which will be further specified for each drug on the following pages.

A.) **Traces of highest concentration with PTX pretreatment**. These figures illustrate the highest concentration tested for the particular drug (solubility dependent) on AtT20-hCB1 and AtT20-hCB2. It also shows the trace of the maximum concentration tested that was blocked by an overnight pretreatment of PTX (200 ng/well). This was to prove the response seen was working through the $G_{i/o}$ pathway. Blue represents the AtT20-hCB1 responses and red represents the AtT20-hCB2 responses.

B.) **Concentrations response curves for Cannabinoid Receptors.** These figures illustrate the concentration response curves for the specific drug ranging from 1pM-30μM depending on solubility and reactivity. They were completed on AtT20-hCB1 and AtT20-hCB2 for all compounds and AtT20-rCB1 has been added where relevant. Blue represents the AtT20-hCB1 responses, red represents the AtT20-hCB2 responses, and black represents the AtT20-rCB1 responses.

C.) **Traces for activity at AtT20-WT challenged with 100 nM SRIF.** These figures illustrate traces of the response of 10 μM concentrations of each drug. After 10 minutes, 100 nM of SRIF was added to show viability of the cells. A DMSO blank (grey line) that was applied after 10 minutes with 100 nM SRIF is also represented to determine if inhibition of the SRIF response was taking place. Some drugs were run concurrently and therefore will use the same DMSO blank trace.

D.) **Traces for agonist activity at HEK293-hTRPA1**. These figures illustrate the maximum increase in calcium change at 30 μM concentrations of each drug on HEK293-hTRPA1 compared to that of a cinnemaldehyde control (300 μM).

E.) **Concentration response curves for agonists/partial agonists at hTRPA1.** These figures illustrate the concentration response curves for all compounds that showed a maximum response at 30 μM that was at least 30% that of CIN max on HEK293-hTRPA1.

F.) **Traces for agonist/antagonist activity at HEK293-hTPRV1.** These figures illustrate the addition of 30 μM SCs to test for agonist activity followed by an addition of 300 nM CAP. A DMSO blank was challenged after 10 minutes with 300 nM CAP as a positive control and to determine if the SCs were causing inhibition of the CAP response signifying antagonist activity. Some compounds were run concurrently and therefore will have the same DMSO blank trace.

G.) **Concentration response curves for agonists/partial agonists at HEK293-hTRPV1**. These figures illustrate the concentration response curves for all compounds that showed a maximum response at 30 μM that was at least 30% that of CAP max on HEK293-hTRPV1

WIN 55,212-2

(R)-(+)-[2,3-Dihydro-5-methyl-3-(4-morpholinylmethyl)pyrrolo[1,2,3-de]-1,4-benzoxazin-6-yl]-1-napthalenylmethanone
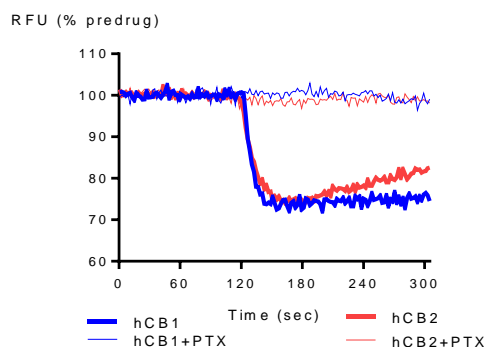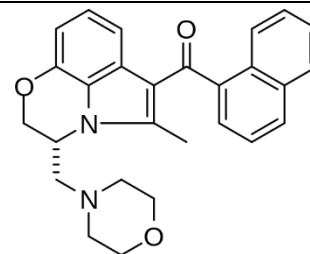
A: Response of AtT20-hCB1 and AtT20-hCB2 to WIN 55,212-2 (10μM).
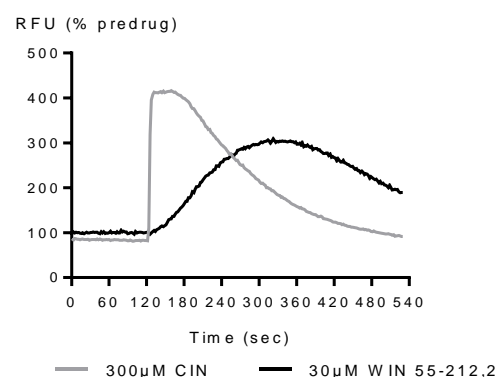
D: Response of HEK293-TRPA1 to WIN 55,212-2 (30μM) and cinnamaldehyde (300μM).
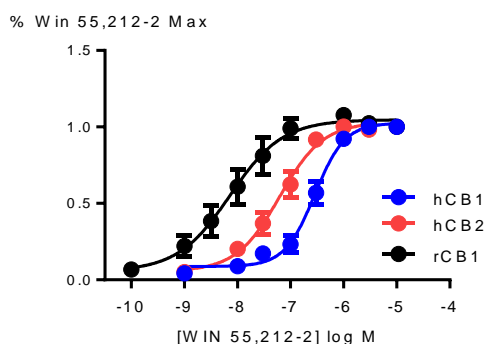
B: Concentration response curves for WIN 55,212-2 in AtT20-hCB1 and AtT20-hCB2
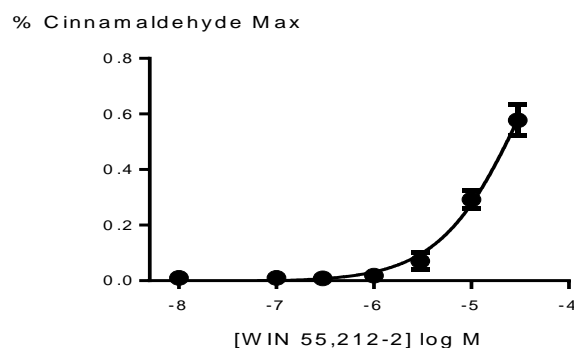
E: Concentration response curve for WIN 55,212-2 in HEK293-TRPA1
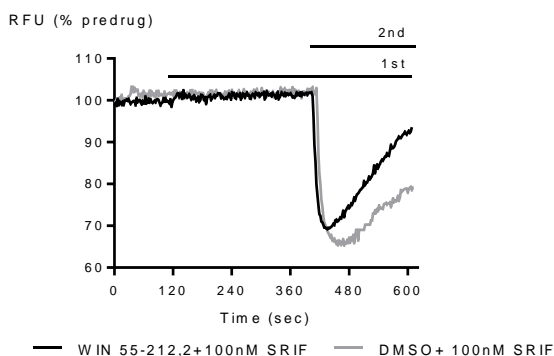
C: Response of AtT20-WT to WIN 55,212-2 (10μM) followed by SRIF (100nM)
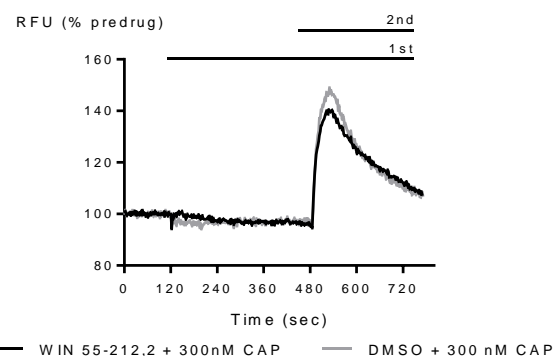
F: Response of HEK293-TRPV1 to WIN 55,212-2 (10μM) followed by capsaicin (300nM)

	pEC50	MAX %	Notes
AtT20-rCB1	8.2 ± 0.1	105 ± 5	
AtT20-hCB1	6.55 ± 0.06	108 ± 10	--
AtT20-hCB2	7.21 ± 0.09	105 ± 10	--
HEK293-TRPA1	4.89 ± 0.15*	58 ± 5	--
HEK293-TRPV1	--	<1	Inhibits max CAP response by <10%
AtT20 WT	--	<1	No change in SRIF max response

*pEC50 assuming that the maximum is equivalent to the maximum of cinnamaldehyde

CP 55,940

2-[(1R,2R,5R)-5-hydroxy-2-(3-hydroxypropyl)
cyclohexyl]-5-(2-methyloctan-2-yl)phenol
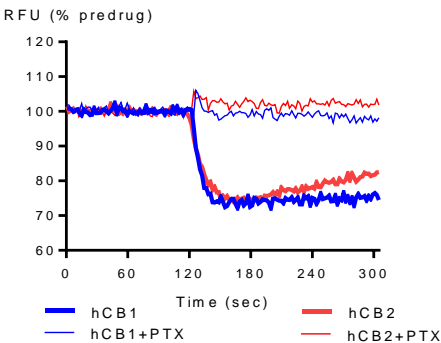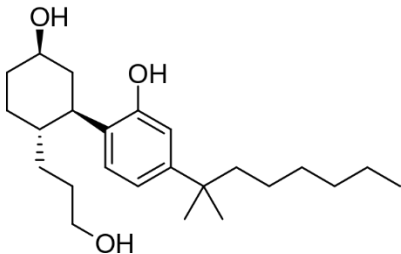
A: Response of AtT20-hCB1 and AtT20-hCB2 to CP
55,940 (10μM).
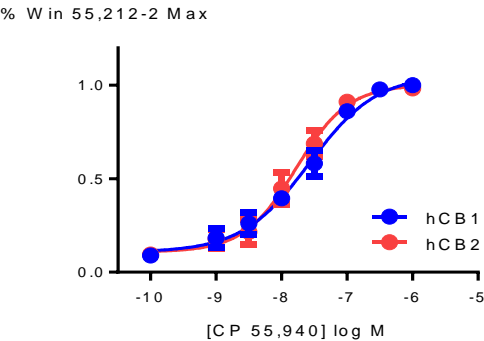
B: Concentration response curves for CP 55,940 in
AtT20-hCB1 and AtT20-hCB2

D: Response of HEK293-TRPA1 to CP 55,940 (30μM) and
cinnamaldehyde (300μM).
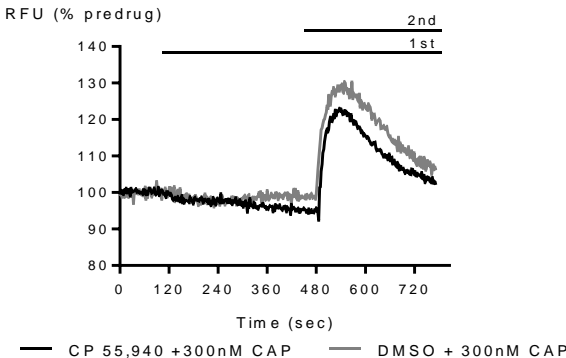
F: Response of HEK293-TRPV1 to CP 55,940 (10μM) followed
by capsaicin (300nM)

C: Response of AtT20-WT to CP 55,940 (10μM)
followed by SRIF (100nM)

	pEC50	MAX %	Notes
AtT20-hCB1	7.6 ± 0.1	106 ± 10	--
AtT20-hCB2	7.8 ± 0.1	100 ± 10	--
HEK293-TRPA1	--	25 ± 3	Max <30% no CRC completed
HEK293-TRPV1	--	≤5	Inhibits average max CAP response by <5%
AtT20 WT	--	<10	Inhibits average max SRIF response by <10%

Anandamide (AEA)

- N-arachidonoyl ethanolamine
- Arachidonoyl ethanolamide

(5Z,8Z,11Z,14Z)-N-(2-hydroxyethyl)icosa-5,8,11,14-tetraenamide
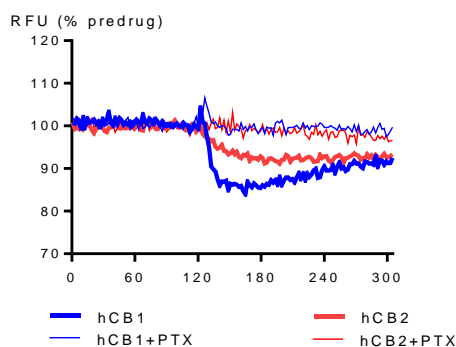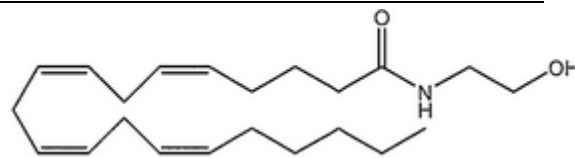
A: Response of AtT20-hCB1 and AtT20-hCB2 to AEA (10μM).
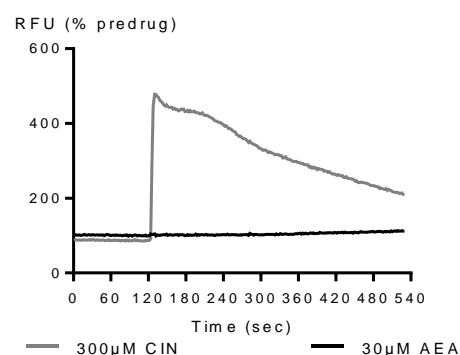
D: Response of HEK293-TRPA1 to AEA (30μM) and cinnamaldehyde (300μM).
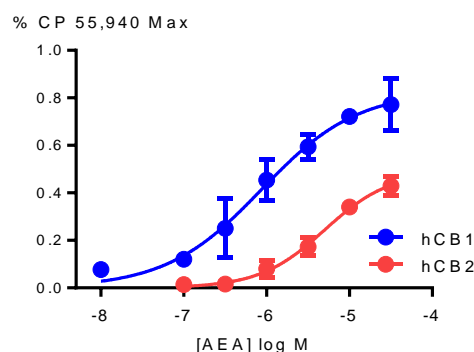
B: Concentration response curves for AEA in AtT20-hCB1 and AtT20-hCB2
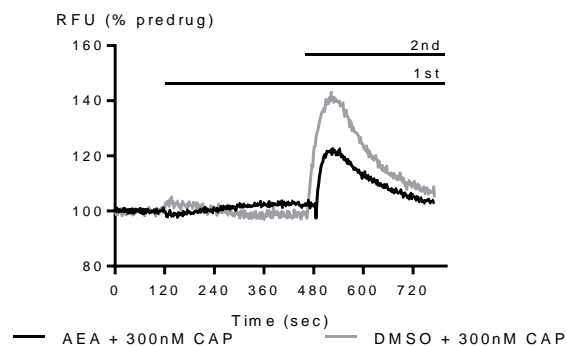
F: Response of HEK293-TRPV1 to AEA (30μM) followed by capsaicin (300nM)
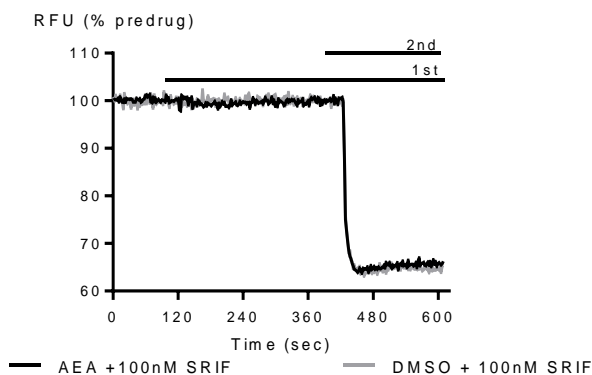
C: Response of AtT20-WT to AEA (10μM) followed by SRIF (100nM)
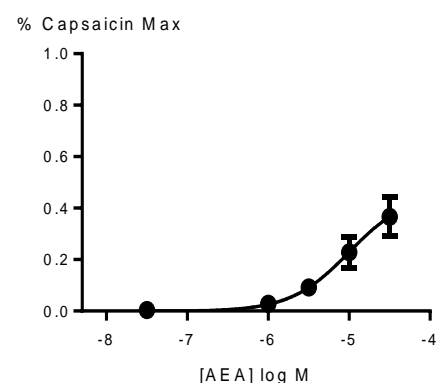
G: Concentration response curve for AEA in HEK293-TRPV1

	pEC50	MAX %	Notes
AtT20-hCB1	6.1 ± 0.2	98 ± 10	--
AtT20-hCB2	5.3 ± 0.2	49 ± 10	--
HEK293-TRPA1	--	<2	Max <30% no CRC completed
HEK293-TRPV1	5.0 ± 0.3	46 ± 2	Inhibits average max CAP response by 42 ± 5
AtT20 WT	--	13 ± 10	No change in SRIF max response

2-Arachidonoyl Glycerol (2-AG)
1,3-Dihydroxy-2-propanyl (5Z,8Z,11Z,14Z)-
5,8,11,14-eicosatetraenoate
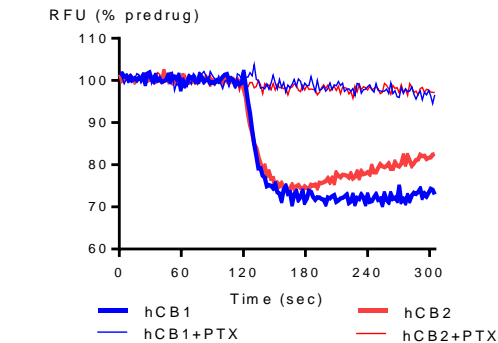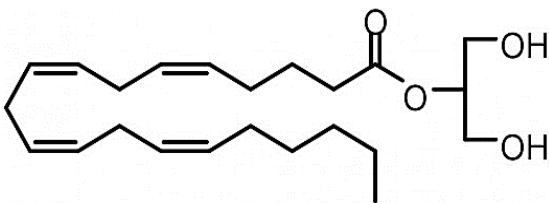

A: Response of AtT20-hCB1 and AtT20-hCB2 to 2-AG (10μM).

B: Concentration response curves for 2-AG in AtT20-hCB1 and AtT20-hCB2

C: Response of AtT20-WT to 2-AG (10μM) followed by SRIF (100nM)
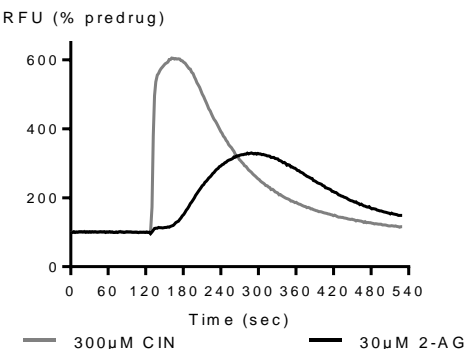
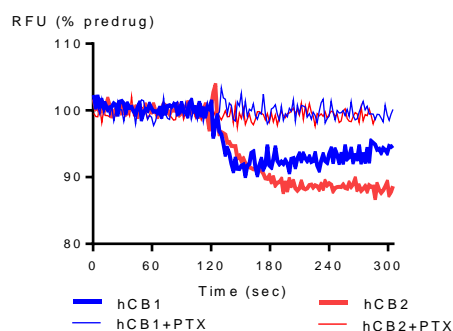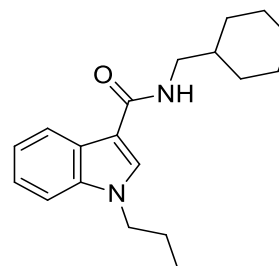D: Response of HEK293-TRPA1 to 2-AG (30μM) and cinnamaldehyde (300μM).
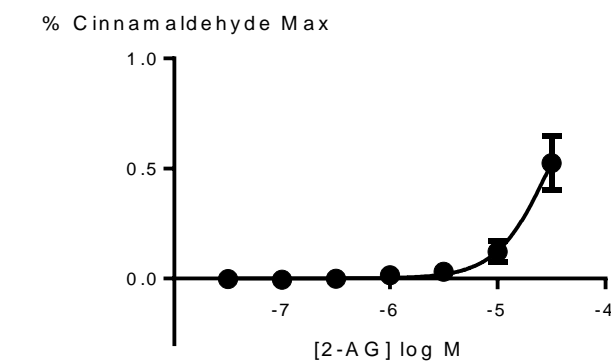
E: E: Concentration response curve for 2-AG in HEK293-TRPA1
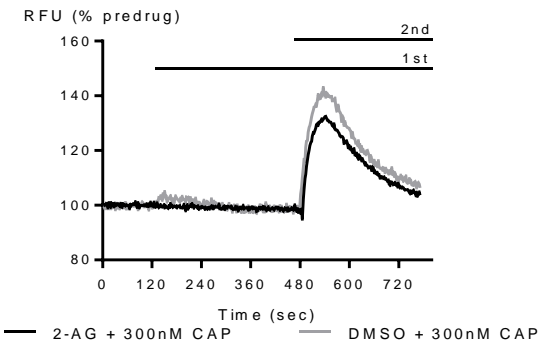
F: Response of HEK293-TRPV1 to 2-AG (30μM) followed by capsaicin (300nM)

	pEC50	MAX %	Notes
AtT20-hCB1	6.6 ± 0.1	83 ± 10	--
AtT20-hCB2	6.5 ± 0.1	100 ± 10	--
HEK293-TRPA1	4.52 ± 0.05*	53 ± 10	--
HEK293-TRPV1	--	<10	Inhibits average max CAP response by <10%
AtT20 WT	--	<5	Inhibits average max SRIF response by <10%

*pEC50 assuming that the maximum is equivalent to the maximum of cinnamaldehyde

Cannabidiol (CBD)

2-[(1R,6R)-6-isopropenyl-3-methylcyclohex-
2-en-1-yl]-5-pentylbenzene-1,3-diol

D: Response of HEK293-TRPA1 to CBD (30μM) and cinnamaldehyde (300μM).
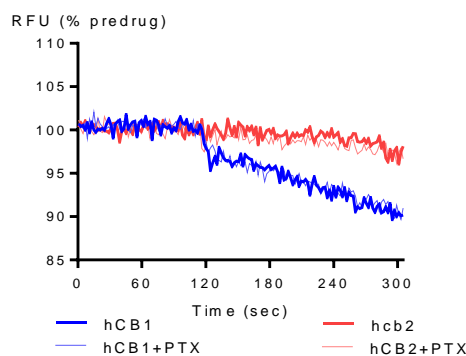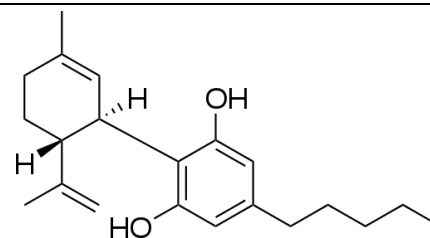
A: Response of AtT20-hCB1 and AtT20-hCB2 to CBD (30μM).

E: Response of HEK293-TRPV1 to CBD (30μM) followed by capsaicin (300nM)
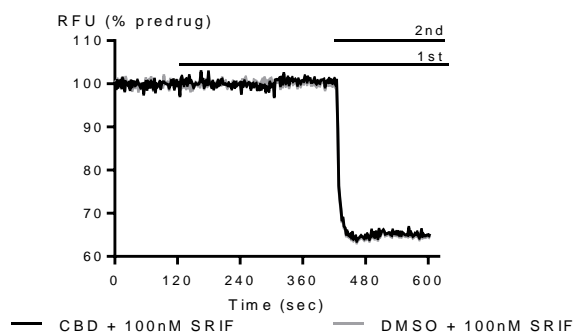
C: Response of AtT20-WT to 2-AG (30μM) followed by SRIF (100nM)
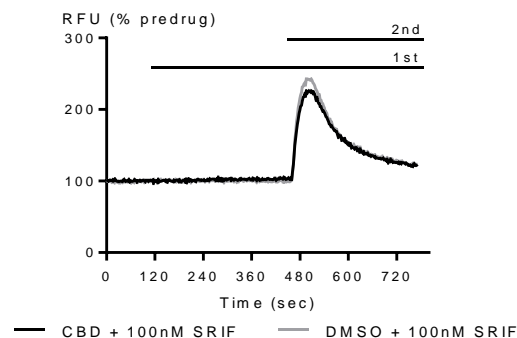
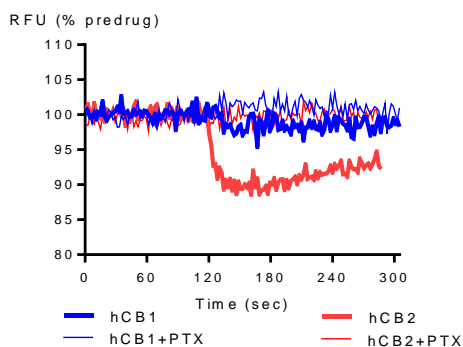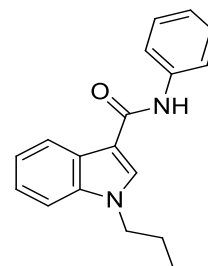F: Response of HEK293-TRPV1 to CBD (30μM) followed by capsaicin (300nM)

	pEC50	MAX %	Notes
AtT20-hCB1	--	18 ±6	--
AtT20-hCB2	--	N.D.	--
HEK293-TRPA1	4.99 ± 0.03	77 ± 5	--
HEK293-TRPV1	--	<10	Inhibits average max CAP response by <10%
AtT20 WT	--	<10	Inhibits average max SRIF response by <10%

N.D. = Not detected

Δ^9-tetrahydrocannabinol (Δ^9-THC)

(−)-(6aR,10aR)-6,6,9-Trimethyl-3-pentyl-6a,7,8,10a-tetrahydro-6H-benzo[c]chromen-1-ol
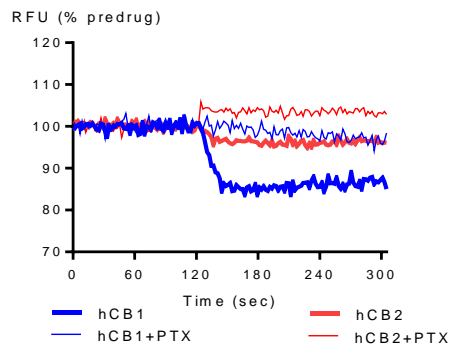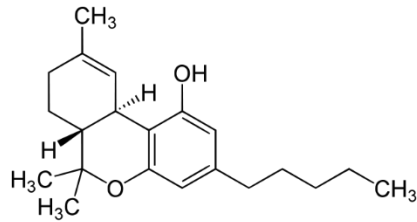
A: Response of AtT20-hCB1 and AtT20-hCB2 to Δ^9-THC (10μM).
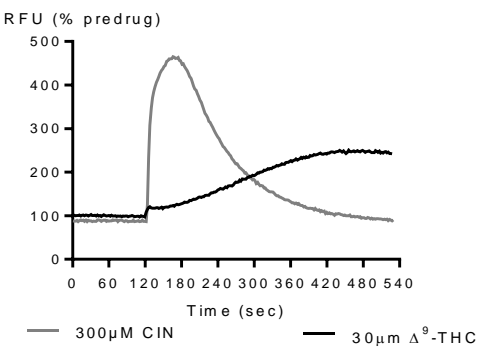
D: Response of HEK293-TRPA1 to Δ^9-THC (30μM) and cinnamaldehyde (300μM).
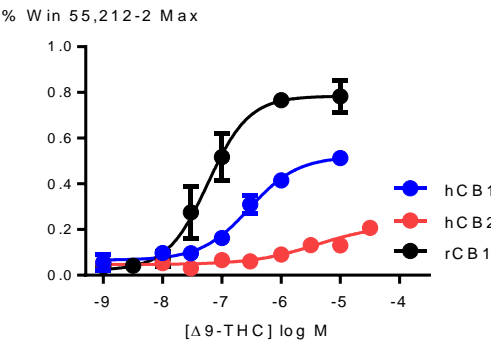
B: Concentration response curves for Δ^9-THC in AtT20-hCB1 and AtT20-hCB2
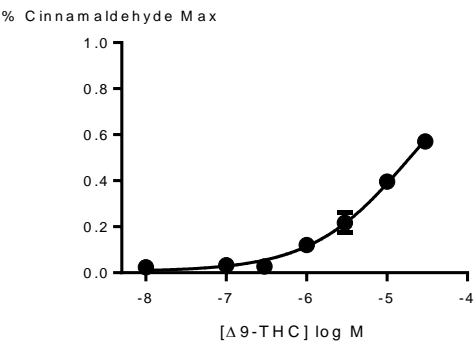
E: Concentration response curve for Δ^9-THC in HEK293-TRPA1
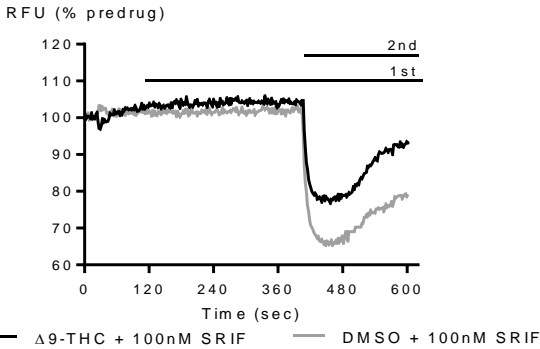
C: Response of AtT20-WT to Δ^9-THC (10μM) followed by SRIF (100nM)
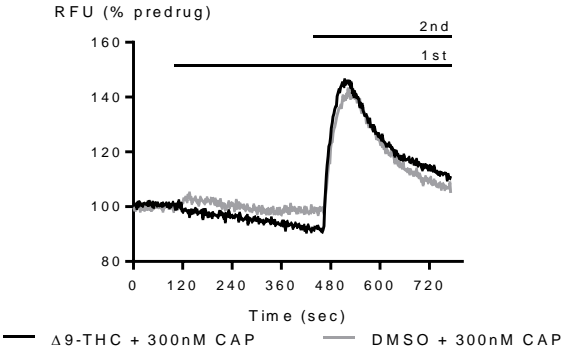
F: Response of HEK293-TRPV1 to Δ^9-THC (30μM) followed by capsaicin (300nM)

	pEC50	MAX %	Notes
AtT20-rCB1	7.24 ± 0.1	78 ± 5	--
AtT20-hCB1	6.5 ± 0.1	52 ± 3	--
AtT20-hCB2	5.4 ± 0.7	22 ± 10	--
HEK293-TRPA1	4.71 ± 0.05*	57 ± 3	--
HEK293-TRPV1	--	<1	Inhibits average max CAP response by <5%
AtT20 WT	--	<5	Inhibits average max SRIF response by 23%

*pEC50 assuming that the maximum is equivalent to the maximum of cinnamaldehyde

JWH-018

1-[(5-Fluoropentyl)-1H-indol-3-yl]-(naphthalen-1-yl)methanone
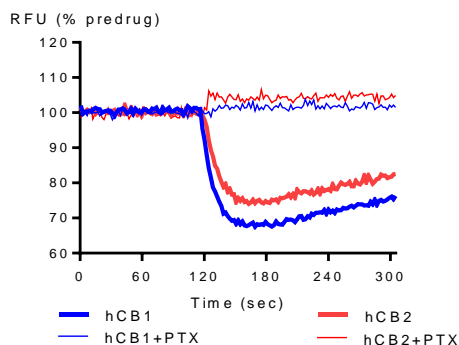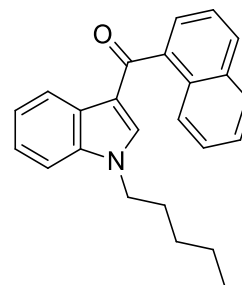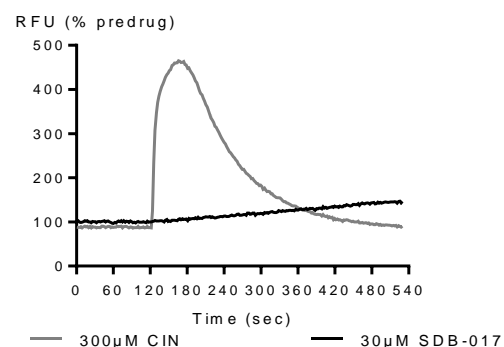

A: Response of AtT20-hCB1 and AtT20-hCB2 to JWH-018 (10μM).
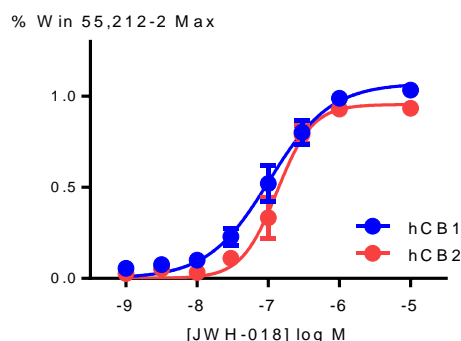
B: Concentration response curves for JWH-018 in AtT20-hCB1 and AtT20-hCB2

D: Response of HEK293-TRPA1 to JWH-018 (30μM) and cinnamaldehyde (300μM).
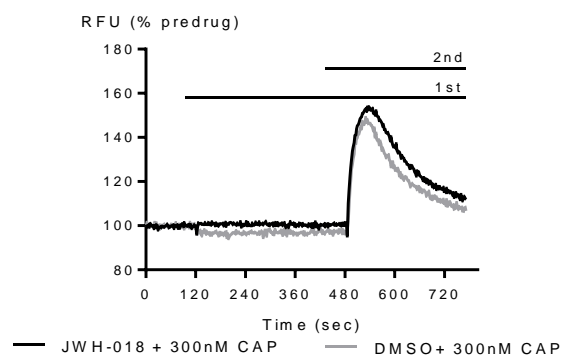
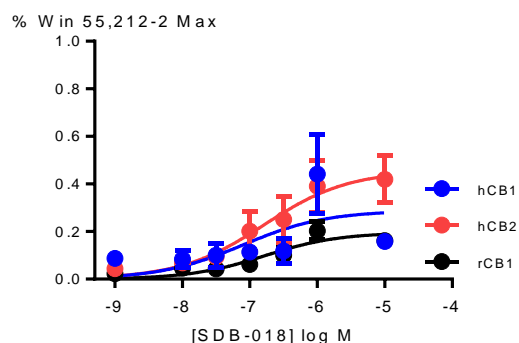F: Response of HEK293-TRPV1 to JWH-018 (10μM) followed by capsaicin (300nM)

C: Response of AtT20-WT to JWH-018 (10μM) followed by SRIF (100nM)

	pEC50	MAX %	Notes
AtT20-hCB1	6.99 ± 0.09	107 ± 6	--
AtT20-hCB2	6.88 ± 0.06	96 ± 4	--
HEK293-TRPA1	--	<10	Max <30% no CRC completed
HEK293-TRPV1	--	<10	Inhibits average max CAP response by <5%
AtT20 WT	--	<1	Inhibits average max SRIF response by <10%

AM-2201

1-[(5-Fluoropentyl)-1H-indol-3-yl]-(naphthalen-1-yl)methanone
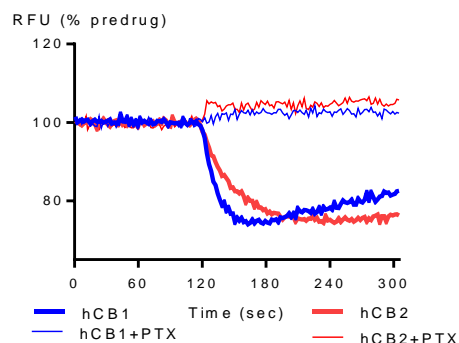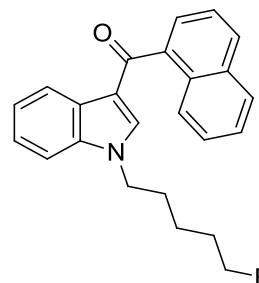
A: Response of AtT20-hCB1 and AtT20-hCB2 to AM-2201 (10μM).
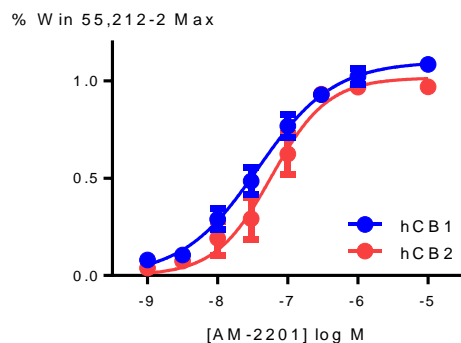
B: Concentration response curves for AM-2201 in AtT20-hCB1 and AtT20-hCB2

D: Response of HEK293-TRPA1 to AM-2201 (30μM) and cinnamaldehyde (300μM).
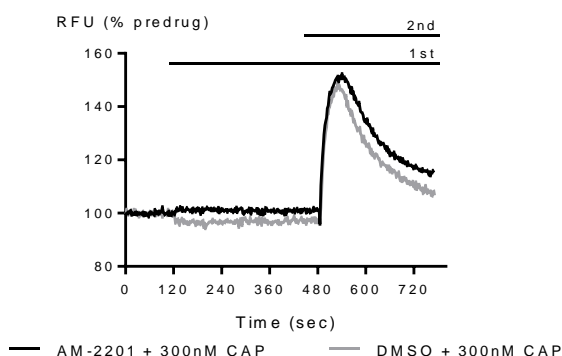
F: Response of HEK293-TRPV1 to AM-2201 (10μM) followed by capsaicin (300nM)

C: Response of AtT20-WT to AM-2201 (10μM) followed by SRIF (100nM)

	pEC50	MAX %	Notes
AtT20-hCB1	7.43 ± 0.09	110 ± 5	--
AtT20-hCB2	7.2 ± 0.1	102 ± 6	--
HEK293-TRPA1	--	<10	Max <30% no CRC completed
HEK293-TRPV1	--	<10	Inhibits average max CAP response by <10%
AtT20 WT	--	<1	Inhibits average max SRIF response by <10%

AB-001

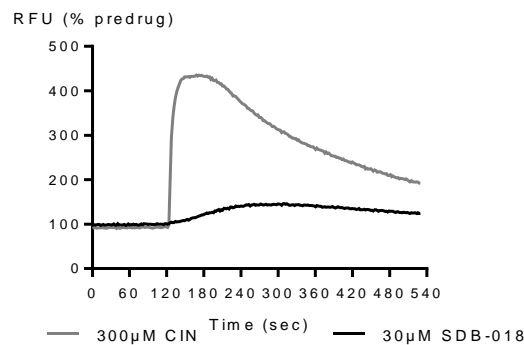Adamantan-1-yl(1-pentyl-1H-indol-3-yl)methanone
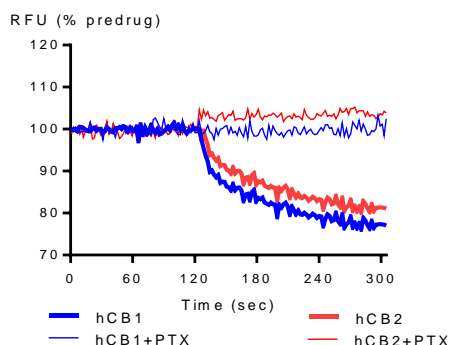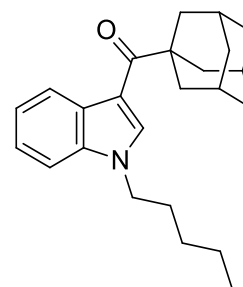
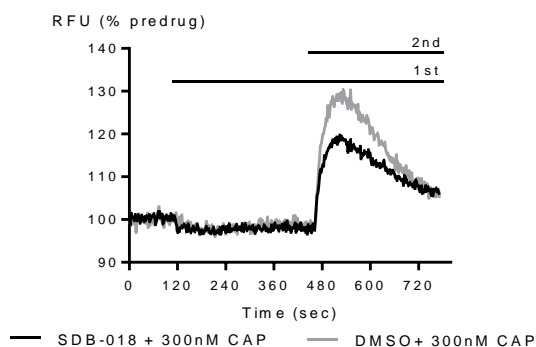A: Response of AtT20-hCB1 and AtT20-hCB2 to
AB-001 (10μM).
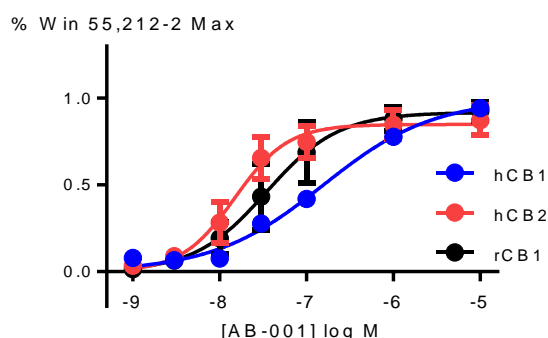
B: Concentration response curves for AB-001 in AtT20-
rCB1, AtT20-hCB1 and AtT20-hCB2
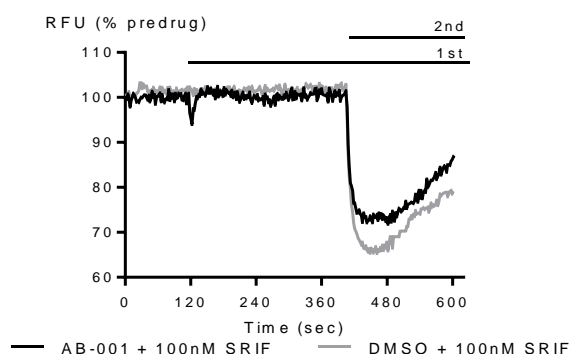
C: Response of AtT20-WT to AB-001 (10μM) followed
by SRIF (100nM)
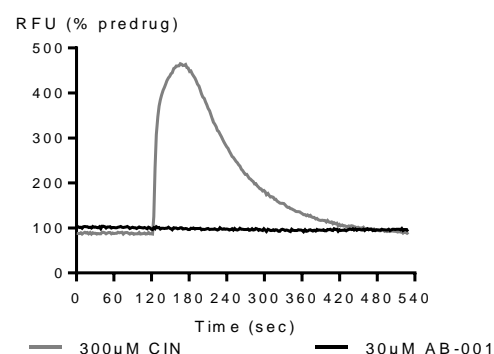
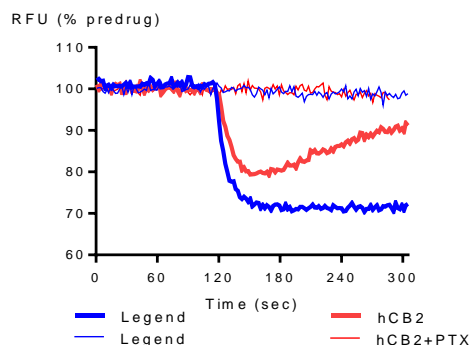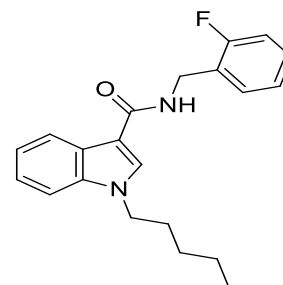D: Response of HEK293-TRPA1 to AB-001 (30μM) and
cinnamaldehyde (300μM).
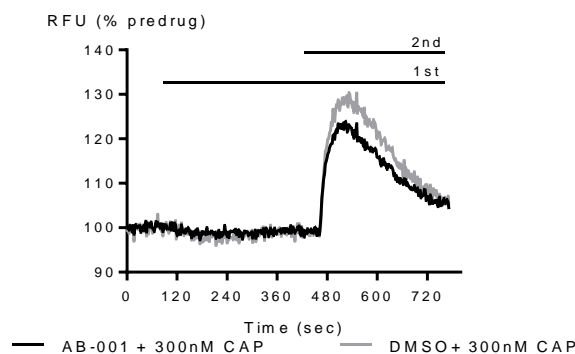
F: Response of HEK293-TRPV1 to AB-001 (10μM) followed by
capsaicin (300nM)

	pEC50	MAX %	Notes
AtT20-rCB1	7.5 ± 0.1	92 ± 5	--
AtT20-hCB1	6.8 ± 0.1	100 ± 8	--
AtT20-hCB2	7.83 ± 0.16	85 ± 5	--
HEK293-TRPA1	--	<5	Max <30% no CRC completed
HEK293-TRPV1	--	<10	Inhibits average max CAP response by <10%
AtT20 WT	--	<1	Inhibits average max SRIF response by 15%

AB-002

2-(Adamantan-1-yl)-1-(1-pentyl-1H-indol-3-yl)ethanone
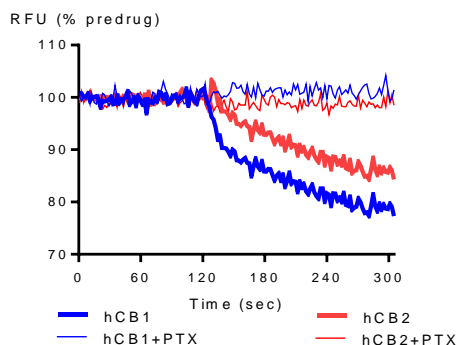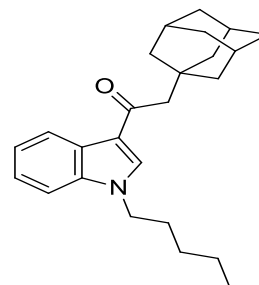
A: Response of AtT20-hCB1 and AtT20-hCB2 to AB-002 (10μM).
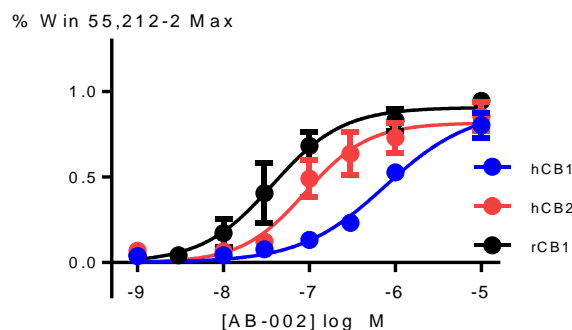
B: Concentration response curves for AB-002 in AtT20-rCB1, AtT20-hCB1 and AtT20-hCB2

D: Response of HEK293-TRPA1 to AB-002 (30μM) and cinnamaldehyde (300μM).
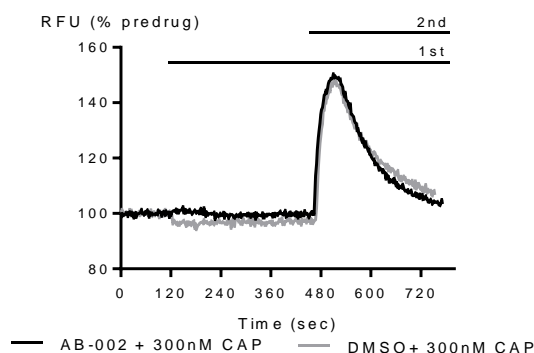
F: Response of HEK293-TRPV1 to AB-002 (10μM) followed by capsaicin (300nM)

C: Response of AtT20-WT to AB-002 (10μM) followed by SRIF (100nM)

	pEC50	MAX %	Notes
AtT20-rCB1	7.0 ± 0.1	91 ± 6	--
AtT20-hCB1	6.1 ± 0.1	89 ± 7	--
AtT20-hCB2	7.4 ± 0.1	82 ± 7	--
HEK293-TRPA1	--	<5	Max <30% no CRC completed
HEK293-TRPV1	--	<10	No change in CAP max response
AtT20 WT	--	<1	No change in SRIF max response

SDB-001
- ## APICA

N-(adamantan-1-yl)-1-pentyl-1H-indole-3-carboxamide
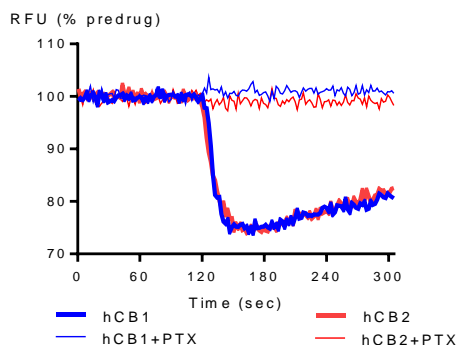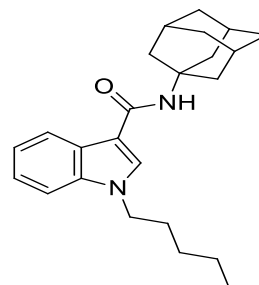
A: Response of AtT20-CB1 and AtT20-CB2 to SDB-001 (10μM).
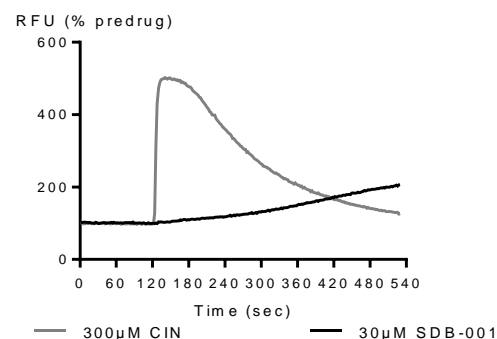
D: Response of HEK293-TRPA1 to SDB-001 (30μM) and cinnamaldehyde (300μM).
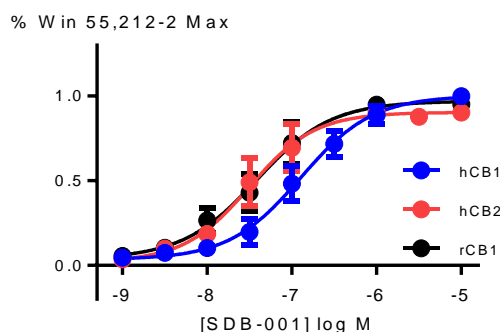

B: Concentration response curves for SDB-001 in AtT20-rCB1, AtT20-hCB1 and AtT20-hCB2
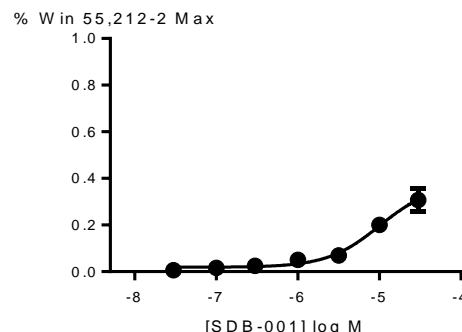
E: Concentration response curve for SDB-001 in HEK293-TRPA1
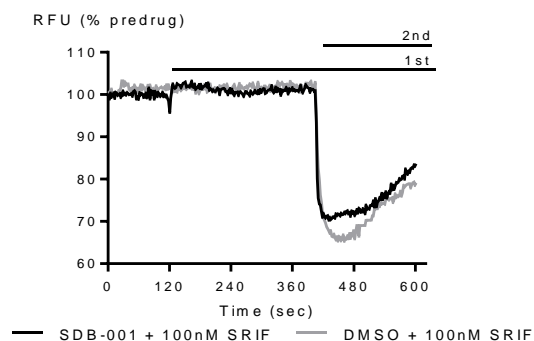
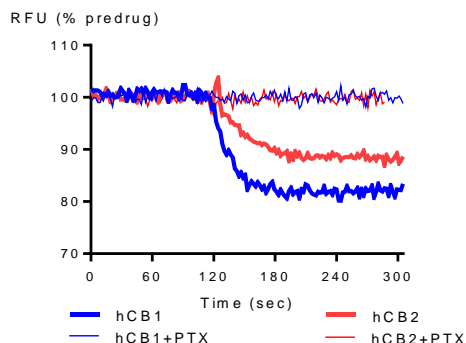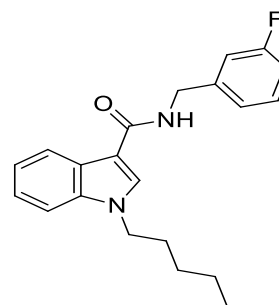C: Response of AtT20-WT to SDB-001 (10μM) followed by SRIF (100nM)
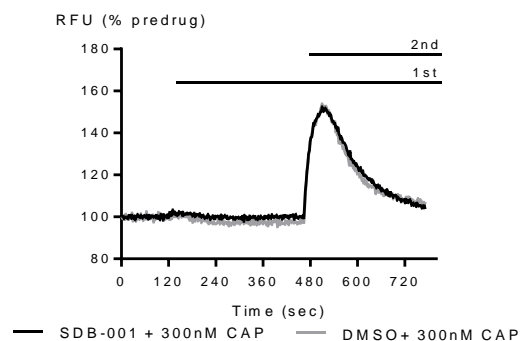
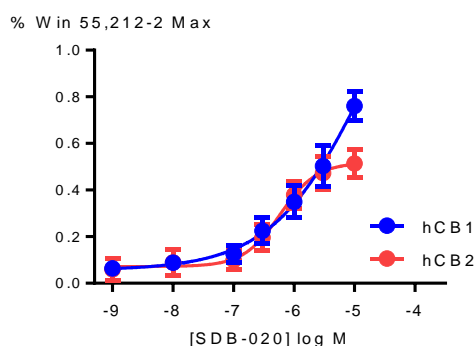F: Response of HEK293-TRPV1 to SDB-001 (30μM) followed by capsaicin (300nM)

	pEC50	MAX %	Notes
AtT20-rCB1	7.42 ± 0.06	97 ± 6	--
AtT20-hCB1	6.89 ± 0.06	100 ± 5	--
AtT20-hCB2	7.50 ± 0.05	90 ± 10	--
HEK293-TRPA1	4.0 ± 0.1*	31 ± 10	--
HEK293-TRPV1	--	<10	No change in CAP max response
AtT20 WT	--	<1	Inhibits average max SRIF response by 12%

*pEC50 assuming that the maximum is equivalent to the maximum of cinnamaldehyde

SDB-002

N-(adamantan-1-ylmethyl)-1-pentyl-1H-indole-3-carboxamide
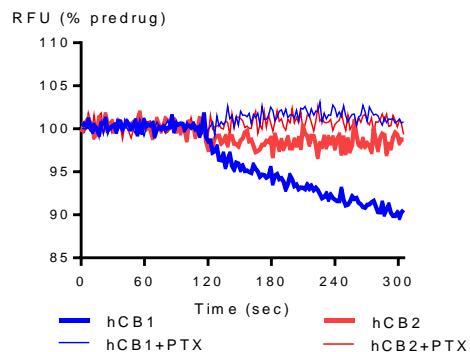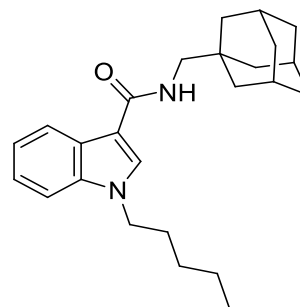
A: Response of AtT20-hCB1 and AtT20-hCB2 to SDB-002 (10μM).
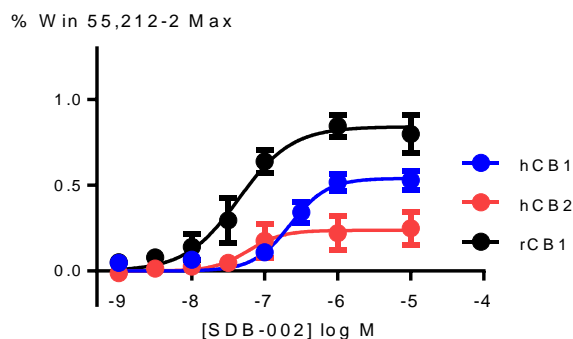
B: Concentration response curves for SDB-002 in AtT20-rCB1, AtT20-hCB1 and AtT20-hCB2
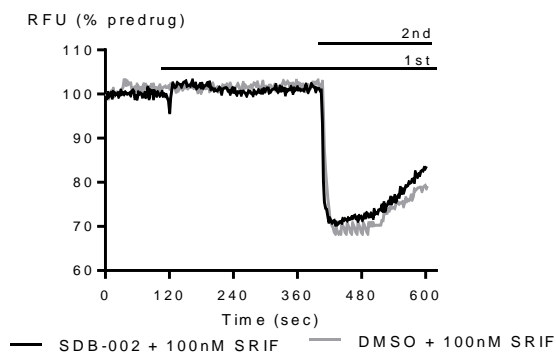
C: Response of AtT20-WT to SDB-002 (10μM) followed by SRIF (100nM)
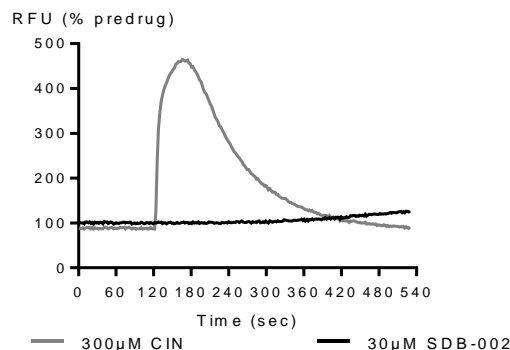
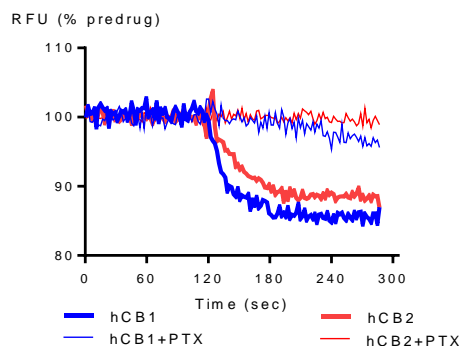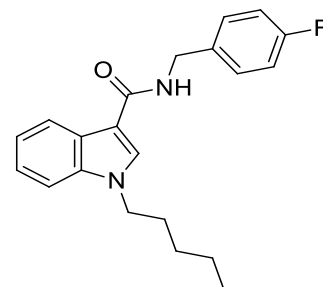D: Response of HEK293-TRPA1 to SDB-002 (30μM) and cinnamaldehyde (300μM).
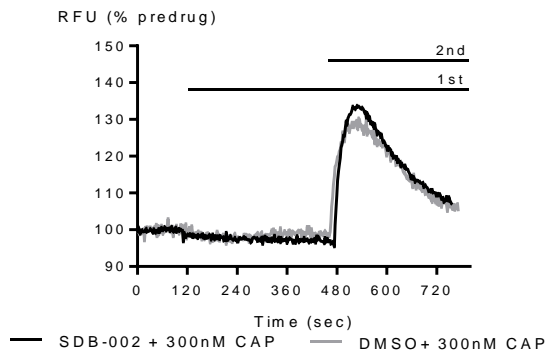
F: Response of HEK293-TRPV1 to SDB-002 (10μM) followed by capsaicin (300nM)

	pEC50	MAX %	Notes
AtT20-rCB1	7.54 ± 0.1	84 ± 6	--
AtT20-hCB1	6.65 ± 0.09	54 ± 4	--
AtT20-hCB2	7.22 ± 0.25	24 ± 4	--
HEK293-TRPA1	--	18 ± 3	Max <30% no CRC completed
HEK293-TRPV1	--	<1	No change in CAP max response
AtT20 WT	--	<1	No change in SRIF max response

SDB-003

N-cyclohexyl-1-pentyl-1H-indole-3-carboxamide
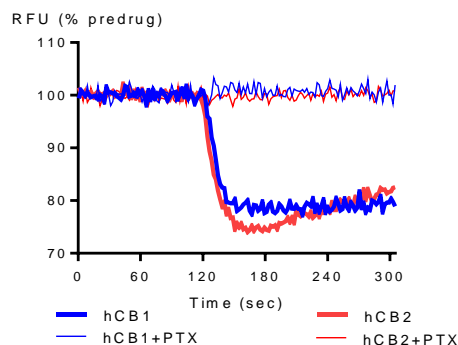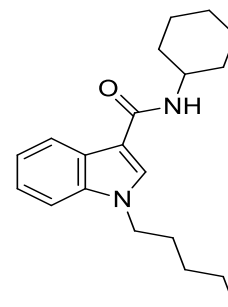
A: Response of AtT20-CB1 and AtT20-CB2 to SDB-003 (10μM).

B: Concentration response curves for SDB-003 in AtT20-rCB1, AtT20-hCB1 and AtT20-hCB2

C: Response of AtT20-WT to SDB-003 (10μM) followed by SRIF (100nM)
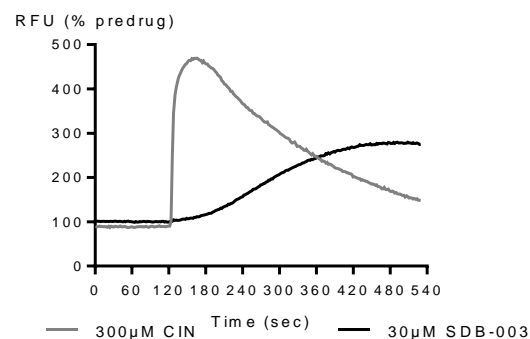
D: Response of HEK293-TRPA1 to SDB-003 (30μM) and cinnamaldehyde (300μM).
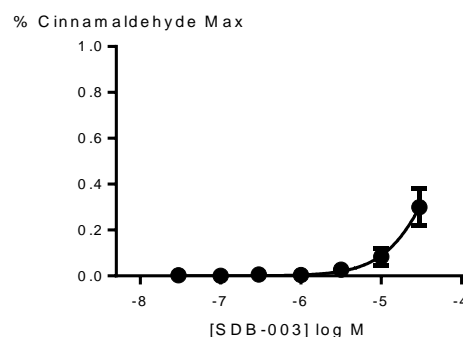
E: Concentration response curve for SDB-003 in HEK293-TRPA1
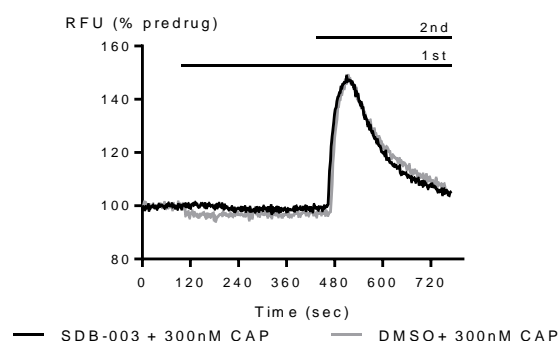
F: Response of HEK293-TRPV1 to SDB-003 (30μM) followed by capsaicin (300nM)

	pEC50	MAX %	Notes
AtT20-rCB1	7.42 ± 0.15	93 ± 7	--
AtT20-hCB1	6.82 ± 0.06	83 ± 3	--
AtT20-hCB2	6.98 ± 0.08	95 ± 5	--
HEK293-TRPA1	$4.2 \pm 0.1*$	30 ± 10	--
HEK293-TRPV1	--	<5	Inhibits average max CAP response by <5%
AtT20 WT	--	<1	Inhibits average max SRIF response by 15%

*pEC50 assuming that the maximum is equivalent to the maximum of cinnamaldehyde

SDB-004

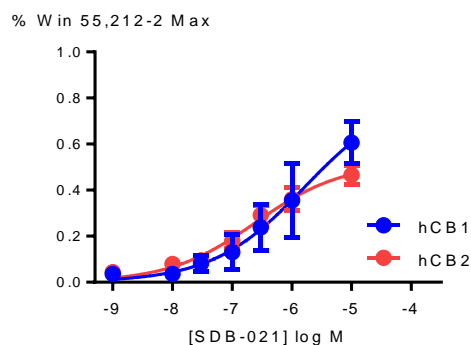N-(cyclohexylmethyl)-1-pentyl-1H-indole-3-carboxamide
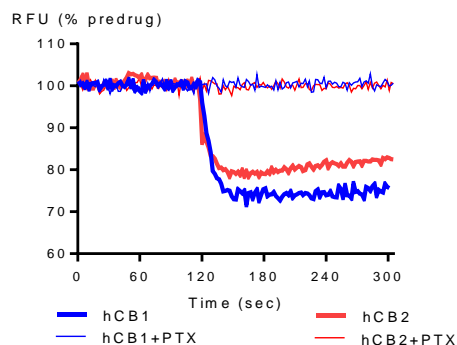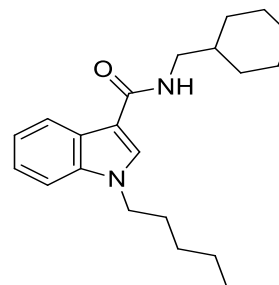

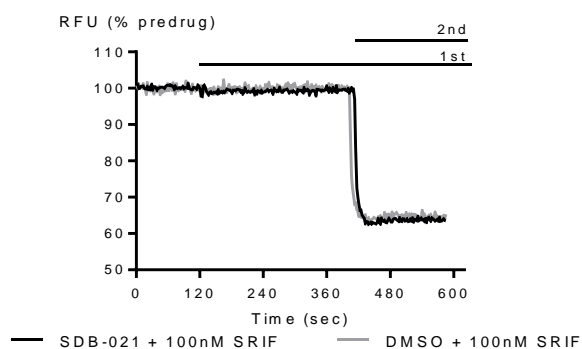

A: Response of AtT20-CB1 and AtT20-CB2 to SDB-004 (10μM).
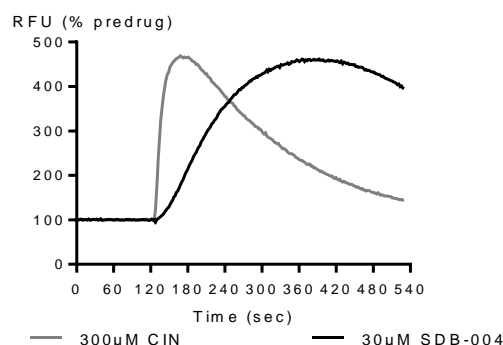
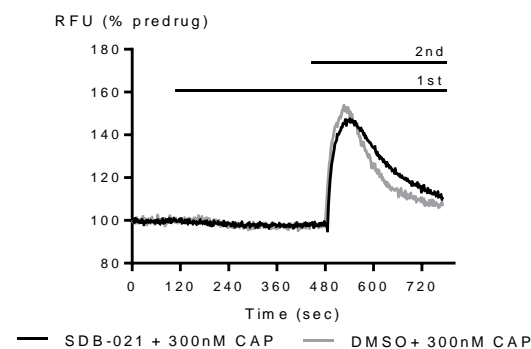D: Response of HEK293-TRPA1 to SDB-004 (30μM) and cinnamaldehyde (300μM).
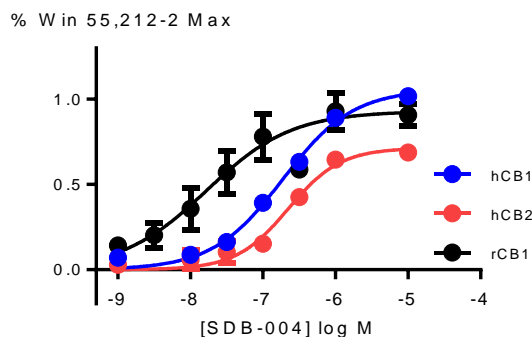
B: Concentration response curves for SDB-004 in AtT20-rCB1, AtT20-hCB1 and AtT20-hCB2
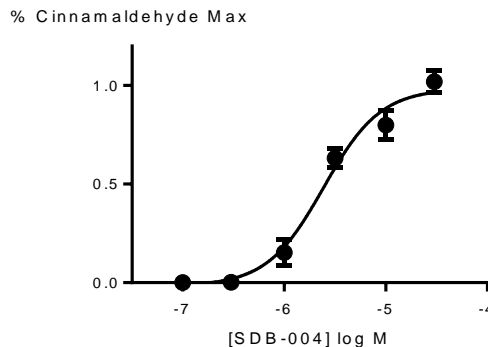
E: Concentration response curve for SDB-004 in HEK293-TRPA1
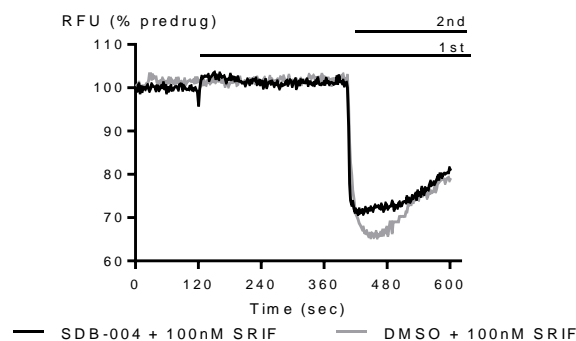
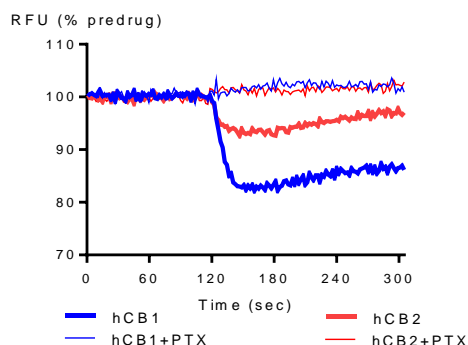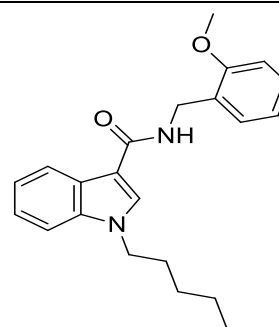C: Response of AtT20-WT to SDB-004 (10μM) followed by SRIF (100nM)
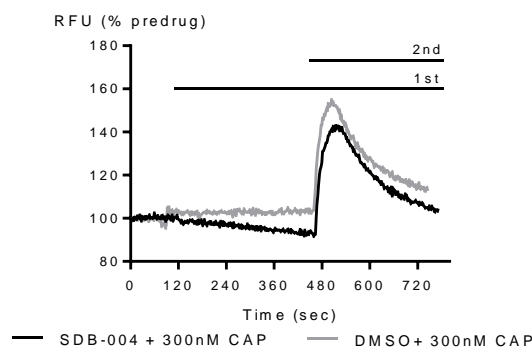
F: Response of HEK293-TRPV1 to SDB-004 (30μM) followed by capsaicin (300nM)

|	pEC50	MAX %	Notes
AtT20-rCB1	7.8 ± 0.2	93 ± 9	--
AtT20-hCB1	6.73 ± 0.06	106 ± 4	--
AtT20-hCB2	6.65 ± 0.09	71 ± 4	--
HEK293-TRPA1	5.61 ± 0.06	98 ± 5	--
HEK293-TRPV1	--	<5	Inhibits average max CAP response by 20%
AtT20 WT	--	<1	Inhibits average max SRIF response by 13%

SDB-005

N-phenyl-1-pentyl-1H-indole-3-carboxamide
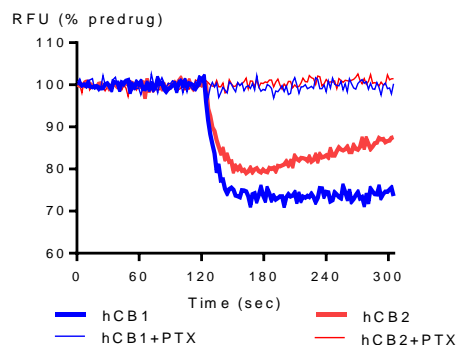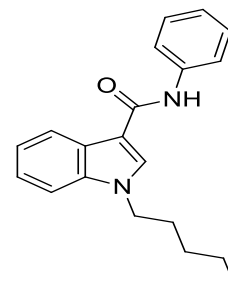


A: Response of AtT20-CB1 and AtT20-CB2 to SDB-005 (10μM).
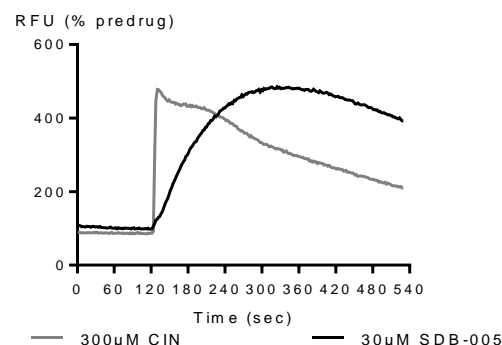
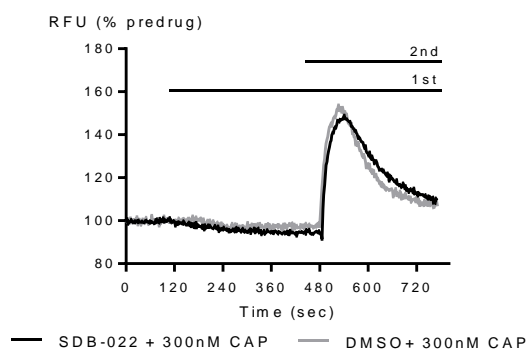D: Response of HEK293-TRPA1 to SDB-005 (30μM) and cinnamaldehyde (300μM).
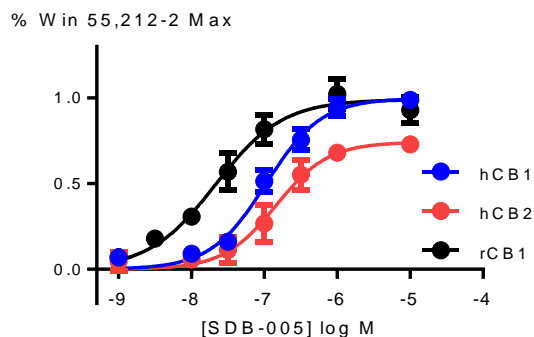
B: Concentration response curves for SDB-005 in AtT20-rCB1, AtT20-hCB1 and AtT20-hCB2
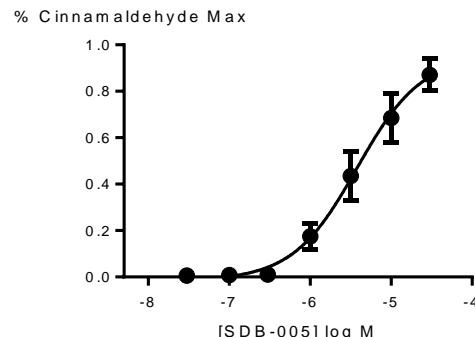
E: Concentration response curve for SDB-005 in HEK293-TRPA1
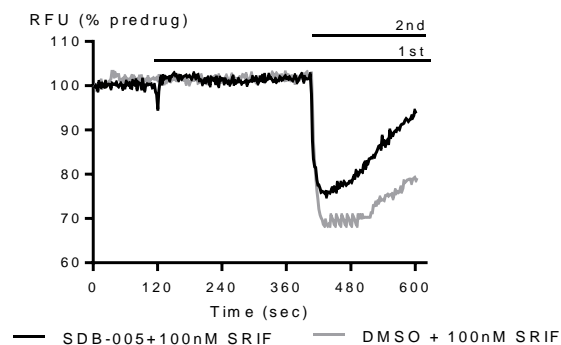
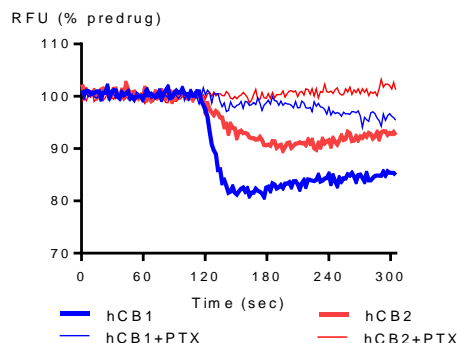C: Response of AtT20-WT to SDB-005 (10μM) followed by SRIF (100nM)
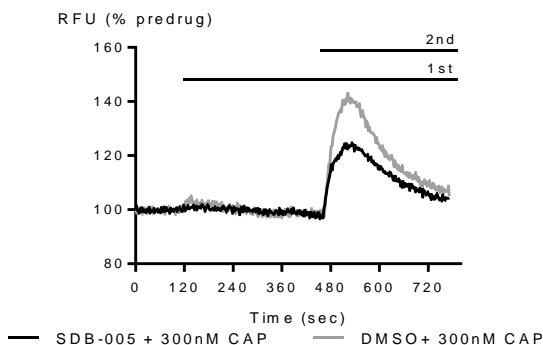
F: Response of HEK293-TRPV1 to SDB-005 (30μM) followed by capsaicin (300nM)

	pEC50	MAX %	Notes
AtT20-rCB1	7.7 ± 0.1	99 ± 6	--
AtT20-hCB1	6.98 ± 0.07	100 ± 4	--
AtT20-hCB2	6.8 ± 0.01	74 ± 6	--
HEK293-TRPA1	5.42 ± 0.16	94 ± 5	--
HEK293-TRPV1	--	<5	Inhibits average max CAP response by 20%
AtT20 WT	--	<1	Inhibits average max SRIF response by 15%

SDB-006

N-benzyl-1-pentyl-1H-indole-3-carboxamide
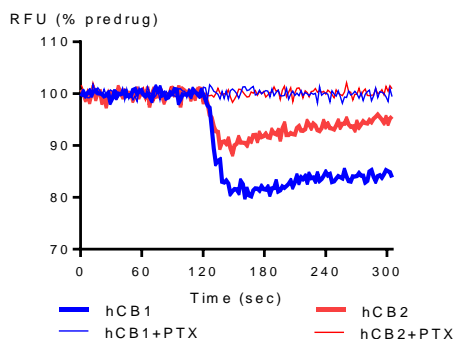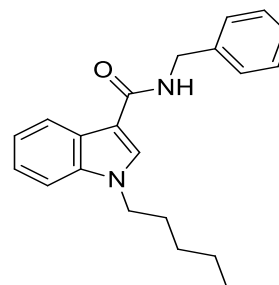
A: Response of AtT20-CB1 and AtT20-CB2 to SDB-006 (10μM).
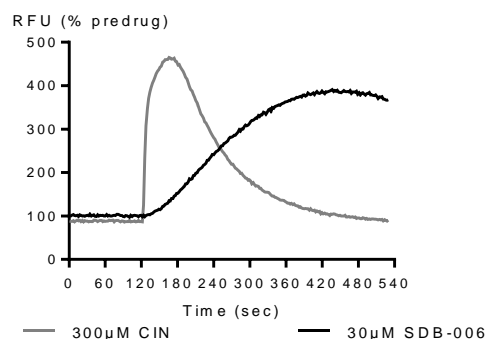
D: Response of HEK293-TRPA1 to SDB-006 (30μM) and cinnamaldehyde (300μM).
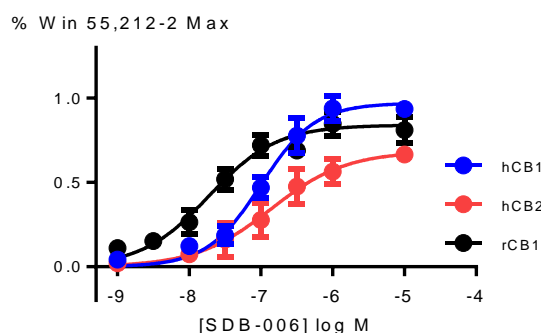
B: Concentration response curves for SDB-006 in AtT20-rCB1, AtT20-hCB1 and AtT20-hCB2
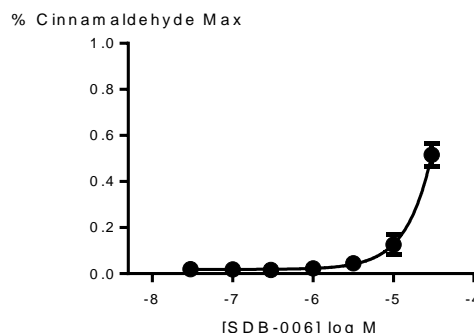
E: Concentration response curve for SDB-006 in HEK293-TRPA1
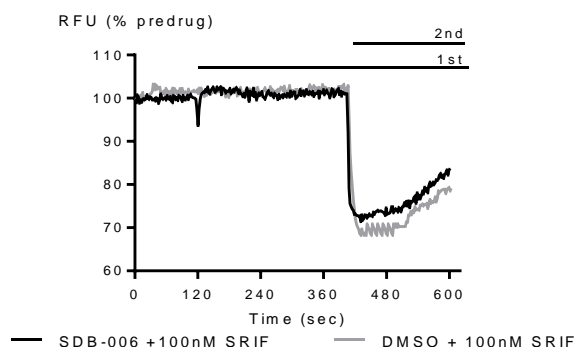
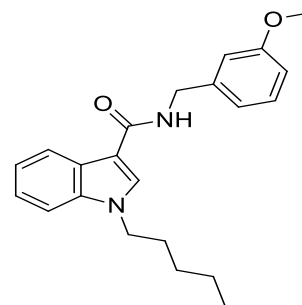C: Response of AtT20-WT to SDB-006 (10μM) followed by SRIF (100nM)
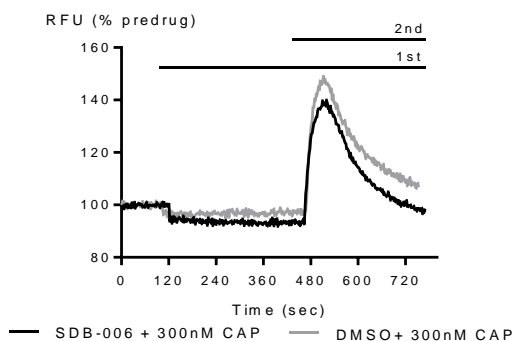
F: Response of HEK293-TRPV1 to SDB-006 (30μM) followed by capsaicin (300nM)

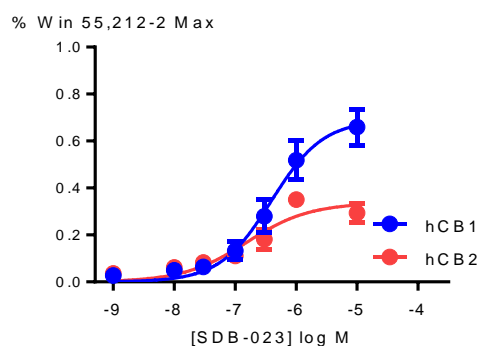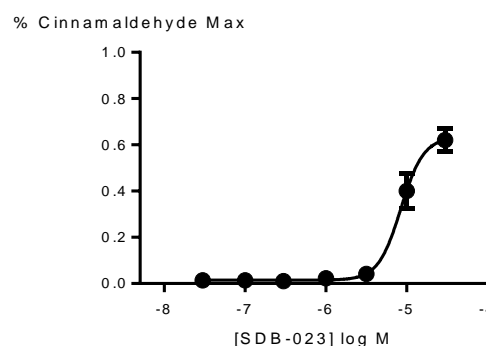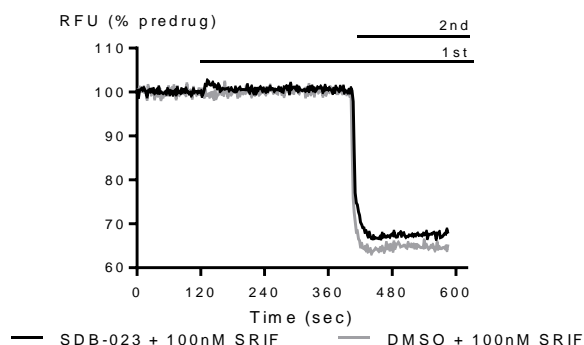|	pEC50	MAX %	Notes
AtT20-rCB1	7.7 ± 0.1	84 ± 5	--
AtT20-hCB1	7.0 ± 0.09	97± 6	--
AtT20-hCB2	6.9 ± 0.2	68 ± 9	--
HEK293-TRPA1	4.54 ± 0.02*	52 ± 6	--
HEK293-TRPV1	--	<1	Inhibits average max CAP response by 10%
AtT20 WT	--	<1	Inhibits average max SRIF response by 15%

*pEC50 assuming that the maximum is equivalent to the maximum of cinnamaldehyde

SDB-007

- STS-135

N-(adamantan-1-yl)-1-(5-fluoropentyl)-1*H*-indole-3-carboxamide
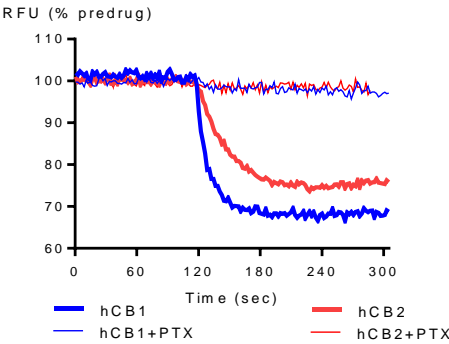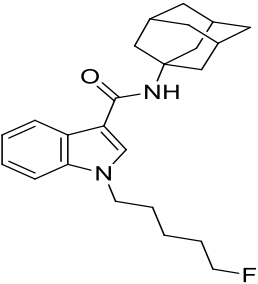
A: Response of AtT20-CB1 and AtT20-CB2 to SDB-007(10μM).

B: Concentration response curves for SDB-007 in AtT20-CB1 and AtT20-CB2

C: Response of AtT20-WT to SDB-007 (10μM) followed by SRIF (100nM)
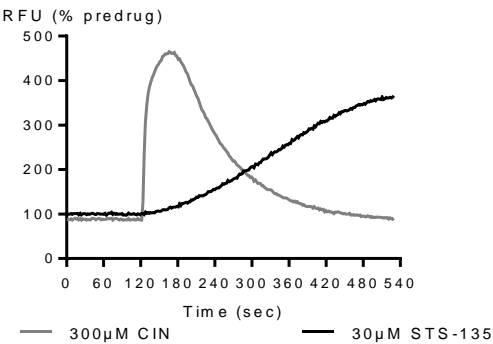
D: Response of HEK293-TRPA1 to SDB-007 (30μM) and cinnamaldehyde (300μM).
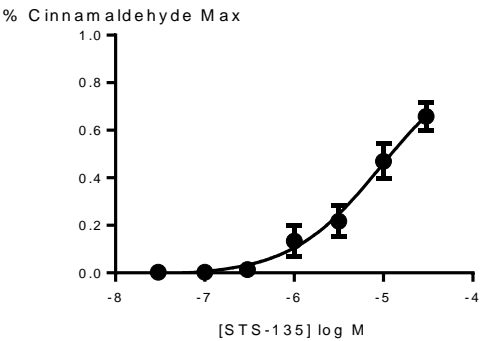
E: Concentration response curve for SDB-007 in HEK293-TRPA1
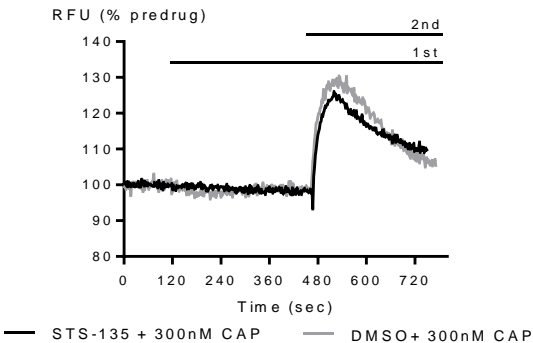
F: Response of HEK293-TRPV1 to SDB-007 (30μM) followed by capsaicin (300nM)

	pEC50	MAX %	Notes
AtT20-hCB1	7.29 ± 0.12	123 ± 8	--
AtT20-hCB2	7.88 ± 0.26	114 ± 12	--
HEK293-TRPA1	4.92 ± 0.07*	66 ± 7	--
HEK293-TRPV1	--	<10	Inhibits average max CAP response by <10%
AtT20 WT	--	<1	Inhibits average max SRIF response by 20%

*pEC50 assuming that the maximum is equivalent to the maximum of cinnamaldehyde

SDB-008

N-(adamantan-1-ylmethyl)-1-(5-fluoropentyl)-
1*H*-indole-3-carboxamide
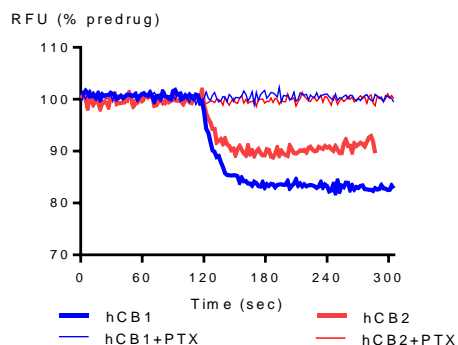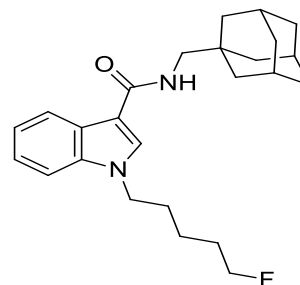
A: Response of AtT20-CB1 and AtT20-CB2 to SDB-008
(10μM).
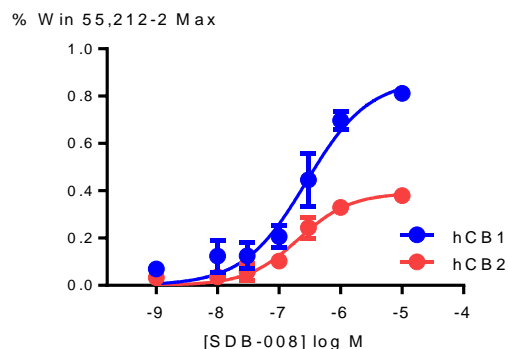
B: Concentration response curves for SDB-008 in
AtT20-CB1 and AtT20-CB2

D: Response of HEK293-TRPA1 to SDB-008 (30μM) and
cinnamaldehyde (300μM).
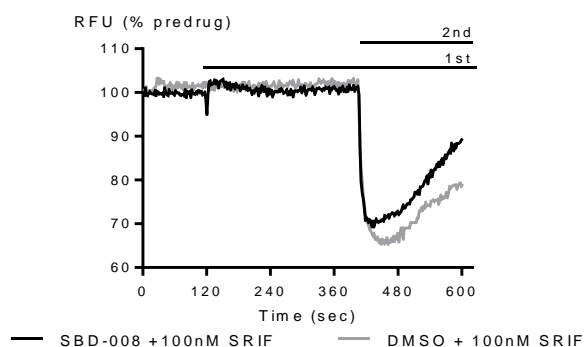
C: Response of AtT20-WT to SDB-008 (10μM)
followed by SRIF (100nM)
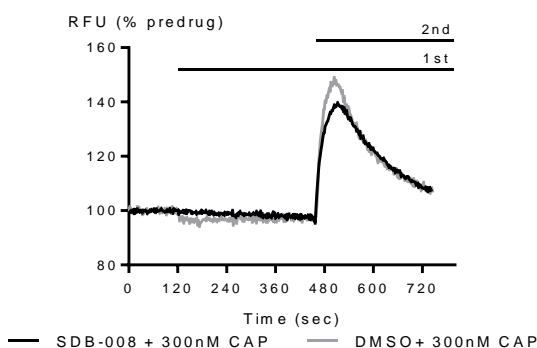
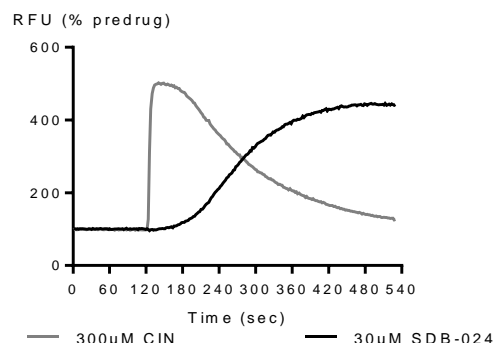F: Response of HEK293-TRPV1 to SDB-008 (30μM) followed
by capsaicin (300nM)

	pEC50	MAX %	Notes
AtT20-hCB1	6.56 ± 0.16	87 ± 8	--
AtT20-hCB2	6.69 ± 0.12	39 ± 3	--
HEK293-TRPA1	--	11 ± 10	Max <30% no CRC completed
HEK293-TRPV1	--	18 ± 10	Inhibits average max CAP response by <13%
AtT20 WT	--	<1	Inhibits average max SRIF response by 20%

SDB-009

N-cyclohexyl-1-(5-fluoropentyl)-1H-indole-3-carboxamide
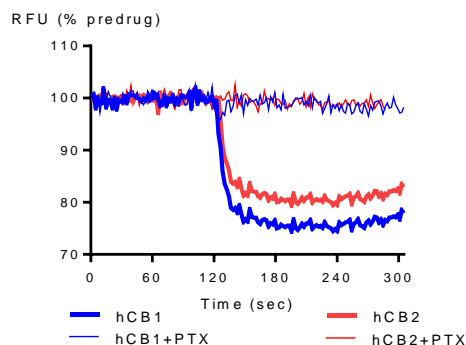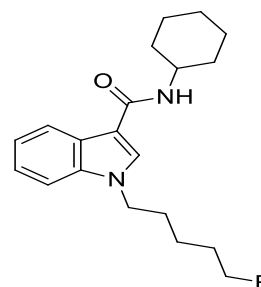
A: Response of AtT20-CB1 and AtT20-CB2 to SDB-009 (10μM).
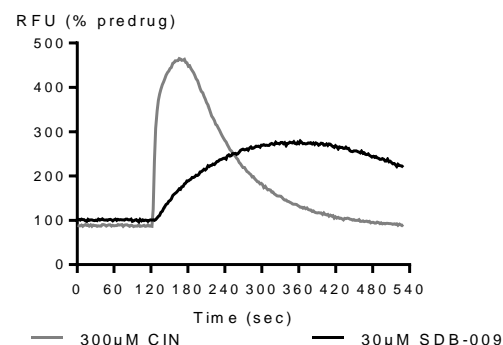
D: Response of HEK293-TRPA1 to SDB-009 (30μM) and cinnamaldehyde (300μM).
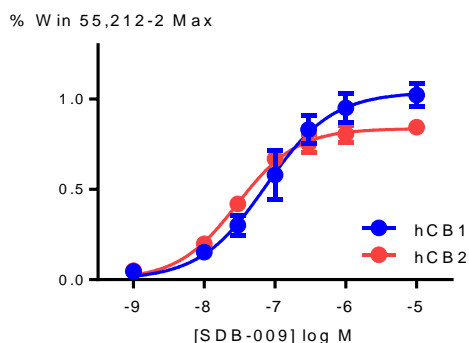

B: Concentration response curves for SDB-009 in AtT20-CB1 and AtT20-CB2
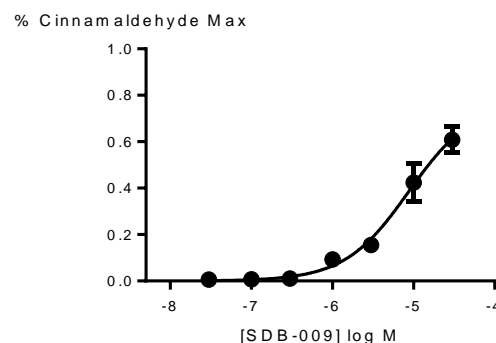
E: Concentration response curve for SDB-009 in HEK293-TRPA1
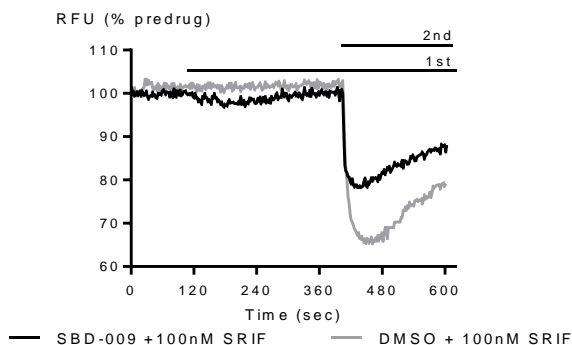
C: Response of AtT20-WT to SDB-009 (10μM) followed by SRIF (100nM)
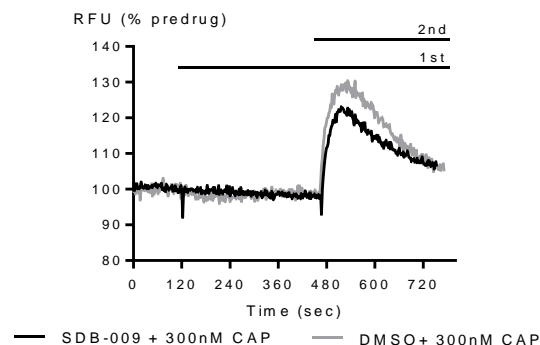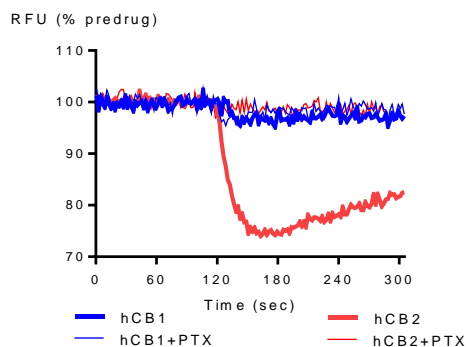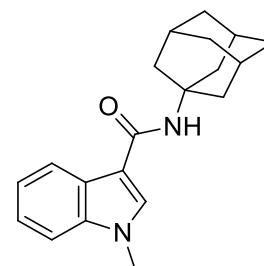
F: Response of HEK293-TRPV1 to SDB-009 (30μM) followed by capsaicin (300nM)

	pEC50	MAX %	Notes
AtT20-hCB1	7.1 ± 0.1	104 ± 7	--
AtT20-hCB2	7.53 ± 0.06	84 ± 3	--
HEK293-TRPA1	5.1 ± 0.2	77 ± 17	--
HEK293-TRPV1	--	<10	Inhibits average max CAP response by <5%
AtT20 WT	--	<5	Inhibits average max SRIF response by 27%

SDB-010

N-(cyclohexylmethyl)-1-(5-fluoropentyl)-1*H*-indole-3-carboxamide
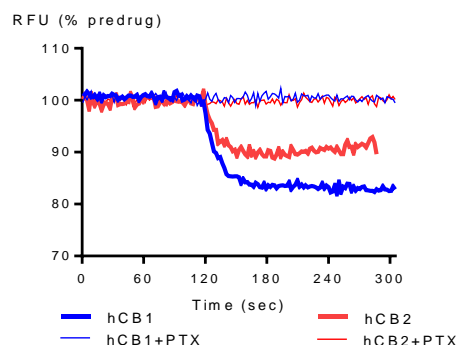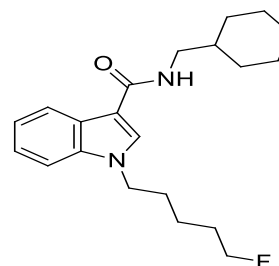
A: Response of AtT20-CB1 and AtT20-CB2 to SDB-010 (10μM).
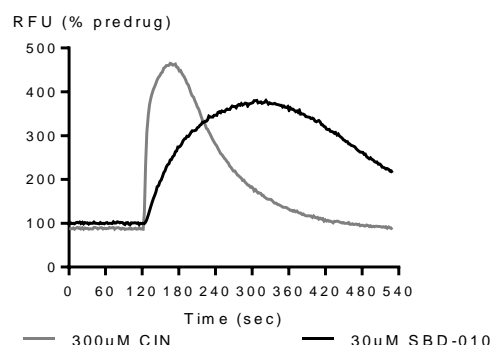
D: Response of HEK293-TRPA1 to SDB-010 (30μM) and cinnamaldehyde (300μM).
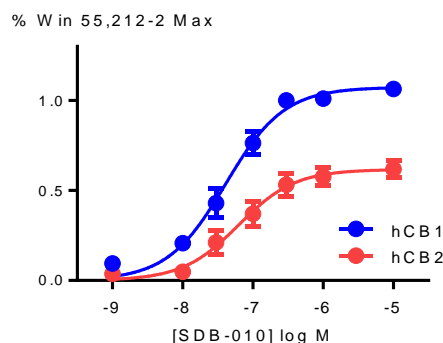
B: Concentration response curves for SDB-010 in AtT20-CB1 and AtT20-CB2
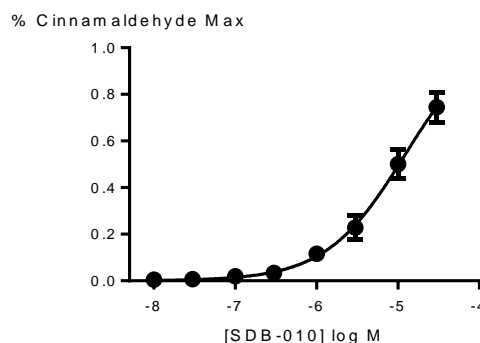
E: Concentration response curve for SDB-010 in HEK293-TRPA1
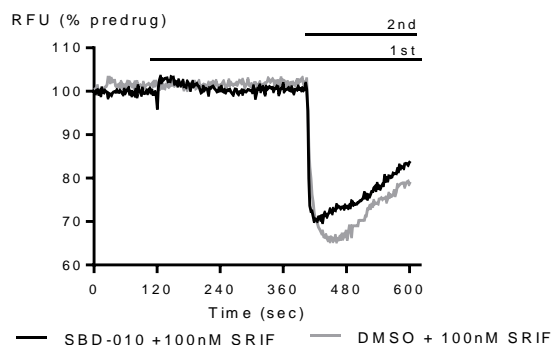
C: Response of AtT20-WT to SDB-010 (10μM) followed by SRIF (100nM)
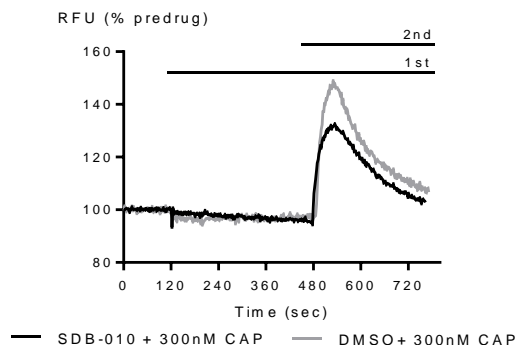
F: Response of HEK293-TRPV1 to SDB-010 (30μM) followed by capsaicin (300nM)

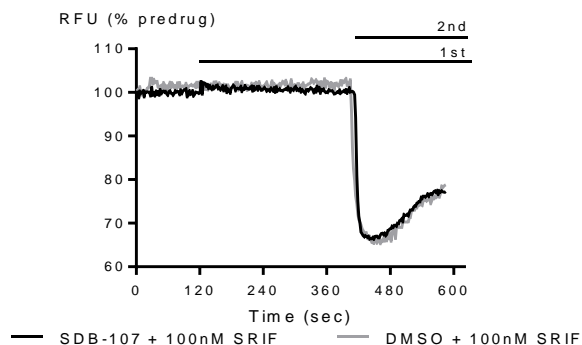|	pEC50	MAX %	Notes
AtT20-hCB1	7.39 ± 0.06	104 ± 4	--
AtT20-hCB2	7.20 ± 0.12	84 ± 4	--
HEK293-TRPA1	4.9 ± 0.3	109 ± 3	--
HEK293-TRPV1	--	12 ± 1	Inhibits average max CAP response by 12%
AtT20 WT	--	<5	Inhibits average max SRIF response by 15%

SDB-011

*N*-phenyl-1-(5-fluoropentyl)-1*H*-indole-3-carboxamide
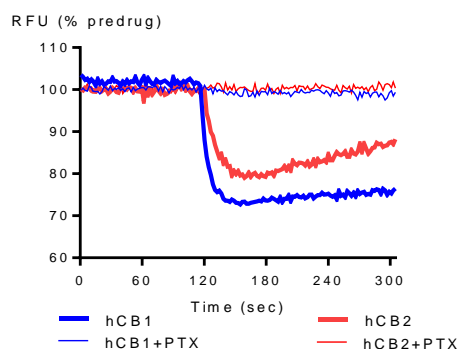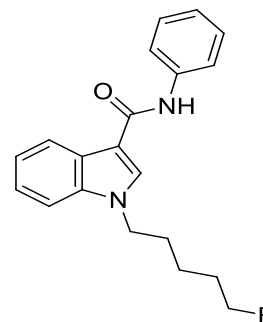
A: Response of AtT20-CB1 and AtT20-CB2 to SDB-011 (10μM).
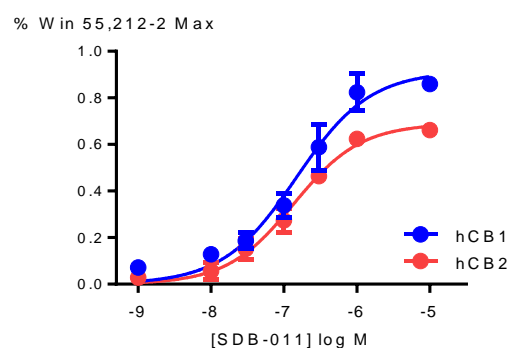
B: Concentration response curves for SDB-011 in AtT20-CB1 and AtT20-CB2

D: Response of HEK293-TRPA1 to SDB-011 (30μM) and cinnamaldehyde (300μM).

F: Response of HEK293-TRPV1 to SDB-011 (30μM) followed by capsaicin (300nM)
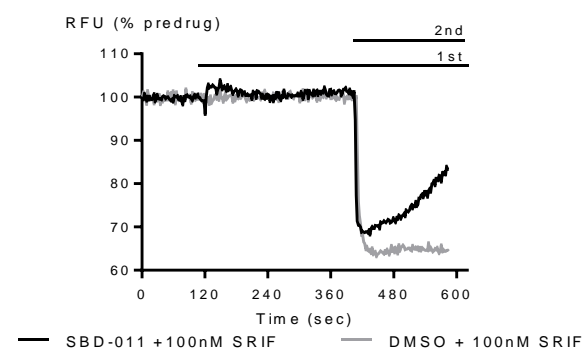
C: Response of AtT20-WT to SDB-011 (10μM) followed by SRIF (100nM)

	pEC50	MAX %	Notes
AtT20-hCB1	6.83 ± 0.13	92 ± 7	--
AtT20-hCB2	6.87 ± 0.09	67 ± 4	--
HEK293-TRPA1	--	<10	Max <30% no CRC completed
HEK293-TRPV1	--	<10	Inhibits average max CAP response by 11%
AtT20 WT	--	<1	Inhibits average max SRIF response by 22%

SDB-012

N-benzyl-1-(5-fluoropentyl)-1*H*-indole-3-carboxamide
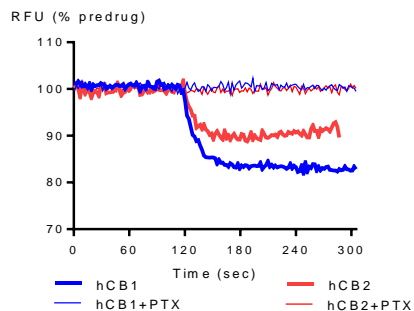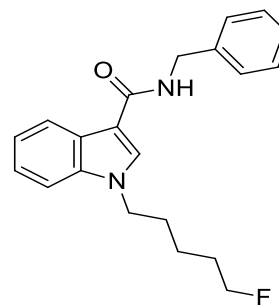
A: Response of AtT20-CB1 and AtT20-CB2 to SDB-012 (10μM).
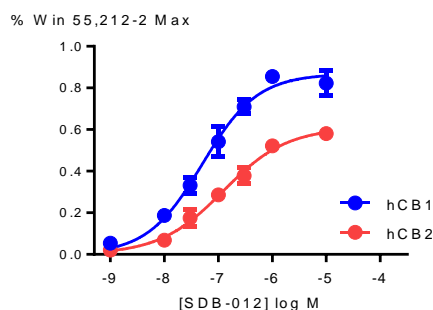
B: Concentration response curves for SDB-012 in AtT20-CB1 and AtT20-CB2

D: Response of HEK293-TRPA1 to SDB-012 (30μM) and cinnamaldehyde (300μM).

F: Response of HEK293-TRPV1 to SDB-012 (30μM) followed by capsaicin (300nM)
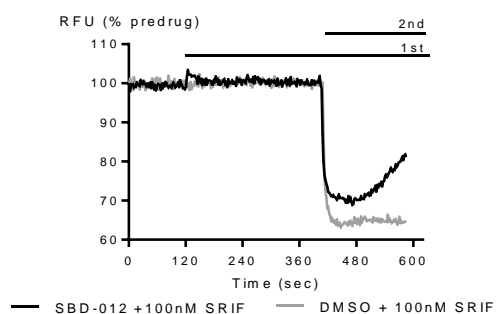
C: Response of AtT20-WT to SDB-012 (10μM) followed by SRIF (100nM)

	pEC50	MAX %	Notes
AtT20-hCB1	7.30 ± 0.09	87 ± 4	--
AtT20-hCB2	6.9 ± 0.1	61 ± 4	--
HEK293-TRPA1	--	<10	Max <30% no CRC completed
HEK293-TRPV1	--	<5	No change in CAP max response
AtT20 WT	--	<1	Inhibits average max SRIF response by 20%

SDB-013

N-benzyl-1-propyl-1*H*-indole-3-carboxamide
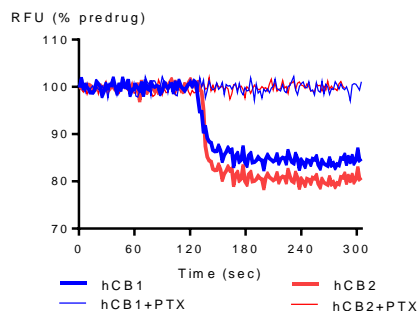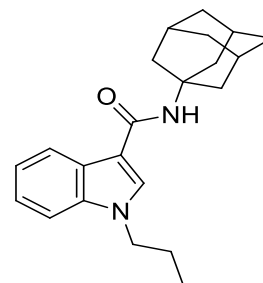
A: Response of AtT20-CB1 and AtT20-CB2 to SDB-013 (10μM).
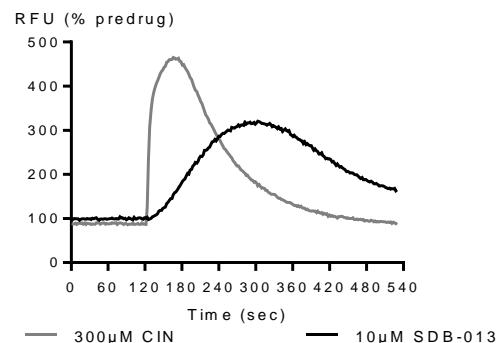
D: Response of HEK293-TRPA1 to SDB-013 (10μM) and cinnamaldehyde (300μM).
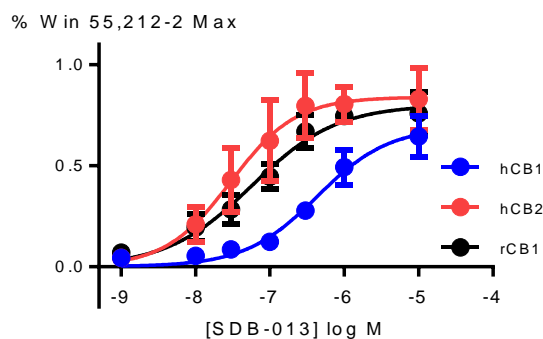
B: Concentration response curves for SDB-013 in AtT20-rCB1, AtT20-hCB1 and AtT20-hCB2
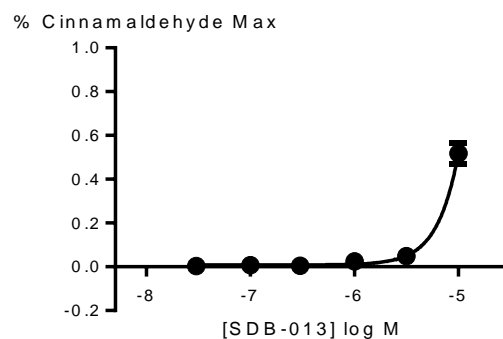
E: Concentration response curve for SDB-013 in HEK293-TRPA1
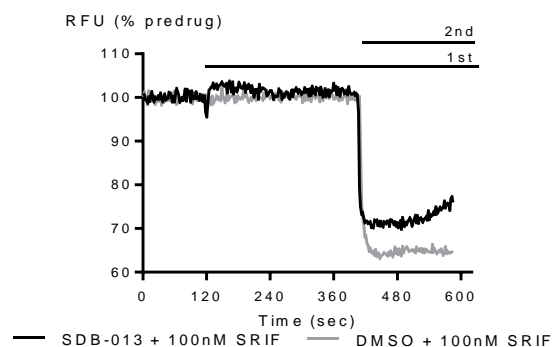
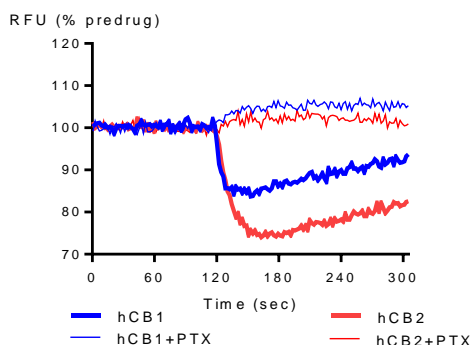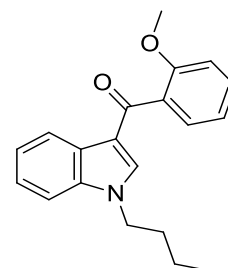C: Response of AtT20-WT to SDB-013 (10μM) followed by SRIF (100nM)
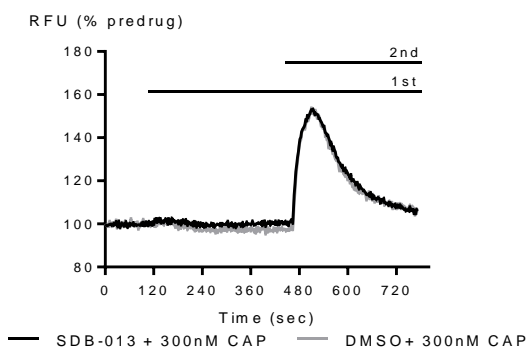
F: Response of HEK293-TRPV1 to SDB-013 (10μM) followed by capsaicin (300nM)

	pEC50	MAX %	Notes
AtT20-rCB1	7.2 ± 0.2	84 ± 7	--
AtT20-hCB1	6.4 ± 0.2	97 ± 8	--
AtT20-hCB2	7.5 ± 0.2	68 ± 10	--
HEK293-TRPA1	5.0 ± 0.01*	55 ± 13	--
HEK293-TRPV1	--	<10	Inhibits average max CAP response by <5%
AtT20 WT	--	<5	Inhibits average max SRIF response by 17%

*pEC50 assuming that the maximum is equivalent to the maximum of cinnamaldehyde

SDB-014

N-(adamantan-1-ylmethyl)-1-propyl-1*H*-indole-3-carboxamide
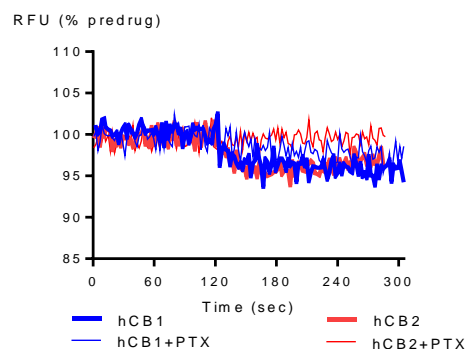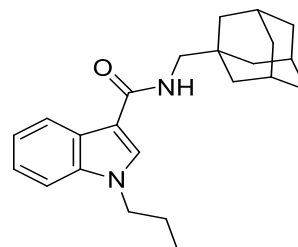

A: Response of AtT20-CB1 and AtT20-CB2 to SDB-014 (10μM).
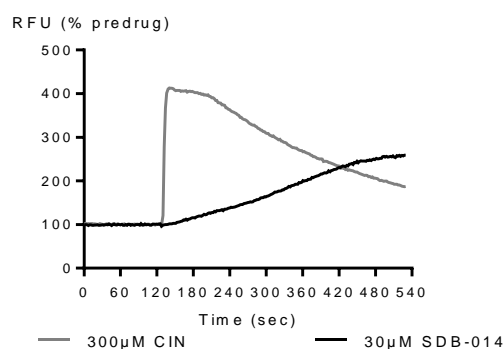


D: Response of HEK293-TRPA1 to SDB-014 (30μM) and cinnamaldehyde (300μM).
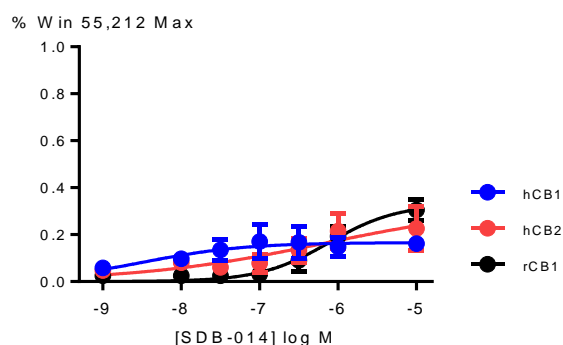
B: Concentration response curves for SDB-014 in AtT20-rCB1, AtT20-hCB1 and AtT20-hCB2
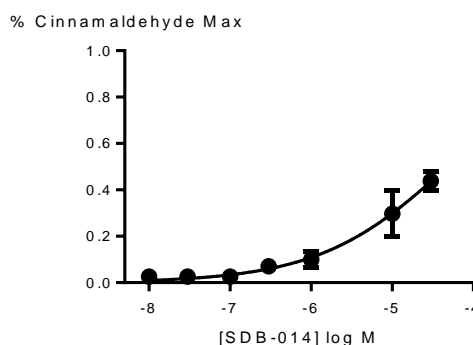
E: Concentration response curve for SDB-014 in HEK293-TRPA1
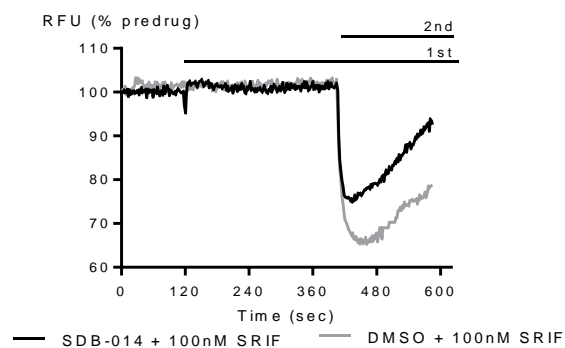
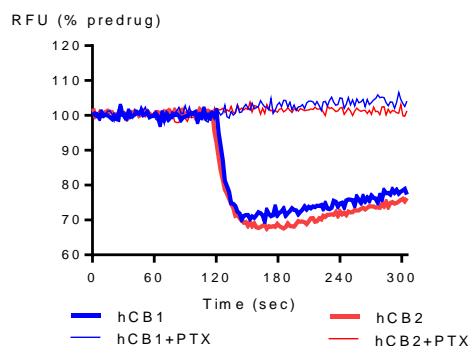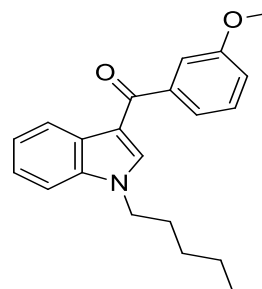C: Response of AtT20-WT to SDB-014 (10μM) followed by SRIF (100nM)
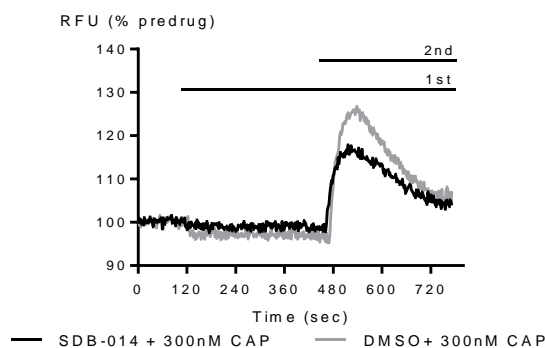
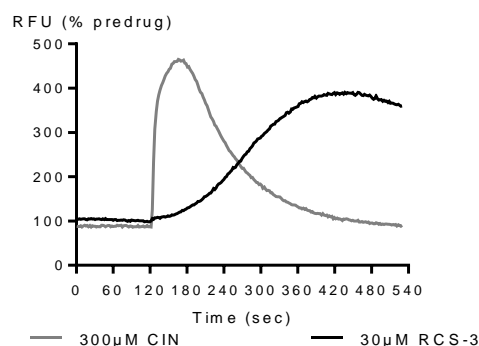F: Response of HEK293-TRPV1 to SDB-014 (30μM) followed by capsaicin (300nM)

	pEC50	MAX %	Notes
AtT20-rCB1	6.12 ± 0.21	33 ± 5	--
AtT20-hCB1	8.48 ± 0.62	17± 3	--
AtT20-hCB2	6.2± 2.6	33 ± 3	--
HEK293-TRPA1	4.32 ± 0.14*	44 ± 4	--
HEK293-TRPV1	--	<1	Inhibits average max CAP response by 10%
AtT20 WT	--	<1	Inhibits average max SRIF response by 15%

*pEC50 assuming that the maximum is equivalent to the maximum of cinnamaldehyde

SDB-015

N-cyclohexyl-1-propyl-1*H*-indole-3-carboxamide
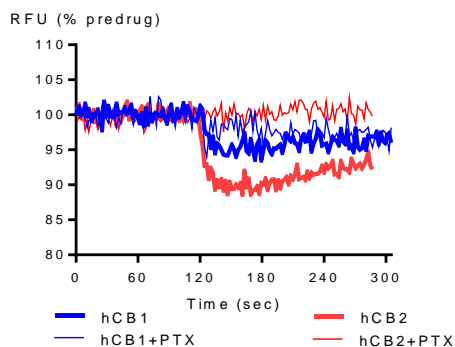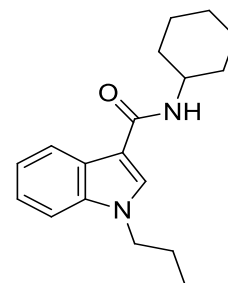
A: Response of AtT20-CB1 and AtT20-CB2 to SDB-015 (10μM).
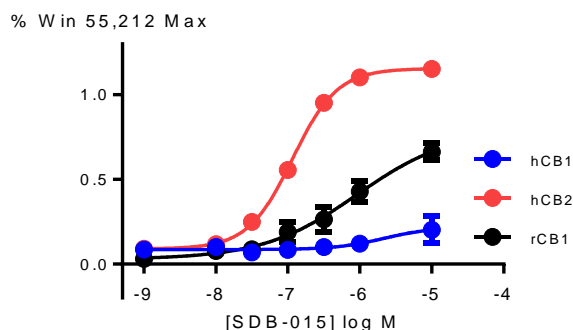
B: Concentration response curves for SDB-015 in AtT20-rCB1, AtT20-CB1 and AtT20-CB2
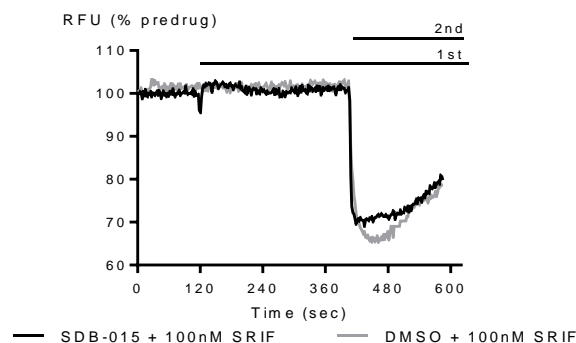
C: Response of AtT20-WT to SDB-015 (10μM) followed by SRIF (100nM)
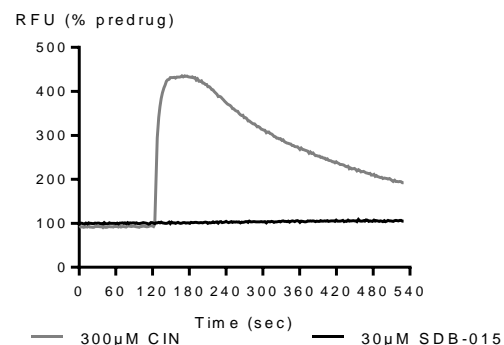
D: Response of HEK293-TRPA1 to SDB-015 (30μM) and cinnamaldehyde (300μM).
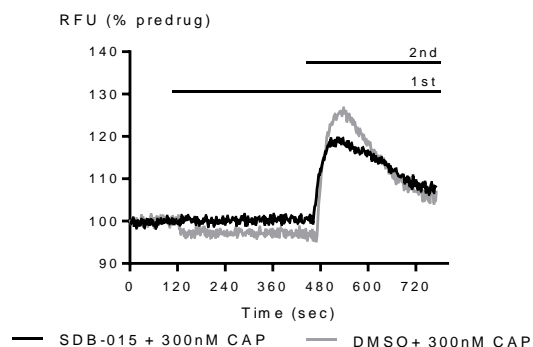
F: Response of HEK293-TRPV1 to SDB-015 (30μM) followed by capsaicin (300nM)

	pEC50	MAX %	Notes
AtT20-rCB1	6.04 ± 0.4	79 ± 2	--
AtT20-hCB1	5.66 ± 2.2	22 ± 2	--
AtT20-hCB2	6.93 ± 0.01	115.5 ± 10	--
HEK293-TRPA1	--	<10	Max <30% no CRC completed
HEK293-TRPV1	--	<1	Inhibits average max CAP response by <10%
AtT20 WT	--	<5	Inhibits average max SRIF response by <10%

SDB-016

*N*-(cyclohexylmethyl)-1-propyl-1*H*-indole-3-carboxamide

A: Response of AtT20-CB1 and AtT20-CB2 to SDB-016 (10μM).
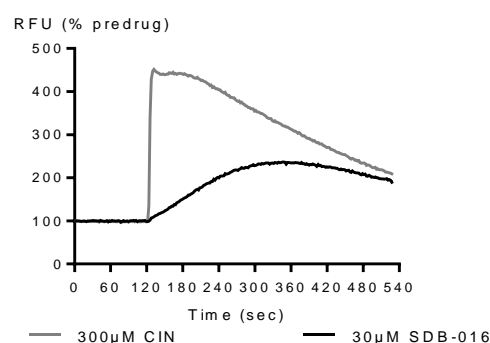
D: Response of HEK293-TRPA1 to SDB-016 (30μM) and cinnamaldehyde (300μM).
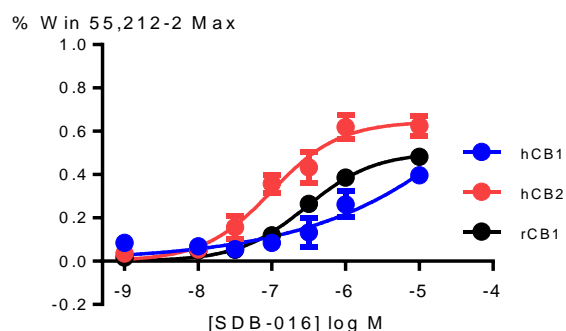
B: Concentration response curves for SDB-016 in AtT20-rCB1, AtT20-hCB1 and AtT20-hCB2
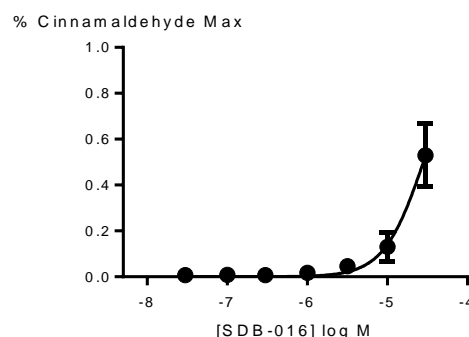
E: Concentration response curve for SDB-016 in HEK293-TRPA1
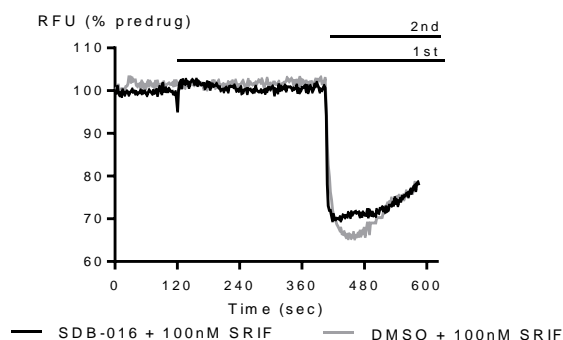
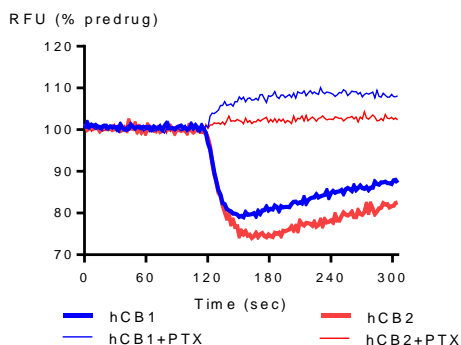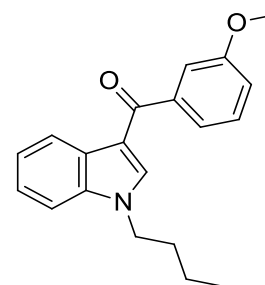C: Response of AtT20-WT to SDB-016 (10μM) followed by SRIF (100nM)
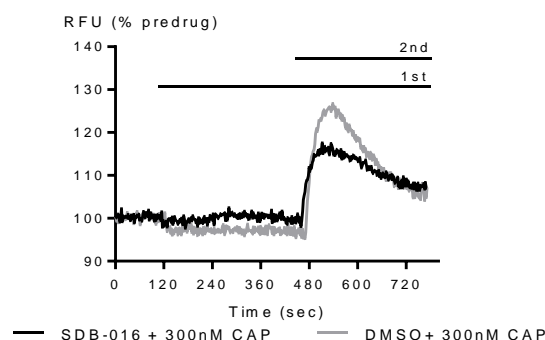
F: Response of HEK293-TRPV1 to SDB-016 (30μM) followed by capsaicin (300nM)

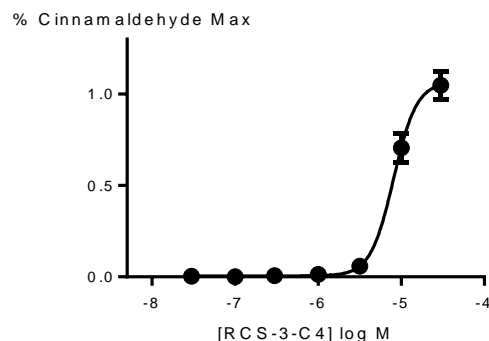|	pEC50	MAX %	Notes
AtT20-rCB1	6.53 ± 0.08	50 ± 3	--
AtT20-hCB1	4.53 ± 0.06**	40 ± 1	--
AtT20-hCB2	7.00 ± 0.13	65 ± 5	--
HEK293-TRPA1	4.55 ± 0.05*	53 ± 10	--
HEK293-TRPV1	--	<1	Inhibits average max CAP response by 15%
AtT20 WT	--	<5	Inhibits average max SRIF response by 18%

*pEC50 assuming that the maximum is equivalent to the maximum of cinnamaldehyde

** pEC50 assuming that the maximum is equivalent to the maximum of WIN 55-212,2

SDB-017

N-phenyl-1-propyl-1*H*-indole-3-carboxamide

A: Response of AtT20-CB1 and AtT20-CB2 to SDB-017 (10μM).
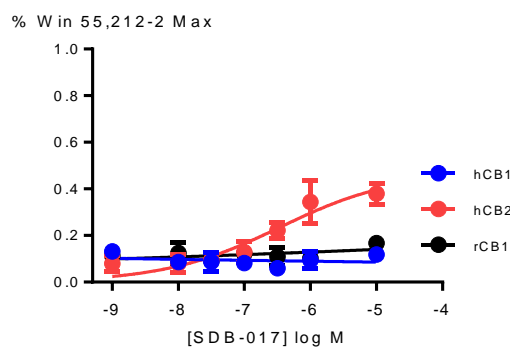
B: Concentration response curves for SDB-017 in AtT20-rCB1, AtT20-CB1 and AtT20-CB2

D: Response of HEK293-TRPA1 to SDB-017 (30μM) and cinnamaldehyde (300μM).
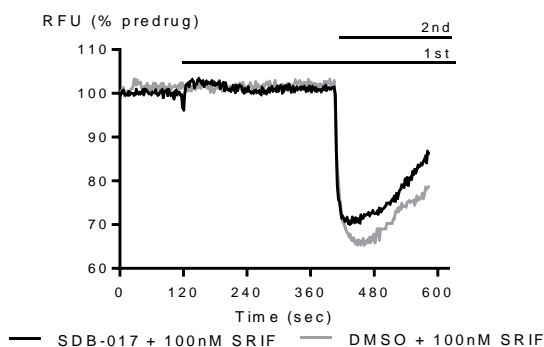
C: Response of AtT20-WT to SDB-017 (10μM) followed by SRIF (100nM)
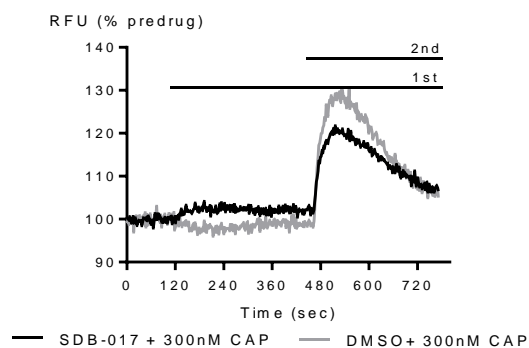
F: Response of HEK293-TRPV1 to SDB-017 (30μM) followed by capsaicin (300nM)

	pEC50	MAX %	Notes
AtT20-rCB1	n.d.	12 ± 8	--
AtT20-hCB1	n.d.	17 ± 2	--
AtT20-hCB2	6.5 ± 0.7	47 ± 15	--
HEK293-TRPA1	--	<5	Max <30% no CRC completed
HEK293-TRPV1	--	<1	Inhibits average max CAP response by <10%
AtT20 WT	--	<5	Inhibits average max SRIF response by 16%

SDB-018

N-benzyl-1-propyl-1*H*-indole-3-carboxamide
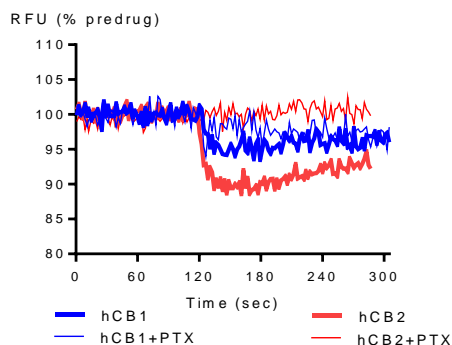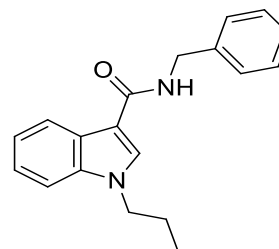
A: Response of AtT20-CB1 and AtT20-CB2 to SDB-018 (10μM).

B: Concentration response curves for SDB-018 in AtT20-rCB1, AtT20-CB1 and AtT20-CB2

D: Response of HEK293-TRPA1 to SDB-018 (30μM) and cinnamaldehyde (300μM).

F: Response of HEK293-TRPV1 to SDB-018 (30μM) followed by capsaicin (300nM)

C: Response of AtT20-WT to SDB-018 (10μM) followed by SRIF (100nM)

	pEC50	MAX %	Notes
AtT20-rCB1	6.8 ± 0.3	20 ± 4	--
AtT20-hCB1	7.1 ± 0.8	29 ±12	--
AtT20-hCB2	6.8 ± 0.4	46 ± 10	--
HEK293-TRPA1	--	<5	Max <30% no CRC completed
HEK293-TRPV1	--	<1	Inhibits average max CAP response by 5%
AtT20 WT	--	<5	Inhibits average max SRIF response by <15%

SDB-019

*N*-(2-fluorobenzyl)-1-pentyl-1*H*-indole-3-carboxamide

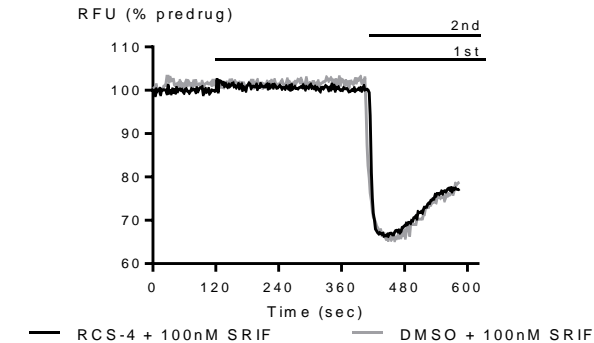A: Response of AtT20-CB1 and AtT20-CB2 to SDB-019 (10μM).
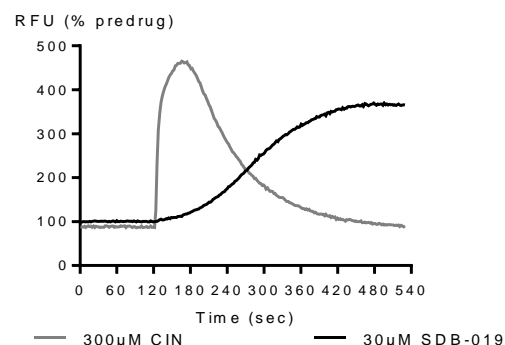
D: Response of HEK293-TRPA1 to SDB-019 (30μM) and cinnamaldehyde (300μM).
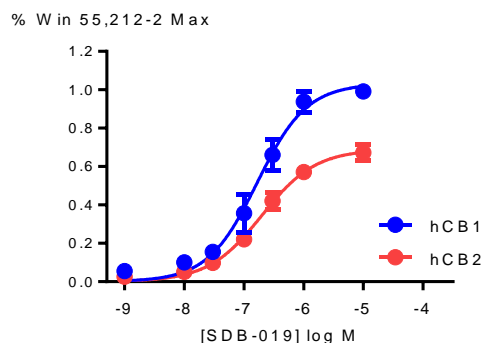

B: Concentration response curves for SDB-019 in AtT20-hCB1 and AtT20-hCB2
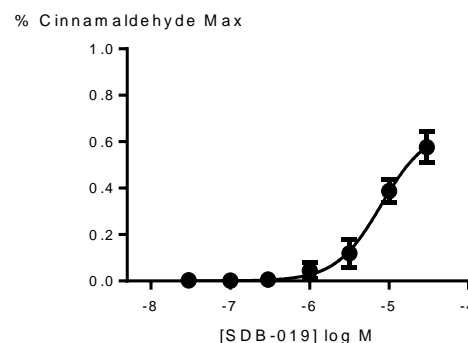
E: Concentration response curve for SDB-019 in HEK293-TRPA1
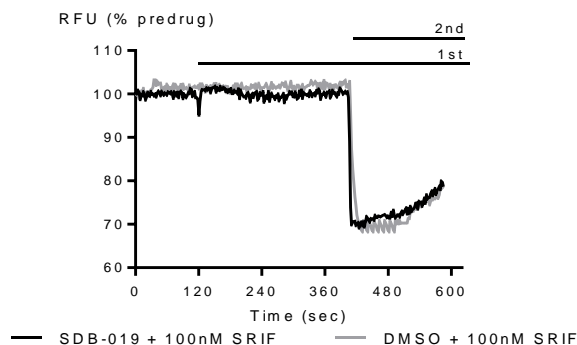
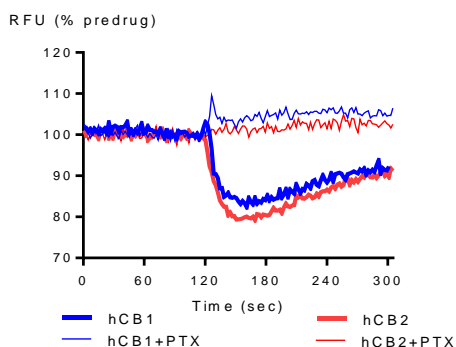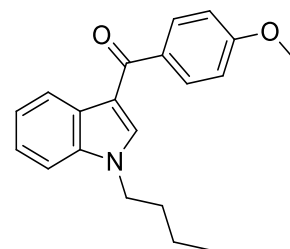C: Response of AtT20-WT to SDB-019 (10μM) followed by SRIF (100nM)
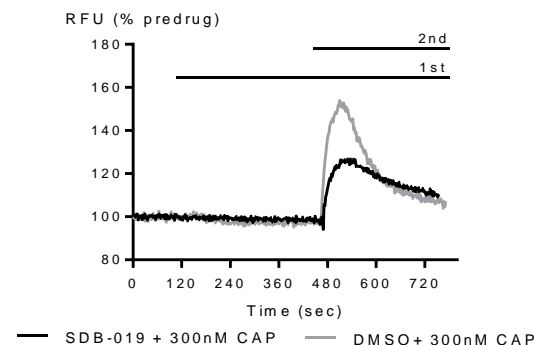
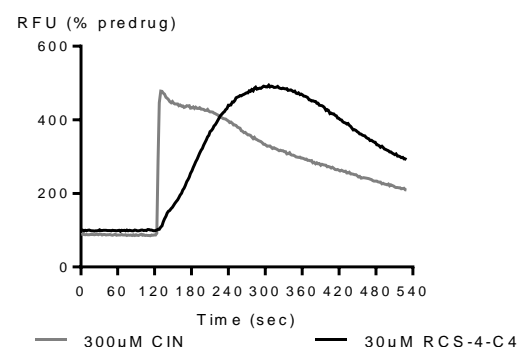F: Response of HEK293-TRPV1 to SDB-019 (30μM) followed by capsaicin (300nM)

	pEC50	MAX %	Notes
AtT20-hCB1	6.78 ± 0.09	103 ± 6	--
AtT20-hCB2	6.70 ± 0.08	69 ± 3	--
HEK293-TRPA1	5.10 ± 0.13	66 ± 10	--
HEK293-TRPV1	--	<10	Inhibits average max CAP response by 25%
AtT20 WT	--	<1	Inhibits average max SRIF response by <10%

SDB-020

N-(3-fluorobenzyl)-1-pentyl-1*H*-indole-3-carboxamide

A: Response of AtT20-CB1 and AtT20-CB2 to SDB-020 (10μM).

B: Concentration response curves for SDB-020 in AtT20-CB1 and AtT20-CB2
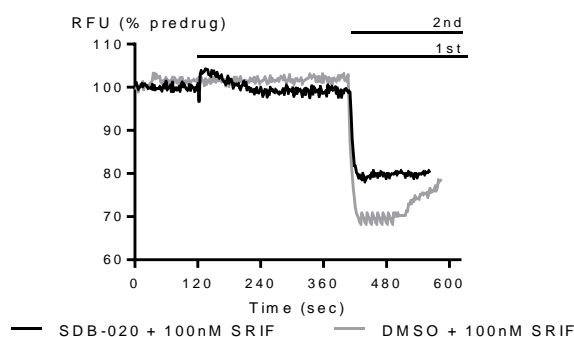
C: Response of AtT20-WT to SDB-020 (10μM) followed by SRIF (100nM)
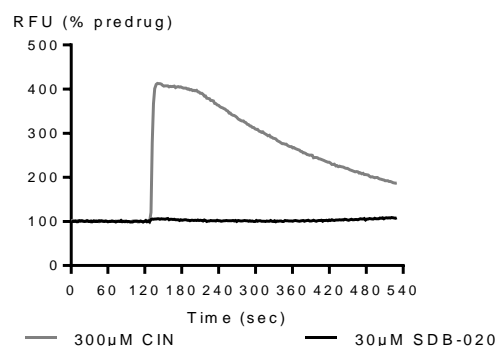
D: Response of HEK293-TRPA1 to SDB-020 (30μM) and cinnamaldehyde (300μM).
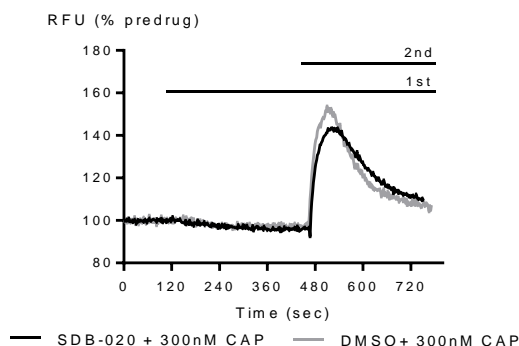
F: Response of HEK293-TRPV1 to SDB-020 (30μM) followed by capsaicin (300nM)

	pEC50	MAX %	Notes
AtT20-hCB1	5.64 ± 0.9**	73 ±4	--
AtT20-hCB2	6.24 ± 0.3	59 ± 13	--
HEK293-TRPA1	--	21 ± 6	Max <30% no CRC completed
HEK293-TRPV1	--	<5	Inhibits average max CAP response by 5%
AtT20 WT	--	<5	Inhibits average max SRIF response by 22%

**pEC50 assuming that the maximum is equivalent to the maximum of WIN 55-212,2

SDB-021

N-(4-fluorobenzyl)-1-pentyl-1*H*-indole-3-carboxamide

A: Response of AtT20-CB1 and AtT20-CB2 to SDB-021 (10μM).

B: Concentration response curves for SDB-021 in AtT20-hCB1 and AtT20-hCB2

C: Response of AtT20-WT to SDB-021 (10μM) followed by SRIF (100nM)
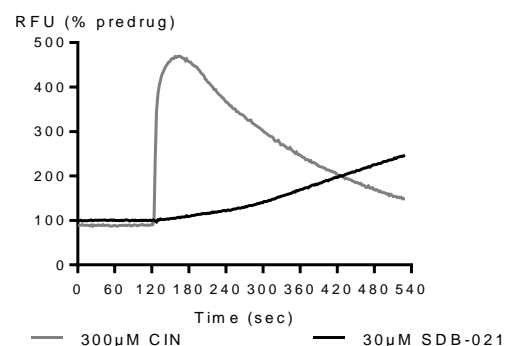
D: Response of HEK293-TRPA1 to SDB-021 (30μM) and cinnamaldehyde (300μM).
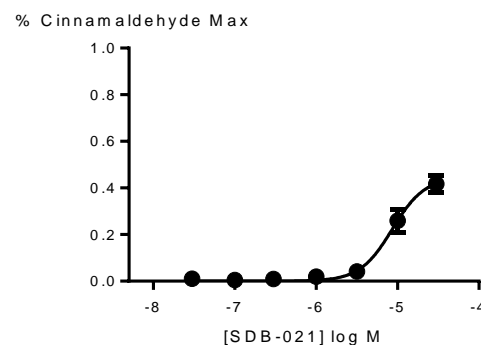
E: Concentration response curve for SDB-021 in HEK293-TRPA1

F: Response of HEK293-TRPV1 to SDB-021 (30μM) followed by capsaicin (300nM)

	pEC50	MAX %	Notes
AtT20-hCB1	5.4 ± 0.2**	61 ± 5	--
AtT20-hCB2	6.6 ± 0.3	52 ± 7	--
HEK293-TRPA1	5.07 ± 0.06	45 ± 4	--
HEK293-TRPV1	--	<5	Inhibits average max CAP response by <5%
AtT20 WT	--	<5	Inhibits average max SRIF response by <5%

**pEC50 assuming that the maximum is equivalent to the maximum of WIN 55-212,2

SDB-022

N-(2-methoxybenzyl)-1-pentyl-1*H*-indole-3-carboxamide

A: Response of AtT20-CB1 and AtT20-CB2 to SDB-022 (10μM).
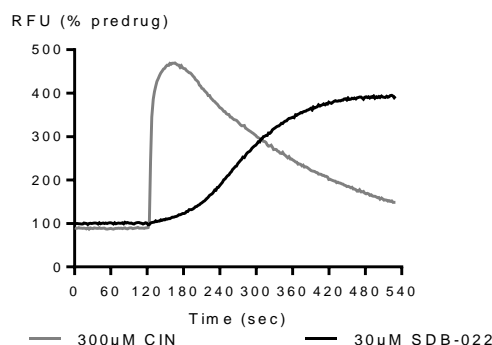
D: Response of HEK293-TRPA1 to SDB-022 (30μM) and cinnamaldehyde (300μM).
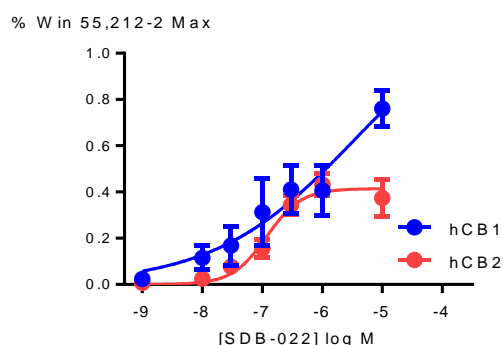
B: Concentration response curves for SDB-022 in AtT20-hCB1 and AtT20-hCB2
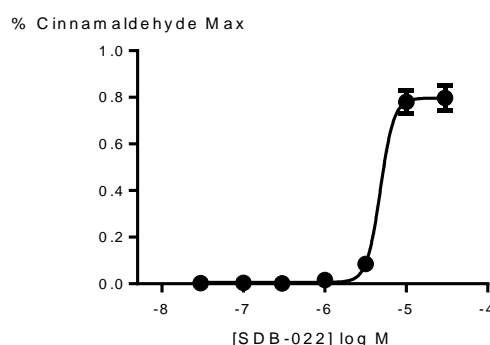
E: Concentration response curve for SDB-022 in HEK293-TRPA1
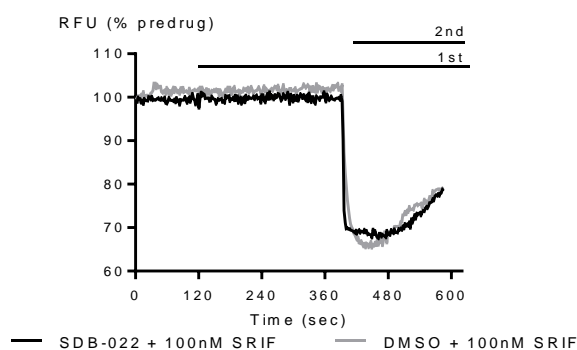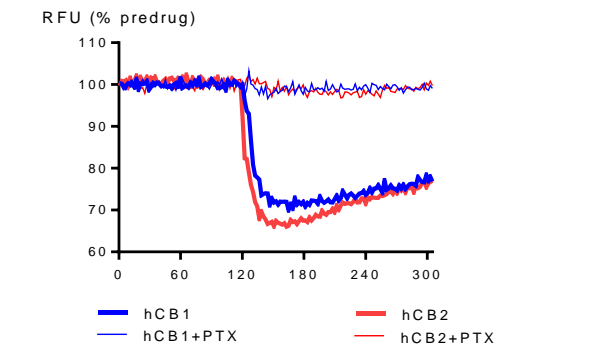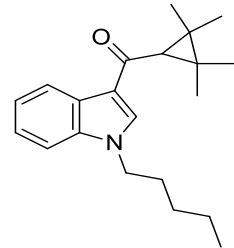

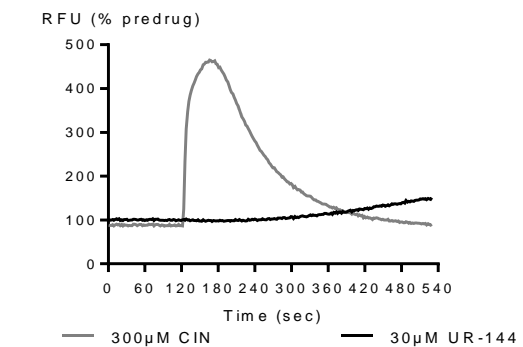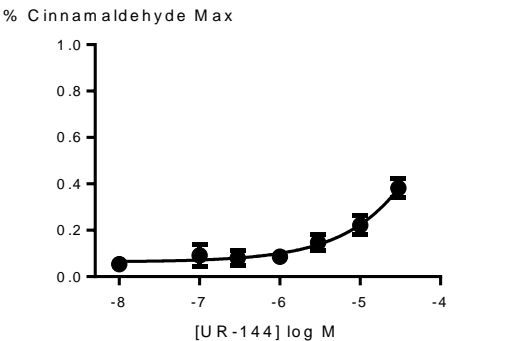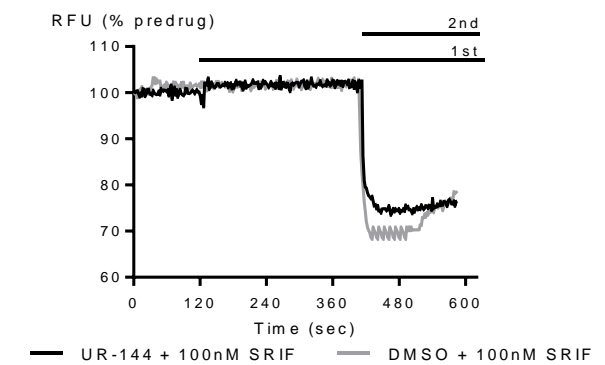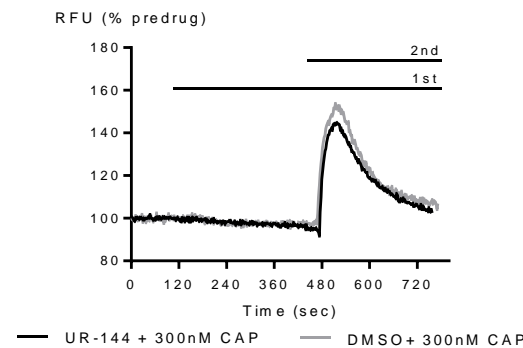C: Response of AtT20-WT to SDB-022 (10μM) followed by SRIF (100nM)

F: Response of HEK293-TRPV1 to SDB-022 (30μM) followed by capsaicin (300nM)

	pEC50	MAX %	Notes
AtT20-hCB1	6.0 ± 0.2**	76 ± 5	--
AtT20-hCB2	6.93 ± 0.1	41 ± 3	--
HEK293-TRPA1	5.32 ± 0.08	80 ± 3	--
HEK293-TRPV1	--	<10	Inhibits average max CAP response by <5%
AtT20 WT	--	<1	Inhibits average max SRIF response by 10%

**pEC50 assuming that the maximum is equivalent to the maximum of WIN 55-212,2

SDB-023

N-(3-methoxybenzyl)-1-pentyl-1*H*-indole-3-carboxamide

A: Response of AtT20-CB1 and AtT20-CB2 to SDB-023 (10μM).

B: Concentration response curves for SDB-023 in AtT20-hCB1 and AtT20-hCB2

C: Response of AtT20-WT to SDB-023 (10μM) followed by SRIF (100nM)
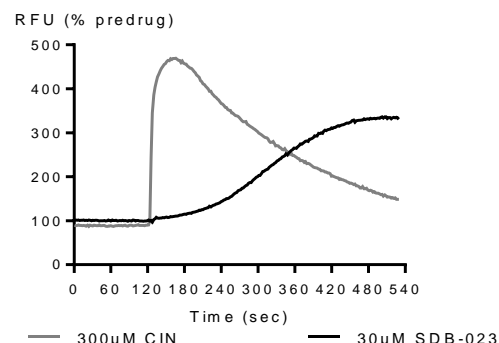
D: Response of HEK293-TRPA1 to SDB-023 (30μM) and cinnamaldehyde (300μM).

E: Concentration response curve for SDB-023 in HEK293-TRPA1
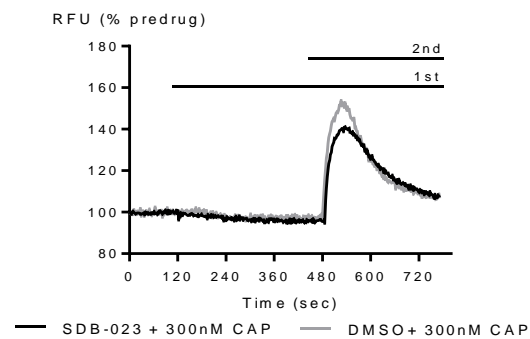
F: Response of HEK293-TRPV1 to SDB-023 (30μM) followed by capsaicin (300nM)

	pEC50	MAX %	Notes
AtT20-hCB1	6.41 ± 0.12	69 ± 7	--
AtT20-hCB2	6.8 ± 0.2	34 ± 4	--
HEK293-TRPA1	5.02 ± 0.04	63 ± 4	--
HEK293-TRPV1	--	<5	Inhibits average max CAP response by <10%
AtT20 WT	--	<5	Inhibits average max SRIF response by <10%

SDB-024

N-(4-methoxybenzyl)-1-pentyl-1*H*-indole-3-carboxamide
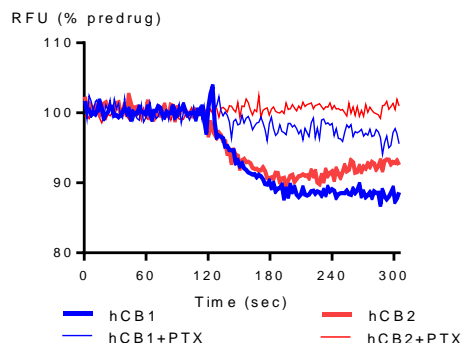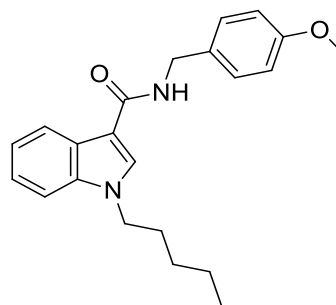
A: Response of AtT20-CB1 and AtT20-CB2 to SDB-024 (10μM).

D: Response of HEK293-TRPA1 to SDB-024 (30μM) and cinnamaldehyde (300μM).
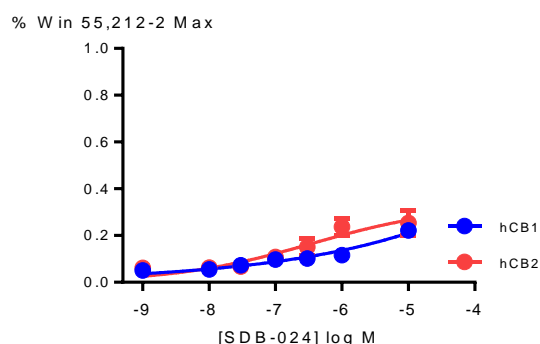
B: Concentration response curves for SDB-024 in AtT20-hCB1 and AtT20-hCB2
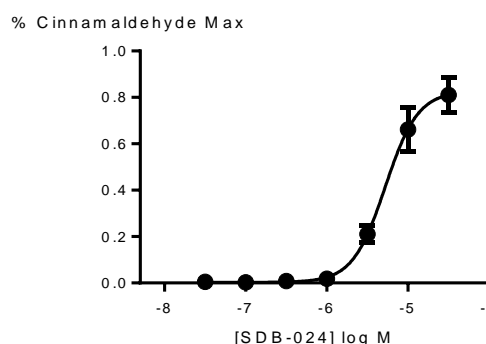
E: Concentration response curve for SDB-024 in HEK293-TRPA1
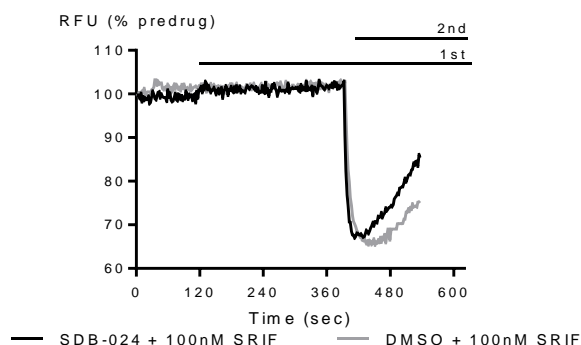
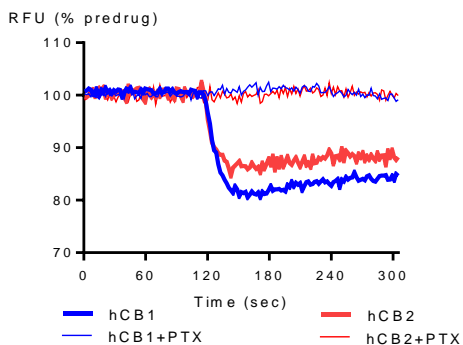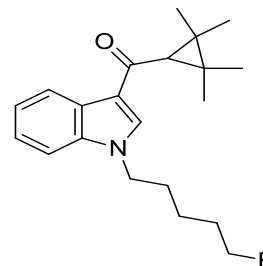C: Response of AtT20-WT to SDB-024 (10μM) followed by SRIF (100nM)
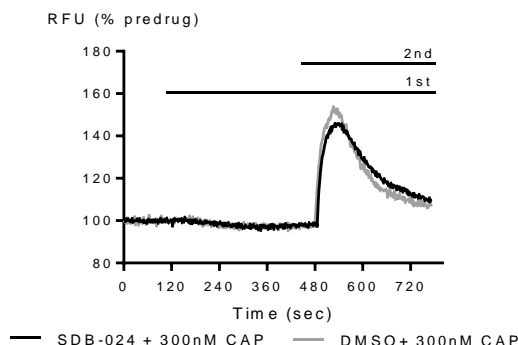
F: Response of HEK293-TRPV1 to SDB-024 (30μM) followed by capsaicin (300nM)

	pEC50	MAX %	Notes
AtT20-hCB1	2.3 ± 0.6**	22 ± 2	--
AtT20-hCB2	3.1 ± 0.6**	24 ± 4	--
HEK293-TRPA1	5.23 ± 0.07	83 ± 6	--
HEK293-TRPV1	--	12 ± 1	Inhibits average max CAP response by <5%
AtT20 WT	--	<1	Inhibits average max SRIF response by <10%

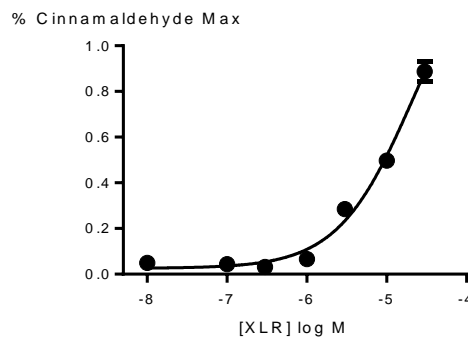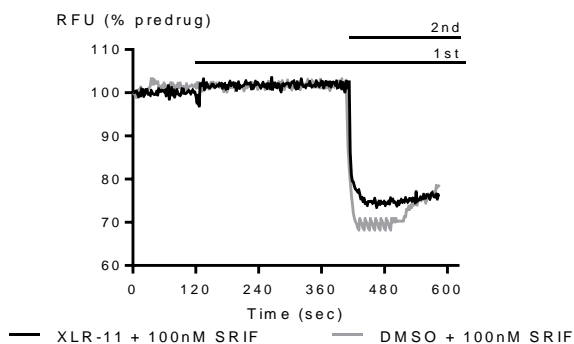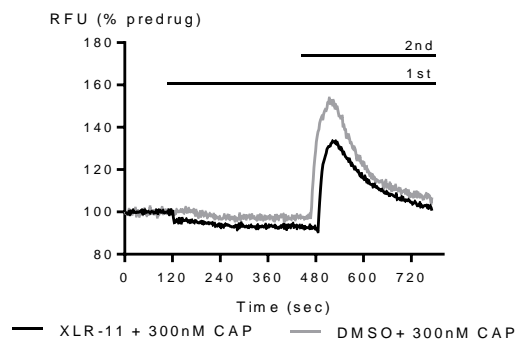**pEC50 assuming that the maximum is equivalent to the maximum of WIN 55-212,2

SDB-107

N-(adamantan-1-yl)-1-methyl-1*H*-indole-3-carboxamide

A: Response of AtT20-CB1 and AtT20-CB2 to SDB-107 (10μM).
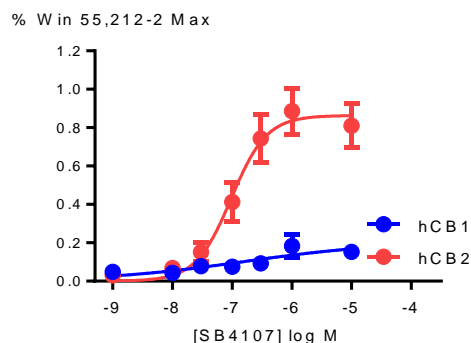
B: Concentration response curves for SDB-107 in AtT20-CB1 and AtT20-CB2

C: Response of AtT20-WT to SDB-107 (10μM) followed by SRIF (100nM)
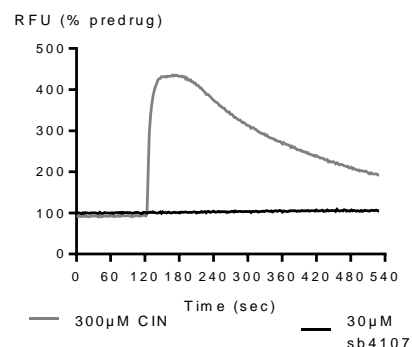
D: Response of HEK293-TRPA1 to SDB-107 (30μM) and cinnamaldehyde (300μM).
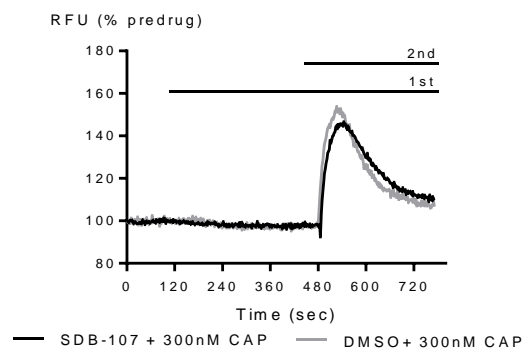
F: Response of HEK293-TRPV1 to SDB-107 (30μM) followed by capsaicin (300nM)

	pEC50	MAX %	Notes
AtT20-hCB1	0.93 ± 1**	20 ± 12	--
AtT20-hCB2	7.0 ± 0.1	86 ± 7	--
HEK293-TRPA1	--	<5	Max <30% no CRC completed
HEK293-TRPV1	--	<5	Inhibits average max CAP response by 10%
AtT20 WT	--	<5	Inhibits average max SRIF response by 10%

**pEC50 assuming that the maximum is equivalent to the maximum of WIN 55-212,2

RCS-2

(1-pentyl-1H-indol-3-yl)(2-methoxyphenyl)methanone
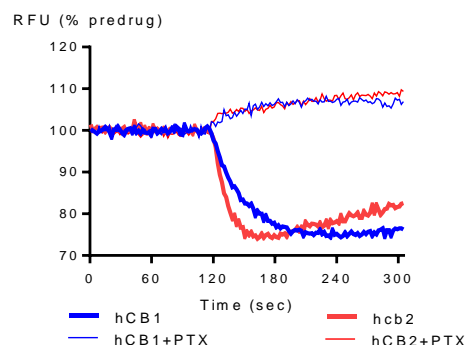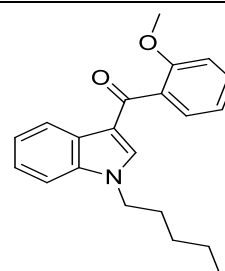
A: Response of AtT20-CB1 and AtT20-CB2 to RCS-2 (10μM).
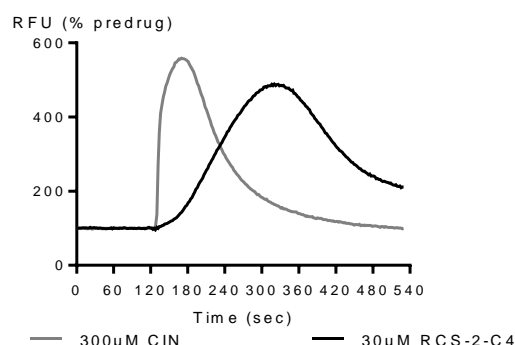
D: Response of HEK293-TRPA1 to RCS-2 (30μM) and cinnamaldehyde (300μM).
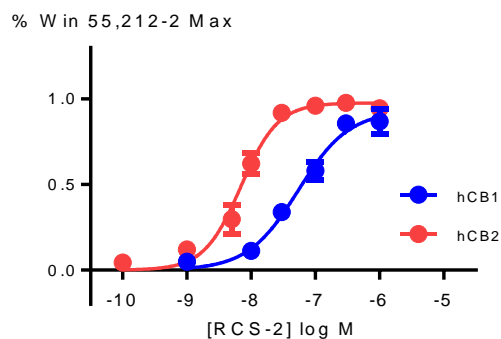
B: Concentration response curves for RCS-2 in AtT20-hCB1 and AtT20-hCB2
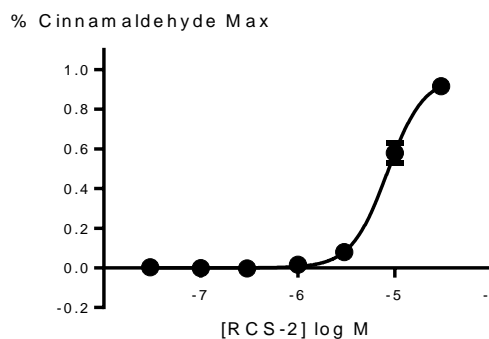
E: Concentration response curve for RCS-2 in HEK293-TRPA1
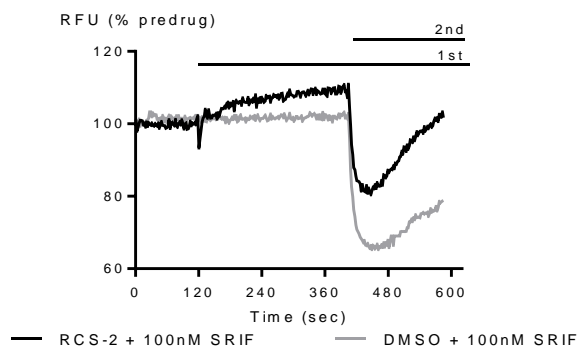
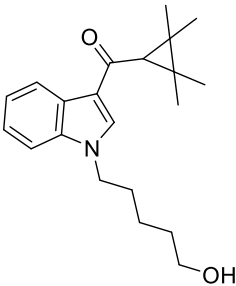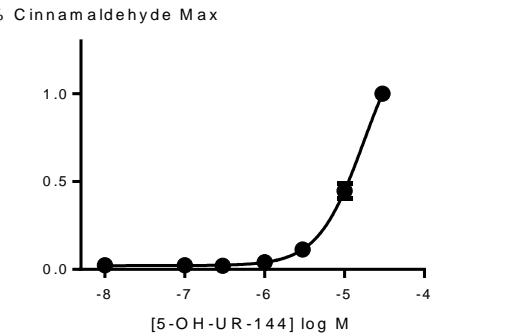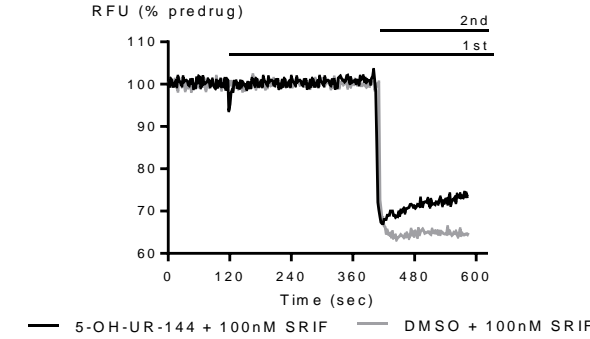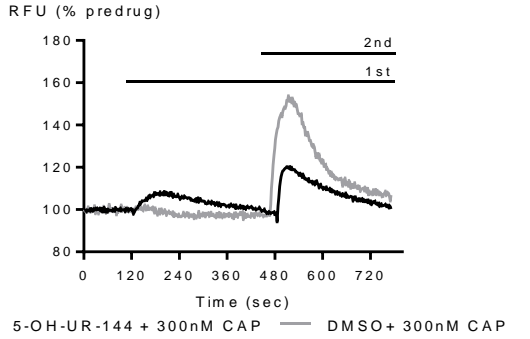C: Response of AtT20-WT to RCS-2 (10μM) followed by SRIF (100nM)
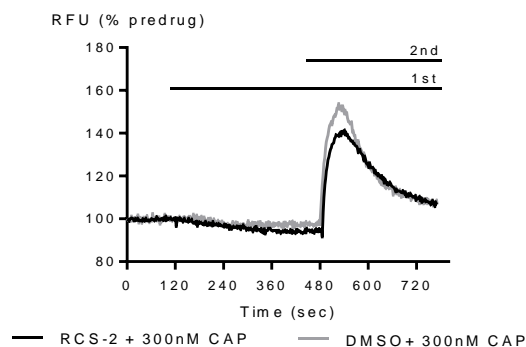
F: Response of HEK293-TRPV1 to RCS-2 (30μM) followed by capsaicin (300nM)

	pEC50	MAX %	Notes
AtT20-hCB1	7.27 ± 0.09	93 ± 6	--
AtT20-hCB2	8.16 ± 0.04	98 ± 3	--
HEK293-TRPA1	5.08 ± 0.03	96 ± 4	--
HEK293-TRPV1	--	<1	Inhibits average max CAP response by 24%
AtT20 WT	--	<1	Inhibits average max SRIF response by 42%

RCS-2-C4

(1-butyl-1H-indol-3-yl)(2-methoxyphenyl)methanone

A: Response of AtT20-CB1 and AtT20-CB2 to RCS-2-C4 (10μM).
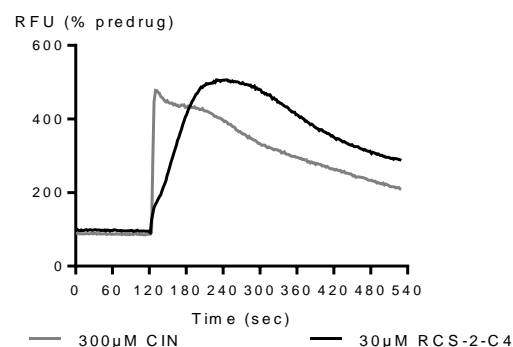
D: Response of HEK293-TRPA1 to RCS-2-C4 (30μM) and cinnamaldehyde (300μM).
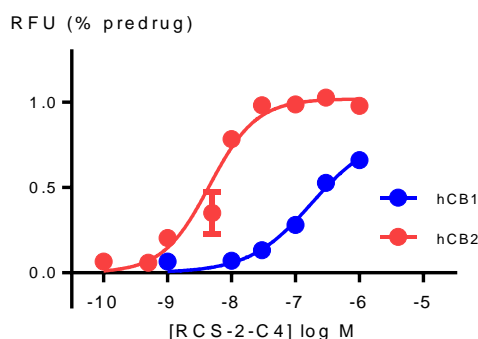
B: Concentration response curves for RCS-2-C4 in AtT20-hCB1 and AtT20-hCB2
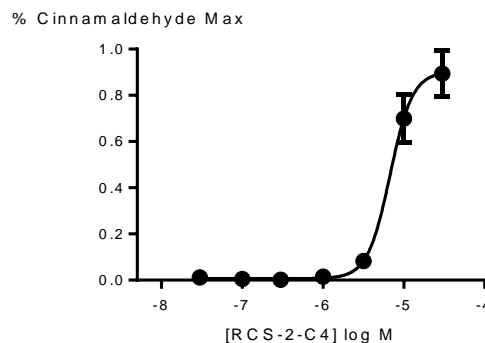
E: Concentration response curve for RCS-2-C4 in HEK293-TRPA1
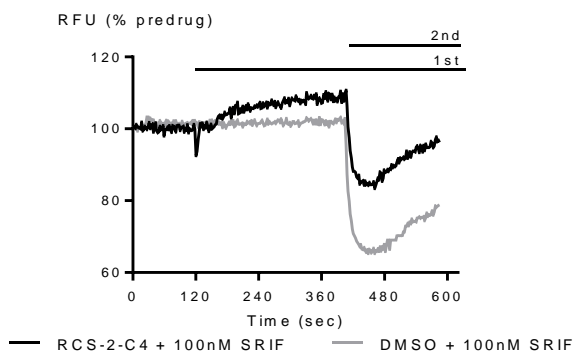
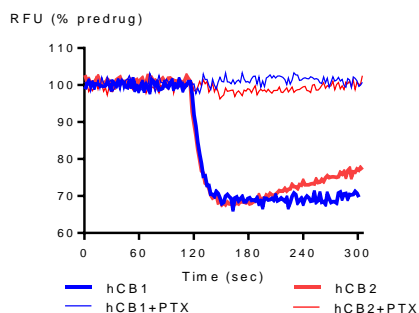C: Response of AtT20-WT to RCS-2-C4 (10μM) followed by SRIF (100nM)
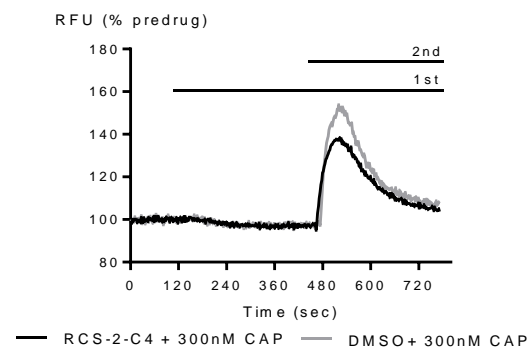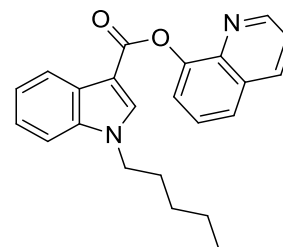

F: Response of HEK293-TRPV1 to RCS-2-C4 (30μM) followed by capsaicin (300nM)

	pEC50	MAX %	Notes
AtT20-hCB1	6.75± 0.13	83 ± 8	--
AtT20-hCB2	8.35 ± 0.05	102 ± 2	--
HEK293-TRPA1	5.17 ± 0.06	90 ± 6	--
HEK293-TRPV1	--	<5	Inhibits average max CAP response by 20%
AtT20 WT	--	<5	Inhibits average max SRIF response by 48%

RCS-3

2-(4-methoxyphenyl)-1-(1-pentyl-indol-3-yl)methanone

A: Response of AtT20-CB1 and AtT20-CB2 to RCS-3 (10μM).

D: Response of HEK293-TRPA1 to RCS-3 (30μM) and cinnamaldehyde (300μM).
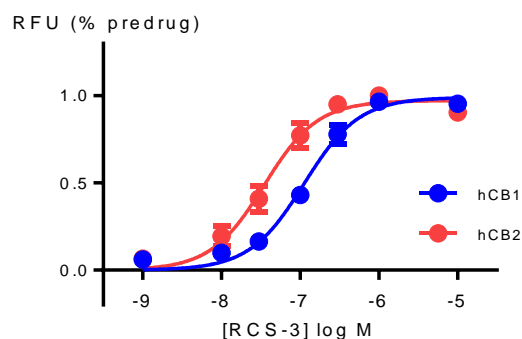

B: Concentration response curves for RCS-3 in AtT20-hCB1 and AtT20-hCB2
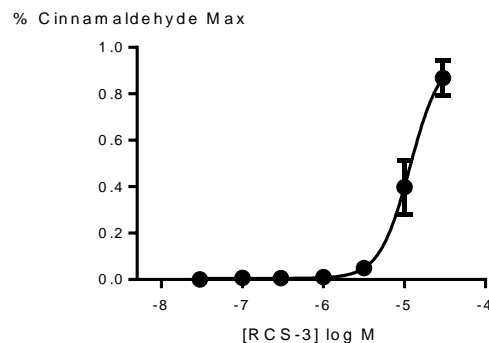
E: Concentration response curve for RCS-3 in HEK293-TRPA1
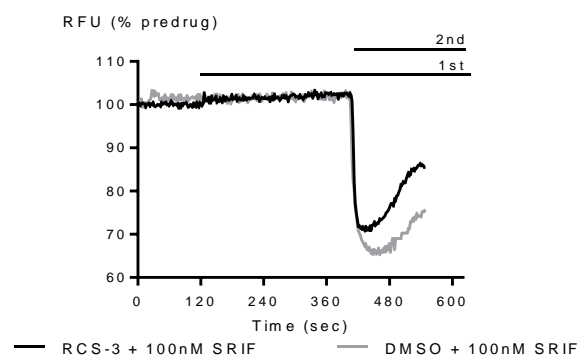
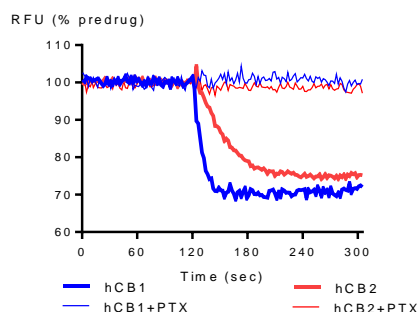C: Response of AtT20-WT to RCS-3 (10μM) followed by SRIF (100nM)
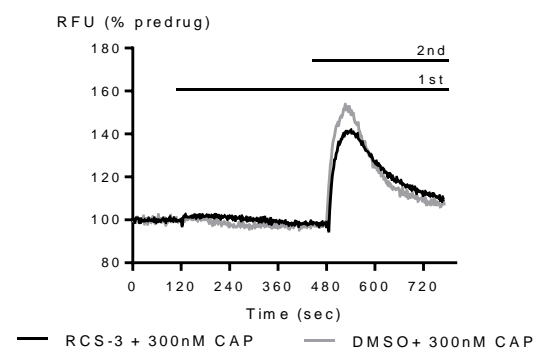
F: Response of HEK293-TRPV1 to RCS-3 (30μM) followed by capsaicin (300nM)

	pEC50	MAX %	Notes
AtT20-hCB1	6.95 ± 0.05	99 ± 3	--
AtT20-hCB2	7.46 ± 0.06	97 ± 4	--
HEK293-TRPA1	4.93 ± 0.11	97 ± 18	--
HEK293-TRPV1	--	<10	Inhibits average max CAP response by 25%
AtT20 WT	--	<1	Inhibits average max SRIF response by 27%

RCS-3-C4

(1-butyl-1H-indol-3-yl)(3-methoxyphenyl)methanone

A: Response of AtT20-CB1 and AtT20-CB2 to RCS-3-C4 (10μM).
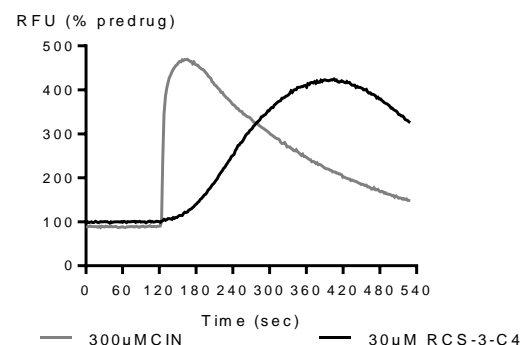
D: Response of HEK293-TRPA1 to RCS-3-C4 (30μM) and cinnamaldehyde (300μM).
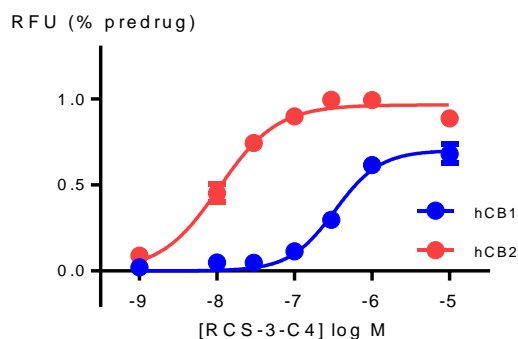
B: Concentration response curves for RCS-3-C4 in AtT20-hCB1 and AtT20-hCB2

E: Concentration response curve for RCS-3-C4 in HEK293-TRPA1
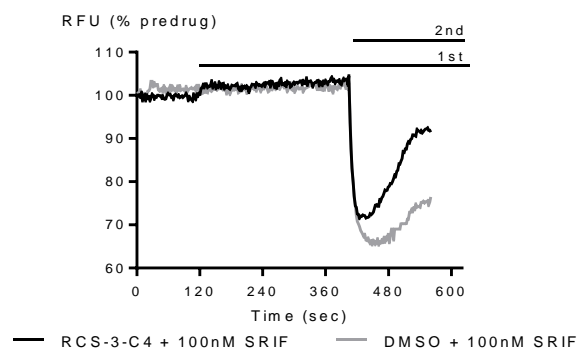
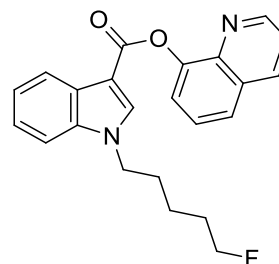C: Response of AtT20-WT to RCS-3-C4 (10μM) followed by SRIF (100nM)
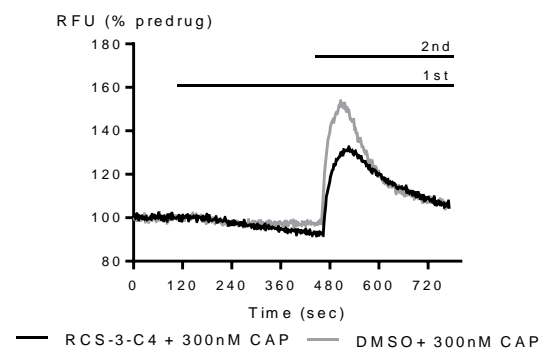
F: Response of HEK293-TRPV1 to RCS-3-C4 (30μM) followed by capsaicin (300nM)

	pEC50	MAX %	Notes
AtT20-hCB1	6.48 ± 0.05	70 ± 3	--
AtT20-hCB2	7.97 ± 0.05	97 ± 2	--
HEK293-TRPA1	5.09 ± 0.03	107 ± 5	--
HEK293-TRPV1	--	15 ± 2	Inhibits average max CAP response by 24%
AtT20 WT	--	<1	Inhibits average max SRIF response by 30%

RCS-4

- **SR-19**
- **BTM-4**
- **OBT-199**

2-(4-methoxyphenyl)-1-(1-pentyl-indol-3-yl)methanone
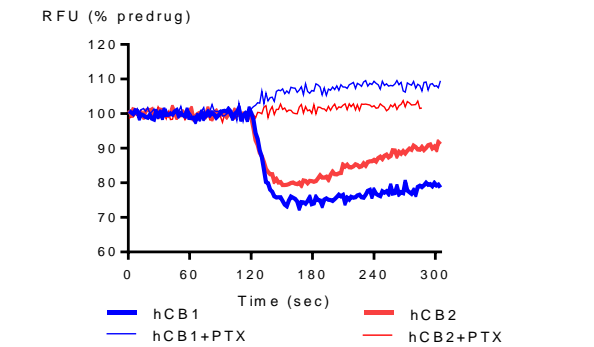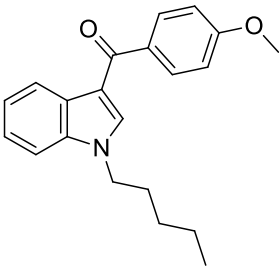
A: Response of AtT20-CB1 and AtT20-CB2 to RCS-4 (10μM).


B: Concentration response curves for RCS-4 in AtT20-hCB1 and AtT20-hCB2

C: Response of AtT20-WT to RCS-4 (10μM) followed by SRIF (100nM)
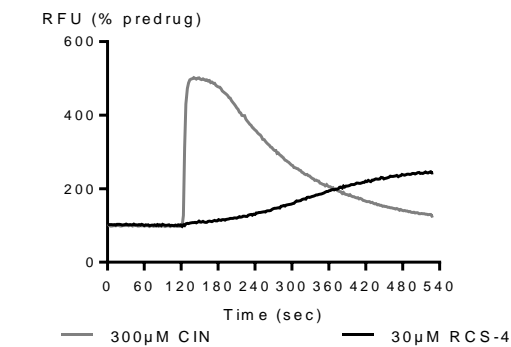
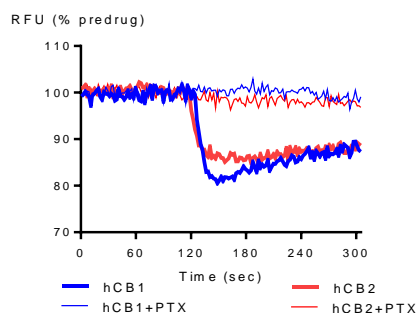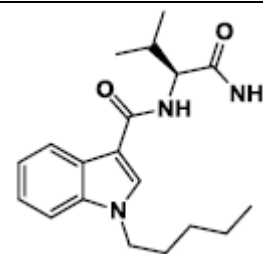D: Response of HEK293-TRPA1 to RCS-4 (30μM) and cinnamaldehyde (300μM).
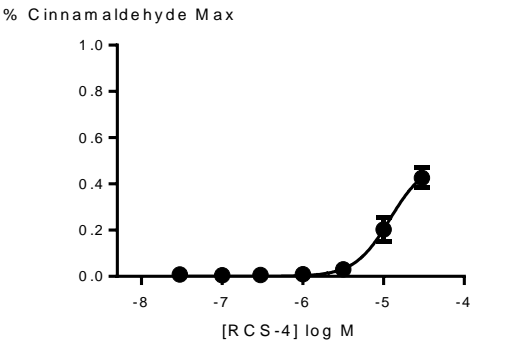
E: Concentration response curve for RCS-4 in HEK293-TRPA1
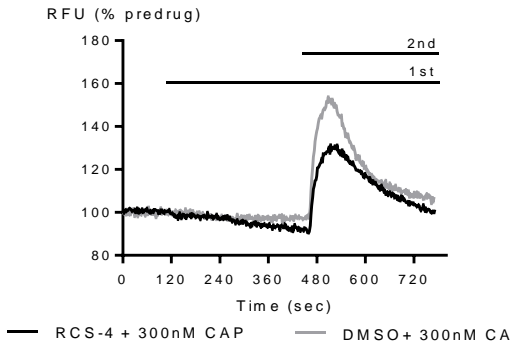
F: Response of HEK293-TRPV1 to RCS-4 (30μM) followed by capsaicin (300nM)

	pEC50	MAX %	Notes
AtT20-hCB1	6.84 ± 0.6	88 ± 4	--
AtT20-hCB2	7.34 ± 0.9	87 ± 4	--
HEK293-TRPA1	4.92 ± 0.13	50 ± 10	--
HEK293-TRPV1	--	<5	Inhibits average max CAP response by 16%
AtT20 WT	--	<1	Inhibits average max SRIF response by <5%

RCS-4-C4

(1-butyl-1H-indol-3-yl)(4-methoxyphenyl)methanone

A: Response of AtT20-CB1 and AtT20-CB2 to RCS-4-C4 (10μM).

D: Response of HEK293-TRPA1 to RCS-4-C4 (30μM) and cinnamaldehyde (300μM).
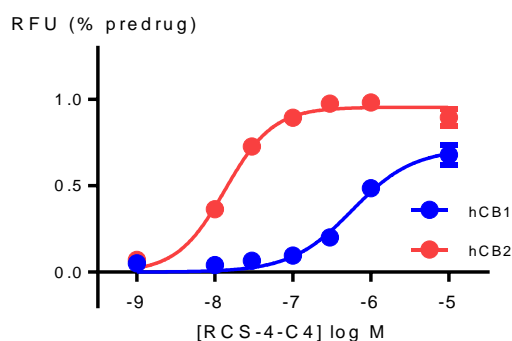
B: Concentration response curves for RCS-4-C4 in AtT20-hCB1 and AtT20-hCB2
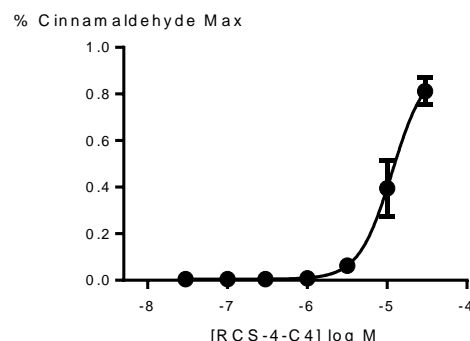
E: Concentration response curve for RCS-4-C4 in HEK293-TRPA1
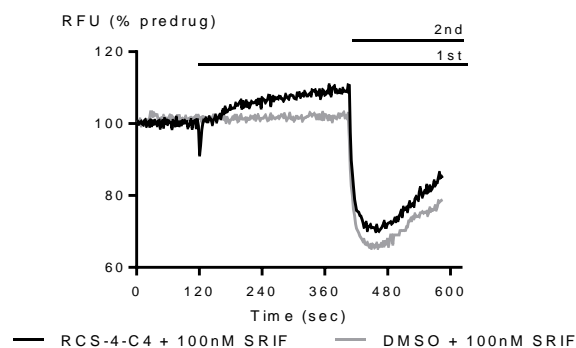
C: Response of AtT20-WT to RCS-4-C4 (10μM) followed by SRIF (100nM)
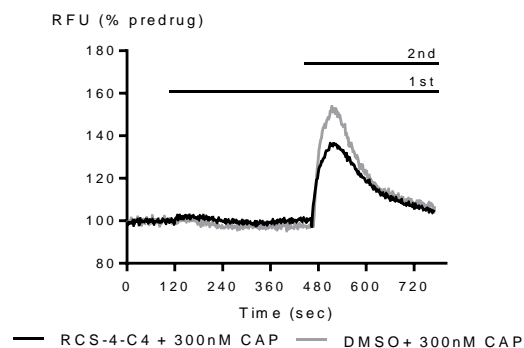
F: Response of HEK293-TRPV1 to RCS-4-C4 (30μM) followed by capsaicin (300nM)

	pEC50	MAX %	Notes
AtT20-hCB1	6.42 ± 0.8	72 ± 4	--
AtT20-hCB2	7.87 ± 0.4	96 ± 2	--
HEK293-TRPA1	4.94 ± 0.12	92 ± 20	--
HEK293-TRPV1	--	15 ± 2	Inhibits average max CAP response by 17%
AtT20 WT	--	<1	Inhibits average max SRIF response by 36%

UR-144
(1-Pentyl-1H-indol-3-yl)(2,2,3,3-tetramethylcyclopropyl)methanone

A: Response of AtT20-CB1 and AtT20-CB2 to UR-144 (10μM).

D: Response of HEK293-TRPA1 to UR-144 (30μM) and cinnamaldehyde (300μM).
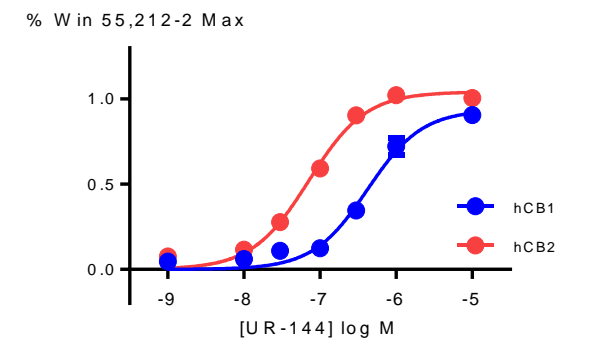
B: Concentration response curves for UR-144 in AtT20-hCB1 and AtT20-hCB2

E: Concentration response curve for UR-144 in HEK293-TRPA1

C: Response of AtT20-WT to UR-144 (10μM) followed by SRIF (100nM)

F: Response of HEK293-TRPV1 to UR-144 (30μM) followed by capsaicin (300nM)

	pEC50	MAX %	Notes
AtT20-hCB1	6.38 ± 0.06	94 ± 4	--
AtT20-hCB2	7.15 ± 0.05	104 ± 3	--
HEK293-TRPA1	$3.91 \pm 0.22*$	38 ± 2	--
HEK293-TRPV1	--	<5	Inhibits average max CAP response by 12%
AtT20 WT	--	<1	Inhibits average max SRIF response by <10%

*pEC50 assuming that the maximum is equivalent to the maximum of cinnamaldehyde

XLR-11

(1-(5-Fluoropentyl)-1H-indol-3-yl)(2,2,3,3-tetramethylcyclopropyl)methanone

A: Response of AtT20-CB1 and AtT20-CB2 to XLR-11 (10μM).
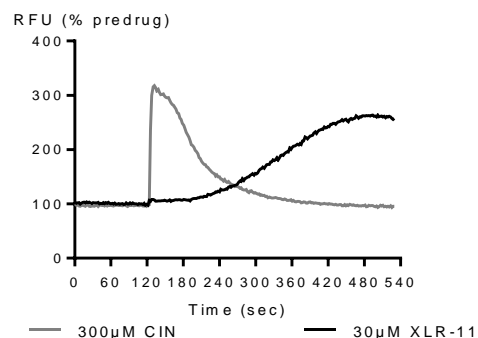
D: Response of HEK293-TRPA1 to XLR-11 (30μM) and cinnamaldehyde (300μM).
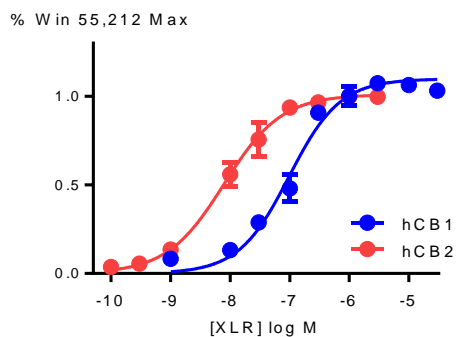
B: Concentration response curves for XLR-11 in AtT20-hCB1 and AtT20-hCB2

E: Concentration response curve for XLR-11 in HEK293-TRPA1

C: Response of AtT20-WT to XLR-11 (10 μM) followed by SRIF (100nM)

F: Response of HEK293-TRPV1 to XLR-11 (30 μM) followed by capsaicin (300nM)

*pEC50 assuming that the maximum is equivalent to the maximum of cinnamaldehyde

	pEC50	MAX %	Notes
AtT20-hCB1	7.01 ± 0.07	110 ± 4	--
AtT20-hCB2	8.10 ± 0.06	101 ± 3	--
HEK293-TRPA1	3.91 ± 0.2*	89 ± 2	--
HEK293-TRPV1	--	<1	Inhibits average max CAP response by 30%
AtT20 WT	--	<5	Inhibits average max SRIF response by <10%

5-OH-UR-144

(1-(5-Hydroxypentyl)-1H-indol-3-yl)(2,2,3,3-tetramethylcyclopropyl)methanone
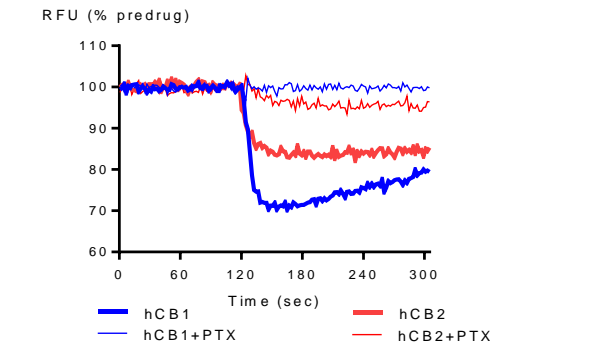
A: Response of AtT20-CB1 and AtT20-CB2 to 5-OH-UR-144 (10μM).
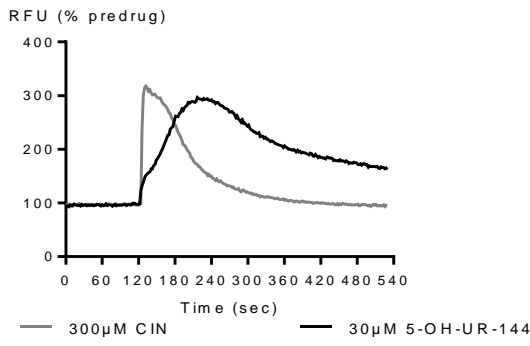
D: Response of HEK293-TRPA1 to 5-OH-UR-144 (30μM) and cinnamaldehyde (300μM).
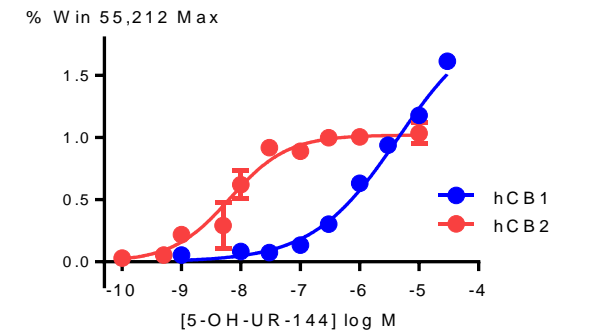
B: Concentration response curves for 5-OH-UR-144 in AtT20-hCB1 and AtT20-hCB2

E: Concentration response curve for 5-OH-UR-144 in HEK293-TRPA1

C: Response of AtT20-WT to 5-OH-UR-144 (10 μM) followed by SRIF (100nM)

F: Response of HEK293-TRPV1 to 5-OH-UR-144 (30 μM) followed by capsaicin (300nM)

	pEC50	MAX %	Notes
AtT20-hCB1	5.36 ± 0.26	159 ± 30	--
AtT20-hCB2	8.18 ± 0.11	102 ± 4	--
HEK293-TRPA1	4.6 ± 0.2	100 ± 5	--
HEK293-TRPV1	--	37 ± 2	Inhibits average max CAP response by 60%
AtT20 WT	--	<10	Inhibits average max SRIF response by 15%

PB-22

Quinolin-8-yl-1-pentyl-1H-indole-3-carboxylate



A: Response of AtT20-CB1 and AtT20-CB2 to PB-22 (10μM).
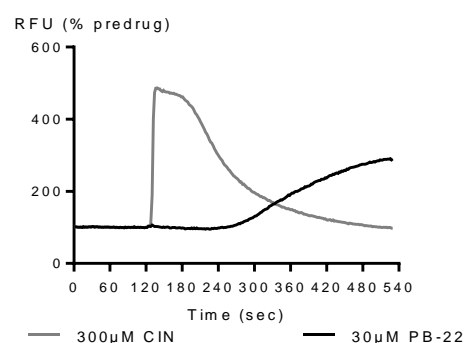
D: Response of HEK293-TRPA1 to PB-22 (30μM) and cinnamaldehyde (300μM).
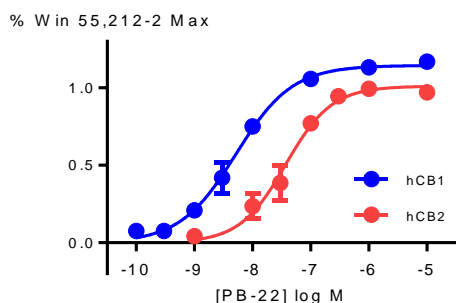
B: Concentration response curves for PB-22 in AtT20-hCB1 and AtT20-hCB2
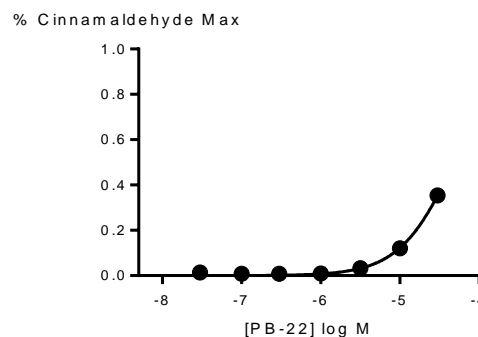
E: Concentration response curve for PB-22 in HEK293-TRPA1
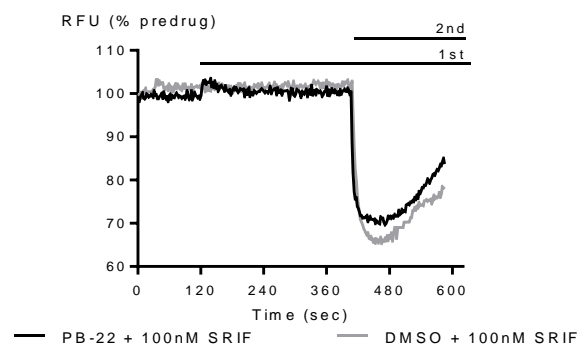
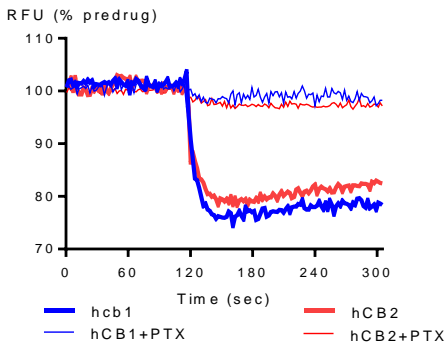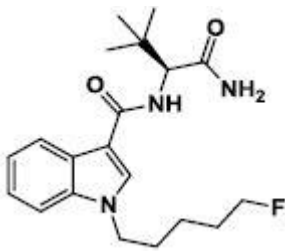C: Response of AtT20-WT to PB-22 (10μM) followed by SRIF (100nM)
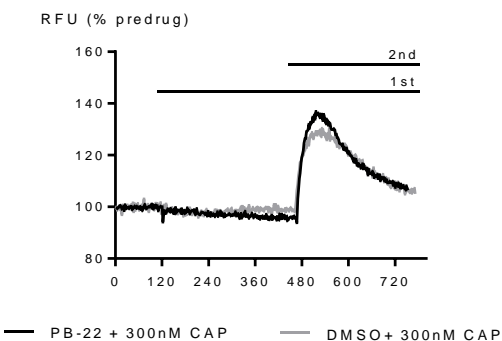
F: Response of HEK293-TRPV1 to PB-22 (30μM) followed by capsaicin (300nM)

	pEC50	MAX %	Notes
AtT20-hCB1	8.30 ± 0.06	114 ± 3	--
AtT20-hCB2	7.43 ± 0.08	101 ± 5	--
HEK293-TRPA1	$4.31 \pm 0.03*$	35 ± 2	--
HEK293-TRPV1	--	<10	Inhibits average max CAP response by <10%
AtT20 WT	--	<5	Inhibits average max SRIF response by 15%

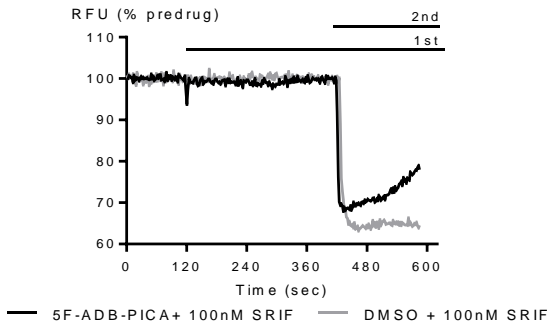*pEC50 assuming that the maximum is equivalent to the maximum of cinnamaldehyde

5F-PB-22

N-cyclohexyl-1-propyl-1*H*-indole-3-carboxamide

A: Response of AtT20-CB1 and AtT20-CB2 to 5F-PB-22 (10μM).
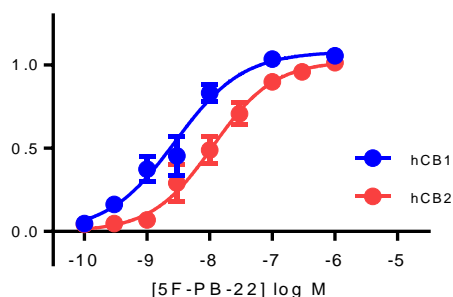
B: Concentration response curves for 5F-PB-22 in AtT20-CB1 and AtT20-CB2
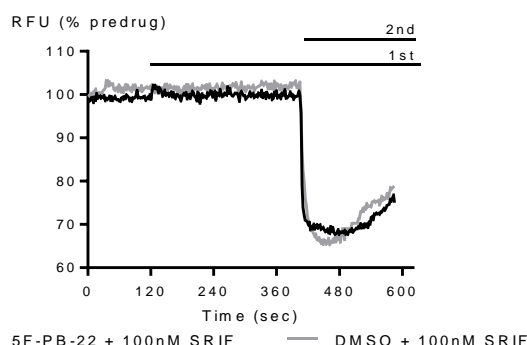
C: Response of AtT20-WT to 5F-PB-22 (10μM) followed by SRIF (100nM)
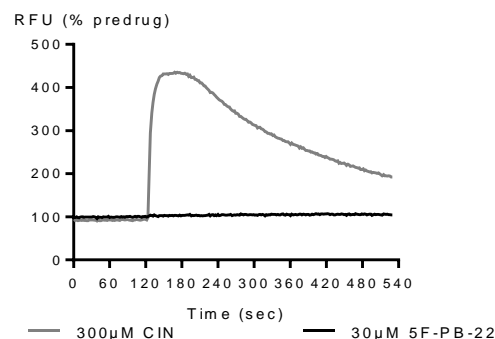
D: Response of HEK293-TRPA1 to 5F-PB-22 (30μM) and cinnamaldehyde (300μM).
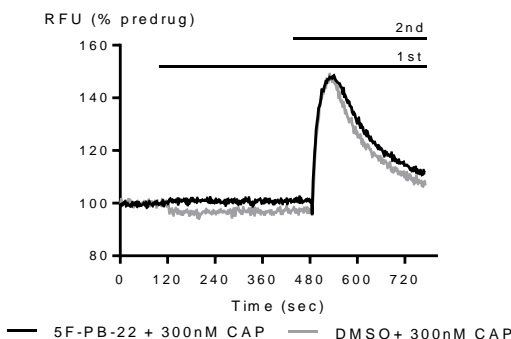
F: Response of HEK293-TRPV1 to 5F-PB-22 (30μM) followed by capsaicin (300nM)

	pEC50	MAX %	Notes
AtT20-hCB1	8.55 ± 0.1	108 ± 5	--
AtT20-hCB2	7.95 ± 0.08	102 ± 4	--
HEK293-TRPA1	--	<10	Max <30% no CRC completed
HEK293-TRPV1	--	<10	Inhibits average max CAP response by <5%
AtT20 WT	--	<5	Inhibits average max SRIF response by 15%

AB-PICA

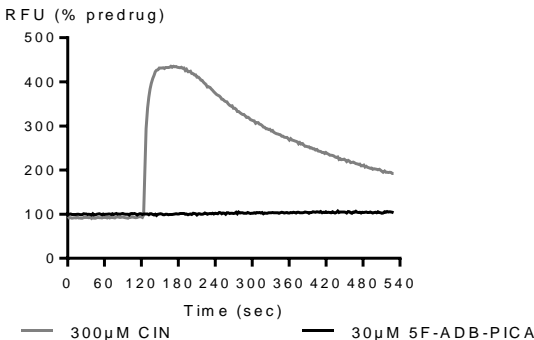(*S*)-*N*-(1-amino-3-methyl-1-oxobutan-2-yl)-1-pentyl-indole-3-carboxamide



A: Response of AtT20-CB1 and AtT20-CB2 to AB-PICA (10μM).
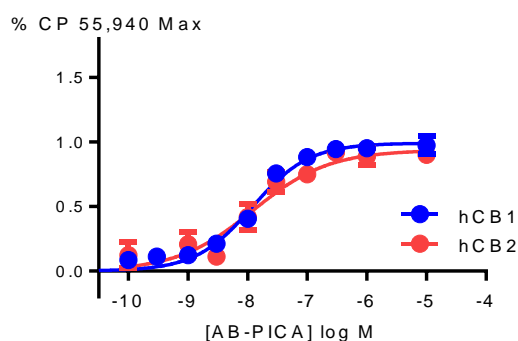
B: Concentration response curves for AB-PICA in AtT20-CB1 and AtT20-CB2
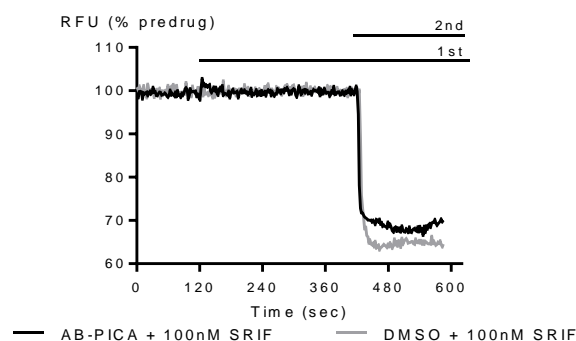
C: Response of AtT20-WT to AB-PICA (10μM) followed by SRIF (100nM)
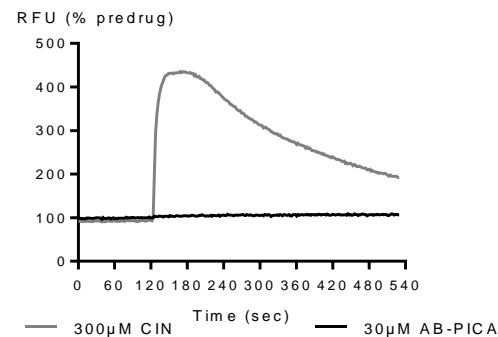
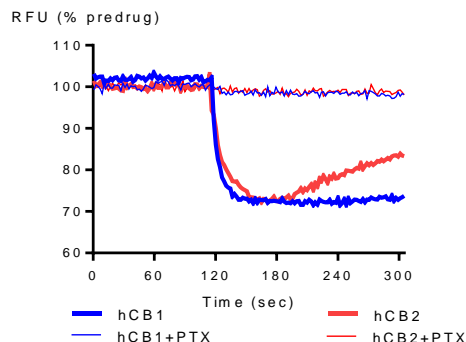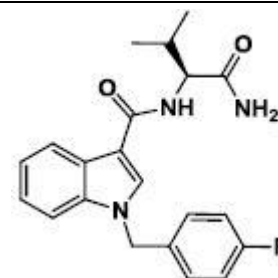D: Response of HEK293-TRPA1 to AB-PICA (30μM) and cinnamaldehyde (300μM).
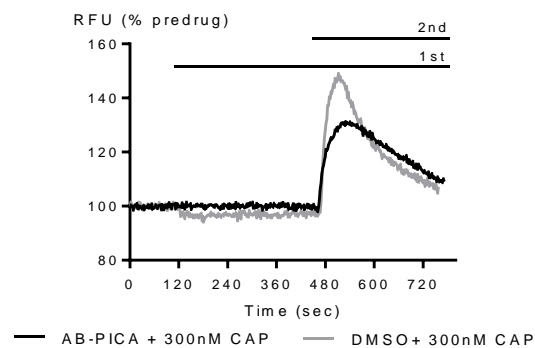
F: Response of HEK293-TRPV1 to AB-PICA (30μM) followed by capsaicin (300nM)

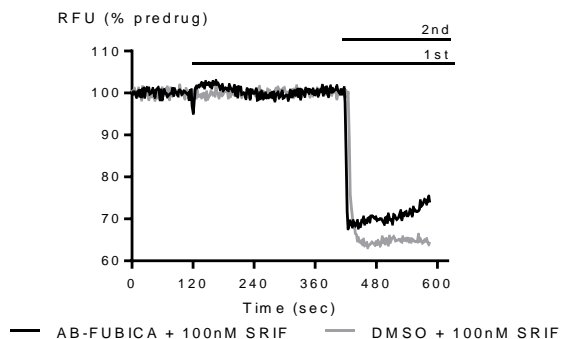|	pEC50	MAX %	Notes
AtT20-hCB1	7.92 ± 0.07	99 ± 3	--
AtT20-hCB2	7.92 ± 0.21	94 ± 9	--
HEK293-TRPA1	--	<5	Max <30% no CRC completed
HEK293-TRPV1	--	<5	Inhibits average max CAP response by 12%
AtT20 WT	--	<5	Inhibits average max SRIF response by 15%

5F-AB-PICA

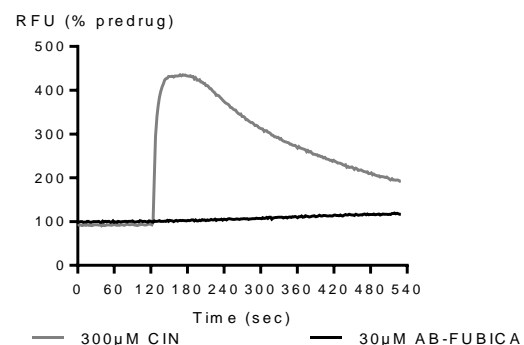(S)-N-(1-amino-3-methyl-1-oxobutan-2-yl)-1-(5-fluoropentyl)-indole-3-carboxamide
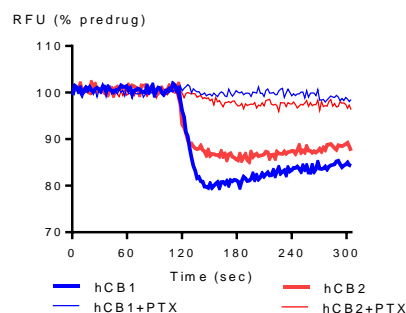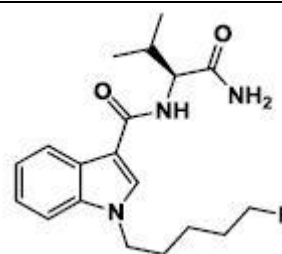
A: Response of AtT20-CB1 and AtT20-CB2 to 5F-AB-PICA (10μM).
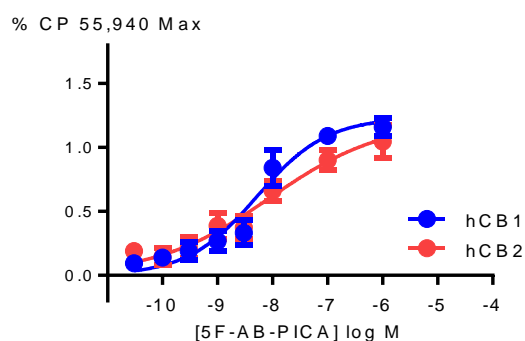
B: Concentration response curves for 5F-AB-PICA in AtT20-CB1 and AtT20-CB2
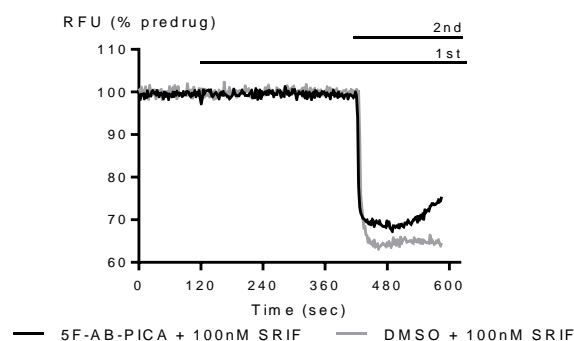
D: Response of HEK293-TRPA1 to 5F-AB-PICA (30μM) and cinnamaldehyde (300μM).

C: Response of AtT20-WT to 5F-AB-PICA (10μM) followed by SRIF (100nM)
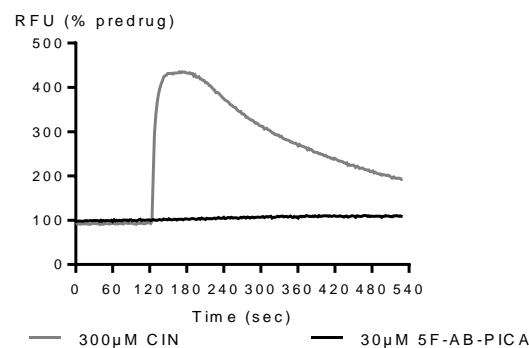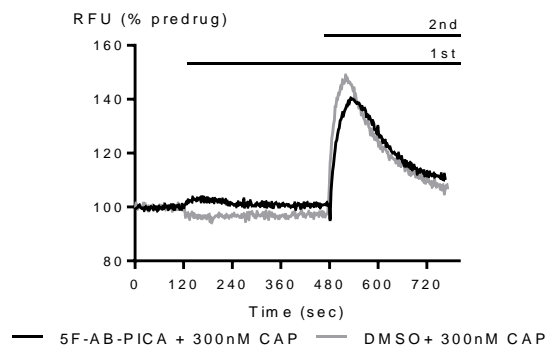
F: Response of HEK293-TRPV1 to 5F-AB-PICA (30μM) followed by capsaicin (300nM)

	pEC50	MAX %	Notes
AtT20-hCB1	8.28 ± 0.21	123± 13	--
AtT20-hCB2	8.05 ± 0.53	121 ± 24	--
HEK293-TRPA1	--	<1	Max <30% no CRC completed
HEK293-TRPV1	--	<10	Inhibits average max CAP response by 17%
AtT20 WT	--	<5	Inhibits average max SRIF response by <10%

ADB-PICA

(S)-N-(1-amino-3,3-dimethyl-1-oxobutan-2-yl)-1-pentyl-indole-3-carboxamide
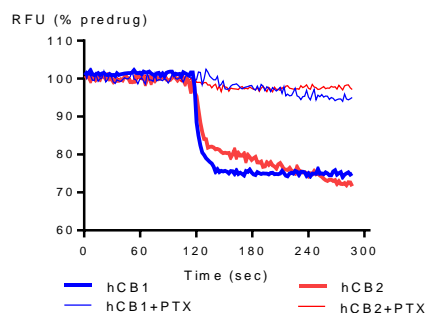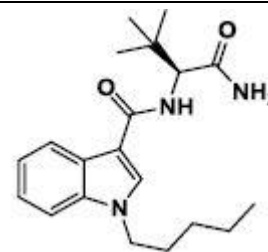
A: Response of AtT20-CB1 and AtT20-CB2 to ADB-PICA (10μM).
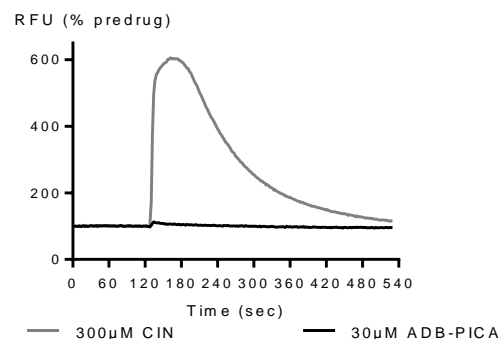
D: Response of HEK293-TRPA1 to ADB-PICA (30μM) and cinnamaldehyde (300μM).
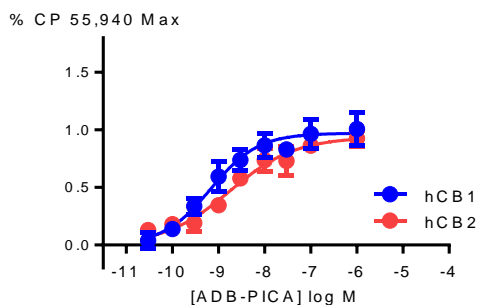
B: Concentration response curves for ADB-PICA in AtT20-hCB1 and AtT20-hCB2
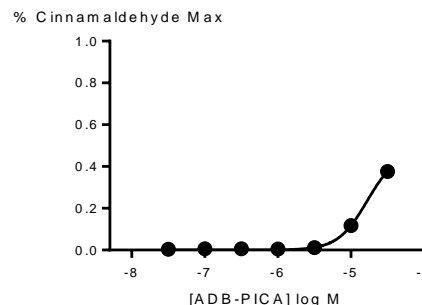
E: Concentration response curve for ADB-PICA in HEK293-TRPA1
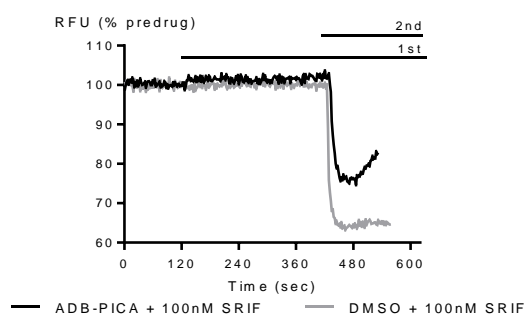
C: Response of AtT20-WT to ADB-PICA (10μM) followed by SRIF (100nM)
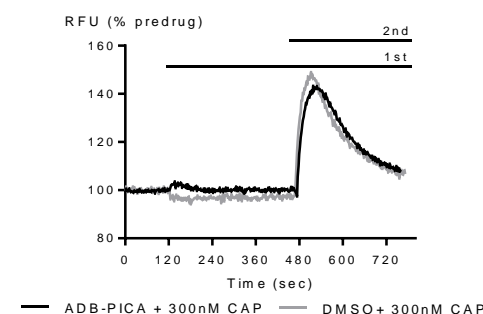
F: Response of HEK293-TRPV1 to ADB-PICA (30μM) followed by capsaicin (300nM)

	pEC50	MAX %	Notes
AtT20-hCB1	9.16 ± 0.16	98 ± 7	--
AtT20-hCB2	8.75 ± 0.18	94 ± 7	--
HEK293-TRPA1	4.34 ± 0.02*	34 ± 1	--
HEK293-TRPV1	--	<10	Inhibits average max CAP response by 25%
AtT20 WT	--	17 ± 10	Inhibits average max SRIF response by 21%

*pEC50 assuming that the maximum is equivalent to the maximum of cinnamaldehyde

---

5F-ADB-PICA

(S)-N-(1-amino-3,3-dimethyl-1-oxobutan-2-yl)-1-(5-fluoropentyl)-indole-3-carboxamide

A: Response of AtT20-CB1 and AtT20-CB2 to 5F-ADB-PICA (10μM).
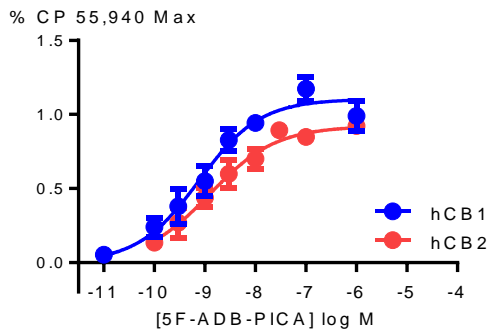
B: Concentration response curves for 5F-ADB-PICA in AtT20-hCB1 and AtT20-hCB2

D: Response of HEK293-TRPA1 to 5F-ADB-PICA (30μM) and cinnamaldehyde (300μM).
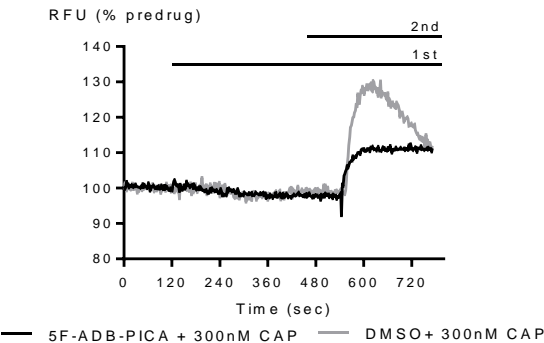
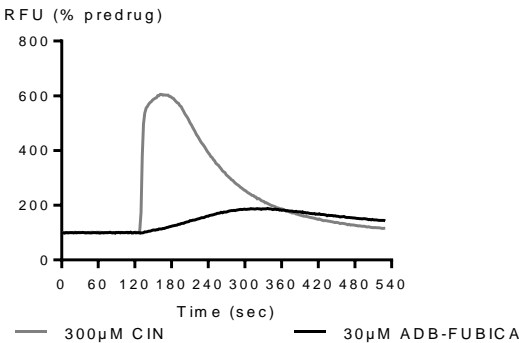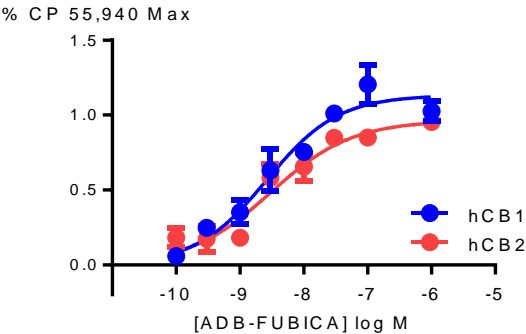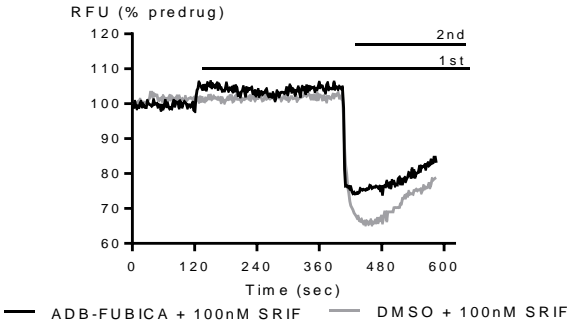F: Response of HEK293-TRPV1 to 5F-ADB-PICA (30μM) followed by capsaicin (300nM)

C: Response of AtT20-WT to 5F-ADB-PICA (10μM) followed by SRIF (100nM)

	pEC50	MAX %	Notes
AtT20-hCB1	9.12 ± 0.14	110 ± 7	--
AtT20-hCB2	8.91 ± 0.14	92 ± 6	--
HEK293-TRPA1	--	<5	Max <30% no CRC completed
HEK293-TRPV1	--	<10	Inhibits average max CAP response by 12%
AtT20 WT	--	<5	Inhibits average max SRIF response by 13%

*pEC50 assuming that the maximum is equivalent to the maximum of cinnamaldehyde

AB-FUBICA

(S)-N-(1-amino-3-methyl-1-oxobutan-2-yl)-1-
(4-fluorobenzyl)-indole-3-carboxamide

A: Response of AtT20-CB1 and AtT20-CB2 to AB-
FUBICA (10μM).
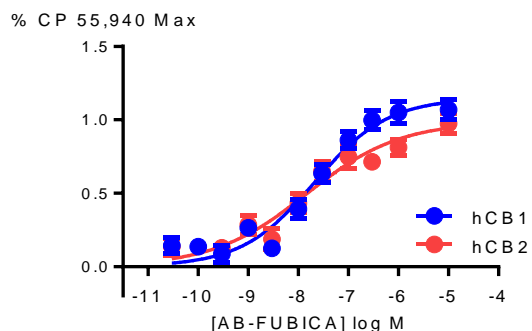
B: Concentration response curves for AB-FUBICA in
AtT20-CB1 and AtT20-CB2

D: Response of HEK293-TRPA1 to AB-FUBICA (30μM) and
cinnamaldehyde (300μM).
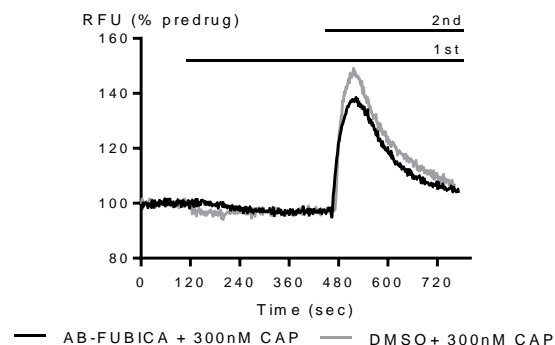
F: Response of HEK293-TRPV1 to AB-FUBICA (30μM)
followed by capsaicin (300nM)

C: Response of AtT20-WT to AB-FUBICA (10μM)
followed by SRIF (100nM)

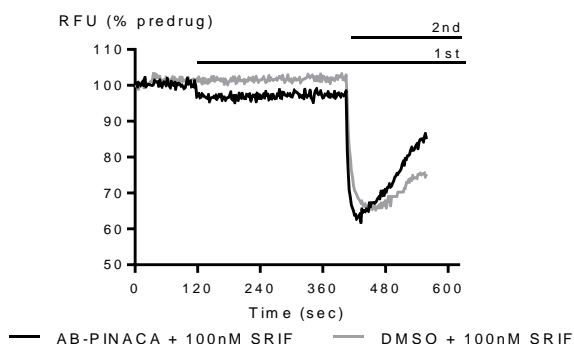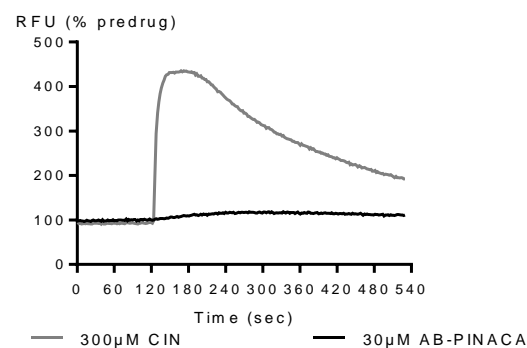|	pEC50	MAX %	Notes
AtT20-hCB1	7.67 ± 0.14	115 ± 7	--
AtT20-hCB2	7.84 ± 0.27	99 ± 10	--
HEK293-TRPA1	--	<5	Max <30% no CRC completed
HEK293-TRPV1	--	<10	Inhibits average max CAP response by 17%
AtT20 WT	--	<5	Inhibits average max SRIF response by 13%

ADB-FUBICA

(S)-N-(1-amino-3,3-dimethyl-1-oxobutan-2-yl)-1-(4-fluorobenzyl)-indole-3-carboxamide
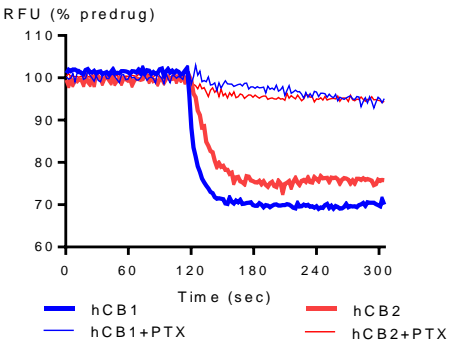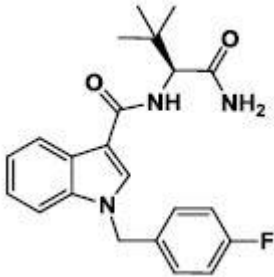
A: Response of AtT20-CB1 and AtT20-CB2 to ADB-FUBICA (10μM).

D: Response of HEK293-TRPA1 to ADB-FUBICA (30μM) and cinnamaldehyde (300μM).

B: Concentration response curves for ADB-FUBICA in AtT20-hCB1 and AtT20-hCB2
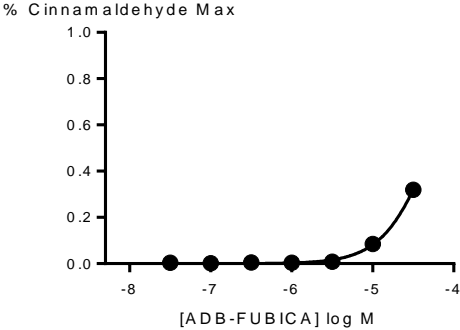
E: Concentration response curve for ADB-FUBICA in HEK293-TRPA1

C: Response of AtT20-WT to ADB-FUBICA (10μM) followed by SRIF (100nM)
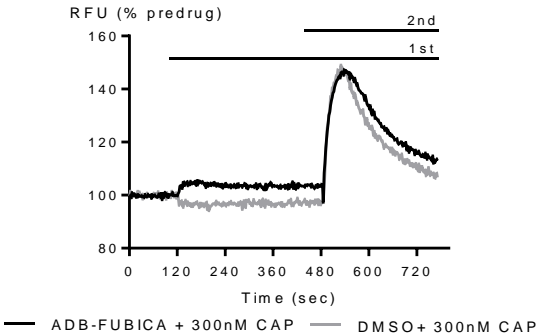
F: Response of HEK293-TRPV1 to ADB-FUBICA (30μM) followed by capsaicin (300nM)

	pEC50	MAX %	Notes
AtT20-hCB1	8.58 ± 0.15	113 ± 8	--
AtT20-hCB2	8.52 ± 0.16	96 ± 7	--
HEK293-TRPA1	4.27 ± 0.03*	32 ± 1	--
HEK293-TRPV1	--	<10	Inhibits average max CAP response by <10%
AtT20 WT	--	<10	No change of max SRIF response

*pEC50 assuming that the maximum is equivalent to the maximum of cinnamaldehyde

AB-PINACA

(S)-N-(1-amino-3-methyl-1-oxobutan-2-yl)-1-pentyl-indazole-3-carboxamide
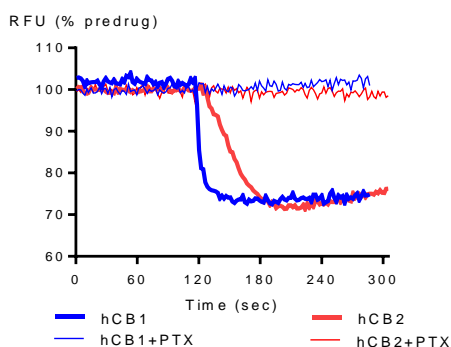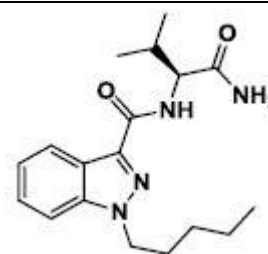
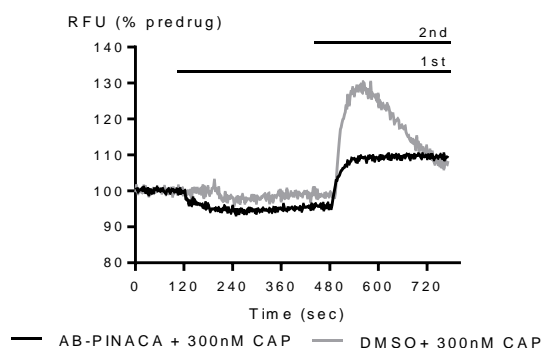A: Response of AtT20-CB1 and AtT20-CB2 to AB-PINACA (10μM).
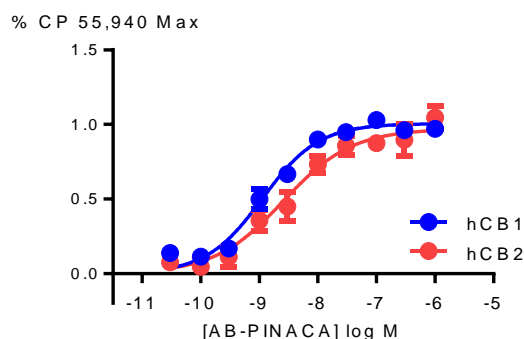
B: Concentration response curves for AB-PINACA in AtT20-CB1 and AtT20-CB2

C: Response of AtT20-WT to AB-PINACA (10μM) followed by SRIF (100nM)

D: Response of HEK293-TRPA1 to AB-PINACA (30μM) and cinnamaldehyde (300μM).
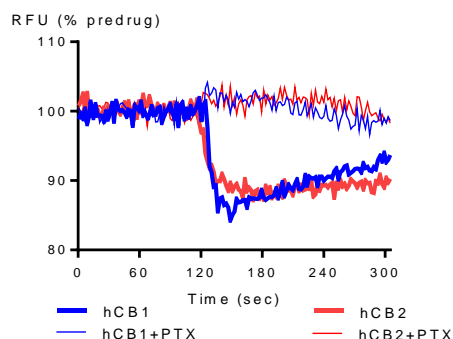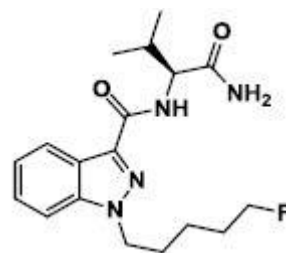

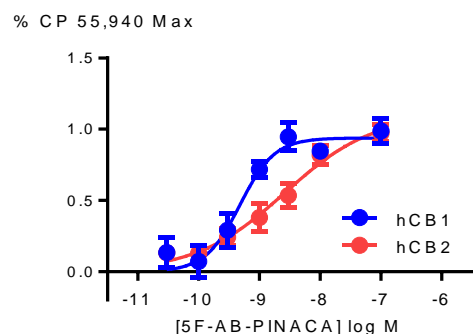F: Response of HEK293-TRPV1 to 5F-AB-PICA (30μM) followed by capsaicin (300nM)

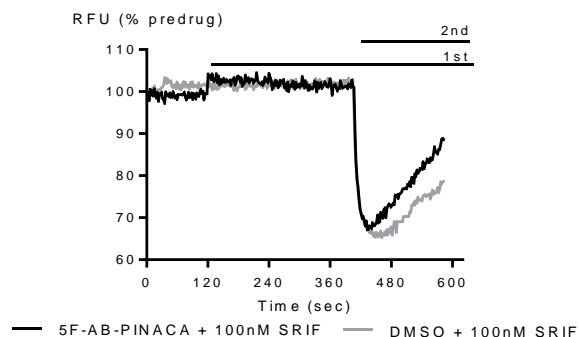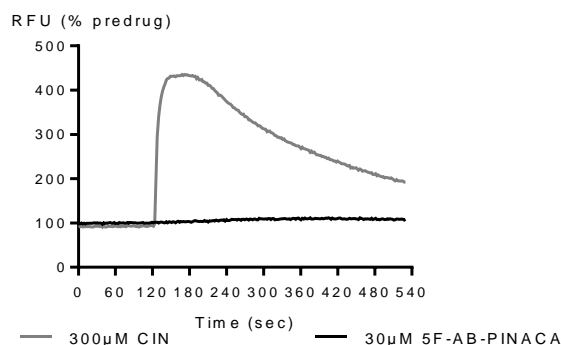|	pEC50	MAX %	Notes
AtT20-hCB1	8.91 ± 0.09	103 ± 4	--
AtT20-hCB2	8.60 ± 0.16	104 ± 8	--
HEK293-TRPA1	--	<5	Max <30% no CRC completed
HEK293-TRPV1	--	<5	Inhibits average max CAP response by 25%
AtT20 WT	--	<5	Inhibits average max SRIF response by 13%

5F-AB-PINACA

(S)-N-(1-amino-3-methyl-1-oxobutan-2-yl)-1-(5-fluoropentyl)-indazole-3-carboxamide

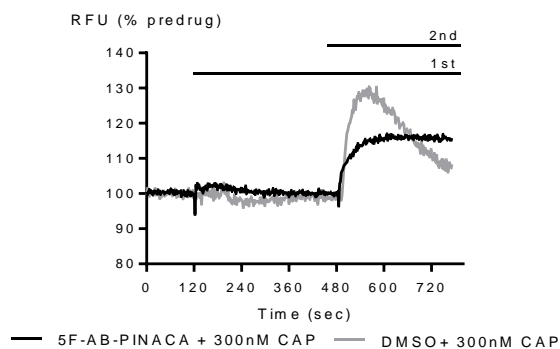A: Response of AtT20-CB1 and AtT20-CB2 to 5F-AB-PINACA (10μM).

B: Concentration response curves for 5F-AB-PINACA in AtT20-CB1 and AtT20-CB2

C: Response of AtT20-WT to 5F-AB-PINACA (10μM) followed by SRIF (100nM)

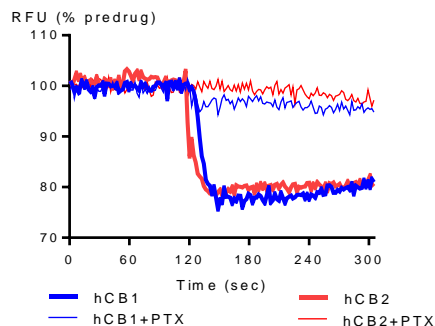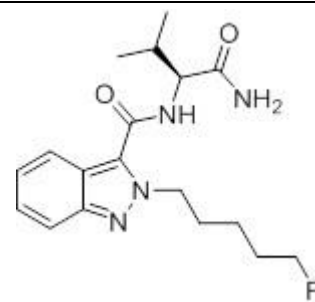D: Response of HEK293-TRPA1 to 5F-AB-PINACA (30μM) and cinnamaldehyde (300μM).

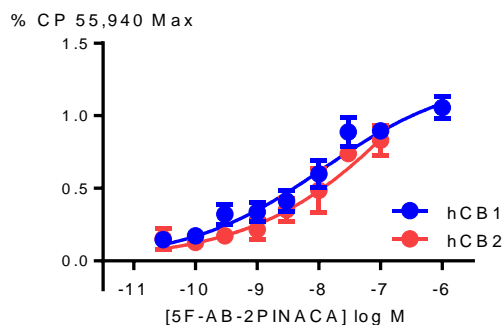F: Response of HEK293-TRPV1 to 5F-AB-PINACA (30μM) followed by capsaicin (300nM)

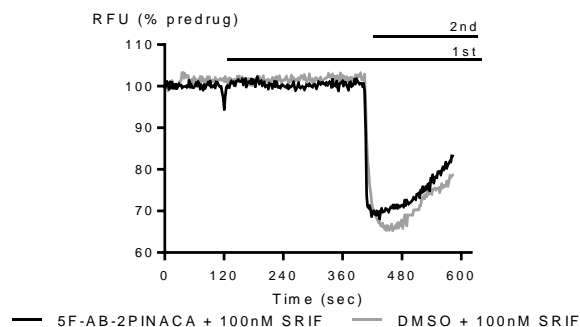|	pEC50	MAX %	Notes
AtT20-hCB1	9.32 ± 0.10	94 ± 6	--
AtT20-hCB2	8.59 ± 0.25	110 ± 13	--
HEK293-TRPA1	--	<5	Max <30% no CRC completed
HEK293-TRPV1	--	<5	Inhibits average max CAP response by <5%
AtT20 WT	--	<1	Inhibits average max SRIF response by 13%

5F-AB-2PINACA

(S)-N-(1-amino-3-methyl-1-oxobutan-2-yl)-**2**-(5-fluoropentyl)-indazole-3-carboxamide
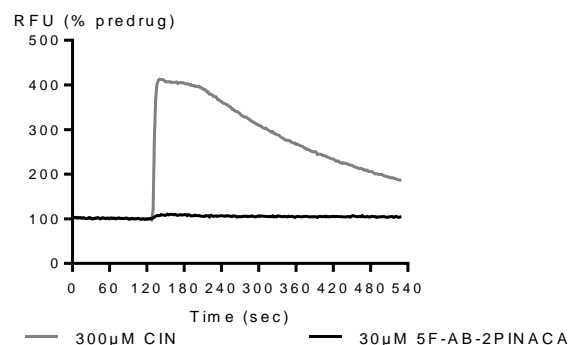

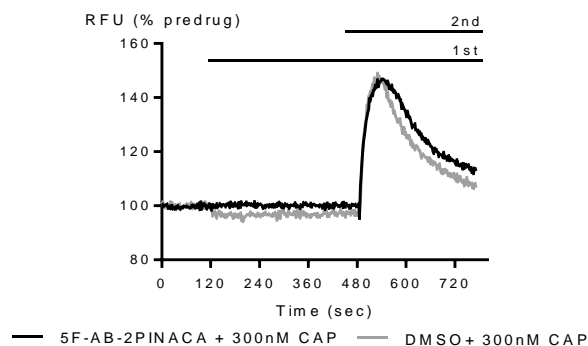A: Response of AtT20-CB1 and AtT20-CB2 to 5F-AB-2PINACA (10μM).

B: Concentration response curves for 5F-AB-2PINACA in AtT20-CB1 and AtT20-CB2

D: Response of HEK293-TRPA1 to 5F-AB-2PINACA (30μM) and cinnamaldehyde (300μM).

C: Response of AtT20-WT to 5F-AB-2PINACA (10μM) followed by SRIF (100nM)
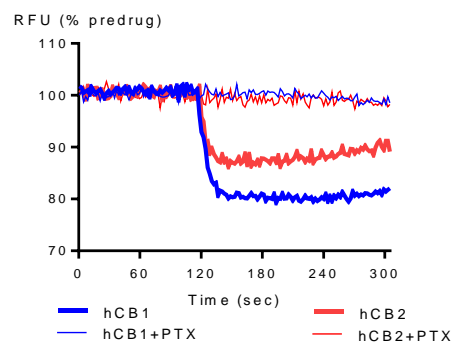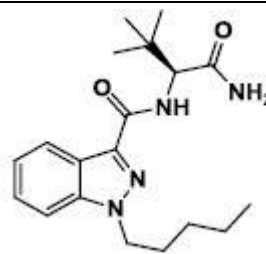
F: Response of HEK293-TRPV1 to 5F-AB-2PINACA (30μM) followed by capsaicin (300nM)

|	pEC50	MAX %	Notes
AtT20-hCB1	7.92 ± 0.46	106 ± 8	--
AtT20-hCB2	8.38± 0.35**	83 ± 10	--
HEK293-TRPA1	--	<5	Max <30% no CRC completed
HEK293-TRPV1	--	<10	Inhibits average max CAP response by 13%
AtT20 WT	--	<5	Inhibits average max SRIF response by 11%

** pEC50 assuming that the maximum is equivalent to the maximum of CP 55.940
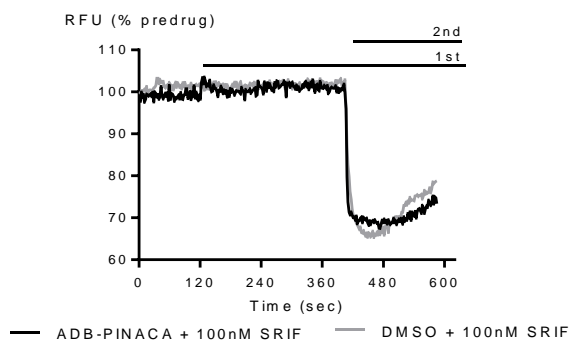
ADB-PINACA

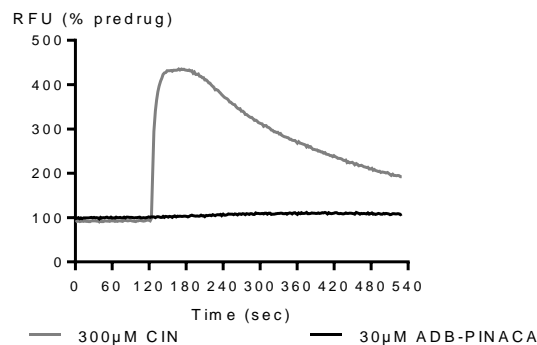(S)-N-(1-amino-3,3-dimethyl-1-oxobutan-2-yl)-1-pentyl-indazole-3-carboxamide

A: Response of AtT20-CB1 and AtT20-CB2 to ADB-PINACA (10μM).
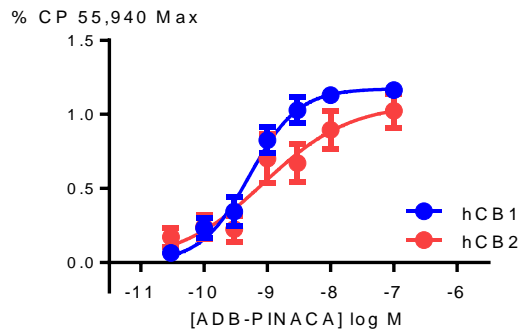
B: Concentration response curves for ADB-PINACA in AtT20-CB1 and AtT20-CB2

D: Response of HEK293-TRPA1 to ADB-PINACA (30μM) and cinnamaldehyde (300μM).
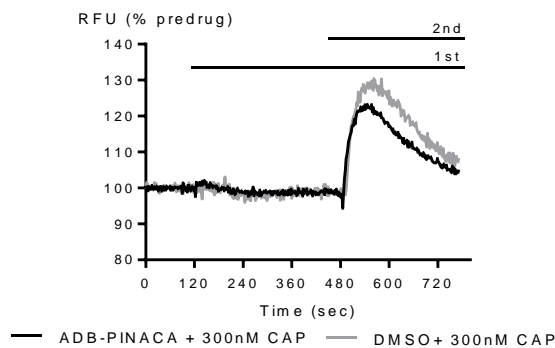
F: Response of HEK293-TRPV1 to ADB-PINACA (30μM) followed by capsaicin (300nM)

C: Response of AtT20-WT to ADB-PINACA (10μM) followed by SRIF (100nM)

	pEC50	MAX %	Notes
AtT20-hCB1	9.28 ± 0.08	117 ± 6	--
AtT20-hCB2	9.06 ± 0.31	107 ± 16	--
HEK293-TRPA1	--	<5	Max <30% no CRC completed
HEK293-TRPV1	--	<5	Inhibits average max CAP response by 28%
AtT20 WT	--	<5	Inhibits average max SRIF response by 22%

5F-ADB-PINACA

(*S*)-*N*-(1-amino-3,3-dimethyl-1-oxobutan-2-yl)-
1-(5-fluoropentyl)-indazole-3-carboxamide

A: Response of AtT20-CB1 and AtT20-CB2 to 5F-
ADB-PINACA (10μM).

B: Concentration response curves for 5F-ADB-PINACA
in AtT20-CB1 and AtT20-CB2

D: Response of HEK293-TRPA1 to 5F-ADB-PINACA (30μM)
and cinnamaldehyde (300μM).
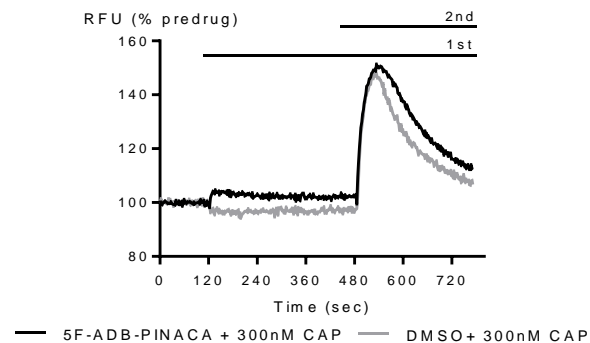
F: Response of HEK293-TRPV1 to 5F-ADB-PINACA (30μM)
followed by capsaicin (300nM)

C: Response of AtT20-WT to 5F-ADB-PINACA
(10μM) followed by SRIF (100nM)

	pEC50	MAX %	Notes
AtT20-hCB1	9.61 ± 0.19	91 ± 7	--
AtT20-hCB2	8.68 ± 0.11	94 ± 5	--
HEK293-TRPA1	--	<10	Max <30% no CRC completed
HEK293-TRPV1	--	<10	Inhibits average max CAP response by 10%
AtT20 WT	--	<1	Inhibits average max SRIF response by 13%

AB-FUBINACA

(*S*)-*N*-(1-amino-3-methyl-1-oxobutan-2-yl)-1-
(4-fluorobenzyl)-indazole-3-carboxamide

A: Response of AtT20-CB1 and AtT20-CB2 to AB-
FUBINACA (10μM).

B: Concentration response curves for AB-FUBINACA
in AtT20-CB1 and AtT20-CB2

C: Response of AtT20-WT to AB-FUBINACA (10μM)
followed by SRIF (100nM)
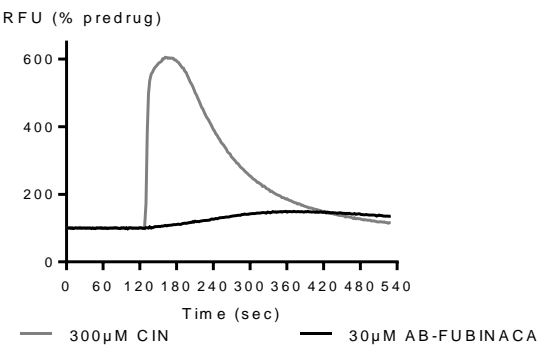
D: Response of HEK293-TRPA1 to AB-FUBINACA (30μM) and
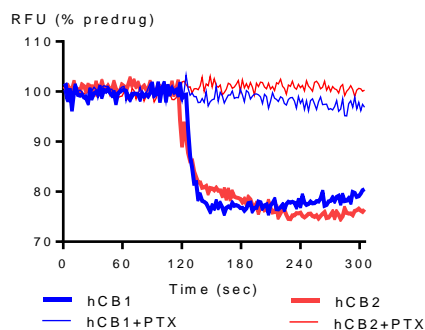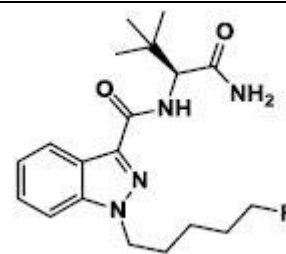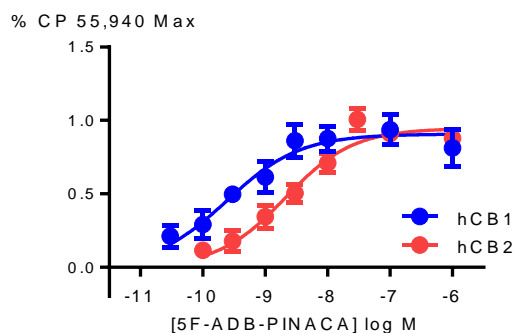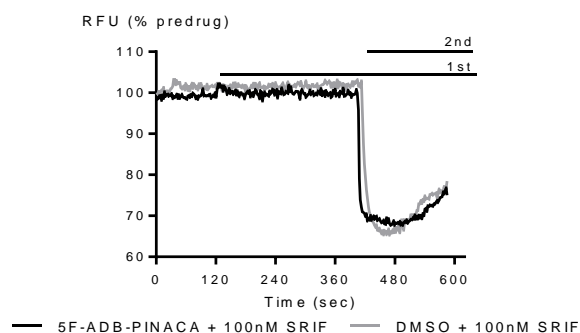cinnamaldehyde (300μM).
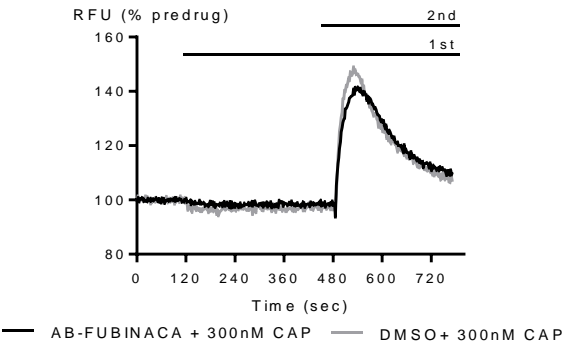
F: Response of HEK293-TRPV1 to AB-FUBINACA (30μM)
followed by capsaicin (300nM)

	pEC50	MAX %	Notes
AtT20-hCB1	8.76 ± 0.10	108 ± 7	--
AtT20-hCB2	8.50 ± 0.2	95 ± 12	--
HEK293-TRPA1	--	<5	Max <30% no CRC completed
HEK293-TRPV1	--	<10	Inhibits average max CAP response by 21%
AtT20 WT	--	<1	Inhibits average max SRIF response by 21%

ADB-FUBINACA

(*S*)-*N*-(1-amino-3,3-dimethyl-1-oxobutan-2-yl)-
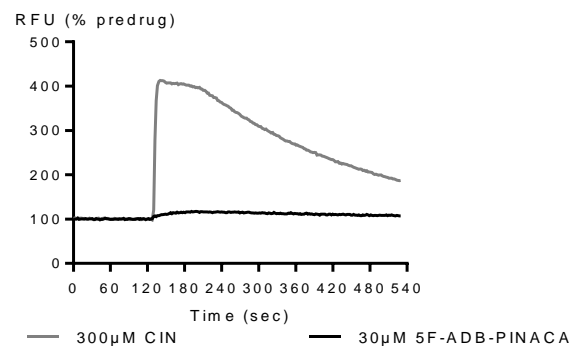1-(4-fluorobenzyl)-indazole-3-carboxamide
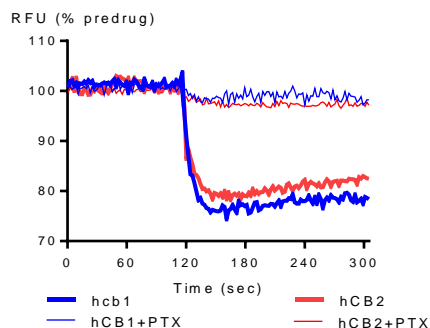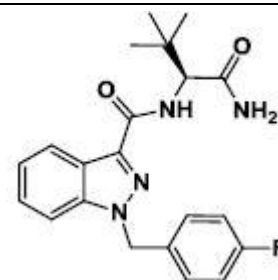
A: Response of AtT20-CB1 and AtT20-CB2 to ADB-FUBINACA (10μM).
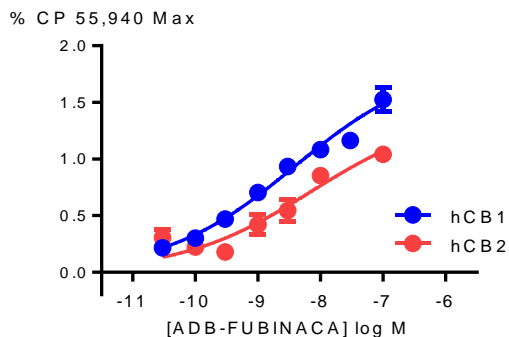
B: Concentration response curves for ADB-FUBINACA in AtT20-CB1 and AtT20-CB2
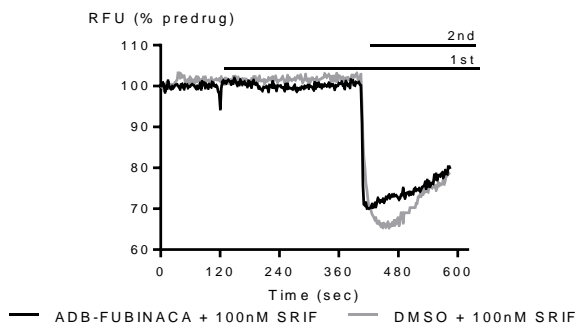
C: Response of AtT20-WT to ADB-FUBINACA (10μM) followed by SRIF (100nM)
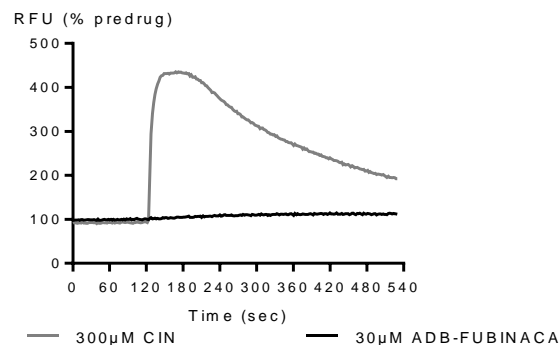
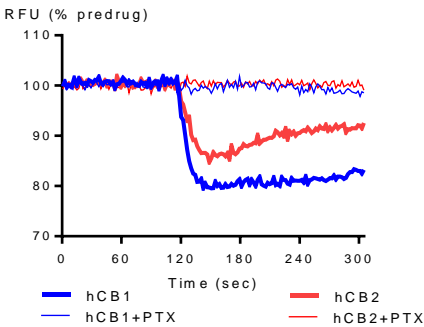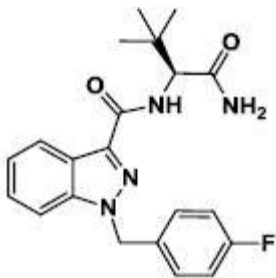D: Response of HEK293-TRPA1 to ADB-FUBINACA (30μM) and cinnamaldehyde (300μM).
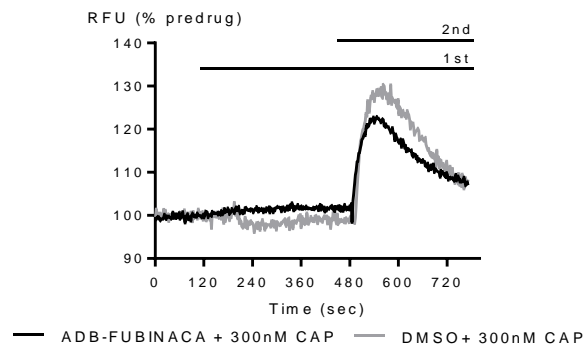
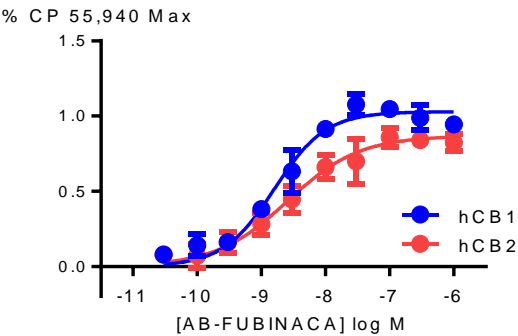F: Response of HEK293-TRPV1 to ADB-FUBINACA (30μM) followed by capsaicin (300nM)

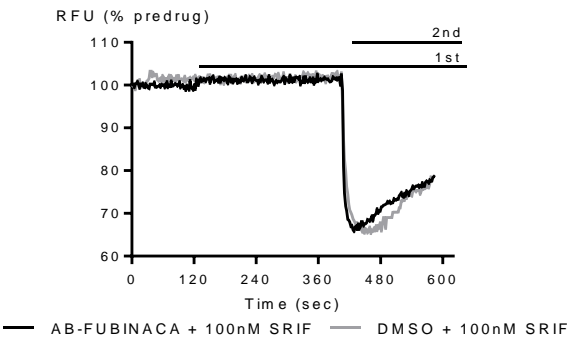|	pEC50	MAX %	Notes
AtT20-hCB1	8.92 ± 0.16	152 ± 11	--
AtT20-hCB2	8.46 ± 0.13	104 ± 7	--
HEK293-TRPA1	--	<5	Max <30% no CRC completed
HEK293-TRPV1	--	<10	Inhibits average max CAP response by 16%
AtT20 WT	--	<1	Inhibits average max SRIF response by 17%

APPENDIX B

Publications with which data has been previously published, by chapter:

Chapter 3/7:

Banister, Sam, Stuart, Jordyn, Kevin Richard, Edington, Amelia, Longworth, Mitchell, Wilkinson, Shane, Beniat, Corinne, Buchanan, Alexandra, Hibbs, David, Glass, Michelle, Connor, Mark, McGregor, Iain, Kassiou, Michael (2015). "The effects of bioisosteric fluorine in synthetic cannabinoid designer drugs JWH-018, AM-2201, UR-144, XLR-11, PB-22, 5F-PB-22, APICA, and STS-135." ACS Chemical Neuroscience.

Chapter 4:

Banister, Sam, Wilkinson, Shane, Longworth, Mitchell, Stuart, Jordyn, Apetz, Nadine, English, Katrina, Brooker, Lance, Goebel, Catrin, Hibbs, David, Glass, Michelle, Connor, Mark, McGregor, Iain, Kassiou, Michael (2013). "The Synthesis and Pharmacological Evaluation of Adamantane-Derived Indoles: Cannabimimetic Drugs of Abuse." ACS Chemical Neuroscience **4**(7): 1081-1092.

Chapter 5:

Banister, Sam, Stuart, Jordyn, Conroy, Trent, Longworth, Mitchell, Manohar, Madhura, Beinat, Corinne, Wilkinson, Shane, Kevin, Richard, Hibbs, David, Glass, Michelle, Connor, Mark, McGregor, Iain, Kassiou, Michael (2015). "Structure–activity relationships of synthetic cannabinoid designer drug RCS-4 and its regioisomers and C4 homologues." Forensic Toxicology: 1-12.

Chapter 6:

Banister, Sam, Moir, Michael, Stuart, Jordyn, Kevin, Richard, Wood, Katie, Longworth, Mitchell, Wilkinson, Shane, Beinat, Corinne, Buchanan, Alexandra, Glass, Michelle, Connor, Mark, McGregor, Iain, Kassiou, Michael. (2015). "Pharmacology of Indole and Indazole Synthetic Cannabinoid Designer Drugs AB-FUBINACA, ADB-FUBINACA, AB-PINACA, ADB-PINACA, 5F-AB-PINACA, 5F-ADB-PINACA, ADBICA, and 5F-ADBICA." ACS Chemical Neuroscience. doi: 10.1021/acschemneuro.5b0011.

APPENDIX C: MASS SPECTROMETRY DATA

Endocannabinoid levels detected after drug treatment HEK293-hTRPV1

HEK293-hTRPV1 — AEA

HEK293-hTRPV1 — 2-AG

HEK293-hTRPV1 — PEA

HEK293-hTRPV1 — OEA

HEK293-hTRPV1 — LEA

	CAPZ	CAPZ+CAP	CAP
AEA	0.6919	0.1259	0.8204
2-AG	0.7786	0.0929	**<0.0001**
PEA	0.8353	0.1613	0.6910
OEA	0.9153	0.2315	0.8537
OEA	0.8320	0.3260	0.8178

p≤0.05   **CAP = capsaicin**

p >0.05   **CAPZ = capsazepine**

Endocannabinoid levels detected after drug treatment in HEK293-WT

	CAPZ	CAPZ+CAP	CAP
AEA	0.9844	**0.0121**	0.9848
2-AG	0.5321	**0.0197**	0.6864
PEA	0.9772	0.1123	0.8832
OEA	0.8685	0.3358	0.4627
OEA	0.9733	0.1439	0.4488

p≤0.05   **CAP = capsaicin**

p >0.05   **CAPZ = capsazepine**

Endocannabinoid levels detected after drug treatment in AtT20-hCB1

	SR14A	SR14A +CP	5-OH-UR-144	XLR-11	CP 55,940
AEA	0.7716	0.7370	0.4957	0.2764	0.9747
2-AG	0.5368	0.3434	0.7580	0.6908	0.0555
PEA	0.2358	0.9851	0.3181	**0.0310**	0.9099
OEA	0.8892	0.9515	0.9303	0.1714	0.9785
OEA	0.6674	0.9618	0.9470	0.6605	0.5317

p≤0.05   SR14A = SR141716A

p >0.05   CP = CP 55,940

Endocannabinoid levels detected after drug treatment in AtT20-hCB2

AtT20-hCB2 — AEA

AtT20-hCB2 — 2-AG

AtT20-hCB2 — PEA

AtT20-hCB2 — OEA

AtT20-hCB2 — LEA

	AM630	AM630 +CP	5-OH-UR-144	XLR-11	CP 55,940
AEA	0.9331	0.2846	0.7076	0.4308	0.5181
2-AG	**0.0305**	0.7216	0.9120	0.5344	0.2454
PEA	0.1651	0.9841	0.9146	0.7677	0.3879
OEA	0.4018	0.2142	0.2158	0.4570	0.6426
OEA	0.0842	0.4750	0.0528	0.3408	0.7583

p≤0.05   **CP = CP 55,940**
p >0.05

Endocannabinoid levels detected after drug treatment in HEK293-hTRPA1

HEK293-hTRPA1 (AEA)

HEK293-hTRPA1 (2-AG)

HEK293-hTRPA1 (PEA)

HEK293-hTRPA1 (OEA)

HEK293-hTRPA1 (LEA)

	CIN	XLR-11	5-OH-UR-144
AEA	0.2166	0.1789	0.3651
2-AG	**0.0056**	0.6499	0.8209
PEA	0.4184	0.3020	0.3403
OEA	0.3952	0.2165	0.2457
OEA	0.3522	0.4673	0.3759

p≤0.05   **CIN = Cinnamaldehyde**

p >0.05

Chromatograms of Biological Samples Compared to the Endocannabinoid Standard

B i o l o g i c a l   S a m p l e   v s.   1   n M   S t a n d a r d

Legend: 1 nM AEA Std. ; 20 μL injection BS
Axes: Intensity, cps (0–40000) vs. Time(min) (3.0–5.5)

B i o l o g i c a l   S a m p l e   v s.   1   n M   S t a n d a r d

Legend: 1 nM PEA Std. ; 20 μL injection BS
Axes: Intensity, cps (0–150000) vs. Time(min) (3.0–5.5)

B i o l o g i c a l   S a m p l e   v s.   1   n M   S t a n d a r d

Legend: 1 nM 2-AG Std. ; 20 μL injection BS
Axes: Intensity, cps (0–9000) vs. Time(min) (3.0–5.5)
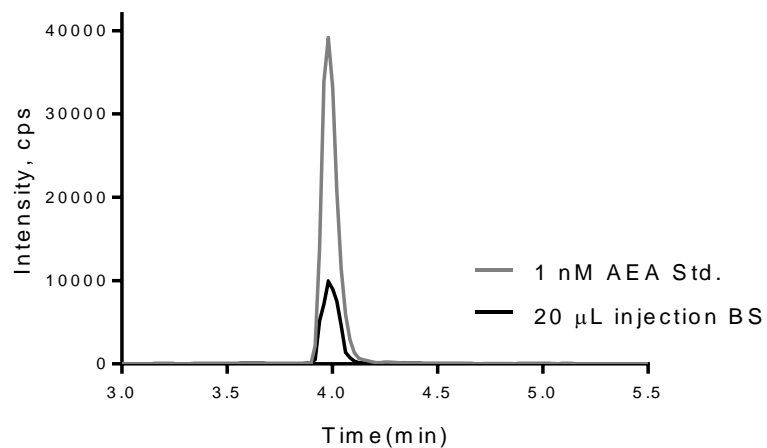
B io lo g ic a l S a m p le v s . 1 n M S ta n d a rd

B io lo g ic a l S a m p le v s . 1 n M S ta n d a rd

Appendix C   Page | 311